Simultaneous removal of nitrate and phosphorus in a biofilm reactor

The aspect of diffusion

Falkentoft, Christina Maria

Publication date:
2000

Document Version
Publisher's PDF, also known as Version of record

DTU

Simultaneous Removal of Nitrate and Phosphorus in a Biofilm Reactor

The Aspect of Diffusion

Christina Maria Falkentoft

Technical University of Denmark
Danmarks Tekniske Universitet

Institut for Miljøteknologi
Department of Environmental Science and Engineering

Simultaneous Removal of Nitrate and Phosphorus in a Biofilm Reactor The Aspect of Diffusion

Cover: Birte Brejl
Printed by: DTU tryk
Department of Environmental Science and Engineering
ISBN 87-89220-55-2

The thesis will be available as a downloadable pdf-file from the department's homepage on: www.er.dtu.dk

Environment & Resources DTU
Library
Bygningstorvet, Building 115, Technical University of Denmark
DK-2800 Kgs. Lyngby
Phone:
Direct (+45) 45 25 16 10
(+45) 45 25 16 00
Fax: (+45) 45 93 28 50
E-mail: gh@er.dtu.dk

Preface - Ph.D.-Study Information

Where?
The host of the Ph.D.-study was the Department of Environmental Science and Engineering (IMT) at the Technical University of Denmark (DTU), Lyngby.
Part of the study (1 year period) was spent at the Department of Water Quality Control and Waste Management at the Technical University of Munich (TUM) in Germany.

When?
The Ph.D.-study was carried out in the period from February 1996 to March 2000. The first version of the thesis was submitted to the Technical University of Denmark 30 June 2000. Following a public Ph.D.-defence at the Department of Environmental Science and Engineering 14 December 2000 a few minor revisions have been made before submitting the present and final version of the thesis.

Who?
The Ph.D.-study was performed by Civ. Eng. Christina Maris Falkentoft.
Professor Poul Harremoës, Technical University of Denmark, was the main supervisor of the project. Ass. Prof.'s Hans Mosbæk and Mogens Henze, Technical University of Denmark, were co-supervisors. The work made at the Technical University of Munich, Germany, was supervised by Professor Peter Wilderer and Dr. Stefan Wuertz.

What?
This Ph.D.-thesis has been submitted as part of the requirements for the Ph.D. degree at the Technical University of Denmark.
The following publications are concurrently submitted as parts of the study:

Falkentoft, C. M., Harremoës, P. and Mosbæk, H. (1999) The significance of Zonation in a Denitrifying, Phosphorus Removing Biofilm. *Wat. Res.* **33**(15), 3303-3310.

Falkentoft, C. M., Harremoës, P., Mosbæk, H. and Wilderer, P. (2000) Combined denitrification and phosphorus removal in a biofilter. Presented at the IAWQ Biofilm Conference in New York, USA, 17-20 Oct. 1999. Published in *Wat. Sci. Tech.* (2000) **41**(4-5), 493-501.

Falkentoft, C. M., Harremoës, P., Mosbæk, H. and Wilderer, P. (2001) Stability of a lab-scale biofilm for simultaneous removal of phosphorus and nitrate. Presented at the international IWA Conference, Paris2000, France, 3-7 July 2000. Published in *Wat. Sci. Tech.* (2001) **43**(1), 335-342.

Falkentoft, C. M., Müller, E., Arnz, P., Harremoës, P., Mosbæk, H., Wilderer, P. and Wuertz, S. (2000) Population changes in a biofilm reactor for phosphate removal as evidenced by the use of FISH. Submitted for *Wat. Res*. June 2000. Acceptance for publication announced Feb. 2001.

Falkentoft, C. M., Arnz, P., Henze, M., Mosbæk, H., Müller, E., Wilderer, P. and Harremoës, P. (2000) Possible Complication regarding phosphate removal with a continuous flow biofilm system: Diffusion limitation. Submitted for *Biotechnol.&Bioeng.* June 2000.

Financing?

The main part of the study was supported by the Danish State Education Fund, Technical University of Denmark.
The stay in Germany was financed by the EU-project BioToBio (Biological Nitrogen Removal: From Biofilms To Bioreactors), and partly by the Research Center for Fundamental Studies of Aerobic Biological Wastewater Treatment (SFB 411, Deutsche Forschungs-gemeinschaft).

Munich, 4 March 2001

Christina Maria Falkentoft

Dansk Sammenfatning (Danish Summary)

Hovedformålet med studiet var at undersøge simultan fjernelse af nitrat og fosfat i et kontinuert biofilm system. En kontinuert laboratorie-skala reaktor, alternerende imellem anaerobe og anoxiske forhold, blev udviklet til brug i undersøgelsen. Fokus var især problematikken vedrørende diffusions begrænsning. Det var tanken, at diffusion muligvis kunne udgøre et alvorligt problem i henhold til succesfuld biologisk fosforfjernelse (bio-P) med en biofilm. En større reaktor, som blev drevet med ilt som elektron acceptor i bio-P-processen, blev som en del af studiet undersøgt af hensyn til sammenligning med den denitrificerende reaktor. Studiet var inddelt i tre dele med følgende undertitler:

DEL A: 'Zone-inddeling og stabilitet af en denitrificerende bio-P reaktor'
DEL B: 'Undersøgelser af en aerob modsat en denitrificerende bio-P reaktor'
DEL C: 'Modellering af en bio-P biofilm'

DEL A. Zone-inddeling og stabilitet af en denitrificerende bio-P reaktor

Udgangspunktet for studiet var udvikling af en laboratorie-skala opstilling. Den naturlige uligevægts tilstand af bio-P processen nødvendiggør konstant overvågning og dataopsamling. Dette kan kun lade sig gøre via automatisk kontrol og on-line måling. Grundige overvejelser og tests af en automatiseret opstilling med on-line nitrat og fosfat målinger blev derfor gennemført forud for de biologiske eksperimenter. pH kontrol blev implementeret senere.
Ingen fuld-, pilot- eller laboratorie-skala biofiltre for bio-P eksisterer i Danmark idag. En biofilm blev derfor først opbygget på et granulært bæremateriale (Biostyr®).
Via batch tests blev teorien om ½. og 0. ordens reaktion i vandfasen udenfor biofilmen eftervist for anaerob fosfatfrigivelse og anoxisk denitrifikation. Dette blev taget som en indikation af en zone-inddelt biofilmstruktur, hvilket er af speciel betydning for fosfatfjernelse. Forudsætningen for denne proces er nemlig, at bakterierne udsættes for alternerende forhold, hvilket kompliceres hvis biofilmen bliver så tyk, at substrat (elektronacceptor eller -donor) ikke kan trænge ind til bunden af filmen. Støkiometriske koefficienter var for anaerob fosfatfrigivelse: 0.25 g P/g acetat-COD, og for anoxisk fosfatoptag: 0.65 g P/g NO_3-N. Begge værdier er lave i sammenligning med litteraturen, hvilken kan betyde at andre bakterier med evne til at lagre organisk stof konkurrerer med bio-P bakterierne. Alternativt kan der være tale om en variant af bio-P metabolismen. Mod slutningen af den 1½-årige forsøgsperiode, måltes den anaerobe koefficient til 0.14 g P/g COD, dog var pH på dette tidspunkt blevet

reduceret fra ~8 til 7, hvilket muligvis forklarer en del af reduktionen i den støkiometriske koefficient.
Signifikant variation i bio-P aktiviteten var observeret i løbet af forsøgsperioden på trods af, at veldefinerede forsøgsbetingelser samt kunstigt substrat med acetat som eneste kulstofkilde blev benyttet. Mikrobiologiske undersøgelser ville have været værdifulde for eftervisning af antagelsen om skift i bakteriepopulationen som årsag til de observerede variationer.

DEL B. Undersøgelser af en aerob modsat en denitrificerende bio-P reaktor

Den eksperimentelle opstilling blev medbragt til det Tekniske Universitet i München, Tyskland, hvor både 20-liters og halvt-fuld-skala sekventielle batch bio-P biofilm reaktorer var i bedrift. Også her benyttedes et granulært bæremateriale (Biolith®). Ilt benyttedes som hoved-elektronacceptoren i processen. Induktion af denitrifikation efter overførsel af biofilmprøver fra disse reaktorer til den anoxiske laboratoriereaktor blev undersøgt. To eksperimentelle forsøgskørsler blev udført. I løbet af første forsøgskørsel, blev faselængder i bio-P cyklussen varieret i intervallet 3 til 16 timer. Efter en ændring af den anaerobe faselængde 1 måned inde i forsøget, reduceredes fosfatfjernelses-aktiviteten, og den forblev på et meget lavt niveau herefter. Årsagen til dette kollaps, blev spekuleret til at være en ændring i bakteriepopulationen bragt omkring af ændringen i faselængden. En ny forsøgskørsel blev startet. Denne gang blev biomasseprøver regelmæssigt udtaget og undersøgt med gensonder og konfokal scanning laser mikroskop for at undersøge eventuelle ændringer i bakteriepopulationen. Faselængderne blev i denne kørsel fastholdt på 3 timer. Imidlertid observeredes i denne kørsel en stigning af aktiviteten efterfulgt af en pludselig aktivitetsreduktion efter ca. 1 måned på helt tilsvarende måde som for første forsøgskørsel. Hermed kunne den først antagne årsag til nedgangen i aktivitet på grund af ændret faselængde afvises.
Gensonde analyserne åbenbarede, at ændringer i den mikrobiologiske population hovedsageligt fandt sted indenfor de første 2 uger efter overførslen fra den aerobe reaktor til den anoxiske forsøgsreaktor. Næsten alle bakterier tilhørende alfa undergruppen af *Proteobakterier* forsvandt, og karakteristiske klynger af *Proteobakterier* fra undergrupperne beta og gamma forsvandt ligeledes. Populationen var domineret af bakterieceller tilhørende beta undergruppen af *Proteobakterier*. Små klynger af gram-positive bakterier med et højt DNA G+C indhold blev gradvist fuldstændigt erstattet med filamentøse bakterier fra samme gruppe. Ingen nævneværdig forandring i populationen kunne verificeres omkring tidspunktet for aktivitetsnedgangen.
Fosfatindholdet i biomassen som blev løsrevet og skyllet ud under returskyl af filteret efter anoxiske faser var lavt: 2.4 ± 0.4 % baseret på den totale tørvægt, hvilket kun er en anelse højere end for ikke-bio-P biomasse.

DEL C: 'Modellering af en bio-P biofilm'

En simplificeret 1-D model baseret på Activated Sludge Model 2d indicerede, at det eksperimentelt observerede lave fosfatindhold kunne forklares via diffusionsbegrænsning af fosfat under anoxiske faser. Ifølge modellen, var en meget tynd biofilm kritisk i henhold til de fosfat-akkumulerende bakteriers konkurrencefordel overfor ikke-fosfat-akkumulerende denitrificerende heterotrofe bakterier i det betragtede kontinuerte system. Vækst af ikke-bio-P heterotrofe bakterier blev understøttet af overgangsperioderne imellem to faser, hvor både acetat og nitrat var tilstede, samt af en signifikant højere væksthastighed i forhold til bio-P-bakterierne. Imidlertid kunne en kombination af en tynd film med længere faselængder medføre et højt fosfatindhold af biofilmen, idet der i en tynd film ikke er diffusions-begrænsning, og vækst af ikke-bio-P-bakterier undertrykkes via lange faselængder. Til gengæld observeredes reduceret fosfatfjernelses-kapacitet grundet den følgende lave koncentration af biomasse. Måden, hvorpå biomasse løsrives under returskyl, har en yderst vigtig betydning for det opnåelige fosfatindhold af overskudsslam fra systemet.

KONKLUSION

Udfra kombinationen af eksperimentelle og modellerings resultater konkluderes, at diffusionsbegrænsning og zone-inddeling kan have kritisk indflydelse i henhold til brug af et kontinuert biofilm system for biologisk fosforfjernelse. En delikat balance eksisterer imellem faselængder, returskyls hyppighed og biofilm tykkelse i forhold til fosfatindholdet i overskudsslammet. Disse forhold er sjældent diskuteret i studier af bio-P med biofiltre. På denne måde kan man få den tanke, at succesfuld bio-P i sådanne anlæg måske er opnået på basis af en tilfældigvis heldig kombination af de forskellige parametre. For at kontrollere processen, er en velkontrolleret returskyls-strategi nødvendig. Optimal proces konfiguration må evalueres på baggrund af spildevandssammensætning og rensningsmål. Modellering syner nødvendig under hensyn til kompleksiteten af processen og anbefales forud for op-skalering. Behovet for en relativt tynd biofilm for undgåelse af diffusionsbegrænsning reducerer mængden af aktiv biomasse og på denne måde også fjernelseskapaciteten til et niveau sammenligneligt med, eller måske endda lavere end, aktiverede slam anlæg?

Summary

The main objective of the study was to investigate simultaneous removal of nitrate and phosphorus in a continuous biofilter system. A continuous lab-scale setup alternating between anaerobic and anoxic conditions was developed for the investigation. No aerobic phase was included in the cycle. The specific focus was on the aspect of diffusion, and it was hypothesised that diffusion limitation could constitute a serious problem for achievement of enhanced biological phosphate removal (EBPR) with a biofilm. A bench-scale reactor operated with oxygen as the electron acceptor was sampled for biomass during part of the study to compare with the denitrifying reactor. The study was divided into three parts with the following sub-titles:

PART A: 'Zonation and Stability of a Denitrifying EBPR Biofilm'
PART B: 'Investigations of an Aerobic versus Denitrifying EBPR Biofilm'
PART C: 'Modelling of an EBPR Biofilm'

PART A. Zonation and Stability of a Denitrifying EBPR Biofilm

The starting point of the study was the development of a lab-scale setup. The inherent non-steady state characteristics of the biological phosphorus removal process makes it of crucial importance to keep constant track of what is going on and record the process history. This can only be achieved by automatic operation and on-line measurements with data logging. For this reason, thorough consideration and time was spent on developing and testing an automated experimental setup with on-line measurements of phosphate and nitrate before initiating the biological experiments. pH control was incorporated later in the study.
No full-, pilot- or lab-scale biofilters for enhanced biological phosphorus removal exist in Denmark. For this reason, a biofilm was first developed on a granular carrier material (Biostyr®).
By batch tests, the theory of ½ and 0 order of reaction in the bulk water depending on penetration depth into the biofilm was verified for anaerobic P-release and anoxic denitrification. This was taken as an indication of a zonated structure of the biofilm, which is of special importance when considering phosphorus removal. The prerequisite for obtaining phosphate removal is to expose the bacteria to alternating conditions, which is complicated if the biofilm gets too thick for the compounds in the bulk water to fully penetrate it.
Stoichiometric coefficients were for anaerobic P-release to COD-uptake 0.25 g P/g COD and for anoxic P-uptake to nitrate removal 0.65 g P/g N. Both values are low compared to the literature for enriched denitrifying cultures which was

taken as an indication of the presence of competing bacteria with the capacity of storing COD. Alternatively, it could be a difference in the metabolism compared to what is normally observed. The anaerobic P release coefficient decreased to 0.14 g P/g COD during the 1½-year period. However, pH was reduced from ~8 to 7 at this time, which might explain some of the reduction of the value.
Significant variation in the bio-P activity was observed despite using well-defined operation and synthetic wastewater with acetate as the only carbon source. Microbiological investigations would have been valuable in order to investigate hypothesised population shifts.

PART B. Investigations of an Aerobic versus Denitrifying EBPR Biofilm

The experimental setup was brought along to the Technical University of Munich, Germany, where both bench- and semi-full-scale sequencing batch biofilm reactors with granular carrier material (Biolith®) was operated for EBPR. Oxygen was the main electron acceptor in these processes. The induction of denitrification upon transferring biofilm samples to the anoxic lab-scale setup was investigated. Two experimental runs were carried out. During the first run, the phase lengths were varied in the range from 3 to 16 hours. By a certain reduction of the anaerobic phase length after 1 month, the phosphate removal activity of the biofilm deteriorated and remained at a very low level. This was speculated to be due to a change in the microbial population caused by the change of operation. Another run was started. This time, biomass samples were regularly investigated with gene probes and confocal laser scanning microscope to see, if population changes could be detected. The phase lengths were kept constant at 3 hours. However, a similar increase followed by a sudden decrease in the activity after 1 month was seen. Hereafter, the activity level stayed relatively constant. The build up of the biofilm, as indicated by the outlet concentrations of phosphate, was nearly identical to the first run, indicating no significant effect of the phase lengths.
The gene probe analysis revealed that the major changes in the microbial population took place within the first 2 weeks after the transfer. Almost all bacteria belonging to the alpha subclass of *Proteobacteria* disappeared and characteristic clusters of the beta and gamma subclasses were lost. The major part of the bacterial population was characterised as beta *Proteobacteria*. Small clusters of Gram-positive bacteria with a high DNA G+C content (GPBHGC) were gradually completely replaced with filamentous GPBHGC. No significant change could be detected around the time of the peak performance in the denitrifying biofilm.
The phosphate content of the biomass that detached during backwash after anoxic phases was measured during the second run and revealed a low value of 2.4 ± 0.4 % of phosphate in the total dry mass, which is only slightly higher than non-bio-P sludge.

PART C: 'Modelling of an EBPR Biofilm'

A simplified 1-D model based on the Activated Sludge Model 2d indicated that the experimentally observed low phosphate contents could be explained by diffusion limitation of phosphate during the anoxic phases. According to the model, a very thin biofilm thickness was critical for the competitive advantage of phosphate accumulating organisms (PAOs) over non-PAO denitrifying heterotrophs for the considered continuous system. The growth of denitrifying heterotrophs was supported by the transition phases where acetate and nitrate were present simultaneously, and by a significantly higher growth rate than the PAOs. However, by combining a thin film with longer phase lengths, high average P contents could be achieved due to no diffusion limitation and suppression of the growth of denitrifying heterotrophs. The payoff was a reduced phosphate removal capacity due to the consequently low amounts of biomass. The mode of detachment of the biofilm biomass plays an important role of the achieved average P content of the biomass removed by backwash.

CONCLUSION

From the combination of experimental and modelling results it is concluded that diffusion limitation and zonation in the film may play a critical role when attempting biological phosphate removal in a continuous biofilm system. A delicate balance between phase lengths, backwash frequency and biofilm thickness in regard to obtainable phosphate contents of the biomass exists. This relationship was seldom addressed in reported studies of EBPR with biofilms, which makes it appear as if good EBPR in many cases may have been achieved on the basis of an accidental fortunate combination of the different parameters. In order to control EBPR in a biofilter system, a well-controlled backwash strategy is required. Optimal process configuration has to be evaluated in relation to wastewater composition and removal objectives. Modelling appears a necessary tool in such an evaluation due to the complexity of the process, and is recommended before up-scaling. The need of relatively thin biofilms to avoid diffusion limitation reduce the concentration of active biomass and might thus reduce the volumetric removal rate to a level similar to (or lower than) activated sludge systems?

Table of Contents

1. Introduction

1.1 Phosphate Removal

Today, it is well known that discharges of nutrients to surface waters can lead to eutrophication. “Eutrophication” means the upsetting of the nutritional balance and is caused by unnatural high abundance of the macro-nutrients nitrogen and phosphorus (Vinconneau *et al.*, 1985). Excessive growth of algae in the water bodies lead to accumulation of organic matter. The effects of this are a reduced recreational appeal, complications regarding the use for drinking water purposes and changes in the food chain. The extreme case of the latter is seen during oxygen depletion with the death of higher organisms.

Removal of phosphorus from wastewater was introduced in Scandinavia in the late 1960s (Henze, 1996a). In the 1970s, phosphorus removal was incorporated in the wastewater treatment strategy of many countries, especially countries with many inland lakes: Sweden, Norway, Finland, Canada, USA and Switzerland (Arvin, 1983). It was at this time realised that release of the nutrients nitrogen and phosphorus with wastewater discharges were the major cause of the eutrophication problems. To prevent eutrophication, at least one of these two nutrients had to be controlled, and due to the greater natural availability of nitrogen, e.g. certain cyanophycae are capable of fixing nitrogen directly from the atmosphere, the control of phosphorus linked to human activities seemed the best control measure. Both nitrogen and phosphorus are essential fertilisers used for agricultural purposes, and also in this aspect it is easier to avoid leaks of phosphorus, since this is strongly held by the clay and humus fractions of the soil as an oppose to nitrogen compounds.

The European Union introduced in 1991 a directive (91/271/EEC) stating effluent requirements for urban wastewater of 2 or 1 mg P/l for small (10.000-100.000 Person Equivalents, PE) or large (> 100.000 PE) treatment facilities. At this time only 13 % of the wastewater in Europe was subjected to phosphate removal, Table 1.1. Also requirements for organic matter and nitrogen were included with values of 25 mg BOD_5/l and 10 mg N/l, respectively.

The EU directive was inspired by the Danish action plan for the aquatic environment that was implemented in 1987 as a direct consequence of large areas with oxygen depletion in the Danish fjords and inland seas (Henze, 1996). Part of this plan involved effluent requirements for wastewater treatment plants of maximum 15 mg BOD_5/l, 8 mg N/l and 1.5 mg P/l. The significant effect on the discharged amounts can be seen in Fig. 1.1. The yearly Danish person equivalent of organic matter and nitrogen has stayed relatively unchanged

during the latest years (22 kg BOD_5/pers/year and 4.4 kg N/pers/year), but the shift towards phosphate-free detergents in washing powder has caused a decrease from approximately 1.5 kg P/pers/year in 1987 to 1 kg P/pers/year today. Whether the trend of replacing phosphate in detergents is a fortunate trend can be discussed due to the relatively unknown environmental effects of the substituting compounds (Vinconneau *et al.*, 1985).
Originally phosphorus was removed by addition of precipitation chemicals. This technology was well established and relatively easy to implement on existing works which had to be upgraded for phosphate removal (Wiecherts, 1985). Also today, chemical treatment is the dominant strategy, but the use of biological removal by activated sludge has increased significantly during the last decade. In this regard, Denmark has been one of the pioneers, refer to Fig. 1.2 which shows the phosphate removal technologies in Scandinavia 1990.
Compared to chemical precipitation, biological removal might be economical beneficial, since the cost of chemicals is avoided and less excess sludge is produced. However, biological removal demand for bigger tank sizes and a chemical dosing system is needed as backup so an economic evaluation has to be made in the individual case. Ecologically it is favourable to avoid the chemicals and hence avoid the extra addition of metal salts that might contain impurities in the form of heavy metals. The success of biological phosphate removal is depending on the wastewater composition. In case of a low content of easily degradable organic matter compared to the phosphate load, it might be impossible to obtain sufficient removal by the biological method alone whereby a combination with chemicals may be necessary.

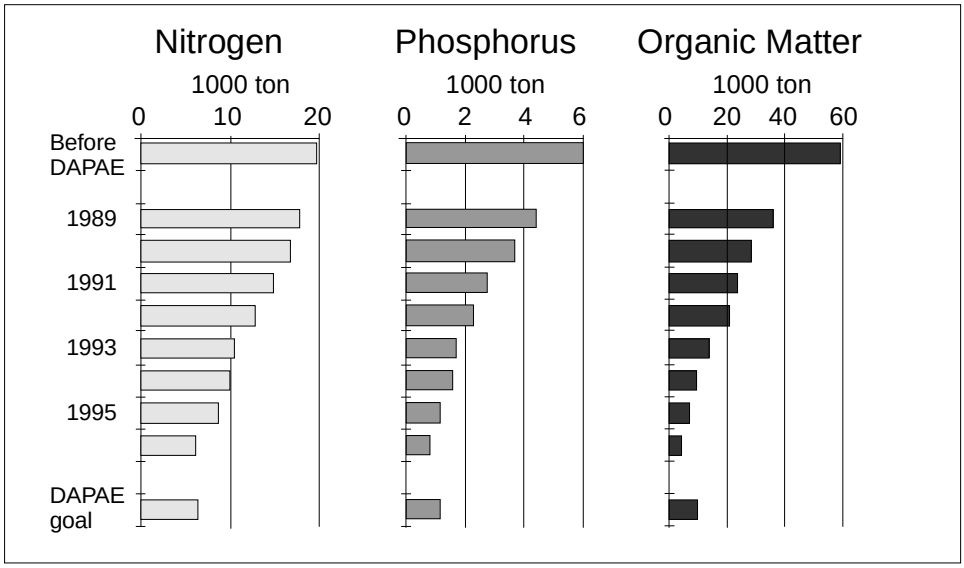

Figure 1.1. Development in discharges of nitrogen, phosphorus and organic matter in Denmark after the introduction of wastewater effluent requirements in 1987. DAPAE is an abbreviation of the Danish Action Plan for the Aquatic Environment. Source: Danish Environmental Protection Agency, EPA.

Table 1.1. Phosphate removal in Europe, 1990. (Source: Henze, 1996a.)

Land (1990)	Connected to sewers, %	No treatment (% of sewered)	**P removal** (% of sewered)
Denmark	98	0	78
Sweden	95	0	90
Norway	77	20	42
Germany	88	4	22
Europe	82	14	13

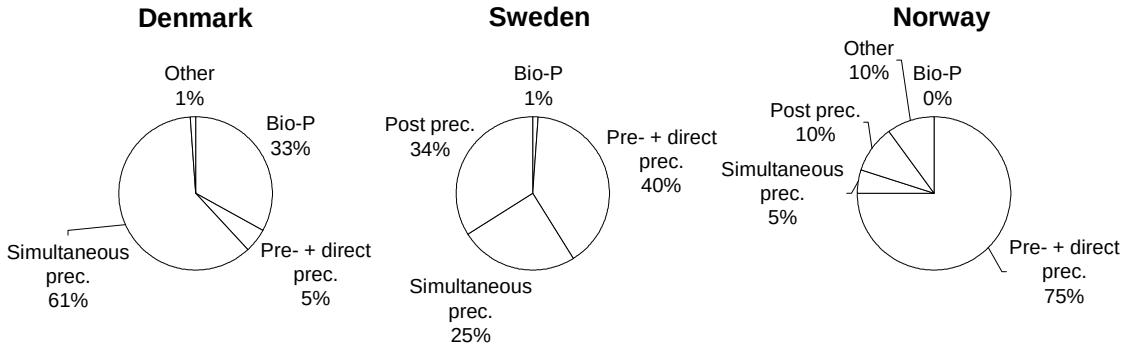

Figure 1.2. Estimated P removal technologies in Scandinavia, 1990 (Henze, 1996a).

Incorporation of bio-P removal in biofilter plants is still at an experimental stage. Research of this alternative is limited, and the author knows no references of full-scale plants. A few pilot plant studies have been reported, e.g. Garzón-Zúñiga and González-Martínez, 1996; Goncalves and Rogalla, 1992ab; Morgenroth, 1998; Muñoz-Colunga and González-Martínez, 1996, and Pastorelli *et al.*, 1999. However, biofilters can have significant advantages. Compared to activated sludge systems biofilters are compact, which can be important when existing facilities in densely urbanised areas have to be upgraded. Biofilter performance is not depending on good sludge settle-ability and ensures very low suspended matter residuals. The problem related to secondary release of phosphate in the final clarifier of the activated sludge systems is not existing, since settling of the excess biomass is a side stream process.

One of the reasons why biofilters are not common for biological phosphorus removal is the complexity of this process combination. When biomass is attached to a fixed carrier material, the alternating conditions of the bio-P process have to be exerted on the reactor tanks in contradiction to activated sludge where the biomass is circulated in the system. For removal of phosphorus from the system, backwash of the filter must take place at a time

where the internal storage of phosphorus in the bacteria is at its highest. Substances that are to be removed by the bacteria have to diffuse into the film. Depending on biofilm thickness and bulk water concentrations this leaves the possibility of creating different zones inside the film. It might e.g. happen that oxygen penetrates only the outer part of the film leaving the inner part anaerobic. In this case there is the possibility of phosphorus release in the anaerobic zone deep in the biofilm at the same time as phosphorus is taken up in the outer part. For these reasons, it appears as if stricter process control might be required for a phosphorus removal biofilter than for an activated sludge plant.

1.2 The Aim of This Study

The current study focuses on the biological removal of phosphorus in a biofilter. Consequences and significance of *diffusion limitation* for successful phosphorus removal with a biofilm was the key issue of the investigation. First, the aim was to experimentally verify that a *zonated* biofilm structure actually is realistic and hence justifies the above-mentioned worries regarding controlling the bio-P process in a biofilter plant. Second, the study aimed at using *nitrate* as the sole electron acceptor for the bio-P process, since this alternative has not yet been thoroughly investigated and the principle is not yet exploited for full-scale operation. However, the simultaneous removal of nitrate and phosphorus is an interesting process due to a frequent lack of sufficient organic matter for complete biological treatment of wastewater. Third, a computer model was used to investigate the *influence of selected process parameters* on the achievable EBPR in the experimentally applied *continuous flow system*.
The scope of the study was directed towards improving the basic understandings of the bio-P process in a biofilm and not towards optimising a system for practical use.

2. State of Knowledge

2.1 Biological Phosphorus Removal – The Metabolism

2.1.1 The Principle of the Process

Phosphate accumulating organisms (PAO's), are able to take up increased amounts of phosphorus compared to the amount required for normal metabolism. The process, so-called enhanced biological phosphate removal (EBPR), occurs if the bacteria are met with conditions alternating between first anaerobic (i.e. no oxygen or nitrate) and then either anoxic (i.e. no oxygen) or aerobic.
During the anaerobic phase, the PAO's take up and store easily degradable organic matter in the form of polyhydroxyalkanoates (PHA), mainly poly-β-hydroxybuturate (PHB) and to a lesser extent polyhydroxyvaleric acid (PHV), while phosphate is released. In the aerobic or anoxic phase they degrade the stored organic matter (if no organic matter is present in the water) while taking up phosphate and storing it as poly-phosphate. The result of a cycle will be a net uptake of phosphate due to the growth of the bacteria.
A third storage compound has in the recent years been acknowledged to be involved in the process. It has been shown to be carbohydrate and is assumed to be glycogen. It is produced during aerobic (or anoxic) conditions from part of the stored PHB and is needed during the anaerobic phase for supplying reducing power and additional energy. Fig. 2.1 schematically illustrates the compound fluxes during the biological phosphate removal process.

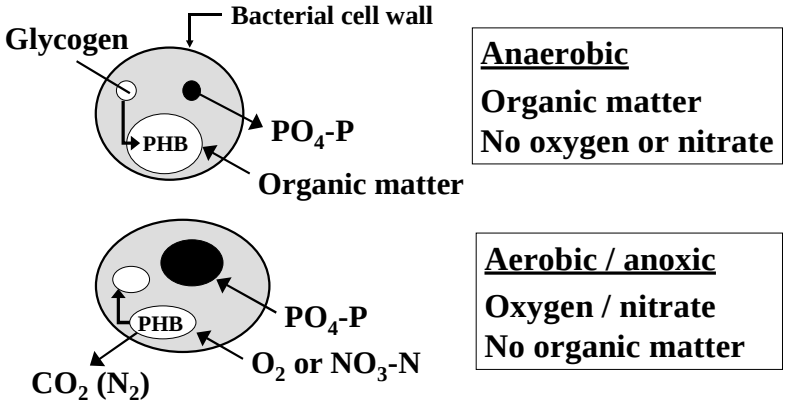

Figure 2.1. Compound fluxes during the biological phosphate removal process.

2.1.2 Metabolic Models

Greenburg *et al.* (1955) were amongst the first to report that phosphate uptake of activated sludge may exceed the basic requirements, if phosphate levels are

more than adequate to maintain satisfactory BOD removal. Srinath *et al.* (1959) observed excessive uptake of phosphate by sludge under aerobic conditions. Levin and Shapiro (1965) demonstrated phosphate uptake and release in activated sludge during aerobic and anaerobic conditions, respectively. Barnard, 1974+1976, summarised guidelines for successful EBPR, such as the need of an initial anaerobic stage without nitrates followed by an aerobic stage. These principles have subsequently been used for the incorporation of the process in many full-scale treatment plants. Since this time, a long list of researchers have investigated the process in order to reveal the metabolism that is used by the phosphate accumulating bacteria, however, full agreement is still not accomplished (Bordacs and Chiesa, 1989; Brdjanovic *et al.*, 1998a; Comeau *et al.*, 1986; Gerber *et al.*, 1986; Marais *et al.*, 1983; Maurer *et al.*, 1997; Mino *et al.*, 1987; Nicholls and Osborn, 1979; Pramanik *et al.*, 1999; Satoh *et al.*, 1992; Smolders *et al.*, 1994abc; Wentzel *et al.*, 1991).
Several historical reviews and evaluations of the model developments can be found in the literature: Filipe and Daigger, 1998; Jenkins and Tandoi, 1991; Kortsee *et al.* 1994; Mino *et al.*, 1998; Seviour and Blackall, 1998; van Loosdrecht *et al.*, 1997a; Wentzel *et al.*, 1991.

The models that form the basis of most discussions are the Comeau/Wentzel (1985/1986), Mino (1987) and the adapted Mino model by Wentzel (1991). They all use acetate as the model carbon source. It is agreed, that poly-phosphate is degraded under anaerobic conditions for supply of energy in the form of ATP. This energy is used for the utilisation of organic acids such as acetate. Readily biodegradable organic matter is in this way removed from the mixed liquor and phosphate generated from poly-P hydrolysis is released from the cells. The stored organic matter is degraded in the subsequent aerobic phase with accompanied synthesis of biomass and polyphosphate. The major difference between the models is the suggested source of reducing power for the anaerobic uptake of organic matter and synthesis of PHA. The Comeau/Wentzel model suggests the reducing power to be supplied from oxidation of acetate through the tricarboxylic acid (TCA) cycle, Fig. 2.2 (top). This theory was strongly doubted by Kortsee *et al.*, 1994, due to improbability of the TCA to function anaerobically. However, several studies have shown the TCA cycle to operate also in anaerobic bacteria (Pereira *et al.*, 1996). The other models suggest intracellular stored carbohydrate (glycogen) to be the source of reducing power as well as an additional energy source. Mino, Fig. 2.2 (bottom), suggested the Embden-Meyerhof-Parnas pathway (EMP) to be the carbohydrate metabolism, whereas Wentzel (adapted Mino) proposed the Entner-Doudoroff pathway (ED).

Comprehensive experimental evidences confirm carbohydrate to be a storage compound in the phosphate removal metabolism (Arun *et al.*, 1989; Bordacs and Chiesa, 1989; Maurer *et al.*, 1997; Mino *et al.*, 1987; Murnleitner *et al.*,

1997; Pramanik *et al.*, 1999; Satoh *et al.*, 1992; Smolders *et al.*, 1994+95), indicating the Mino model to be the most plausible approach. Liu *et al.*, 1994, verified enzymatically that the carbohydrate stored in an EBPR sludge was glycogen and this was also shown by Smolders *et al.*, 1994a, via a glycogen staining technique followed by electron microscopy. However, disagreement still exists regarding the proposed glycogen metabolisms. Pereira *et al.*, 1996, even suggested a combination of the Mino and Comeau/Wentzel model, i.e. supply of reduction equivalents during anaerobic conditions from both glycogen and the TCA cycle. This suggestion was based on experimental data obtained by in vivo ^{13}C-NMR and ^{31}P-NMR techniques for tracking C and P transformations. Also based on ^{13}C-NMR, Maurer *et al.*, 1997, suggested the ED pathway to be the main glycogen metabolism.

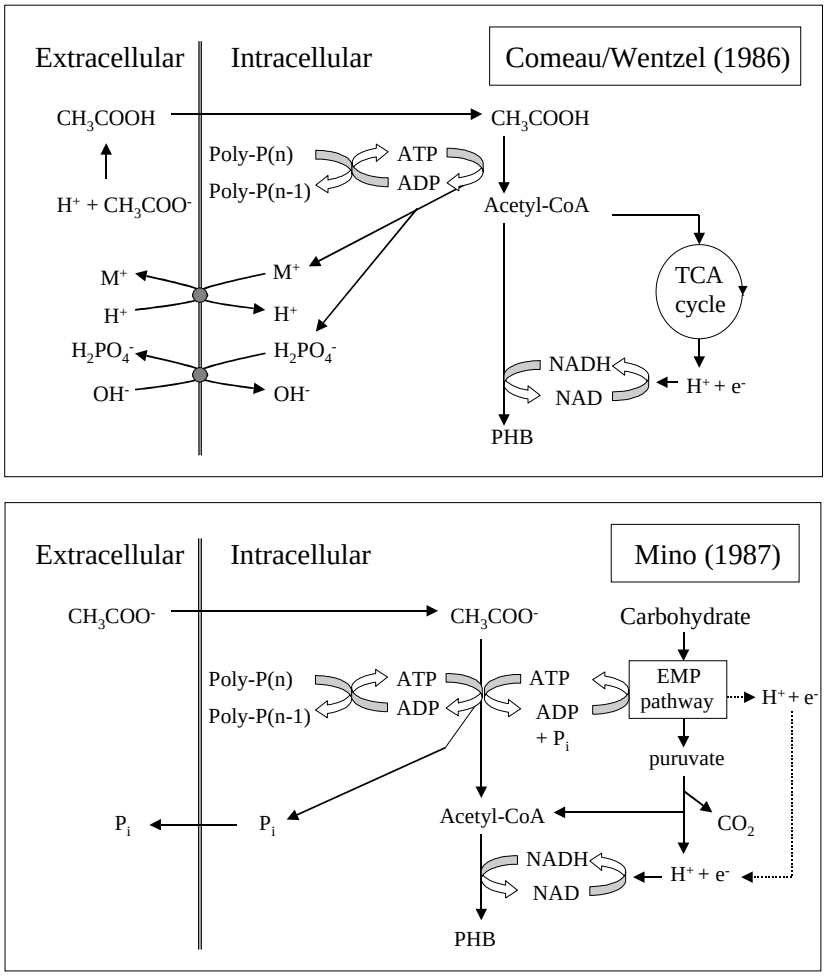

Figure 2.2. The biochemical models proposed by Comeau/Wentzel (top) and Mino (bottom) for the anaerobic behaviour of phosphate accumulating bacteria. The main difference is the supply of reduction equivalents for PHB formation from organic acids, either by the TCA cycle or the Embden-Meyerhof-Parnas pathway. M^+: positively charged cation, PHB: Poly-β-hydroxybuturate, TCA: Tricarboxylic acid cycle, EMP: Embden-Meyerhof-Parnas.

Figure 2.3 illustrates the biochemical model proposed by Comeau/Wentzel for the aerobic behaviour of phosphate accumulating bacteria. The Mino model is similar, but includes carbohydrate formation from part of the PHB. The adapted Mino model additionally outlines a hypothesis for the pathway of carbohydrate regeneration from PHB, which was not addressed in the first Mino model.

All of the above investigations were made with activated sludge (AS) cultures. No EBPR with biofilms have focused on elucidating possible metabolic differences compared to AS.

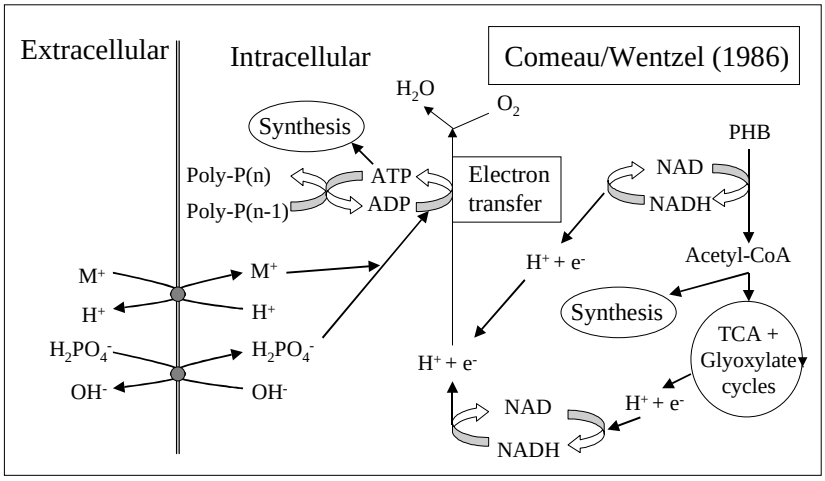

Figure 2.3. The biochemical model proposed by Comeau/Wentzel for the aerobic behaviour of phosphate accumulating bacteria. The Mino model included carbohydrate formation from part of the PHB.

2.1.3 Anaerobic Stoichiometry and The Influence of pH

The suggested models lead to different anaerobic stoichiometric coefficients. Smolders *et al.*, 1994ac, 1995, made a thorough investigation of the stoichiometry of the process. They tested a proposed detailed metabolic model against experimental findings and found close agreement with the suggestion by the Mino models (involvement of carbohydrate/glycogen), Table 2.1. According to the developed model, the stoichiometric ratios of PHB/acetate, glycogen/acetate and CO_2/acetate should be pH independent, whereas a strong dependence on pH should exist for the phosphate released to acetate taken up. The literature cites values of this ratio in the interval 0.15-0.88 mol P/C-mol acetate (Mino *et al.*, 1998). Smolders *et al.* found a linear dependence of this in the tested pH interval of 5.5 to 8.5 with the lowest coefficient: 0.25 P-mol/C-mol for the lowest pH. The ratio increased to 0.75 P-mol/C-mol at pH 8.5. The pH dependency was explained by an increasing electrical potential difference across the cell membrane with increasing pH (assuming that the internal pH and

the overall proton motive force of the cell is kept constant). Consequently more energy is needed for transport of a negatively charged ion, like acetate, against the negative electrical potential of the cell. Fleit, 1995, disagreed with this theory and suggested the transport of un-dissociated short chain fatty acids (SCFA) into the cell by simple diffusion. Filipe and Daigger, 1998, consequently developed a revised metabolic model to explain the anaerobic pH phenomenon based on simple diffusion as the transport mechanism.
Liu *et al.*, 1996a, confirmed a linearly increasing phosphate/acetate ratio in the pH interval 6.4-8.4, but obtained a constant value in the interval 5.5-6.4 and a greatly increasing value below pH 5.5. Additionally they found that acetate uptake significantly decreased for pH below 6.0 as oppose to Smolders *et al.*, 1994a, that found a constant acetate uptake rate.
Satoh *et al.*, 1992, and Christensson *et al.*, 1998, found coefficients that also were in good agreement with the Mino model (included in Table 2.1).

Table 2.1. Theoretical conversion ratios for the models with the TCA cycle and glycogen as source of reduction equivalents and measured ratios of the anaerobic metabolism. The moles are based on C-mol for the organic compounds (see text).

(Mol/Mol)	Theoretical			Experimental findings	
Ratio	TCA	Glycogen□	Satoh *et al.*,1992	Smolders *et al.*,1994a	Christensson *et al.*,1998
CO_2/HAc	0.11	0.17	-	0.17-0.22	-
Glycogen/HAc	-	0.50	0.60	-	0.70
PHB/HAc	0.89	1.33	1.30	1.2-1.3	1.30
PO_4/HAc	$0.5+\alpha1^{*}$	$0.25+\alpha1^{*}$	0.43◆	0.26-0.75	-
PO_4/HAc, pH 7	0.75**	0.50**	-	0.48	0.50

□ The only difference between the Mino and adapted Mino model is that the PO_4/Hac ratio for the adapted model is (0.33+α1) (Filipe and Daigger, 1998).
* α1 varies from 0-0.5 depending on pH, increases with pH.
** Assuming linear increase of α1 from 0 to 0.5 in the pH interval 5.5–8.5 (α1 = 0.25 for pH 7).
◆ pH varied in the experiments in the interval 7.0-8.5.

The literature often reports stoichiometric coefficients based on gram or COD. For conversion to C-mol (used by e.g. Smolders *et al.*), the following compositions are assumed:

Acetate:	$C_2H_4O_2$	Mv = 60 g/mol,	COD: 1.07 gCOD/g
PHB:	$C_4H_6O_2$	Mv = 86 g/mol,	COD: 1.67 gCOD/g
Glycogen:	$C_6H_{10}O_5$	Mv = 162 g/mol,	COD: 1.19 gCOD/g

Hence: 1 C-mol = 0.5 mol acetate
1 C-mol = 0.25 mol PHB
1 C-mol = 0.17 mol glycogen

2.1.4 Co-transport of Cations

Concurrent phosphate and metal release or uptake has been observed in several investigations, Table 2.2. It appears that the metallic cations K^+, Mg^{2+} and Ca^{2+} are co-transported with phosphate molecules in a total molar ionic charge ratio of 1.0 (Comeau *et al.*, 1986). The cations are speculated to stabilise the negatively charged polyP chains by acting as counter-ions (Wentzel *et al.*, 1989) and investigations of electron-dense granules in sludge cells and *Acinetobacter* spp. with electron microscopy energy dispersive X-ray analysis indicate this postulate to be correct (Bonting *et al.*, 1993; Buchan, 1983; Heymann *et al.*, 1989; Sicko-Goad *et al.*, 1975). The typically observed molar ratios are 0.3 (K/P), 0.26 (Mg/P) and 0.05 (Ca/P). Na^+ was by Fukase *et al.*, 1982, shown to also be involved.
Lindrea *et al.*, 1994, found correlation between lowered influent Mg^{2+} concentrations and deterioration of the EBPR process in a full- and lab-scale system. Brdjanovic *et al.*, 1996, observed serious deterioration of the phosphate removal process in a lab-scale SBR during shortage of K^+ in the influent.

Table 2.2. Molar ratios of cations co-transported with phosphorus (modified from Comeau *et al*, 1986, and Wentzel *et al.*, 1989).

	(Mol Metal ion / Mol P)				
	Mg^{2+}	K^+	Ca^{2+}	Na^+	Charge Balance
Arvin and Kristensen, 1985	0.32	0.23	-	-	0.87
Comeau *et al.*, 1985	0.24	0.34	0.06	-	0.94
Fukase *et al.*, 1982	0.28	0.31	0.05	0.12	1.09
Jardin and Pöpel, 1994	0.30	0.26	-	-	0.86
Miyamoto-Mills *et al.*, 1983	0.26	0.27	-	-	0.79
Wentzel *et al.*, 1989	0.26	0.30	0.05	0	0.92

2.1.5 Denitrifying PAOs

Not all PAO's are able to denitrify. Barker and Dold, 1996, presented a review of the denitrification ability of PAOs. No consensus exists as to whether two different types of PAO bacteria exist or if only different levels of denitrifying enzyme-production is induced in different PAO-populations (Wachtmeister *et al.*, 1997). Most research, however, support the theory of different populations (Bortone *et al.*, 1996; Kerrn-Jespersen and Henze, 1993; Kuba *et al.*, 1997a;

Meinhold *et al.*, 1999), and it is today generally accepted to divide PAOs into 3 different categories (Barker and Dold, 1996; Lötter, 1985; Wentzel *et al.*, 1986):

1) Unable to utilise oxidised nitrogen (nitrate or nitrite) as electron acceptor
2) Able to reduce nitrate to nitrite only
3) Able to reduce nitrate to free dinitrogen gas

Lötter *et al.*, 1986, reported 32-43% of *Acinetobacter* spp. strains to be capable of reducing nitrate to nitrite whereas only 6-12 % are capable of full denitrification to nitrogen gas.
Kuba *et al.*, 1997a, stated that the occurrence of denitrifying bio-P bacteria in full-scale treatment plants to a great extent is depending on plant design and control procedures. They investigated 2 treatment plants and found respectively 10-30 % and 30-50% of the bacteria population in the sludge carrying the denitrifying capability. ~50% was also reported in investigations by Kuba *et al.*, 1997b, Meinhold *et al.*, 1999 and Wachtmeister *et al.*, 1997. Filipe and Daigger, 1999, used computer modelling to verify the strong dependence of plant design (anoxic/aerobic zone) on the competition between the different groups of PAOs. They concluded that introduction of even a relatively small aerobic zone in EBPR systems has an adverse affect on the accumulation of denitrifying PAOs.
Murnleitner *et al.*, 1997, developed an integrated metabolic model for the aerobic and denitrifying biological phosphorus removal.
Brdjanovic *et al.*, 1999, Meinhold *et al.*, 1999, and Wachtmeister *et al.*, 1997, suggested several methods for quantifying the relative fraction of denitrifying PAOs compared to the total PAO population in activated sludge.

The current study is working with alternation between first anaerobic and then anoxic conditions. No aerobic phase is included. In this way it is expected to obtain an enriched denitrifying population of PAO's. Vlekke *et al.*, 1988, showed the feasibility of biological phosphate removal with nitrate as the only electron acceptor. This has subsequently been confirmed in several investigations (Bortone *et al.*, 1994; Kerrn-Jespersen and Henze, 1993; Kuba *et al.*, 1993; Sieker, 1999). The advantage of using anoxic conditions instead of aerobic is that the organic substrate is used for simultaneous removal of nitrate and phosphate, whereby both energy requirements (aeration) and sludge production are decreased (Kuba *et al.*, 1996a; Wanner *et al.*, 1992). Also, the available organic matter content of wastewater is often a limiting factor for complete N and P removal leading to a frequent need of external addition to the process. In practise an aerobic phase is needed in order to obtain nitrification. This is optimally done in a two-sludge system separating the nitrifying sludge from the mainstream process (Filipe and Daigger, 1999; Kuba *et al.*, 1996b) in order to overcome the competitive disadvantage of the denitrifying PAOs compared to non-denitrifying PAOs during circulation through aerobic conditions.

2.1.6 Aerobic and Anoxic Stoichiometry

Less attention has been directed at elucidating the details of the aerobic phosphate metabolism (Smolders, 1995). This is peculiar since phosphate is actually taken up in the aerobic phase, whereby the aerobic uptake capacity is determining the excess phosphate removal capacity. The energy requiring processes during the aerobic/anoxic conditions are:

1) Growth (biomass production) and maintenance
2) Uptake of phosphate and synthesis into polyphosphate
3) Formation of glycogen

Smolders *et al.*, 1994b, developed a metabolic model of the aerobic metabolism and supported this by experimental investigations. This was a continuation of the work initiated by Wentzel *et al.*, 1989, who developed a conceptual model based on experimental data, but without PHB, glycogen or biomass measurements. Smolders *et al.*, 1994b, found that the overall energy requirement for the P-metabolism is substantial: 25% of the acetate consumed during anaerobic conditions and 60% of the oxygen consumption is used for the synthesis of polyphosphate and glycogen. This was explained to be the reason for a relatively low yield coefficient of PAOs compared to strictly aerobic heterotrophs (13% lower), however due to the storage of polyP, the total sludge production is comparable or even higher than a conventional aerobic treatment process. They found that the oxygen consumption for cell growth and glycogen production was not significantly influenced by the phosphate uptake. Smolders *et al.*, 1994b, did not address the effect of internal PHB pools on the phosphate uptake process. This is a subject that subsequently has been discussed by several researchers (Brdjanovic *et al.*, 1998b; Meinhold *et al.*, 1998; Petersen *et al.*, 1998; Temmink *et al.*, 1996). The conclusion is that it is essential to maintain a base level of internal PHB storage pools to obtain good phosphate uptake, since the uptake rate is directly related to the amount of PHB. Control strategies to avoid wasting of internal PHB by excessive aeration in full-scale plants are important.

Kuba *et al.*, 1993, investigated and compared process rates and stoichiometry of aerobic (A/O) respectively anoxic (A_2) phosphate removal in sequencing batch reactors (SBR), Table 2.3. They found good phosphate removal with comparable capacity of the two systems and concluded anoxic phosphate removal to be of considerable potential. The A_2 system showed a lower sludge production (due to a ~25% lower biomass yield) and better sludge settle-ability. Kerrn-Jespersen *et al.*, 1994, found for an A_2 fixed-film reactor stoichiometric coefficients in agreement with Kuba *et al.*: 0.52 gP/gAC for phosphate release and 2.0 gP/gN for P uptake (1.3 gP/gN when nitrite accumulated). Sieker, 1999, found for another A_2 biofilm system lower coefficients: 0.15-0.25 gP/gAc and

0.6-1.0 gP/gN for the anaerobic and anoxic phase, respectively. The by Sieker reported process rates were also lower, 4.5-6.5 mgP/(gTS h) for phosphate release and 5-7 mgN/(gTS h) for nitrate utilization.
The reported nitrate utilization rates for sludge taken from EBPR plants and tested under anoxic conditions are significantly lower (factor ~10) than the values found by Kuba *et al.*, 1993 (Kerrn-Jespersen and Henze, 1993; Meinhold *et al.*, 1999; Kuba *et al.*, 1997a). This is due to the mixed cultures in the sludge used in these tests – no culture enrichment of denitrifying PAOs.

Table 2.3. Investigation of the use of oxygen (A/O) or nitrate (A_2) as the only electron acceptor in the phosphate removal process. Kuba *et al.*, 1993.

Phase			A_2 SBR	A/O SBR
Anaerob	Released-P/consumed-HAc	(gP/gC)	1.0-1.5	1.1-1.3
		(mol P/mol C)	0.39-0.58	0.43-0.50
		(gP/gAc)	0.41-0.61	0.45-0.53
	P release rate	(mgP/l/h)	90-130	110-190
		(mgP/gSS/h)	20-30	30-50
	HAc consumption rate	(gCOD/l/h)	0.20-0.31	0.27-0.37
		(gCOD/gSS/h)	0.05-0.06	0.06-0.09
Anox/Aerob	P uptake/NO_3-N utilized	(gP/gN)	2.10	
		(mol P/mol e-)	0.19	
	P uptake/O_2 utilized	(gP/gO_2)		0.91
		(mol P/mol e-)		0.23
	NO_3-N utilization rate	(mgN/l/h)	41-56	
		(mgN/gSS/h)	11-14	
	O_2 utilization rate	(mgO_2/l/h)		20-100
		(mgO_2/gSS/h)		10-30
Overall	Growth yield	(gSS/gCOD)	0.25-0.30	0.35-0.40
	VSS/SS	(gVSS/gSS)	0.65-0.70	0.65-0.70
	P content (calculated)	(mgP/gSS)	100-170	90-110
	Maximum releasable P	(mgP/gSS)	50-60	60-70
	SVI	(ml/gSS)	50	100

The typical phosphorus content of non-EBPR wastewater sludge is in the range 1-2 % of the biomass dry weight (Appeldorn *et al.*, 1992; Henze *et al.*, 1997; Scheer, 1995; Seviour and Blackall, 1998; Smolders *et al.*, 1996; Surampalli *et al.*, 1997). This phosphorus is incorporated in the cell composition and can only be released by decay. The phosphorus contents of EBPR sludge from treatment plants varies in the interval 4-7 % and for enriched PAO sludges up to ~16 % can be obtained, depending on the experimental conditions, Table 2.4a + 2.4b (activated sludge + biofilm systems). The reactor scales in Table 2.4ab are

categorised into: lab (< ~5L), bench (~5-50 L), pilot (50-5000 L) and full-scale (> 5000 L) (Janning, 1998). Wentzel *et al.*, 1989, reported a phosphorus content of 38 % for an enriched culture, but this very high value has not been reproduced in other investigations.

Table 2.4a. Reported phosphorus contents of EBPR activated sludge.

Reference	Reactor (Scale, Type)	C-source	% P
Abugararah *et al.*, 1991	Pilot, UCT	Domestic wastewater	4.3
		Isobutyric acid	7.0
		Acetate	9.8
Appeldorn *et al.*, 1992	Full, *non*-EBPR	Domestic wastewater	1.7-1.9
	Full/pilot, EBPR	Domestic wastewater	2.5-3.5
	Lab, SBR	Acetate/glucose (9:1)	11
Arun *et al.*, 1989	Bench, SBR	Acetate/peptone/yeast/ lactic acid/glutamic acid	3.9-6.5
Belia and Smith, 1997	Bench, SBR	Acetate	8, 16*
Christensson *et al.*, 1998	Lab, Continuous	Acetate	14
Converti *et al.*, 1995	Bench, Alternating	Acetate/propionate/glucose/ peptone	10*
Kawaharasaki *et al.*, 1999	Lab, SBR	Acetate/peptone	6
Kim and Chuang, 1996	Bench, SBR	Glucose	5.8
Kuba *et al.*, 1993	Lab, SBR	Acetate	9-11
		Acetate	10-17**
Larose *et al.*, 1997	Bench, SBR	Acetate	5-15
Lee *et al.*, 1997	Bench, Continuous	Presettled wastewater	4.5-6.1
Lie *et al.*, 1997	Full, Continuous	Municipal wastewater	6.2
Liu *et al.*, 1996a	Lab, SBR	Acetate/peptone	8-12
Malnou *et al.*, 1984	Pilot, Continuous	Domestic sewage/meat extract /milk powder/peptone	5.5-7
Mamais and Jenkins, 1992	Bench, Continuous	Presettled wastewater	6.9
Mino *et al.*, 1987	Lab, Continuous	Acetate/propionate/yeast/ glucose/peptone	3.2-6.4
Randall *et al.*, 1997	Lab, SBR	Glucose	6
	Lab, SBR	Starch	3.7
Satoh *et al.*, 1992	Lab, Continuous	Acetate/propionate/lactate	6.1-7.1
Vlekke *et al.*, 1988	Lab, SBR	Domestic wastewater	3**-3.5
Wentzel *et al.*, 1989	Bench, Continuous	Acetate	38

* Bioaugmented with *Acinetobacter* spp.

** Nitrate used as sole electron acceptor

Table 2.4b. Reported phosphorus contents of sludge from biofilm EBPR systems.

Reference	Reactor (Scale, Type)	C-source	% P
Castillo *et al.*, 1999a	Lab, SBR, Membrane	Acetate	4.2-5.2
Goncalves *et al.*, 1994a	Pilot, Continuous, Floating Bed	Presettled wastewater	2.9-4.1
González-Martínez and Wilderer, 1991	Lab, SBR, Fixed bed	Acetate/peptone/glucose	4.5-6.1*
Kerrn-Jespersen *et al.*, 1994	Lab, Alternating, Fixed bed	Acetate	8-10◆
Morgenroth, 1998	Bench, SBR, Fixed bed	Acetate	6.5 (2-14)*
Pastorelli *et al.*, 1999	Pilot, SBR, Floating bed	Presettled wastewater/acetate	7.5-9
Rovatti *et al.*, 1995	Bench, SBR, Fixed bed	Glucose	4.3**
Sieker, 1999	Bench, SBR, Fixed bed	Presettled wastewater	3.5-4.5*◆

* Biofilm characterised as "thin, ** Biofilm thickness calculated to 24-32 μm
◆ Nitrate used as the electron acceptor

2.1.7 Process Kinetics

2.1.7.1 Monod type kinetics

The kinetics of growth, uptake and release processes are typically approximated by Monod type expressions, refer to e.g. the Activated Sludge Model (ASM) 2D (Henze *et al.*, 1999) that also presents a default list of kinetic and stoichiometric constants. Some of these are estimated on the basis of very scarce experimental findings, due to the present lack of knowledge on PAO kinetics. Establishment of kinetic constants etc. for PAOs is complicated by the fact, that no pure cultures have been isolated yet (chapter 2.2). An example of the kinetic expression for anoxic phosphate uptake is shown below (ASM2D). Switching functions are included, e.g. in order to take into account that: the bacteria can include a limited amount of phosphate relative to its own mass, phosphate uptake does not take place when acetate is present in the bulk water, and phosphate uptake can only take place when an electron acceptor is available and the bacteria has internally stored PHA available.

$$r_{PP} = q_{PP} \cdot \eta_{NO3} \cdot \frac{K_A}{K_A + S_A} \cdot \frac{S_{NO3}}{K_{NO3} + S_{NO3}} \cdot \frac{S_{PO4}}{K_{PS} + S_{PO4}} \cdot \frac{\frac{X_{PHA}}{X_{PAO}}}{K_{PHA} + \frac{X_{PHA}}{X_{PAO}}} \cdot \frac{K_{MAX} - \frac{X_{PP}}{X_{PAO}}}{K_{IPP} + K_{MAX} - \frac{X_{PP}}{X_{PAO}}} \cdot X_{PAO}$$

2.1.7.2 Growth rate

PAOs are in all presented models assumed to grow only during conditions with the presence of an electron acceptor, and the growth rate of PAOs is considered to be significantly lower than the growth rate of traditional aerobic heterotrophs. Morgenroth, 1998, used in modelling maximum specific growth rates of 1 d^{-1}, respectively, 6 d^{-1} based on ASM2 (Henze *et al.*, 1995). ASM2D list typical

maximum growth rates in the temperature interval 10-20 ^{o}C: aerobic heterotrophs 3-6 d^{-1}, denitrifying heterotrophs 2-5 d^{-1}, PAOs 0.7-1 d^{-1} and nitrifiers 0.3-1 d^{-1} (Henze *et al.*, 1999). Jenkins and Tandoi, 1991, reported maximum growth rates of *Acinetobacter calcoaceticus lwoffi* grown under either anaerobic/aerobic alternating or pure aerobic conditions of 0.84 d^{-1} and 4.8 d^{-1}, respectively. Wentzel *et al.*, 1987, observed a similar low growth rate of enhanced PAO cultures: 0.75-0.95 d^{-1}. Ubukata and Takii, 1994, found a growth rate of 1.43 d^{-1} of an isolate of PAOs tested under aerobic conditions. The survival of PAOs in treatment plants is based on the competitive advantage over traditional heterotrophs obtained by their anaerobic substrate storage capacity. The strong competitive advantage of bacteria with the capacity of storing substrates during famine-feast conditions in e.g. wastewater treatment plants was discussed by van Loosdrecht and Heijnen, 1997. PAOs additionally have been shown to have significantly lower decay rate (Wentzel *et al.*, 1989: 0.04 d^{-1}; Smolders *et al.*, 1994b: 0.06 d^{-1}) than aerobic heterotrophs (Marais and Ekama, 1976: 0.24 d^{-1}).

2.1.7.3 Impact of sludge retention time (SRT)

A consequence of the relative low growth rate has been addressed in several studies of the minimum sludge retention time (SRT) required for EBPR. Mamais and Jenkins, 1992, found washout of PAOs for SRT < 2.9 d at 14^{o}C. McClintock *et al.*, 1993 found washout of PAOs for SRT < 5 d at 10^{o}C. According to Henze *et al.*, 1997, washout of nitrifiers at this temperature can be expected already at aerobic SRT < 10 d, hence for single-sludge systems, nitrification is more sensitive to the sludge age than the phosphate removal process in agreement with observations of McClintock *et al.* Scheer and Seyfried, 1996, claimed optimal SRT for EBPR would be the smallest possible sludge age allowing for successful nitrification and denitrification. This was in agreement with Henze *et al.*, 1997; and Rodrigo *et al.*, 1996, who used modelling to support experimental findings of an optimal SRT of about 10 d at 20 ^{o}C. They explained the disadvantage of long SRTs by increased P release by decay of PAOs and a decrease in the relative fraction of PAOs in the mixed culture for longer SRTs. This explanation appears peculiar when considering the literature cited above, where PAOs are characterised by very low decay rates whereby one would expect a competitive advantage for longer sludge ages.

2.1.8 Environmental Factors

Environmental factors of general importance for biological processes are also influencing the biological phosphate removal process:

- Temperature
- Toxic substances
- Substrate concentration
- Substrate type

The responses are largely corresponding to denitrifying and aerobic heterotrophs (Henze *et al.*, 1997). Additional factors are of special importance for the EBPR process (Malnou *et al.*, 1984; Scheer and Seyfried, 1996):

- pH (discussed above)
- Type of organic substrate, especially the fraction of SCFAs
- COD/N/P ratio of the wastewater
- Anaerobic/anoxic/aerobic phase lengths
- Recirculation of nitrate/oxygen into the anaerobic reactor

2.1.8.1 Temperature

The effect of temperature on EBPR was studied in several investigations. Baetens *et al.*, 1999, and Kumar *et al.*, 1996, present reviews. For the effect on overall EBPR efficiency, very contrasting observations are noted. The at first most logical observation of higher efficiancy at elevated temperatures (20-37^{o}C) as generally observed for biological processes was verified by some investigations (Converti *et al.*, 1995; Jones and Stephenson, 1996; McClintock *et al.*, 1993; Scheer, 1995) whereas the opposite finding of improved efficiency by lower temperatures (5-15^{o}C) was reported by other authors (Barnard *et al.*, 1985). Helmer and Kunst, 1997, found no significant effect on the efficiency when reducing the temperature stepwise from 15 to 5^{o}C.

The temperature effects on the kinetics of EBPR have been more consistent, with increasing P release and uptake rates in the temperature range, 5-30^{o}C (Boughton *et al.*, 1971; Mamais and Jenkins, 1992; Romanski *et al.*, 1997; Shapiro *et al.*, 1965). Maximum aerobic P uptake was found between 15 and 20^{o}C by Baetens *et al.*, 1999, whereas Brdjanovic *et al.*, 1997, found the anaerobic P release rate to peak at this temperature. The stoichiometry of the anaerobic process was in both of these investigations showed to be relative insensitive of temperature, whereas some effect on the aerobic stoichiometry was shown by Brdjanovic *et al.*, 1997.

Suggestions of the inconsistency of the observed temperature effects in the literature were given by Baetens *et al.*, 1999. First, it should be realised that acclimation to temperature changes is a slow process and sufficient acclimation periods might not have been applied in all studies whereby a mixture of short and long term effects are reported. Second, long term effects might influence the biomass population of the system. This is of special importance in systems where nitrification and denitrification are included since lower temperatures are critical for nitrifiers. In case of washout of the nitrifiers and hence also decreased denitrification activity, an enrichment of PAOs take place, which might be the explanation of improved EBPR by reduced temperatures found in some investigations. However, in case the lower temperatures due to slower PAO kinetics lead to leakage of organic substrate into the aerobic stage of the process, an increase in the relative proportion of non-PAO-heterotrophs is the result. Third, low temperatures decrease the hydrolysis and fermentation rates in the anaerobic stage, which might affect EBPR. If a relative low fraction of

easily degradable COD is present in the influent water, lower fermentation lead to less easily degradable substrate available for the PAOs. Hence, also the wastewater composition might influence the observed temperature effect.
Based on the above, it is concluded that prediction of temperature effects on a full-scale treatment plant is far from straight-forward and has to be evaluated in each individual case based on the above discussion.

2.1.8.2 Type of organic substrate

Developed metabolic models have used acetate as the model substrate for EBPR, and the vast majority of EBPR investigations have used acetate as the organic substrate. However, at an early stage it was realised that several simple carbon compounds could trigger the phosphate release process and this has been verified in numerous investigations (Abu-ghararah and Randall, 1991; Arun *et al.*, 1989; Comeau *et al.*, 1986; Fuhs and Chen, 1975; Gerber *et al.*, 1986; Satoh *et al.*, 1992, 1996). However, it is generally accepted that short chain fatty acids (SCFA) are the most favourable substrates for EBPR. This fact is supported by a consistent observation of improved EBPR upon inclusion of an additional fermentation step in the process (e.g. high rate anaerobic digestion of primary settled sludge) with recycling of the fermentation products into the anaerobic reactor (Danesh and Oleszkiewicz, 1997; Goncalves *et al.*, 1994b; Lötter and Pitman, 1992; Oldham, 1985; Randall *et al.*, 1994).

2.1.8.3 COD/N/P ratio

The COD/N/P ratio is another important factor for the success of EBPR. The theoretical need for removal of phosphate is around 4 g COD(acetate)/g P, but due to consumption of fermentation products by non-PAOs, the practical ratio is around 10 g COD/g P (Henze, 1996a). For removal of nitrate by denitrification a COD/N ratio of around 4-6 g COD/gN is necessary in practise (Henze *et al.*, 1997) and this ratio might be higher in case of significant aerobic COD consumption, e.g. in alternating plants (Henze *et al.*, 1994). For combined nitrogen and phosphorus removal, the competition for organic substrate increases the overall need for organic substrate significantly. Henze, 1996b, infer the need for additional chemical phosphate removal for COD/P ratios below 40-50 by simultaneous N and P removal. In this aspect, it is favourable to exploit the ability of anoxic P uptake. Kuba *et al.*, 1996a, found that the need of COD in a two-sludge system with anoxic phosphate removal could be reduced up to 50 % compared to traditional systems with aerobic P uptake. They found for an inlet concentration of phosphate of 15 mg P/l that a COD/N/P ratio of 27:7:1 could support complete treatment.

2.1.8.4 Anaerobic/anoxic/aerobic phase lengths

Relatively few investigations of the effect of different anaerobic, anoxic and aerobic phase lengths are found in the literature (Castillo *et al.*, 1999a; Fukase *et al.*, 1985; González-Martinez and Wilderer; Malnou *et al.*, 1984), and no

theoretically based design criteria exist. Most design is based on empirical guidelines. The optimal combination of the different phases is a balance between the different organisms (PAOs, denitrifiers, aerobic heterotrophs and nitrifiers) and will naturally depend on removal objectives and wastewater composition. An overview of some phase length combinations found in the literature is given in Table 2.5 (compare with Table 2.4).

Table 2.5. Phase length combinations as observed in the literature.

Reference	**Anaerobic [h]**	**Anoxic [h]**	**Aerobic [h]**	**Settling [h]**	**Anaerobic (Anox+Aerob)**
Activated sludge systems					
Abugararah *et al.*, 1991	2.1	0.7	3.2	-	0.54
Appeldorn *et al.*, 1992	1.25	0	2.75	2	0.45
Arun *et al.*, 1989	0.83	0	1.33	0.75	0.62
Belia and Smith, 1997	2	0	5	4	0.4
Christensson *et al.*, 1998	1.7	0	3.7	-	0.46
Kawaharasaki *et al.*, 1999	1	0	1.5	0.5	0.67
Kim and Chuang, 1996	2.8	0	3.2	2	0.88
Kuba *et al.*, 1993	2.5	3	0	0.5	0.83
Larose *et al.*, 1997	3	0.5	3.5	1	0.75
Liu *et al.*, 1996a	0.83	0	1.33	0.83	0.62
Malnou *et al.*, 1984	1.6	0.6	0.9	-	1.07
Mamais and Jenkins, 1992	1.45	0	4.6	1.7	0.32
Mino *et al.*, 1987	1.06	0	2.88	-	0.37
Randall *et al.*, 1997	2	0	4	2	0.5
Satoh *et al.*, 1992	2	0	4.8	-	0.42
Vlekke *et al.*, 1988	3	4	0	1	0.75
Average	**1.8 ±0.7**	**-**	**3.2 ±1.3***	**-**	**0.6 ±0.2**
Biofilm systems					
Castillo *et al.*, 1999	1.5-3	0	4.5-9	-	0.25
Goncalves *et al.*, 1994a	1.75	0	9.6	-	0.18
Kerrn-Jespersen *et al.*, 1994	2	4	0	-	0.50
Morgenroth, 1998	2	0	5.5	-	0.36
Pastorelli *et al.*, 1999	1.6	0	4.4	-	0.36
Sieker, 1999	1	3	0	-	0.33
Average	**1.7 ±0.4**	**-**	**6.5 ±3.7***	**-**	**0.3 ±0.1**

* Investigations with anoxic P uptake excluded

An average of 1.8 ± 0.7 hours anaerobic and 3.2 ± 1.3 hours aerobic phase lengths, i.e. a ratio of 0.6 ± 0.3 for the phosphate release versus uptake phases, is found for 16 investigations of bio-P removal with activated sludge. Pitman,

1991, recommends for full-scale treatment plants with simultaneous N and P removal an un-aerated fraction of maximum 0.45.
The obtained phosphorus content of the sludge (Table 2.4) is in Fig. 2.4 plotted against the release/uptake phase length ratio. No correlation is seen for activated sludge systems in the tested ratio interval from 0.32-1.07. This is, however, not surprising due to the very different operation systems and wastewater compositions in the investigations. In comparison, investigations with biofilm systems are very scarce and difficult to assign average values, but a linear trend appeared when plotting the data (the dotted line). An explanation why biofilm systems exhibit a linear relationship is lacking, and due to the limited available data set, further investigation is required to confirm the apparent trend.

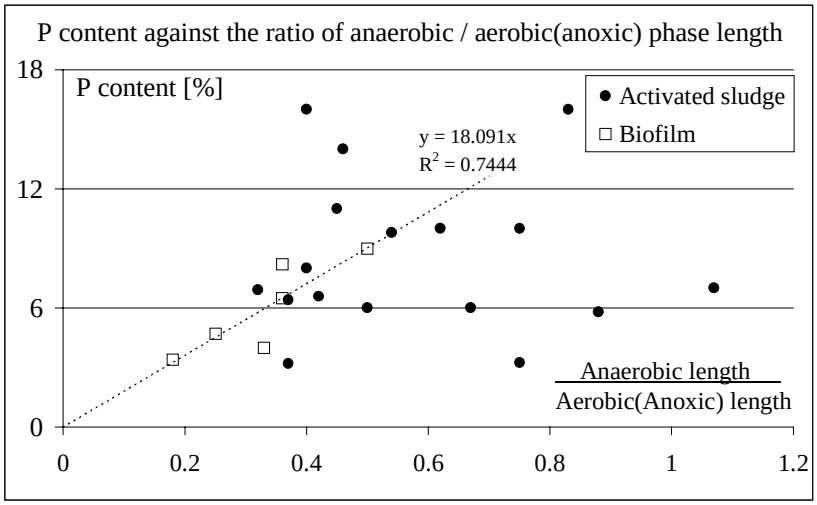

Figure 2.4. The phosphorus content of sludge as a function of the relative ratio of the P release versus P uptake phase lengths. No correlation is found. The systems were operated with different systems and wastewater and hence are not directly comparable. Data from Table 2.5.

Henze *et al.*, 1997, suggested a minimum of 1 hour (10°C) anaerobic phase length and inferred improved bio-P up to 3 hours. Scheer and Seyfried, 1996, reported for the German speaking regions of Europe that more than 60% of the wastewater treatment plants (WWTP) with EBPR operate with an anaerobic contact time of less than 2, and in 30% less than 1 hour. By modelling they concluded, that longer contact time could only partially be recommended.
Results of the investigations of the effect of the relative ratio of the phase lengths have not been consistent. González-Martinez and Wilderer, 1991, tested cycle lengths of 6, 8 and 12 h with the anaerobic phase making up 25, 43 and 63 % of the cycle. They did not find conclusive results, but a tendency of better P removal for the highest relative ratio of the anaerobic phase. Muñoz-Colunga and González-Martinez, 1996, tested 8 and 12 h cycles with different anaerobic ratios and found a similar inconclusive result, but with a tendency of better

removal for lower ratios. Castillo *et al.*, 1999a, also tested total cycle durations of 6, 8 and 12 h but with a fixed anaerobic phase ratio of 25%. They observed best P removal for the longest cycle length, i.e. the lowest anaerobic phase ratio.

2.1.8.5 Recirculation of nitrate/oxygen into the anaerobic reactor

If excessive nitrate or oxygen is recirculated to the anaerobic reactor, fermentation is inhibited and facultative non-PAO bacteria will consume part of the easily degradable organic matter. Hence, consistent recirculation of significant amounts of electron acceptor to the anaerobic tank is detrimental for the capacity of EBPR (less internal COD available for P uptake) and for the PAO population (loss of their competitive advantage based on anaerobic storing of COD). This fact was generally accepted relatively early in the EBPR development (Arvin, 1985; Barnard, 1976; Fukase *et al.*, 1985; Hascoet *et al.*, 1985; Malnou *et al.*, 1984; Osborn and Nicholls, 1978; Simpkins and McLaren, 1978).

2.1.9 Simultaneous Presence of COD and Electron Acceptor

In many EBPR systems transient periods of simultaneous presence of nitrate and COD occur (chapter 2.5). The question is in this regard: How do PAOs react to such a situation?

Comeau *et al.*, 1986, hypothesised uptake of phosphate during the aerobic zone with either internal or external organic matter. Wentzel *et al.*, 1986, proposed storage of both phosphorus and PHB under anoxic conditions with external organic matter available. Gerber *et al*., 1986, observed release of phosphate during the presence of nitrate and several, but not all, organic substrates tested. Acetate, formate and propionate caused phosphate release, whereas organic compounds such as citrate, succinate, glucose, ethanol and methanol did not induce release in the presence of nitrate. Gerber *et al*., 1986, hypothesised the difference to be because, anaerobiosis was needed in order to convert these substrates into products which trigger the release, i.e. anaerobic conditions were not considered to bring about the release by itself but via the role as a fermentation zone where acidogenic bacteria transform organic matter into volatine fatty acids. Hascoet *et al.*, 1985, observed release of phosphate during simultaneous presence of COD and nitrate, however the release was significantly reduced compared to true anaerobic conditions. Kuba *et al.*, 1994, suggested based on experimental observations, that the bacteria both store acetate (80%) and simultaneously degrade it (20%) directly. The P release rate will be reduced compared to strict anaerobic conditions, because the bacteria oxidise part of the acetate directly via nitrate and use part of this energy for PHB production - quote: ”PHB (Poly-β-hydroxybutyrate) was always produced and phosphorus was released by DPB (denitrifying, phosphorus removing bacteria) sludge when nitrate and HAc were simultaneously present. The

reducing power ($NADH_2$) and the energy (ATP) for this process seemed to be obtained from HAc oxidation by nitrate as well as from polyphosphate degradation."
Barker and Dold, 1996, concluded from a literature review of experimental studies: "P uptake/PHB oxidation appear to occur simultaneously with P release/PHB storage when SCFAs are available under anoxic conditions". This statement was based on studies with mixed bio-P-cultures whereby different bacteria groups might do the different processes and only the net effect is observed in the water phase. Wachtmeister *et al.*, 1997, made experiments with enhanced denitrifying bio-P and reached the same conclusion as Kuba *et al.*, 1994, that "a complex behaviour for phosphorus release occurs when electron acceptors (oxygen or nitrate) and electron donors (COD) are both present, probably because energy can be obtained from the direct COD oxidation (with oxygen or nitrate), leading to less phosphorus release".
In the Activated Sludge Model 2d (Henze *et al.*, 1999) that includes denitrifying PAO's, no acetate/organic substrate inhibition term is included for the anoxic P uptake. Similarly, no electron acceptor inhibition term is included for anaerobic storage of organic matter. This is explained by observations indicating storage of COD also during aerobic or anoxic conditions.
Brdjanovic *et al*., 1998b, report experimental data with activated, phosphorus-removing sludge where phosphate was released under aerobic conditions with acetate present. Simultaneous with the P release, internal PHB levels increased and internal glycogen contents decreased.

From the above, the conclusion is made, that EBPR cultures apparently partly take up and store COD and partly oxidise it directly during the simultaneous presence of an electron acceptor. However, since no pure culture studies have been made, it is not verified whether the net effect is caused by a single or by different organisms.

2.1.10 Terminology – Phases

When talking about simultaneous presence of COD and electron acceptor, it gets a bit confusing regarding defining anaerobic or anoxic (aerobic) conditions.
In the following when talking about a **phase** it is defined by the state of the bacteria upon the start of the phase. The definition of phase is determined by which compounds are present internally in the bacteria cells.

By the beginning of an **anaerobic phase**, the bacteria have just been through an anoxic (or aerobic) phase and have high internal polyphosphate storage, whereas their internal storage of organic matter is empty/low. COD is present in the bulk water, and occasionally an electron acceptor is present (e.g. during the transition from an anoxic to an anaerobic phase in a continuously operated system before all nitrate is washed out).

When talking about an **anoxic (or aerobic) phase** it too is defined by the storage inside the bacteria. By the beginning of an anoxic (or aerobic) phase, the bacteria have just been through an anaerobic phase so their internal organic storage is full/high whereas the P storage is empty/low. Nitrate (or oxygen) is present in the bulk water, and occasionally COD may be present (e.g. during the transition from an anaerobic to an anoxic phase in a continuously operated system before all COD is washed out).

Figure 2.5 summarises the theory according to Kuba *et al.* (1994) for a system with alternating anaerobic and anoxic conditions, i.e. denitrifying EBPR. The title of the figure indicates the transition, either from anaerobic to anoxic phase or the other way. Acetate is used as the model COD.

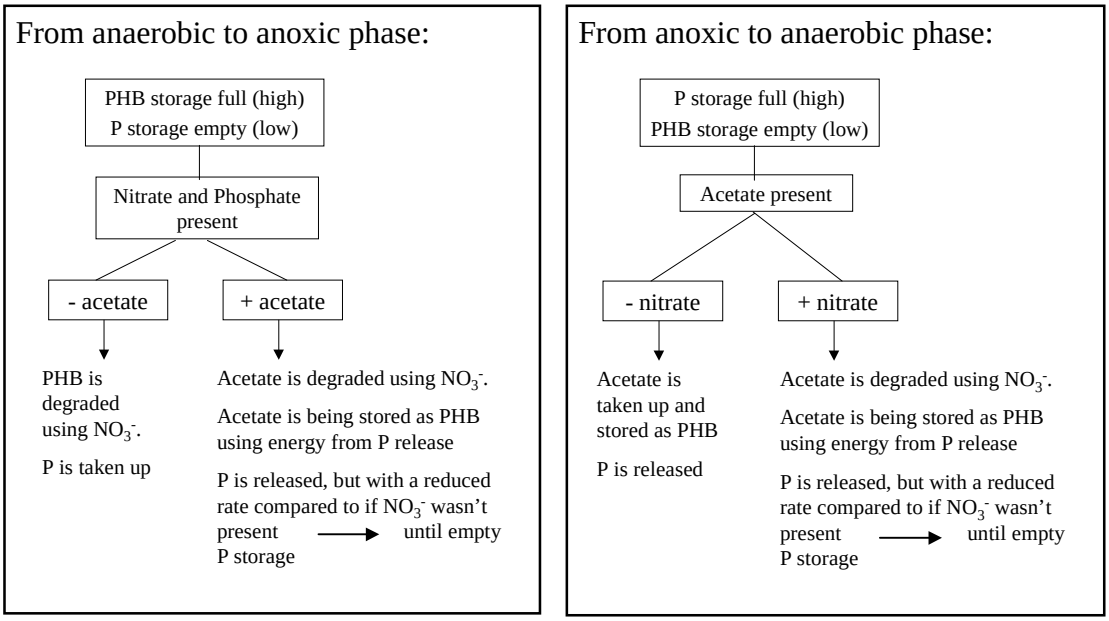

Figure 2.5. Hypothesis for simultaneous presence of acetate and nitrate during transistion between anaerobic and anoxic phases. Theory according to Kuba *et al.*, 1994.

2.1.11 An Exception To The Rule → ??

A recent finding by Barak and van Rijn, 2000, contradicts all of the hitherto established theories of the EBPR process. Excess P uptake (9 % of the dry weight) by a pure culture of *Paracoccus denitrificans* was observed during aerobic or anoxic conditions, but *only* during simultaneous presence of acetate. Acetate uptake stopped during anaerobic conditions and phosphate was released. Growth (based on protein measurements) took place during both aerobic/anoxic and anaerobic conditions on the premise that the internal

phosphate storage pools weren't depleted. PHB levels increased during aerobic conditions with acetate present. During anoxic conditions, no increase in PHB was seen, but PHB levels increased during subsequent anaerobic conditions upon depletion of the internal phosphate pools. Internal glycogen contents decreased during anaerobic conditions. A summary of the observed metabolism and a comparison with the normal PAO metabolism is given in Table 2.6. The investigated strain, *Paracoccus denitrificans*, was isolated from a fluidised, denitrification bed reactor. An anaerobic digestion basin was part of the system, however, since attached biomass was used, circulation of the bacteria through alternating conditions did not take place. Barak and van Rijn referred to a few other investigations that supported the findings of the atypical metabolism. Other isolates of denitrifying bacteria were also found to be capable of polyphosphate storage and the authors suggested this trend to possible be common among many denitrifiers. The findings of high accumulation of phosphate in denitrifying bacteria not exposed to alternating conditions were found also during long-term operation.
The possibility of simultaneous denitrification and phosphorus removal without alternating conditions would simplify wastewater treatment enormously, however, a theoretical and metabolic model of the process has yet to be revealed along with further experimental investigations.

Table 2.6. Atypical metabolism of a denitrifying bacteria, *Paracoccus denitrificans* with the capability of simultaneous excess phosphate storage and denitrification with acetate. The established metabolism of PAOs is included for comparison. Barak and van Rijn, 2000.

Organism(s)	**Anaerobic metabolism**	**Aerobic/anoxic metabolism**
P. denitrificans	Unable to use external carbon source for PHA synthesis; degrade glycogen for PHA synthesis; degrade polyphosphate; release phosphate; degradation of poly-phosphate provides energy for growth	Produce polyphosphate and grow on energy provided by external carbon source; produce glycogen; in the absence of an external carbon source, cells with PHA do not grow and do not produce poly-phosphate
PAOs	Use external carbon source for PHA synthesis; release phosphate; degrade polyphosphate; degrade glycogen	Produce polyphosphate by degradation of PHA; produce glycogen;grow in the absence of an external carbon source on PHA; when present, exter-nal carbon source might inhibit polyphosphate synthe-sis or is used for PHA production but not for growth

Penetrating so many secrets, we cease to believe in the unknowable. But there it sits nevertheless, calmly licking its chops.

- H. L. Mencken (1880-1956) American journalist, writer.

BOX 1 Metabolic Model of EBPR

The metabolic model proposed by Mino *et al.*, 1987, which includes glycogen as a storage compound, appears reasonable based on experimental observations.
The anaerobic stoichiometry of phosphate released to COD taken up increases with pH from ~ 0.26-0.75 mol P/mol C in the pH interval 5.5-8.5.
The metal ions, K^+ and Mg^{2+}, are taken up and released simultaneously with phosphate in the relative molar ratios of 0.3 (K/P) and 0.26 (Mg/P). Apparently these ions chemically stabilise the poly-phosphate chains.
PAOs grow relatively slow, maximum growth rate is around 1 d^{-1} (20^{o}C). In return, the PAOs have a low decay rate (0.04 d^{-1}). Investigations on growth rates and kinetics are limited and suffer from the lack of a pure PAO culture.
PAOs can grow on several simple carbon compounds, but SCFAs are considered most favourable. This assumption is based on lab experiments as well as improvement of full-scale EBPR plants by addition of fermentation products.
Typical phosphorus content of EBPR sludge from wastewater treatment plants is 4-7%, compared to ~1.5% for non-EBPR. In laboratory experiments with enhanced PAO cultures, the content can be increased up to ~16%.
Some PAOs can use nitrate as the sole electron acceptor. If this process is used for simultaneous N and P removal, the overall COD demand can be reduced to near half. The yield coefficient of anoxic growth is smaller than of aerobic leading to lower sludge production.
Recirculation of nitrate or oxygen into the anaerobic tank has a negative effect on EBPR, since PAOs loose their competitive advantage of anaerobic COD storage.
Combined presence of nitrate and COD lead to phosphate release at a reduced rate compared to strict anaerobic conditions since part of the COD is oxidised directly.

Some open questions:
Do all PAOs use the same glycogen metabolism during anaerobic conditions? Is this the EMP or the ED pathway, or a combination of one of these with the TCA cycle, or others? How are the glycogen pools restored during aerobic conditions?
Are SCFAs transported over the cell membrane in un-dissociated form via simple diffusion or in dissociated form via energy consuming active diffusion?
What is the effect of different ratios between the anaerobic and aerobic (alternatively anoxic) phase lengths?
Is the EBPR metabolism identical for activated sludge and biofilm organisms?
What is the temperature optimum for EBPR and is this different in full-scale plants compared to lab-scale experiments with enhanced PAO cultures due to the interactions between different bacteria groups in full-scale?
Can denitrifying capability be induced in every PAO culture? I.e. do many PAOs possess a denitrifying enzyme system that can be induced if necessary, or is it different PAO groups that use oxygen or nitrate as the electron acceptor. If so, are both groups always present to some extent in EBPR plants?
Which metabolism accounts for the recent observation of simultaneous phosphate storage and denitrification directly with acetate? Does this mechanism suggest a treatment alternative of the future?

2.2 Biological Phosphorus Removal – The Microorganisms

2.2.1 Culture-dependent Methods → *Acinetobacter*

Ever since the discovery of the excess phosphate uptake induced by the characteristic alternating conditions, researchers have been chasing the organism(s) responsible for the process. Fuhs and Chen, 1975, isolated strains resembling members of the *Acinetobacter-Moraxella-Mima* group from EBPR sludge and showed that an *A. lwoffi*-like organism was able to aerobically store PHB and poly-P. Acetate uptake occurred aerobically, accompanied by P uptake and growth. Upon transferring these bacteria to anaerobic conditions, some P release was observed, but no acetate measurements were made whereby anaerobic uptake was not confirmed. Fuhs and Chen concluded that the anaerobic phase of the EBPR process simply was needed in order to produce the fermentation products such as acetate that was needed for simultaneous COD and excess P uptake during aerobiosis. An overwhelming list of investigations with *Acinetobacter* spp. followed in the subsequent years (Bayly *et al.*, 1991; Beacham *et al.*, 1990; Belia and Smith, 1997; Brodish, 1985; Cloete *et al.*, 1985; Deinema *et al.*, 1980, 1985; Lötter, 1985; Lötter *et al.*, 1986; Ohtake *et al.*, 1985; Suresh *et al.*, 1985).

Based on a literature review, Jenkins and Tandoi, 1991, concluded, that none of the investigations with pure cultures of *Acinetobacter* spp. had been able to duplicate all of the key aspects of EBPR, mainly anaerobic uptake of COD had not been shown. Another problem was that none of the pure culture experiments had been performed according to the alternating anaerobic/aerobic conditions of EBPR, but mostly in pure aerobic environments.

Other isolates capable of excess storage of phosphate have been isolated, but none of them gained significant attention. Suresh *et al.*, 1985, showed high phosphorus content (31%) and P uptake/release activity of *Pseudomonas vesicularis*. Gersberg and Allen, 1985, observed significantly higher P uptake rates of a pure culture of *Klebsiella pneumoniae* than of a parallel pure *Acinetobacter calcoaceticus* culture. Nakamura *et al.*, 1991, 1995, isolated a bacterium from EBPR, which was capable of P uptake, P release and anaerobic uptake of some carbon sources (different from acetate) with internal storage as glycogen. They named it *Microlunatus phosphovorus* NM-1. Kawaharasaki *et al.*, 1998, developed an oligonucleotide probe for this strain and showed only minor presence in an EBPR sludge (3%). Stante *et al.*, 1997, isolated and investigated a culture of *Lampropedia* spp. All the phenomena of EBPR could be verified for this culture, however, the ratio of phosphate release to acetate taken up was very low. Mino *et al.*, 1998, further stated that the morphology with a unique sheet-like cell arrangement seldom is observed in EBPR sludge.

2.2.2 Culture-independent Methods → NOT *Acinetobacter*

2.2.2.1 Introduction of culture-independent methods

By the recent introduction of innovative, non-culture dependent methods, it has become possible to detect species that are not culturable in the lab and avoid the bias introduced by cultivation. Possibly, only a minor fraction of the bacteria population of a complex ecological system like activated sludge can be cultured under defined laboratory conditions applying only a few substrates (Amann *et al.*, 1995; Kämpfer *et al.*, 1996; Spring *et al.*, 1992; Wagner *et al.*, 1993).

One of the new methods that has gained particular popularity within the field of characterisation of microbial populations in wastewater treatment plants is "Fluorescent In Situ hybridisation" (FISH) using rRNA targeted oligonucleotide probes. This method was introduced in the late 80'ties (Amann *et al.*, 1990ab; DeLong *et al.*, 1989; Giovannoni *et al.*, 1988; Stahl *et al.*, 1988) and is today subjected to constant development with addition of new probes. The principle of the method is to add small pieces of DNA labelled with a fluorescent dye to a sludge sample, let the sample and DNA strings react on a microscopic slide under certain defined conditions (that makes the bacteria cell wall permeable) and finally wash the sample. DNA strings that are compatible with ribosomal RNA of the targeted bacteria group, attach and can subsequently be seen via an epifluorescent microscope (e.g. a confocal laser scanning microscope, CLSM), Fig. 2.6. Via digital image analysis, quantification of different bacteria groups based on the microscopic images, is possible. The specificity of the probes can be chosen according to different investigation aims, from subspecies to the kingdom level. For a detailed description of the method, including a discussion of rRNA as the target molecule and probe design, refer to Amann, 1995. Amann *et al.*, 1995, and Muyzer and Ramsing, 1995, discussed some of the potentials and limitations of FISH and other new molecular techniques.

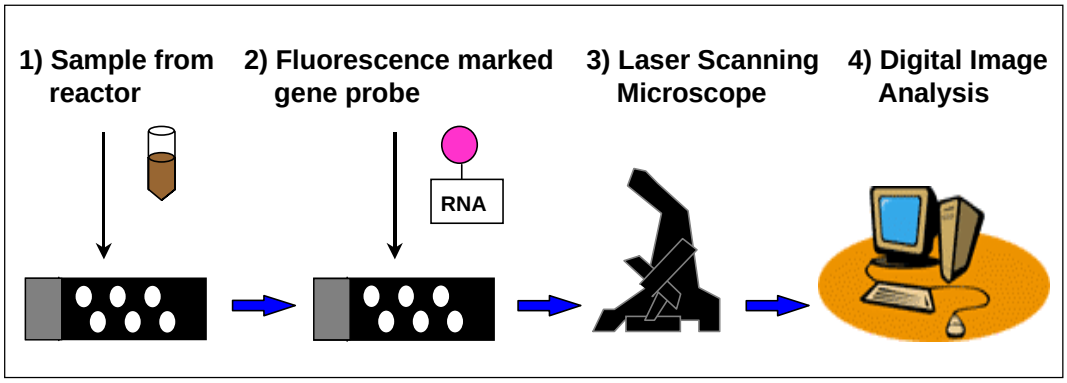

Figure 2.6. Principle of "Fluorescent In Situ hybridization (FISH)" using rRNA targeted oligonucleotide probes. A sludge sample is mounted on a microscopic slide, a fluorescently marked DNA string is added, reaction is allowed, and the slide is finally washed to remove excess DNA strings. The bacteria cells that took up the DNA string are now visible in an epifluorescence microscope.

For development of probes, a combination with another new method: Direct rRNA retrieval from the sludge sample, by the use of e.g Polymerase Chain Reaction (PCR) for sequencing and amplification of genes, is recommended (Snaidr *et al.*, 1997). No isolation and cultivation is needed by this method. It is possible to identify new sequences directly based on the sludge sample and subsequently develop probes for in situ analysis and quantification.

Upon the development of the refined microbial characterisation methods based on RNA sequences, it was proposed to use an rRNA approach for studies of microbial ecology (Olson *et al.*, 1986). A so-called molecular phylogenetic tree for all living cells is seen in Fig. 2.7. The lengths of the branches quantitatively represents the evolutionary distance separating organisms, based on the rRNA divergence (Brown, 1999). A close-up on the bacteria part of the tree is seen in Fig. 2.8. This figure illustrates the major group-specific genetic probes that have been developed so far (Amann *et al.*, 1995).

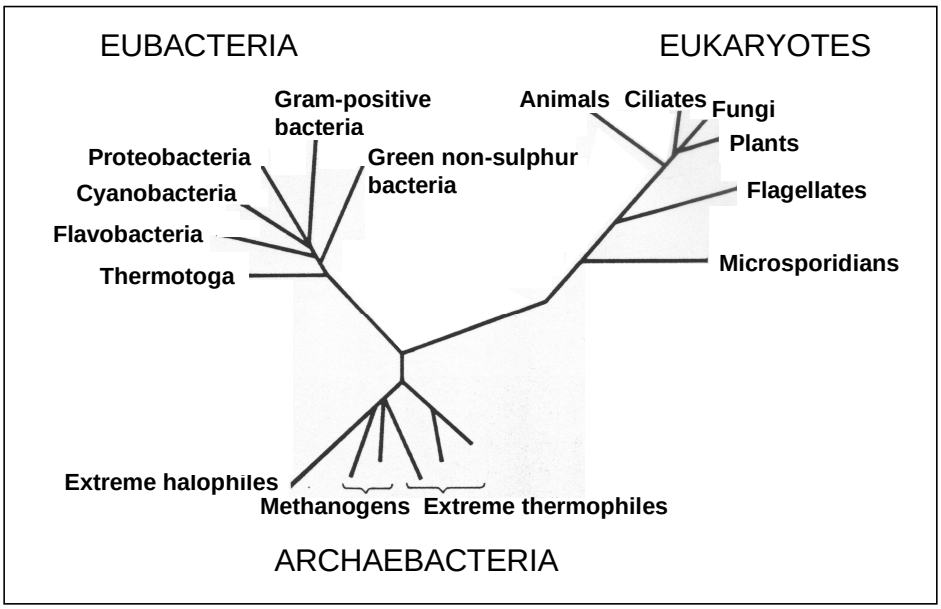

Figure 2.7. A molecular phylogenetic tree for all living organisms (3 evolutionary groups). The lengths of the branches quantitatively represents the evolutionary distance based on the rRNA divergence (Brown, 1999).

A comment should be made regarding the use of PCR and FISH – and other new characterisation methods – the sole verification of the presence of a certain bacteria group does not answer the question of function. High cell numbers of a certain bacteria group in e.g. an EBPR plant can only indicate the involvement of this group in the process. Nielsen *et al.*, 1999b, and Lee *et al.*, 1999, suggested the combination with microautoradiography (MAR) for a simultaneous in situ determination of the identities, activities, and specific

substrate uptake profiles of individual bacterial cells within complex microbial communities. The method is based on incubation with radioactively labelled substrates before the biomass sampling. FISH in combination with the detection of radioactivity can reveal, which bacteria groups took up the different substrates. The method appears a promising tool for elucidating metabolic pathways. However, the need of an isotope-laboratory makes the method of limited general applicability.

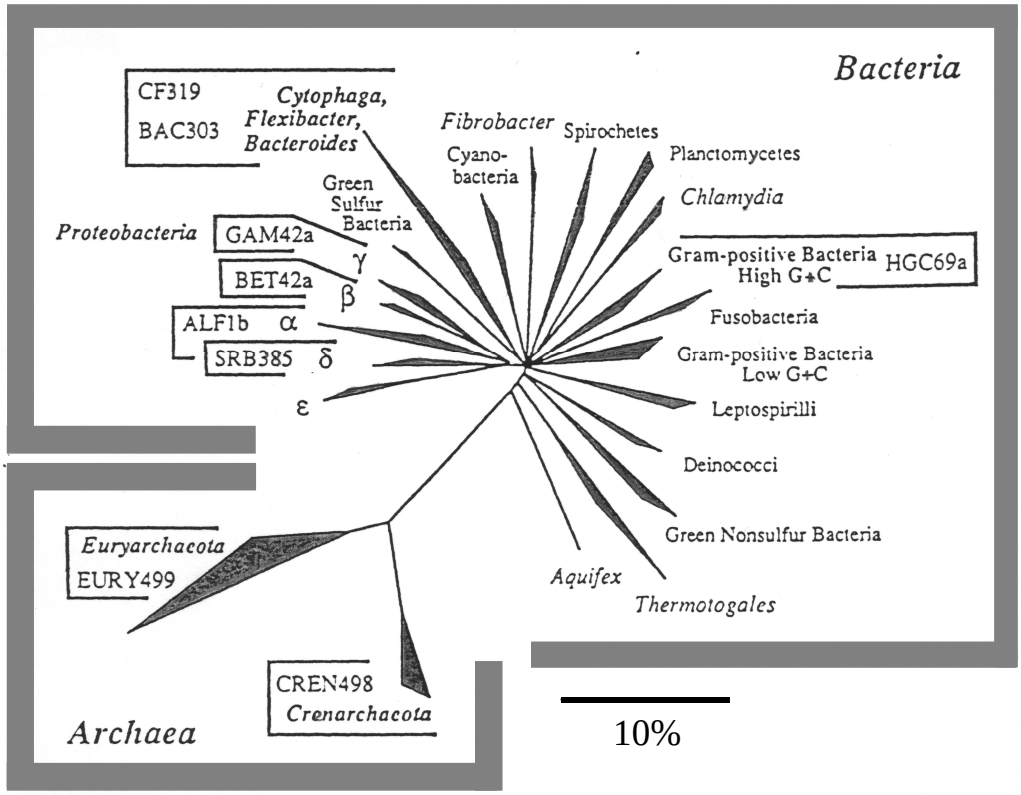

Figure 2.8. A phylogenetic tree illustrating major groups belonging to the *Bacteria* and *Archaea* groups. The branches currently targeted by upper-level oligonucleotide probes are identified. The bar corresponds to 10 % estimated rRNA sequence divergence (Amann *et al.*, 1995).

2.2.2.2 Results of culture-independent methods

As summarised in a recent review by Mino *et al.*, 1998, it has during the last decade been demonstrated, that *Acinetobacter* spp. actually constitutes only a minor fraction of the bacteria population in activated sludge for phosphorus removal (Auling *et al.*, 1991; Bond *et al.*, 1995; Oerther *et al.*, 1998; Sudiana *et al.*, 1998; Wagner *et al.*, 1994a). The reason that *Acinetobacter* spp. was falsely attributed the great importance in the bio-P process was due to the bias introduced by the traditional culture-dependent methods used to analyse microbial communities (Erhart, 1997; Wagner *et al.*, 1994a).

Investigations of sludge from enhanced biological phosphate removal processes by mainly the use of FISH have generally considered the bacteria groups belonging to: the alpha, beta and gamma subclasses of *Proteobacteria*, *Acinetobacter*, the *Cytophaga-Flavobacterium* cluster of the *Flexibacter-Cytophaga-Bacteroides* phylum and Gram-positive bacteria with a high G+C DNA content (Bond *et al.*, 1995; Kawaharasaki *et al.*, 1999; Sudiana *et al.*, 1998; Wagner *et al.*, 1994a). More detailed analysis of the bacterial community in enhanced biological phosphorus removal sludge (and non-bio-P sludge) was made by Erhart (1997).

Of other probes that have been used in activated bio-P sludge can be mentioned: Probes specific for populations of nocardiaform actinomycetes (Schuppler *et al.*, 1998) and a probe specific for *Microlunatus phosphovorus* (Kawaharasaki *et al.*, 1998+1999).

The general findings have been, that the beta sublass of *Proteobacteria* dominate most sludge, both EBPR and non-bio-P sludge (Bond *et al.*, 1995; Hiraishi *et al.*, 1998; Snaidr *et al.*, 1997; Sudiana *et al.*, 1998). Other major groups represented were the alpha subclass of *Proteobacteria*, planctomycete group and *Flexibacter-Cytophaga-Bacteroides* group (Bond *et al.*, 1995). Members of the class *Actinobacteria* (gram positive with a high DNA G+C contents) were found to be the second most dominant group after the beta subclass by Hiraishi *et al.*, 1998.

In the EBPR sluge was found larger predominance of: Gram-positive bacteria with a high G+C content (Bond *et al.*, 1999; Erhart, 1997; Kawaharasaki *et al.*, 1999; Kämpfer *et al.*, 1996; Wagner *et al.*, 1994a), the alpha subclass of *Proteobacteria* (Kawaharasaki *et al.*, 1999), the *Rhodocyclus* group within the beta subclass (Bond *et al.*, 1995). Melasniemi *et al.* (1998) found that *Micrococcus*, *Staphylococcus* and *Acidovorax* were the most dominant bacteria genera in EBPR sludge and also strains related to actinomycetes. Lee *et al.*, 1999, identified phosphate uptake by beta subclass bacteria.

Hiraishi *et al.* (1998) found that the bacterial community apparently was more influenced by the wastewater type than by the plant operation. They found larger differences in the populations for different wastewater sludges than when comparing EBPR to standard processes. This strongly argues for specifying the operating conditions used for any investigation of a microbial population.

Hesselmann *et al.*, 1999, worked with a lab-scale reactor and obtained a very enriched culture showing good phosphate removal. They developed a specific probe for a bacteria related to the *Rhodocyclus* group that was shown to make up 81% of the population (quantified in situ by FISH). They suggested the name: *Candidatus* Accumulibacter phosphatis for this organism. The setup was operated with oxygen. This bacteria has subsequently been found in laboratory EBPR sludges from different continents (Crocetti *et al.*, 2000), making it of high potential as a significant PAO bacteria. Crocetti *et al.*, 2000, additionally found a linear correlation between the sludge P content and the percent of cells binding the new probe.

From the above it is concluded, that the microorganism(s) responsible for EBPR still need to be identified. It appears from the different investigations, that it is likely more than one species that is capable of excess phosphate storage and hence might be able to perform EBPR if the conditions are right. None of the investigations focused on denitrifying PAOs or biofilms. Interactions between different groups should be investigated further. The difficulty in obtaining a pure culture could perhaps be related to interspecies symbiotic relations? This was indicated in a study by Doll *et al.*, 1999.

2.2.3 Microorganisms Competing with The PAOs

Bacteria capable of anaerobic uptake and storage of COD in the form of PHA without the use of polyphosphate as energy source were first described by Cech and Hartman, 1990, 1993. The morphology of these bacteria was identified to be different from the typical PAO clusters of large cocci cells with intracellular Neisser-positive (Jenkins *et al.*, 1993) inclusions. Instead, they typically occurred as large cocci arranged in tetrads and only the cell walls tested positive with the Neisser stain. Cech and Hartman, 1993, named this bacteria "G bacteria" because it dominated their so-called G reactor, where G was referring to the feed: glucose. Subsequently the G has been generally accepted, however as referring to glycogen, the storage compound of the "glycogen-accumulating-organisms" (GAOs). Cech and Hartman, 1993, stated that the observed molar ratio of phosphate released to acetate taken up in the anaerobic stage varied from 0 to 0.78 and depended on the ratio of the numbers of PAO bacteria to "G bacteria". The existence of glycogen-accumulating organisms has been verified in several subsequent investigations (Blackall *et al.*, 1997; Bond *et al.*, 1999; Liu *et al.*, 1994, 1996b; Satoh *et al.*, 1992, 1994; Sudiana *et al.*, 1999; Tasli *et al.*, 1997). Mino *et al.*, 1998, summarises some of the investigations and conclusions made regarding GAOs. The typical metabolisms of GAOs and PAOs are compared in Table 2.7. Apparently the involvement of phosphate is the only metabolic difference.

The causes of GAO appearance (mainly observed in lab-scale reactors) have been studied in several investigations following the publications by Cech and Hartman (Brdjanovic *et al.*, 1998a; Carruci *et al.*, 1995, 1997, 1999, Liu *et al.*, 1994, 1996ab, 1997; Matsuo, 1994, Mino *et al.*, 1994, 1995; Satoh *et al.*, 1992, 1994, Sudiana *et al.*, 1999; Tasli *et al.*, 1997). However, no definitive conclusions have yet been reached. In many investigations, an adverse effect on EBPR was observed when supplying high ratios of glucose in the feed (Appeldorn *et al.*, 1992; Cech and Hartman, 1993; Tasli *et al.*, 1997). However, also feed without glucose, but with e.g. propionate or peptone has supported growth of GAOs (Matsuo, 1994; Satoh *et al.*, 1992, 1994). Liu *et al.*, 1994, 1996ab, 1997, used a very low phosphorus/carbon feeding ratio (2/100, wt/wt) to suppress the growth of PAOs. Hence, they obtained an enriched GAO

population with a medium containing high amounts of acetate. Batch tests were used to verify anaerobic uptake of many different organic carbon sources by this GAO culture.

Table 2.7. Comparison of metabolisms of PAOs and GAOs. Mino *et al.*, 1998.

Metabolism	**PAOs**	**GAOs**
In the anaerobic phase		
Uptake of external organic substrates	+	+
Consumption of intracellular glycogen	+	+
Accumulation of intracellular PHA	+	+
Consumption of intracellular polyphosphate and consequent release of orthophosphate	+	–
In the aerobic phase		
Recovery of intracellular glycogen	+	+
Consumption of stored PHA	+	+
Growth	+	+
Recovery of intracellular polyphosphate	+	–

A theoretical explanation for the likeliness of GAO dominance when other carbon sources, such as glucose or propionate, are used instead of acetate, was provided by Maurer *et al.*, 1997. They concluded from metabolic considerations, that polyphosphate is an essential energy pool for uptake and storage of acetate during anaerobic conditions, whereas uptake and storage of e.g. glucose is less energy demanding whereby the organisms have the possibility of replacing the polyphosphate by glycogen. For acetate as the major carbon source, they inferred good EBPR due to the need of high polyphosphate storage. As of today, no experimental investigations with high acetate and phosphate concentrations in the feed reported growth of GAOs. Mino *et al.*, 1994, 1995, developed a simplified metabolic model, that also indicated no need of polyphosphate for glucose metabolism, due to enough energy produced by glycogen.

An exception to the typical PAO and GAO metabolisms was observed by a research group in Italy (Carruci *et al.*, 1995, 1997, 1999). Their results are summarised in Carruci *et al.*, 1999. They described bacteria capable of anaerobically removing glucose from the water phase, but without the synthesis of PHA. However, when testing the same sludge using acetate, the typical PAO metabolism with PHA formation was observed for anaerobic acetate uptake. The morphological characteristics of the bacteria resembled the descriptions of G bacteria by Cech and Hartman, 1993, and this was true for periods of both

good and poor EBPR activity. Carruci *et al.* suggested the need to consider additional metabolisms for anaerobic substrate uptake and synthesis of internal glycogen pools. The authors also reported good EBPR with glucose as the sole organic carbon source over extended time periods. In one case, no EBPR had been seen in a glucose fed system for 5 months, but following an accidental failure in the aeration for 3 days, EBPR was re-established and lasted 3 months before it again deteriorated. The dominance of bacteria similar to the previously described G bacteria also during periods of good EBPR indicate either that the G bacteria can perform EBPR under certain environmental conditions or survival of PAO bacteria in competition with the GAOs.

Brdjanovic *et al.*, 1998a, tested the behaviour of an enriched PAO culture under conditions of poly-P limitation and surplus glycogen content of the biomass. Under these conditions, almost no acetate was taken up in the anaerobic phase, which indicates that PAOs cannot use glycogen conversion to PHA as the sole energy source under anaerobic conditions as is observed for GAOs. However, since the enriched PAO population was acclimatised during normal EBPR conditions, it cannot from this investigation be definitely excluded that PAO bacteria can induce the GAO metabolism during non-optimal EBPR conditions.

Cech and Hartman, 1994, investigated the influence of bacterial grazers (rotifiers, ciliates and flagellates) on the competition between PAOs and GAOs. They found indications of higher grazing of PAOs compared to GAOs, possible due to compact flocs of GAOs that were more predator-resistant. Flagellates grazing on the PAO was also suggested as a reason for a decrease in EBPR activity observed by Cech and Hartman, 1993.
Matsuo, 1994, found an influence of the anaerobic sludge retention time. For 3 continuous flow EBPR systems, a long anaerobic SRT stabilised EBPR (tested range: 0.9-6.4 d), when the aerobic SRT was maintained constant at 5.6 d. A type of organisms similar to the GAO described by Cech and Hartman, 1993, was present in all systems, but to a much higher extent in the systems with low EBPR activity. Whether the long anaerobic SRT directly favoured the PAOs metabolism or whether it suppressed the growth of grazers was not investigated.
Brdjanovic *et al.*, 1999, suggested a quantification method of the relative proportion of PAOs and GAOs in a sludge sample based on measurements of acetate consumption with and without depletion of the internal poly-P pool of the cells in an anaerobic batch test.

Microbial investigations of GAOs, except for traditional morphological characterisations, are very limited. Blackall *et al.*, 1997, isolated and suggested the name *Tetracoccus cechii* for two strains of G bacteria resembling the bacteria described by Cech and Hartman. The strains were described as 1-2 μm cocci, arranged in tetrads and belonging to the alpha subclass of *Proteobacteria*. They were shown unable to reduce nitrate further than to nitrite.

Bond *et al.*, 1999, used FISH to compare sludges with high and low EBPR activity. The phosphate activity was defined by the phosphorus content of the sludge, 9-12% and 1.5%, for high and low activity, respectively. The low-EBPR sludge was obtained by limiting the phosphate content of the feed. Their findings are shown in Table 2.8. Significantly higher dominance of bacteria belonging to the alpha subclass of *Proteobacteria* appeared in the low EBPR sludge (42% compared to 9-10%) in agreement with the findings of Blackall *et al.*, 1997. Also bacteria belonging to the gamma subclass were present to a higher extent (16%) compared to the good EBPR sludge (1-2%). These groups flourished on the expense of bacteria belonging to the beta subclass. Gram-positive bacteria with high G+C DNA contents were well represented in all sludges (35-43%).
Nielsen *et al.*, 1999a, identified 6 types of bacteria from a reactor with deteriorated EBPR. One type belonged to the alpha subclass of *Proteobacteria* and the others to the gamma subclass. The bacteria from the alpha subclass were different from the type identified by Blackall *et al.*, 1997. According to FISH, the gamma types constituted ~35% of the total population and were characterised as large cocci, 3-4 μm.
Sudiana *et al.*, 1999, also used FISH to characterise PAO and GAO enriched populations fed with either acetate or glucose. Also in this investigation, a low P/TOC ratio (2/100) was used to suppress PAO growth. However, no significant differences between the sludges could be detected with FISH. The alpha subclass constituted 14-19%, the beta subclass 30-39%, the gamma subclass 11-12%, *Acinetobacter* 3-5% and Gram-positive HGC 11-16%.

Table 2.8. FISH analysis applied on sludge with good and poor EBPR capacity. Reproduced from Bond *et al.*, 1999.

		P content of sludge		
Probe	Specificity	High: 12%	High: 9%	Low: 1.5%
		% of total cells		
ALF1b	Alpha *subclass of Proteobacteria*	9	10	42
BET42a	Beta *subclass of Proteobacteria*	56	42	13
GAM42a	Gamma *subclass of Proteobacteria*	2	1	16
HGC69a	*Gram-positive bacteria with a high G+C DNA content*	35	43	40
CF	*Cytophaga/flavobacteria*	9	12	6

> The most beautiful experience we can have is the mysterious. It is the fundamental emotion which stands at the cradle of true art and true science.
>
> - *Albert Einstein (1879-1955) U. S. physicist, born in Germany.*

BOX 2 Microorganisms of EBPR

Acinetobacter spp. was since the discovery of excess P uptake by Fuhs and Chen, 1975, thought to be of major importance for EBPR. By the introduction of culture-independent characterisation methods in the early 90'es, it was shown that a serious bias in the favour of *Acinetobacter* spp. had been introduced by the traditional culture-dependent methods. In reality, *Acinetobacter* spp. was present in very low cell numbers in EBPR plants.
Till today, no pure culture of a phosphate-accumulating organism (PAO) has been obtained, and no single organism doing all of the typical characteristics of enriched PAO cultures has been identified.
FISH analysis have indicated that gram-positive bacteria with a high G+C content might be important for EBPR, and bacteria belonging to the beta subclass of *Proteobacteria* has been found to in situ take up phosphate. However, no conclusive results have yet been obtained.
Recently, an 81% pure PAO culture was found to be made up of a *Rhodocyclus*-like organism (Hesselmann *et al.*, 1999). The name *Candidatus* Accumulibacter phosphatis has been suggested. This organism was subsequently identified in EBPR sludge from different continents (Crocetti *et al.*, 2000).

So-called glycogen accumulating organisms (GAOs) have been seen to compete with PAOs for organic substrate during the anaerobic phase and under certain operating conditions oust PAOs with deterioration of the EBPR process as a consequence. The wastewater composition might be a determining factor for the competition, with e.g. acetate being in high favour of PAOs. GAOs were first described by Cech and Hartman, 1990, as large cocci arranged in tetrads. This finding has been confirmed in several studies. Blackall *et al.*, 1997, isolated an organism resembling the one described by Cech and Hartman and suggested the name *Tetracoccus cechii*. It was identified as belonging to the alpha subclass of *Proteobacteria* and was shown unable to reduce nitrate further than nitrite. Bond *et al.*, 1999, supported this finding, since FISH analysis of sludge exhibiting high (9-12 % P content) or low (1.5 % P content) phosphate removal activity had a significant difference in the proportion of alpha bacteria, 9-10 % and 42 %, respectively.

Some open questions:
Can a large group of different organisms perform EBPR?
At least a few species must be able to perform EBPR, since it has been shown that not all PAOs can denitrify → which groups perform anoxic EBPR? Can the recently *Rhodocyclus*-like organism denitrify?
Are interspecies relations of importance for EBPR and hence the reason for the failed attempts of obtaining a pure culture?
Are PAOs and GAOs different organisms or can the groups adapt their metabolisms to a given/changed environment?
Can some GAOs denitrify further than nitrite?
Will the same PAO cultures be present in activated sludge and biofilms?

2.3 Biofilm Models

2.3.1 What is a Biofilm?

Biofilms are collections of microorganisms, predominantly bacteria, that are enmeshed within a three dimensional gelatinous matrix of extracellular polymers secreted by the bacteria (Bryers, 1993). The extrapolymeric substances (EPS) can anchor bacteria to all kinds of material – such as metals, plastics, soil particles, medical implant materials, and tissue - as of today, no inert surface resistant to bacterial colonisation has been found (Costerton, 1995). The only prerequisite for biofilm formation is that some amount of water is available.
A biofilm can be formed by a single bacterial species, but more often biofilms consist of many species of bacteria, as well as fungi, algae, protozoa, debris and corrosion products. The relative ratio of bacterial cells and EPS has been reported to vary significantly, from 10 to 90% of the organic matter (Nielsen *et al.*, 1997). EPS is mainly represented by polysaccharides (up to 65%) and is for this reason also known as the glycocalyx matrix. However, also other substances are present, such as proteins (10-15%), nucleic acids, lipids, DNA and humics (Lazarova and Manem, 1995; Nielsen *et al.*, 1997). The polysaccharides produced vary depending on the species but are typically made up of repeating oligosaccharides, such as glucose, mannose, galactose, xylose, and others (Buckman, 2000). Within the same strain of bacteria, the saccharide chains may shift according to the physiological state of the cell and environmental conditions. Almost all investigations concerning the chemical structure and biochemical nature of EPS composition have been made with culture media or activated sludge samples. The EPS matrix of complex biofilm communities - from e.g. wastewater treatment plants - may differ considerable in comparison (Lazarova and Manem, 1995; Zhang *et al.*, 1998). Jahn and Nielsen, 1995, found that proteins and in some cases humic substances made up the major components of some biofilms, both mixed cultures from technical systems and pure cultures. This finding was supported by a study of biofilms in an industrial prototype circulating bed reactor by Lazarova *et al.*, 1998.

The vast majority of microbial life is made up of attached growth and in this regard, it is striking that microbiologist first in the early 80'es started to study biofilms. Costerton, 1995, speculated that planktonic cells may represent a simple mode of growth specialised to accomplish dispersal and the colonisation of new habitats. He inferred that the study of planktonic growth as done by microbiologists during the last 15 decades, in this way would be similar to confining a study of plants and animals to the examination of their spores, gametes, seeds and other propagules. It is today clear, that biofilm bacteria are phenotypically, physiologically and ecologically profoundly different from their planktonic counterparts (Costerton *et al.*, 1994).

2.3.2 Why is Attached Growth Preferential?

The life in a biofilm offers several advantages compared to planktonic growth:

1) Protection against washout of slow growing bacteria under conditions of relatively low hydraulic residence times, e.g. nitrifiers in wastewater treatment plants or slow-growing bacterial species capable of degrading xenobiotics (Bishop, 1997).

2) Higher nutrients concentrations. The EPS matrix is usually composed of charged polymers, mainly anionic, that act as an ion exchanger attracting organic molecules and inorganic ions from the passing water (Costerton, 1999b; Flemming, 1995).

3) Life in a microbial community offers interspecies interactions that might be beneficial for the individual cell, a well-known example is the juxtaposed positions of nitrate- and nitrite-oxidising nitrifiers. James *et al.*, 1995, gives an overview of different types of interspecies bacterial interactions. Microniches inside a biofilm can make it possible for e.g. anoxic or anaerobic bacteria to survive in an otherwise aerobic environment.
   Nutrient cycling by bacteria lysis should also be mentioned.

4) Protection against toxic compounds (e.g. antibiotics) and to some extent predation. The current 'rule of thumb' in biofilm microbiology is that biofilm bacteria can survive sterilants and/or antibiotic concentrations 1000-1500 higher than planktonic cells of the same species (Costerton, 1999a).

Costerton, 1999a, stated that bacteria cultivated as planktonic cells in laboratories often loose their ability to adhere to surfaces. This has an important constraint in making extrapolation from data obtained with 'tamed' lab cultures to wild bacteria cells found in the environment.

2.3.3 Biofilm Formation

Adhesion of bacterial cells to a surface and development of a biofilm include several steps, Fig. 2.9. The initial step of formation plays an important role and has a considerable impact on the structure and physico-chemical properties of the mature biofilm (Lazarova and Manem, 1995). The influence of surface (or substratum) structure on biofilm stability and development was studied in a biofilm airlift suspension (BAS) reactor by Gjaltema *et al.*, 1997a, who concluded that the physicochemical surface characteristics were less important compared the key factor: surface roughness. Increased roughness promoted biofilm accumulation, probably due to the shield from shear that is offered by rough surfaces (van Loosdrecth *et al.*, 1995).

In order to attach, planktonic cells must be able to 'sense' when they are close to a surface. It is known that planktonic bacterial cells release both protons and signalling molecules as they move through bulk fluids. When approaching a surface, a relative concentration difference on the side of the bacteria closest to the surface develops which might be the way that bacteria register surfaces (Costerton, 1999a). The first attachment to a surface is reversible, and it is observed that bacteria appear to 'explore' the surface by different species-specific behaviour, e.g. by rolling, before proceeding to the next step of irreversible adhesion. Within a few minutes after committed adhesion, cells upregulate specific genes coding for enzymes involved in the synthesis of EPS. The attached cells initiate the formation of discrete microcolonies that form the basic organisational units of biofilms (Costerton, 1999a).

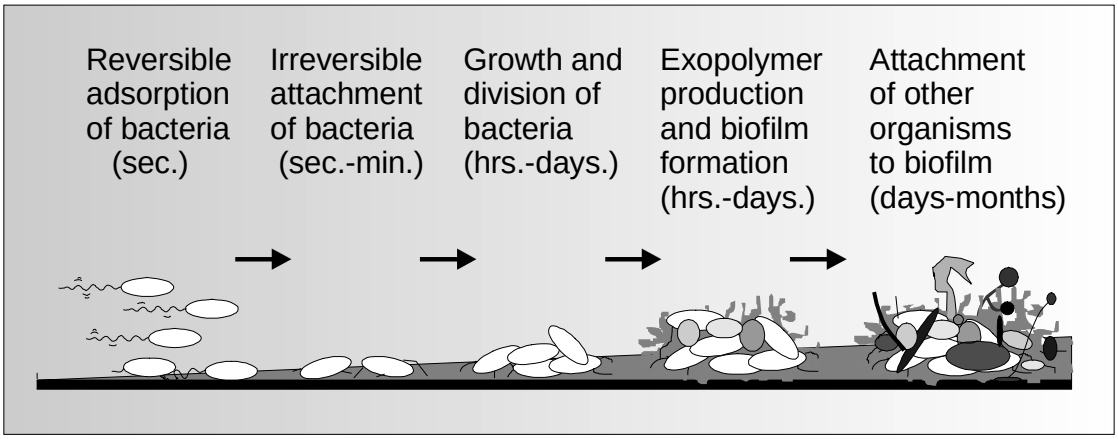

Figure 2.9. A series of steps proceed biofilm formation. First a few cell are attached, these start producing EPS, more cells attach, and a biofilm community develops. (Reproduced from ASM, 2000).

Once anchored to a surface, biofilm microorganisms carry out a variety of detrimental or beneficial reactions (by human standards), depending on the surrounding environmental conditions. For wastewater treatment, the use of biofilms has been exploited for over a century (Arvin and Harremoës, 1990), but only within the last two decades have the advantages of biofilms come into focus of also other areas of biotechnology, such as the production of bioactive substances; cultivation of plant and animal cells and biosensors (Bryers, 1994; Lazarova and Manem, 1995). More traditionally, biofilms have been the subject of annoyance in many industrial and medical fields, the term biofouling is used for the unwanted growth of biofilms. Figure 2.10 illustrates some of the fields that are concerned with the impacts of biofilms. Bryers, 1994, and Flemming and Melo, 1995, discussed some of the beneficial and detrimental impacts and control measures.
The ubiquitous nature of biofilms makes them a very interdisciplinary issue.

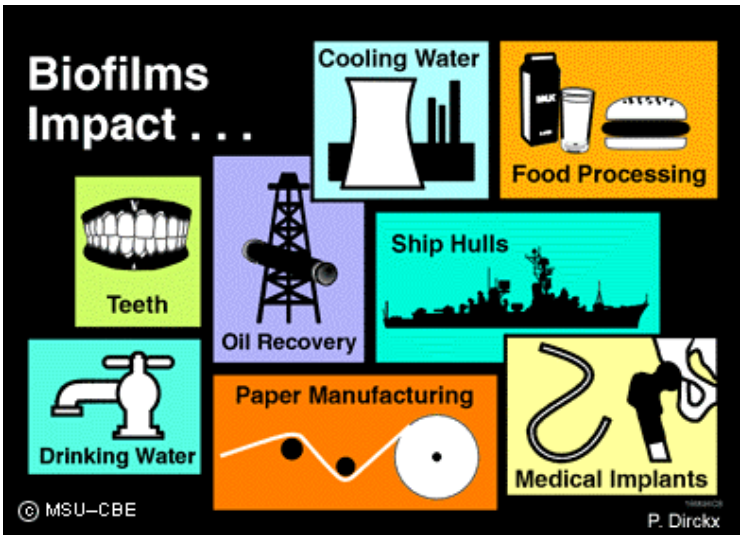

Figure 2.10. In many fields of industry and medicine, biofilms are deleterious and extensive efforts are committed to their removal/prevention. (CBE, 2000).

2.3.4 Biofilm Structures

The structure of biofilms has been a hot scientific topic during the 90'es and until today. The original perception, that biofilms are structurally homogeneous with little variation of biofilm properties such as porosity, pore size distribution, density and microbial populations, was mainly based on light microscopy with limited resolution and on scanning electron microscope which demanded the biofilm to be dehydrated before examination. Once the confocal laser scanning microscope (CLSM) was introduced, it became possible to non-destructively examine successive focal planes of living, hydrated biofilms (Lawrence *et al.*, 1991). A comparison of different microscopic methods for the examination of biofilms is supplied by Stewart *et al.*, 1995, and Surman *et al.*, 1996. The result of the new methods was a dramatic change of the biofilm view.
The conceptual biofilm structure model developed by Costerton *et al.*, 1994, from CLSM observations (Fig. 2.11) is today well known. It predicts the growth of microorganisms in a mushroom-shaped manner. The microcolonies are situated in the top of these 'mushrooms' with a stalk of EPS and microorganisms constituting the binding link to the surface. Some of the mushrooms might fuse together, but leaving water channels open so that water from the bulk can penetrate most of the biofilm via convective flow. Water channels inside biofilms have been directly observed by tracking fluorescent particles using a combination of CLSM and normal optical microscopy (Stoodley *et al.*, 1994).
Costerton, 1995, defined biofilms as 'the highest phenotypic expression of the bacterial genome' and inferred that the mushroom biofilm structure was no accidental structure, but directed according to growth control of the inhabiting

bacteria by complex cell-to-cell communication including quorum sensing (Davies *et al.*, 1998). This assumption was supported by the significant change of bacterial gene expression when attached to a surface. He assumed the mushroom-structure to be a general growth mode for all biofilms, however, this assumption has subsequently been questioned by other researchers (Bishop, 1997; van Loosdrecht *et al*, 1995; Wimpenny and Colasanti, 1997).

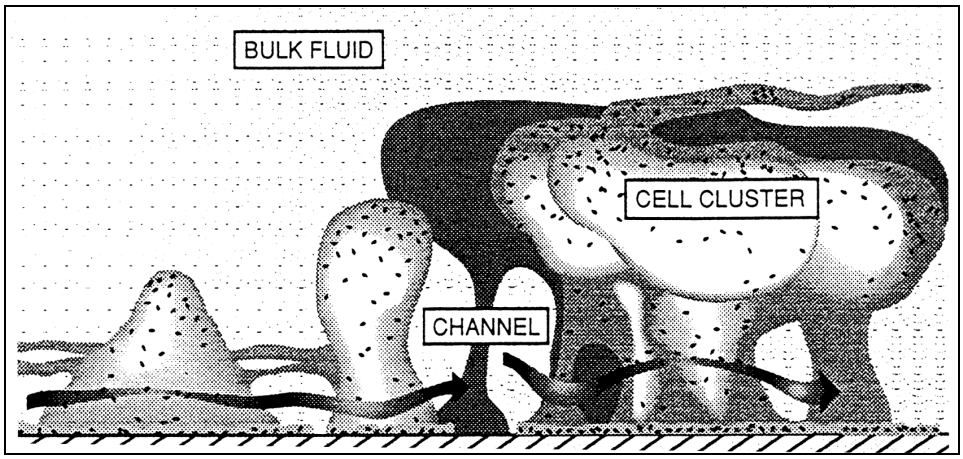

Figure 2.11. The 'Mushroom' model of biofilm structure. Costerton *et al.*, 1994.

Bishop, 1997, summarised some shortcomings of the biofilm investigations with CLSM. Mainly relatively thin, young biofilms have been studied due to the limited penetration depth of the laser light, maximum ~200 μm. Hence the biofilms might not have had the time to develop into more mature biofilms. Many wastewater treatment biofilms are up to 2 mm thick, i.e an order of magnitude thicker than most studied films. Large porous structures have not been reported in these thick films, and microelectrode studies of dissolved oxygen (D.O.) profiles with depth have not shown internal increases of D.O. concentrations which would be expected in a porous film with channels separating biomass clusters. Bishop speculated and cited references to support the idea, that these thick films possibly began as microclusters separated by voids, but with time these colonies overlapped and grew together to form a continuous biofilm. Another aspect of criticism is that most of the investigated biofilms were monocultures or a consortium of only two or three species, whereas biofilms in wastewater treatment systems are formed by a complex mixed culture. It is possible that the species in a monoculture do form and maintain channels between microcolonies, but in a mixed culture other species eventually fill in these channels making the mature biofilm more continuous.

van Loosdrecht *et al.*, 1995, suggested the ratio between biofilm surface loading and shear rate to be the essential environmental factor determining the steady-

state biofilm structure. Additionally, characteristics of the individual organism, such as yield and growth rate, play a role. Based on experimental observations of biofilm formation in a BAS reactor, they concluded that high loading and low shear lead to highly heterogeneous structures with many pores and protuberances, Fig. 2.12-right, whereas low loading and high shear result in thin, patchy biofilms. With an appropriate ratio, relatively smooth biofilms can be obtained.
Basically biofilms tend to become heterogeneous structures, but this is in most systems balanced by shear forces (causing detachment). For biofilms of slow-growing organisms – slow due to either physiological, e.g. nitrifiers, or substrate limitation - the proturbances will erode before they can reach macroscopic proportions, leading to the formation of a smooth biofilm. In contrast, if shear rate is low, heterogeneous structures can develop, which eventually lead to instability and sloughing as observed in e.g. trickling filters. Biofilm density seems to be influenced similarly with formation of denser structures for higher shear. Newly formed biomass volume generally has relatively low density (Peyton, 1996). If proturbances prevail, most substrate is consumed by bacteria situated in these with less substrate remaining for the base biofilm and hence no increase of the base density. In contrast, if shear forces rapidly erode proturbances, substrate can diffuse into the 'older' biofilm, where growth of cells increases the biofilm density.

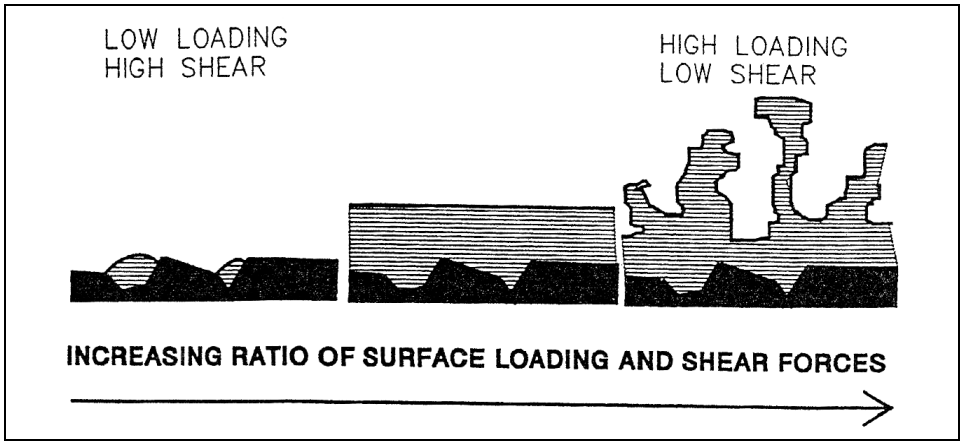

Figure 2.12. Dependence of biofilm structure on loading and shear rate. van Loosdrecht *et al.*, 1995.

Wimpenny and Colasanti, 1997, discussed different extremes of biofilm structures. They considered 3 distinct biofilm structures:

1) *The water-channel model* - alias the "Mushroom" model by Costerton *et al.*, 1994, Fig. 2.11.

2) *The heterogeneous mosaic biofilm model*. This model predicts a biofilm structure made of a thin, cohesive film (~5 μm) from which separated stacks of microcolonies extend, Fig. 2.13. This model stemmed from observations of biofilms in drinking water systems.
3) *The dense biofilm model*. This is the original perception of biofilms with a relatively smooth surface and without noteworthy channels, Fig. 2.12-middle.

They supplied examples of observations of dense biofilms without apparent internal water channels (dental plaque, biofilms on inner surfaces of medical catheters), that were characterised by high nutrient availability. Additionally they developed a biofilm 'cellular automaton' (CA) model to predict biofilm development based on a simple set of rules (diffusion, growth rate, substrate concentration etc.). They found that the most compact structures formed during high substrate availability, and inferred from their findings, that whenever a mushroom structure is observed, this is most likely accidental and based solely on diffusion limitation as a mechanism. The reason for proturbances to form is diffusion limitation in areas of high cell density (due to high substrate consumption). New cells grow in the direction of higher substrate concentrations, i.e. towards lower cell density, i.e. upwards instead of horizontally. The findings were in line, but not in full agreement with van Loosdrecht *et al.*, 1995. van Loosdrecht *et al.*, 1997b, pointed out, that the model of Wimpenny and Colasanti suffered from not including detachment processes.

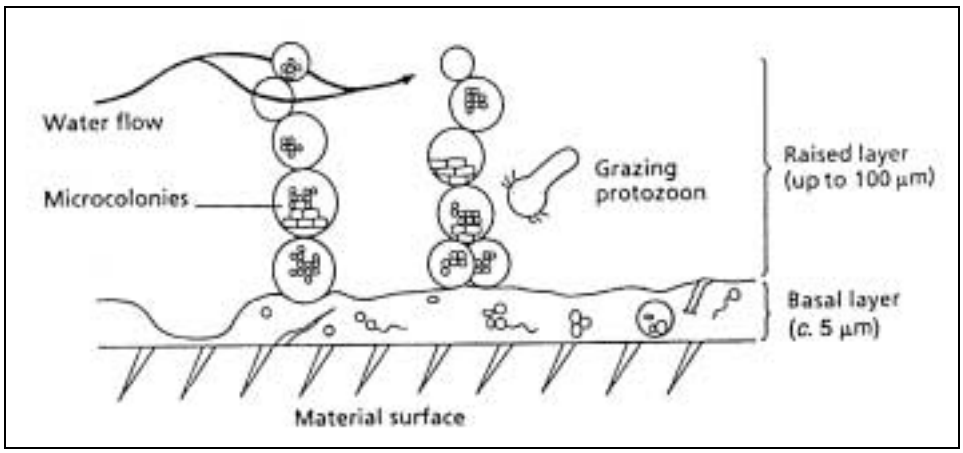

Figure 2.13. The heterogeneous mosaic biofilm model. Based on observations of biofilms in drinking water distribution systems. Wimpenny and Colasanti, 1997.

Table 2.9 illustrates the result of a brainstorming session at the first international workshop on "Biofilms in aerobic wastewater treatment: An interdisciplinary

approach", arranged by the Research Center for Fundamental Studies of Aerobic Biological Wastewater Treatment (SFB 411), TUM, Munich, Germany, Oct. 1998. Much dispute ruled regarding the *most* important factors for biofilm structure, however, some agreement was reached that: Microbial population, hydrodynamics/shear, substrate type, concentration and kinetics, and physico/chemical properties of the environment were major factors.

Table 2.9. Brainstorming session at the SFB411 Biofilm Workshop in Munich, Germany, Oct. 1998.

What are the most important factors determining biofilm structure and hence transport processes within?

- EPS
- Detachment
- Mass transfer
- Physiology of cells
- Cell-to-cell interactions
- Internal structure of the biofilm
- Particulate matter
- Morphology of the biofilm
- Structure depends on the scale observed
- **Microbial population**
- Microbial distribution
- Grazing activity
- **Hydrodynamics/shear**
- **Substrate type**
- **Substrate concentration and kinetics**
- Electrostatic behaviour of the environment
- **Physico/chemical properties of the environment**
- Type of substratum
- Roughness of substratum

The new, innovative microbial characterisation methods have been used for investigations of a wide variety of biofilms: drinking-water pipes (Manz *et al.*, 1993), sulphate-reducing bacteria in anaerobic fixed-bed reactors (Amann *et al.*, 1992), nitrifiers in different biofilms (Biesterfeld *et al.*, 1998; de Beer and Schramm, 1999; Schramm *et al.*, 1996), the rumen of animals (Stahl *et al.*, 1988), hot spring microbial mats (Ferris *et al.*, 1997) etc. The possibilities are boundless due to the infinite types of biofilms. In order to obtain information on distribution of different bacterial species in a thick biofilm, a microsectioning method is necessary. The cryo-cutting method described by Kristensen and Christensen, 1982, is suitable for this purpose. Often, the molecular characterisation techniques are combined with microelectrodes as first reported by Ramsing *et al.*, 1993. In this way, it is possible to obtain both information of the spatial distribution of different organisms as well as their metabolic function in the biofilm. A zonated biofilm structure with redox microniches, e.g. sulphate reduction in aerobic systems, has been verified in several investigations with microelectrodes (Okabe *et al.*, 1998; Ramsing *et al.*, 1993; Santegoeds *et al.*, 1998; Yu and Bishop, 1998).

``The great tragedy of Science - the slaying of a beautiful hypothesis by an ugly fact. "

- T. H. Huxley 1825-95: Collected Essays (1893-4)
'Biogenesis and Abiogenesis'

2.3.5 Biofilm Detachment

Detachment is by definition balancing the growth of a biofilm in steady-state (Trulear and Characklis, 1982; van Loosdrecht *et al.*, 1995). For this reason, it is important to distinguish between non-steady and steady-state biofilms when discussing detachment. A growing biofilm adapt to the prevailing detachment forces of a given environment until a steady-state film structure, less susceptible to detachment forces, is obtained. The mechanisms for adaptation are not clear. However, for this reason, a distinction should also be made regarding detachment for an active versus a non-growing (Gjaltema *et al.*, 1997b) biofilm subjected to identical detachment conditions as discussed by Kwok *et al.*, 1998. Experimental findings by Tijhuis *et al.*, 1996, and Kwok *et al.*, 1998, confirmed the hypothesis regarding biofilm structure proposed by van Loosdrecht *et al.*, 1995 (previous section).
Detachment can be defined as the transport of particles from the attached solid matrix into the fluid phase. Attachment can be considered as a separate process or included in the detachment, leading to a net detachment rate. 5 different types of detachment exist (Fig. 2.14):

1) Erosion – removal of small groups of cells from the surface, caused by shear forces of the moving fluid.
2) Abrasion – removal of small groups of cells from the surface as a result of collision with particles, e.g. in fluidised bed or biofilm airlift reactors, or during backwash of fixed beds.
3) Sloughing – removal of big cloaks of biofilm pieces as a cohesive mass, sometimes exposing the bare substratum.
4) Predator grazing.
5) Human intervention.

Detachment mode of bacterial cells from a biofilm has been the focus of several investigations, however without resulting in one definitive relationship in the form of a single mathematical formula covering a wide range of conditions. Stewart, 1993, and Morgenroth, 1998, summarised some of the empirical mathematical expressions that are found in the literature, Table 2.10. Generally, dependencies on: biofilm thickness (L_f), shear stress (τ), growth rate (μ), biofilm volumetric mass density (ρ_f) and biomass concentration (X) have been applied.
Most biofilm models found in the literature incorporate a continuous detachment process, but as discussed by Morgenroth, 1998, this might be appropriate for many natural biofilm systems or for unwanted biofilms where detachment mainly is caused by shear of the fluid. However, this is no reasonable approach for wastewater treatment processes where regular backwash is used as an integrated part of the process for biofilm thickness control. For this case, Morgenroth defined a detachment rate of zero during

normal operation and a detachment function removing all biomass above a set thickness during backwash. Detachment is of particular importance for EBPR with biofilms, since backwash (removal of biomass) is the only way of removing phosphate from the system (Morgenroth and Wilderer, 1998). This aspect shall be addressed in more detail later.

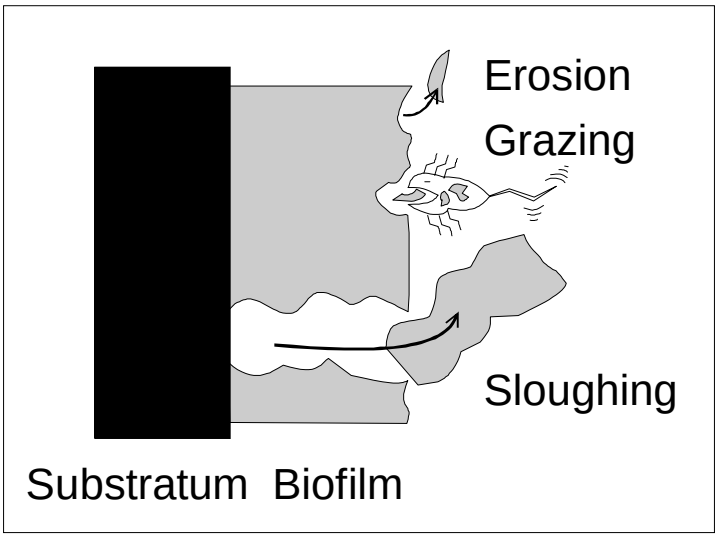

Figure 2.14. Different types of detachment from biofilms.

Table 2.10. Examples of empirical mathematical formulas used to describe biofilm detachment rate. (Modified from Stewart, 1993, and Morgenroth, 1998).

Expression	Reference
$k_d * \tau * \rho_f$	Bakke *et al.*, 1990
$k_d * X_f^2$	Bryers, 1984
$k_d * \rho_f * L_f$	Kreikenbohm and Stephen, 1985
$k_d * \rho_f * L_f * \tau^{0.58}$	Rittmann, 1982
$L_f * (k_d + k_d' * \mu)$	Speitel and DiGiano, 1987
$k_d * \mu_s * \rho_f * a^2$	Stewart, 1993
Constant biofilm	Wanner and Gujer, 1984
$k_d * \rho_f * L_f^2$	Wanner and Gujer, 1986
0 during normal operation $k_d * (L_f - L_{base\ thickness})$ during backwash	Morgenroth, 1998

k_d and k_d': detachment coefficients, ρ_f : biofilm volumetric mass density, L_f : biofilm thickness, τ: surface shear stress, (μ_s) μ: (maximum specific) growth rate, a: dimension of the growth zone in the biofilm, X_f : biomass concentration, $L_{base\ thickness}$: biofilm thickness after backwashing.

2.3.6 Advanced Computer Aided Biofilm Modelling

2-D cellular automaton model: Hermanowicz, 1998, presented a two-dimensional cellular automaton model similar to the one of Wimpenny and Colasanti, 1997, however with detachment included. Detachment was modelled using proportionality to the shear strength versus biofilm strength. Via relatively simple mathematical rules, he included influences from the factors: Diffusion as the transport process, the liquid boundary layer thickness between the bulk fluid and the biofilm surface, liquid shear stress and biofilm strength. From these few rules, all reported biofilm structures could be predicted, from the very dense over a mushroom and into a stalk-like structure. Results of 3 simulations are shown in Fig. 2.15a-c. The biofilm structure is shown in the lower left corner with biomass in black and water in white. The other three parts of each figure show the cell growth rate, substrate concentration and cell age with a white colour representing the highest value.

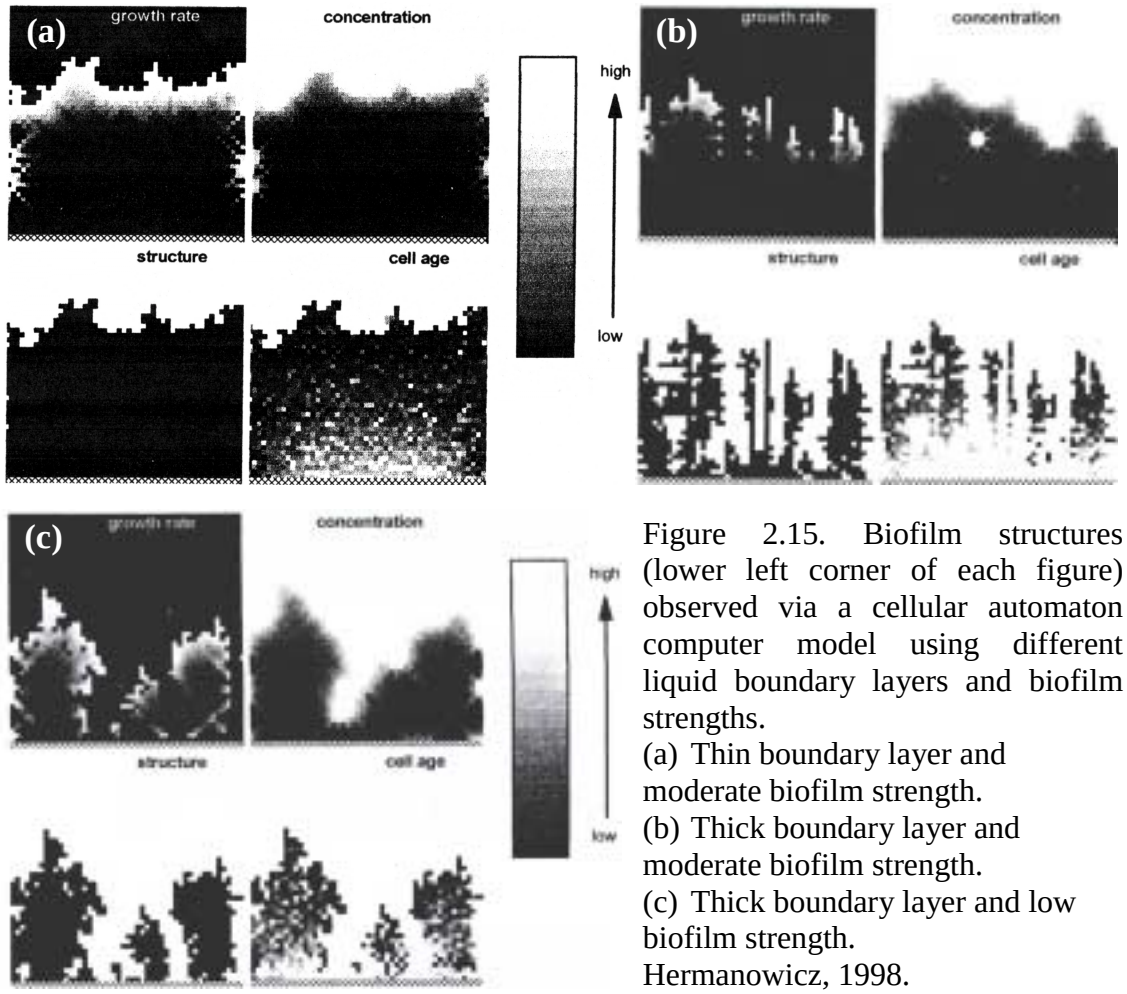

Figure 2.15. Biofilm structures (lower left corner of each figure) observed via a cellular automaton computer model using different liquid boundary layers and biofilm strengths.
(a) Thin boundary layer and moderate biofilm strength.
(b) Thick boundary layer and moderate biofilm strength.
(c) Thick boundary layer and low biofilm strength.
Hermanowicz, 1998.

The determining factor was identified as the external mass transfer. When significant external mass transfer was present (simulated by a high boundary layer), open structures developed. The biofilm strength determined the appearance of the open structure, moderate strength led to a stalk-like structure (Fig. 2.15b), whereas lower strength resulted in a mushroom-like structure (Fig. 2.15c). If the biofilm had a moderate strength, and the boundary layer was thin, a dense, homogeneous structure with a relatively smooth surface developed (Fig. 2.15a). Hermanowicz, 1999, made an additional study of the effect of the bulk concentrations of substrate. Still, the liquid boundary layer was found to be the major factor, however at some conditions dramatic changes could occur even for small changes in the bulk concentration.

3-D cellular automaton model: One step further from the 2-D to 3-D models based on the cellular automaton approach was made by Picioreanu *et al.*, 1998ab, 1999, and Noguera *et al.*, 1999a. The principle of this type of modelling of a biofilm is the mathematical description of space as made up of small, cubic boxes, Fig. 2.16. The individual cubes contain biomass, water in the liquid boundary layer or bulk water. According to a set of mathematical rules, the individual cells respond in a defined way to environmental inputs.

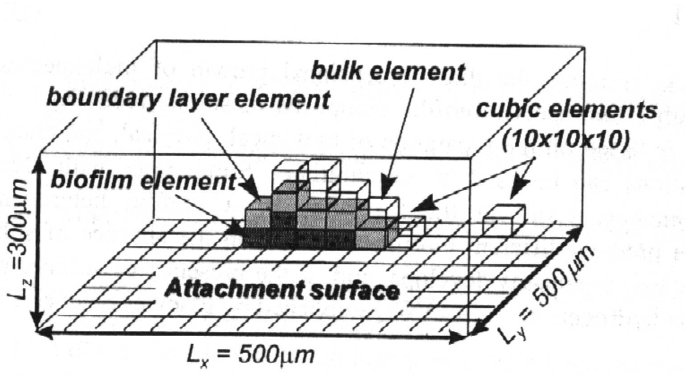

Figure 2.16. Schematic 3-D modelling of biofilms via cellular automaton is based on a mathematical description of the physical domain as made up of small cubes. These cubes can be filled with biomass, water in the boundary layer or the bulk water. Noguera *et al.*, 1999a.

The complexity of 3-D models demand for high-speed computers and long calculation times. In order to achieve reduction in complexity (simulation time), it is useful to apply a time-scale analysis. Some reactions can be considered in a pseudo-equilibrium, while calculating phenomena of other time-scale regions, Fig. 2.17 (Picioreanu *et al.*, 1999).
The potential of 3-D models in illustrating biofilm development and structure depending on different environmental factors is colossal. However, as stated in a recent biofilm models status report of Noguera *et al.*, 1999b, the interaction

between mathematical modelling and experimental verification cannot be overemphasised. This bridge has not yet been completed. An example of the result of a 3-D model simulating evolution in time of a two-species biofilm grown on a spherical carrier is shown in Fig. 2.18. For more details on the 3-D models is referred to the original papers.

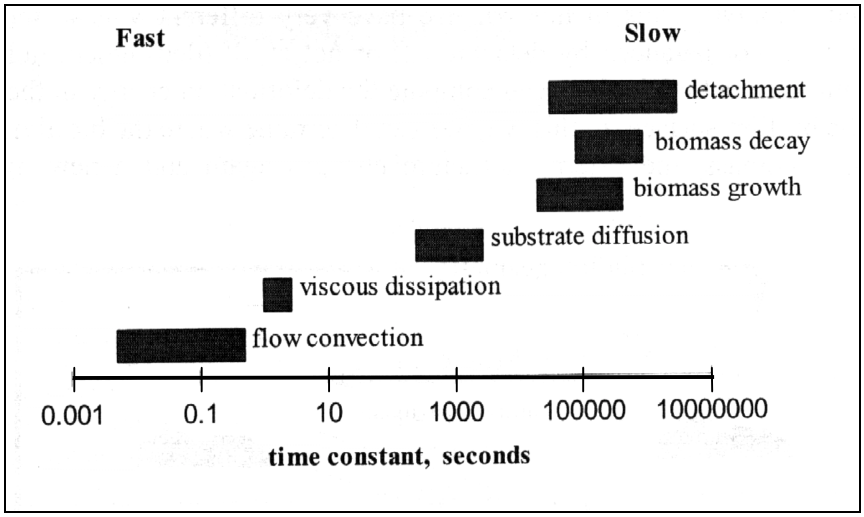

Figure 2.17. Illustration of reactions of different time-scales involved in biofilm models, Picioreanu *et al.*, 1999.

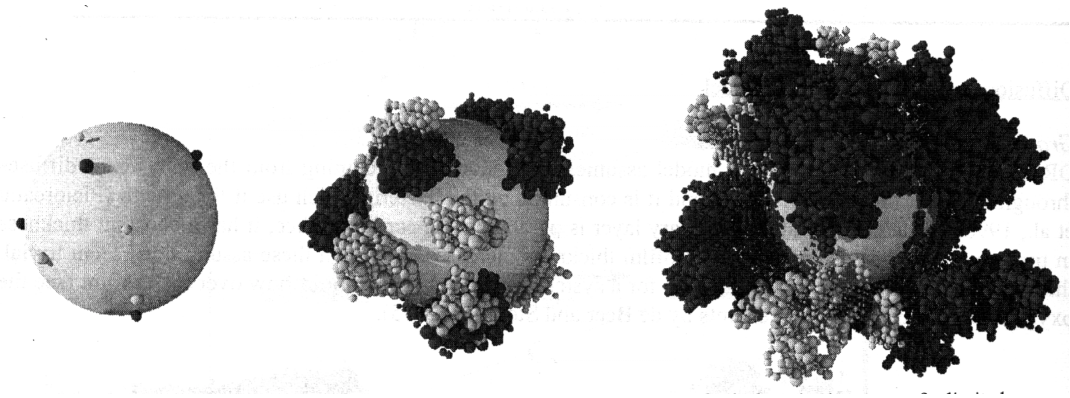

Figure 2.18. Simulated evolution of a two-species biofilm grown on a spherical carrier under mass transfer limiting conditions. Picioreanu *et al.*, 1999.

Examples of other advanced models: Rittmann *et al.*, 1999, developed a 3-D model that was used to study the effect of clusters on substrate flux in a biofilm. An interesting result was that a cluster-channel (mushroom) structure might create a competitive disadvantage for slow-growing organisms, such as nitrifiers or species specialised in degradation of xenobiotics. The reason was a reduction in the volume of micro-niches with depletion of substrate for the fast-growing

organisms (such as organic matter for aerobic heterotrophs) due to diffusion into the cluster from all sites of the cluster exposed to channels with convective flow.
Bungartz *et al.*, 2000, combined 3-D mathematical simulation and image analysis with experimental microscopic observations of a real biofilm to investigate the effect of biofilm structure on fluid flow.
Xavier *et al.*, 2000, used computer modelling to determine 2- and 3-D 'developmental axis' during biofilm formation. Real biofilms were observed microscopically. The fractal dimension of axial branching was used to quantify the level of structural complexity. It was found, that most of the biofilm was characterised by a well-defined and constant pattern of linear branching in all measured scales. During biofilm formation, biofilm clusters individually branched upwards. The tips of the branching axis did not cross, whereby the diffusion channels between cell clusters were kept open, reflecting structural optimisation of access to the liquid medium. Different diffusion/hydrodynamics were not discussed.

'Quantification' of Biofilm Structure: A problem regarding description, comparison and modelling of biofilm structure is the difficulty regarding characterisation and "quantification" of biofilm structure. Lewandowski *et al.*, 1999, summarised some of the parameters that hitherto have been used: density, porosity, specific surface area, mean pore radius, fractal dimension, surface roughness, compactness, cluster size and shape etc. They suggested 4 parameters to be general applicability for quantitative description of biofilm structure. These had the quality of reaching steady state along with the biofilm as verified experimentally:

1) *Textural Entropy*
2) *Areal Porosity*
3) *Fractal dimension*
4) *Maximum diffusion distance*.

The values are determined from horizontal layers of the biofilm obtained by confocal laser scanning microscopy. For description of the 4 parameters is referred to the source.

2.3.7 Which Biofilm Model is The Best?

In the context of the IAWQ Specialty Conference on "Microbial Ecology of Biofilms: Concepts, Tools and Applications", held in Lake Bluff, Illinois, USA, Oct. 1998, a specialist group was selected for a discussion of the present status and future directions of biofilm modelling. A summary report of this meeting was supplied by Noguera *et al.*, 1999b. Many of the people represented at this meeting, met again the following month at the first "International Workshop on Biofilms in Aerobic Wastewater Treatment: An interdisciplinary Approach"

held in Munich, Germany and arranged by SFB411. A book from this workshop is expected this year and shall contain several papers discussing different modelling approaches.

An illustration of the development of biofilm models over the last 3 decades is given in Fig. 2.19. Model complexity is a direct reflection of the advances in computational tools. In the 70'es, 1-D models of a completely homogeneous biofilm (Atkinson and Favies, 1974; Harremoës, 1978) dominated. These models consisted of simple algebraic equations, which described the spatial profile of a substrate in the biofilm and which could be evaluated by the simple means of a pocket calculator (Wanner, 1998). In the 80'es these were refined to stratified, dynamic 1-D models including multisubstrate-multispecies biofilms (Wanner and Gujer, 1986). These models were based on a set of differential equations and demanded for numerical calculations by computers. A computer software program, AQUASIM, for these models was developed by Reichert, 1994, and made available for biofilm research. This program has gained significant appreciation world-wide and is under constant development according to new experimental findings, however the 1-D approach is maintained (Wanner and Reichert, 1996). The 90'es were the decade of multi-dimensional models as described in the previous section.

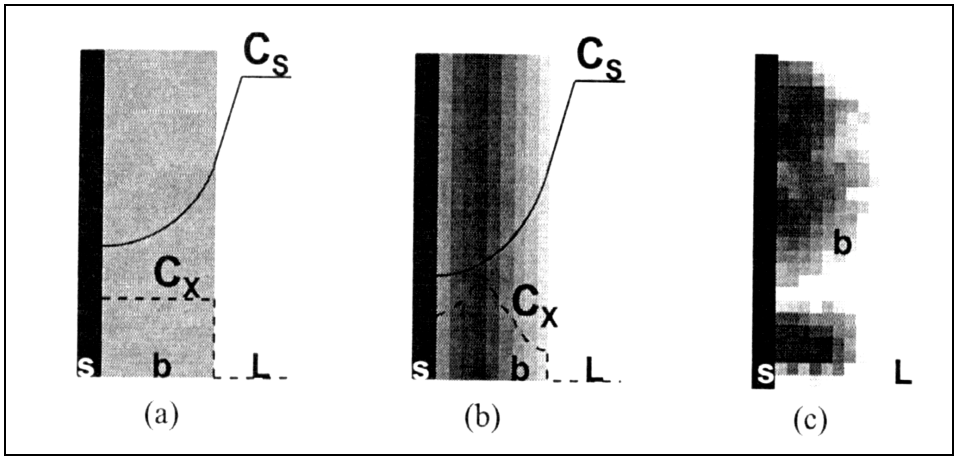

Figure 2.19. Evolution of biofilm models from (a) uniform biomass distribution and 1-D substrate gradient in the 70'es, to (b) 1-D stratified biomass and multisubstrate-multispecies biofilms in the 80'es, to (c) complex multidimensional models at the end of the 90'es. s: substratum, b: biofilm, L: bulk liquid, C_s: substrate concentration and C_x: cell concentration. Noguera *et al.*, 1999.

One could now ask oneself: Which is the BEST model? However, one quickly reaches the conclusion that no answer can be given, since the best model depends on the modelling objectives.

The golden rule of modelling:

'Models should be as simple as possible and as complex as needed'

- Oskar Wanner, 1998

Wanner, 1998, discussed model selection. Looking at the model evolution, it is evident that all the models are based on the same physical principles and that progress primarily meant increased complexity. Modelling objectives should be evaluated on the desired scale of modelling – which are the relevant properties and dominant processes in a given situation? Possible simplifications should be evaluated, especially considering the available data base. The less simplifying assumptions made, the more realistic the model, but the more information, i.e. data, is needed. There is little point in including a wide set of parameters into a model if these in practise are impossible to observe/measure.
Bishop, 1997, commented that if the heterogeneous 3-D structure of a biofilm is a general trend, it is likely that biofilm property variability will need to be averaged to overcome the non-predictable in-homogeneities. Modelling of the biofilm kinetics may need to be done on a macro-, rather than a micro-scale, especially if the modelling aims at practical purposes (Bishop and Rittmann, 1995).
Biofilm models may broadly be classified into two categories (Noguera *et al.*, 1999b) according to their objectives (Fig. 2.20):

1) Models for *practical engineering* applications, such as design, troubleshooting, real-time operation and education.
2) Models as *research tools* for developing further understanding of specific biofilm phenomena, such as biofilm structure, population dynamics and structural heterogeneities.

Despite the very different kinds of models and experimental findings discussed in the previous sections, one factor stands out as of common and all-determining influence: the transport via molecular diffusion. Whether this be from the surface and inwards through a dense biofilm, or from an internal channel into a dense cluster (de Beer and Stoodley, 1995). As suggested by Morgenroth, 1998, and Morgenroth *et al.*, 2000, it is possible to break a multi-dimensional biofilm model into smaller 1-D pieces, where diffusion perpendicular to the surface is the main transport process. This can e.g. be illustrated by Fig. 2.21. Here iso-oxygen-curves and oxygen gradients (arrows) of a heterogeneous biofilm are shown based on microelectrode measurements, de Beer *et al.*, 1994. For evaluations of basic phenomena of a biological process dependent on redox zones, such as EBPR, the use of a 1-D diffusion based model can be a valuable tool as shown by Morgenroth, 1998. Regarding predictions of layered structures of relatively dense films and for studying competition between microbial

species, 1-D model concepts were often in good qualitative agreement with many experimental studies (Wanner, 1995). The 1-D diffusion controlled biofilm model is for these reasons selected for more description in the next section.

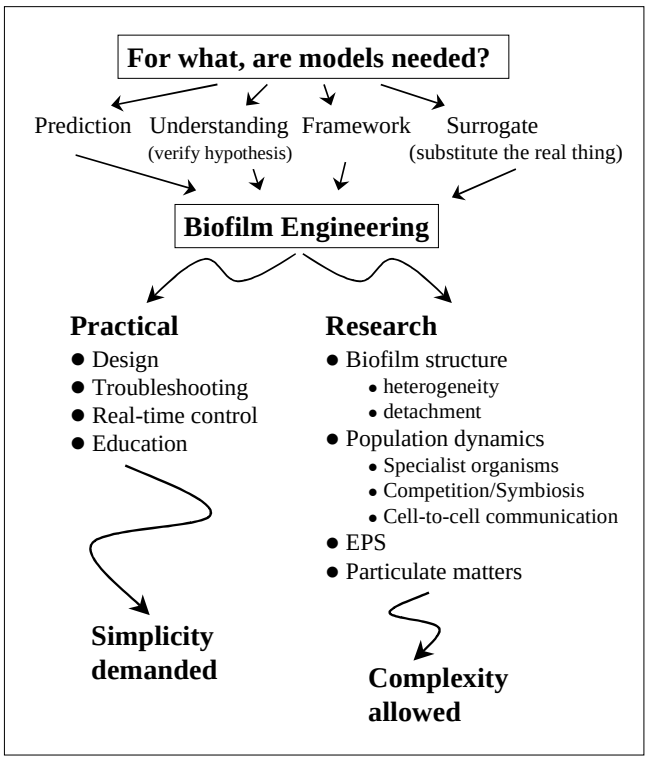

Figure 2.20. Model selection has to be made according to the modelling objectives. A more complex model is far from always the best choice.

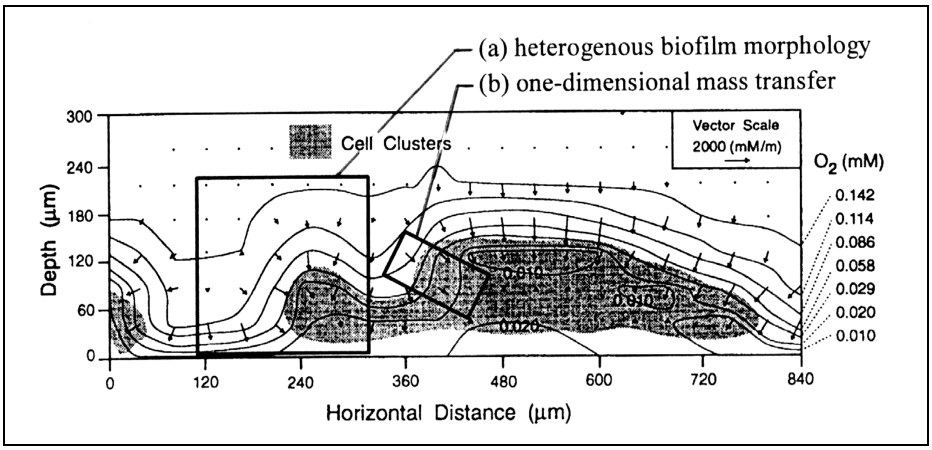

Figure 2.21. A heterogeneous biofilm structure (a) may be approximated by a sum of 1-D slices. Transport of compounds in each slide is controlled by 1-D diffusion from one layer to the next, with concentration gradients perpendicular to the individual layers (b). Morgenroth, 1998 - based on microelectrode measurements by de Beer *et al.*, 1994.

2.3.8 One-Dimensional Diffusion Model

2.3.8.1 Fick's Law and Concentration Profiles

Diffusion of substances into and out of a biofilm is assumed to be controlled by molecular diffusion described by Fick's first Law, refer to Fig. 2.22:

$$N = -D \cdot \frac{\partial S}{\partial x} \tag{2.1}$$

- N is the transport of substance through an infinitesimal slice of the biofilm
- D is the diffusion coefficient
- S is the concentration of the soluble substance
- x is a position co-ordinate (zero at the surface of the film)

A mass balance of the slice gives:

$$\text{In} + \text{Produced} = \text{Out} \tag{2.2a}$$

$$N + r_f \cdot dx = N + \left(\frac{\partial N}{\partial x}\right) \cdot dx \tag{2.2b}$$

$$r_f = \left(\frac{\partial N}{\partial x}\right) \Leftrightarrow \frac{\partial^2 S}{\partial x^2} = \frac{-r_f}{D} \tag{2.2c}$$

- r_f is the reaction rate inside the biofilm

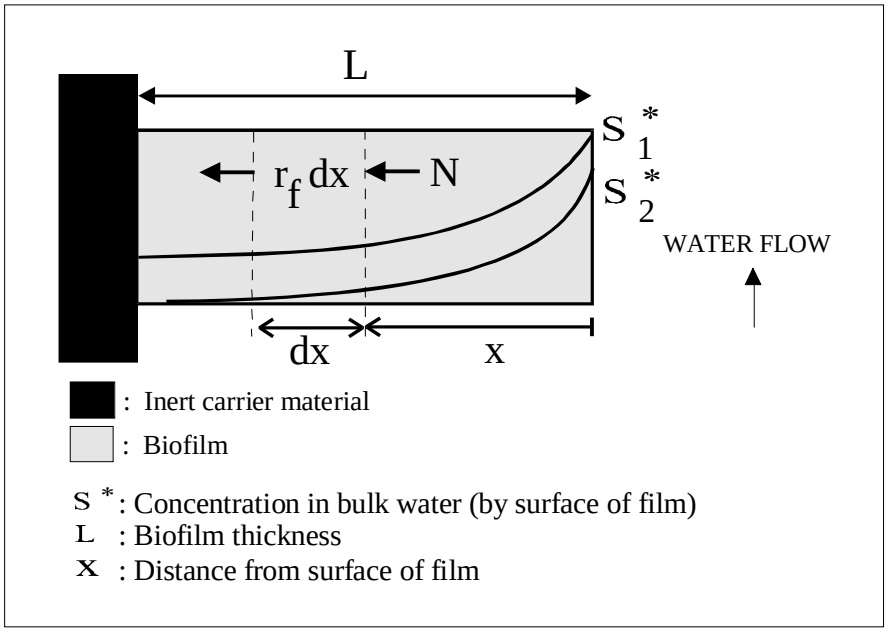

Figure 2.22: Diffusion of two substrates into a biofilm. Refer to the text for a mass balance.

A detailed theory of Fick's law and diffusion in biofilms can be found elsewhere (Harremoës, 1978; Henze *et al.*, 1997) and will not be given here. The main features in regard to concentration profiles and what these will look like are (Fig. 2.23):

1) By the bottom of the biofilm (x = L), the profile will be perpendicular to the carrier material, since no transport can take place into the inert carrier material, that is dS/dx = 0.
2) Curves will be smooth and breakpoints can only occur in case of changes in the diffusion coefficient, that is dS/dx (x^+) = dS/dx (x^-) unless change in D. Change in D happens at the biofilm surface since diffusion generally is lower in biofilms compared to water.
3) In case of production in the biofilm, $r_f > 0$ equal to $d^2S/dx^2 < 0$, the curve will be *convex*. For transport of the product out of the film (unless involved in other reactions) the concentration in the biofilm must be higher than the bulk concentration.
4) In case of removal in the biofilm, $r_f < 0$ equal to $d^2S/dx^2 > 0$, the curve will be *concave*. For transport of reactant from the bulk water in to the film, the concentration in the bulk water must be higher than inside the film.
5) In case of no production or removal, $r_f = 0$ equal to $d^2S/dx^2 = 0$, the curve will be *liniar* (but not always horizontal).

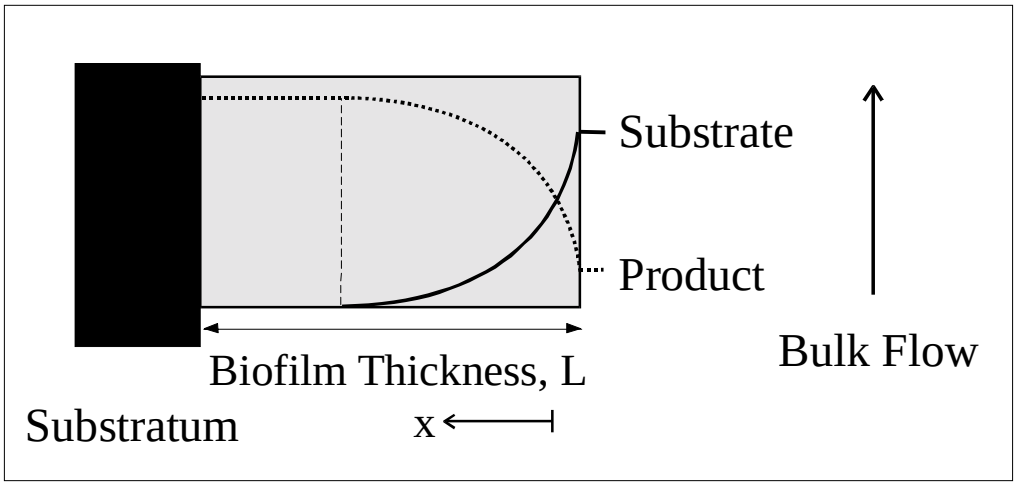

Figure 2.23: The shape of concentration profiles inside a biofilm depend on the reaction that the compound is involved in – production, removal or no reaction.

2.3.8.2 Penetration Depth and Limiting Substrate.

For a reaction to take place inside a biofilm, diffusion into the biofilm of both the electron acceptor and the electron donor are required. In the case where at least one of the substrates does not fully penetrate the biofilm, we are talking

about diffusion limitation, and the substrate that penetrates shortest into the biofilm is called the limiting substrate.
The intrinsic process in the biofilm is assumed to follow Monod-type kinetics, but as stated by Jansen and Harremoës (1984), the Monod constant is low in many cases, so the reaction rate within the biofilm for practical applications can be considered as a zero order of reaction.

How deep a substrate will penetrate the biofilm is determined by the relative penetration depht, β, which is calculated (Henze *et al.*, 1997):

$$\beta = \sqrt{\frac{2 \cdot D \cdot S}{(k_{0f} \cdot L^2)}} \qquad (2.3)$$

- D is the diffusion coefficient
- S is the concentration of the soluble substance at the surface of the film
- k_{0f} is the zero order rate constant inside the film
- L is the biofilm thickness

If β > 1 the film is fully penetrated for the considered substrate concentration, and if β < 1 the film is only partly penetrated.

Which of two redox components that will be the potential rate limiting substrate is determined by the relationship between the diffusion coefficients and zero order rate constant of the two components (Henze *et al.*, 1997):

$$\frac{C^*_{acceptor}}{C^*_{donor}} \lessgtr \frac{D_{donor}}{D_{acceptor}} \cdot \frac{k_{0,acceptor}}{k_{0,donor}} = \frac{D_{donor}}{D_{acceptor}} \cdot \frac{1}{\nu_{acceptor,donor}} \qquad (2.4)$$

If < applies to the equation, the electron acceptor will be the potentially rate limiting substrate, whereas the electron donor will be potentially rate limiting if > applies.

2.3.8.3 Order of Reaction in Bulk Water.
Looking at bulk concentrations, a half or zero order of reaction will be observed. Half order of reaction will appear if the substrate considered is rate limiting. With r_a being the area specific removal rate, the results of the theory can be written:

0. order bulk reaction:

$$r_a = k_{0a} = k_{0f} \cdot L = r_{a,\max} \qquad \text{when} \quad \beta = \sqrt{\frac{2 \cdot D \cdot C^*}{k_{0f} \cdot L^2}} \geq 1 \qquad (2.5)$$

½. order bulk reaction:

$$r_a = k_{\frac{1}{2}\,a} \cdot \sqrt{C^*} = \sqrt{2 \cdot D \cdot k_{0f}} \cdot \sqrt{C^*} \qquad \text{when} \quad \beta < 1 \tag{2.6}$$

The reaction rate in the bulk water can be determined by a mass balance over the reactor:

$$r_A = \frac{(S_{in} - S_{out}) \cdot Q}{A^*} \qquad \left[\text{g} / (\text{m}^2 \cdot d)\right] \tag{2.7}$$

- Q is the water flow and A^* is the surface area of the biofilm

A plot of the removal rate against the square root of the substrate concentration results in a straight line for a ½ order of reaction (partly penetrated film) and a horizontal line for zero order reaction (full penetration), Fig. 2.24. The concentration that lead to transition from ½ to 0 order ($S_{transition}$), can be used to calculate the biofilm thickness, since at this point, $\beta = 1$:

$$\beta = 1 \Leftrightarrow \frac{2 \cdot D \cdot S_{transistion}}{k_{0f} \cdot L^2} = 1 \Leftrightarrow L = \frac{2 \cdot D \cdot S_{transition}}{r_{a,\max}} \tag{2.8}$$

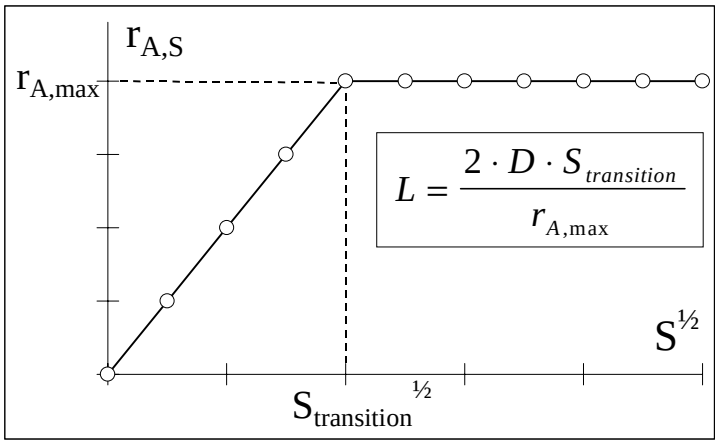

Figure 2.24. Transition from half to zero order of reaction in the bulk water outside a biofilm. By plotting the reaction rate as a function of the square root of the concentration, a ½ order reaction manifests itself in a straight line. For concentrations higher than what fully penetrates the film ($S_{transition}$), a horizontal line occur (0 order) since the removal rate cannot be increased any further.

2.3.9 Zonation in a Biofilm

Evidently from the above, different redox zones can evolve in a diffusion limited biofilm. Figure 2.25 shows an example of development of a zonated

biofilm with aerobic conditions in a zone closest to the bulk fluid, a denitrification zone below and an anaerobic zone without oxygen or nitrate by the bottom of the film.

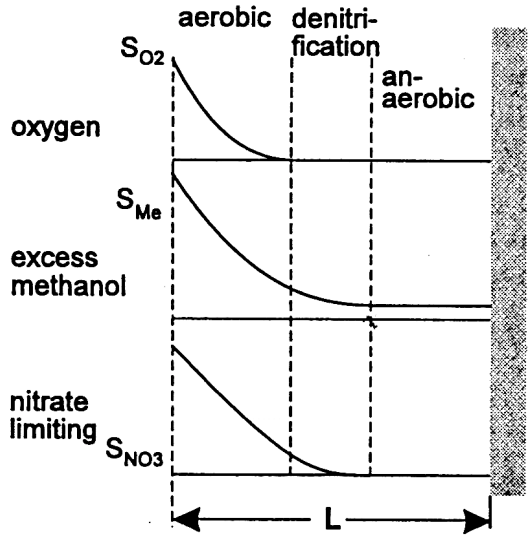

Figure 2.25. Zonation in a diffusion limited biofilm. Riemer and Harremoës, 1978.

Hagedorn-Olsen *et al.* (1994) verified that the denitrification rate of a biofilm decreased according to a linear proportionality with the square root of the oxygen concentration, Fig. 2.26. For an oxygen concentration leading to full penetration of the film ($O_2^{½}$ = 2.45 ⇒ O_2 = 6.0 mg/l), no denitrification took place.

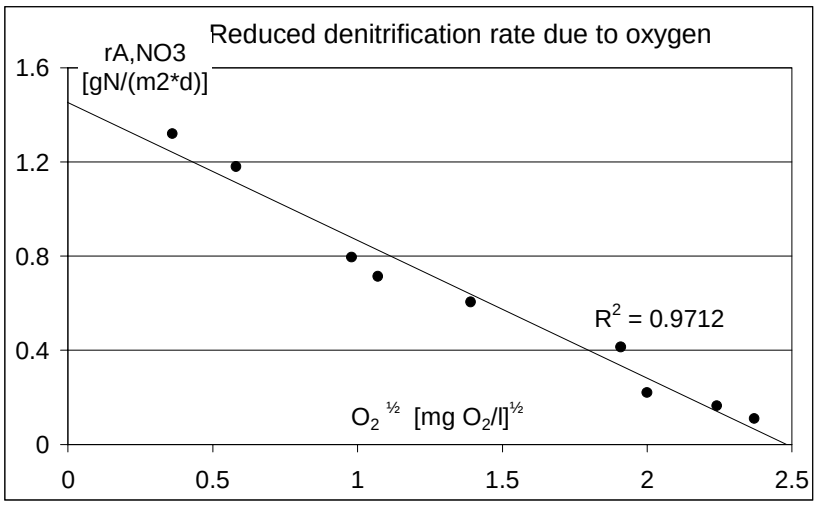

Figure 2.26. Verification of the ½ order bulk reaction theory. Denitrification rate is reduced proportionally to the square root of the oxygen concentration. For a fully aerobic film, $O_2^{½}$ = 2.45 ⇒ O_2 = 6.0 mg/l, no denitrification can take place. Data from Hagedorn-Olsen *et al.*, 1994.

The aspect of redox zones is of particular importance when considering EBPR as discussed in the next chapter.

Methane production, or sulphate reduction resulting in H_2S production or FeS precipitation in bottom, anaerobic zones of a biofilm might cause disintegration of the biofilm matrix (by bubble formation or chemical reactions, respectively) leading to sloughing (Henze *et al.*, 1997; Nielsen and Keiding, 1998). As discussed by Okabe *et al.*, 1998, the sulphur cycle in aerobic biofilms is very complex, since sulphide flux across a biofilm-water interface cannot describe sulphur transformation within biofilms due to an internal sulphur cycle. Sulphate reduction can be anticipated in the deep anaerobic zone of a biofilm. Reoxidation of sulphide with oxygen and/or nitrate would be possible once the sulphide diffuse towards the surface of the biofilm, Fig. 2.27. A substantial part of the oxygen consumption in aerobic biofilms is expected to be caused by this phenomenon (Kühl and Jorgensen, 1992; Norsker *et al.*, 1995).

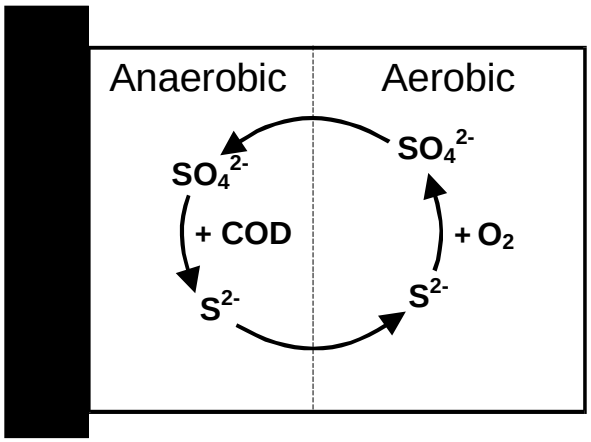

Figure 2.27. The sulphur cycle in a zonated biofilm might account for considerable oxygen (or nitrate) consumption in aerobic wastewater treatment. Sulphate in the deep anaerobic biofilm layers is reduced to sulphide, which diffuse to the outer layers of the biofilm and react with oxygen to form sulphate, which then again might be reduced in the anaerobic zone – the sulphur cycle.

2.3.10 Removal of Particulate Matter in a Biofilm

A situation where a model based on molecular diffusion does not suffice for description of compound degradation in a biofilm, is when considering removal of particulate matter. First, the diffusion of macromolecules into a biofilm is much slower than diffusion of soluble substrates, e.g. the molecular diffusion coefficient of acetate is a factor 10^4 higher than diffusion of a 5 μm particle, and it appears unlikely that particles deposited on a biofilm surface penetrate far into the biofilm matrix, because they will be detained/filtered in the outmost layer of

the film (Bouwer, 1987). This is based on the perception of a biofilm as being dense with no significant channels. As already discussed, also open structures with channels exist and in these, convective flow plays an important role for transport of particles (Reichert and Wanner, 1997). Second, organic macromolecules cannot be assimilated directly by the bacterial cell, but must be hydrolysed into small-molecular-weight compounds (less than ~1000 atomic mass units, amu) by extracellular enzymes before they can be transported across the bacterial cell wall (Confer and Logan, 1997). Confer and Logan, 1998, stated that macromolecules greater than 1000 amu can constitute 50-60 % of dissolved organic carbon in wastewater. Fig. 2.28 illustrates size ranges of typical municipal wastewater compounds.

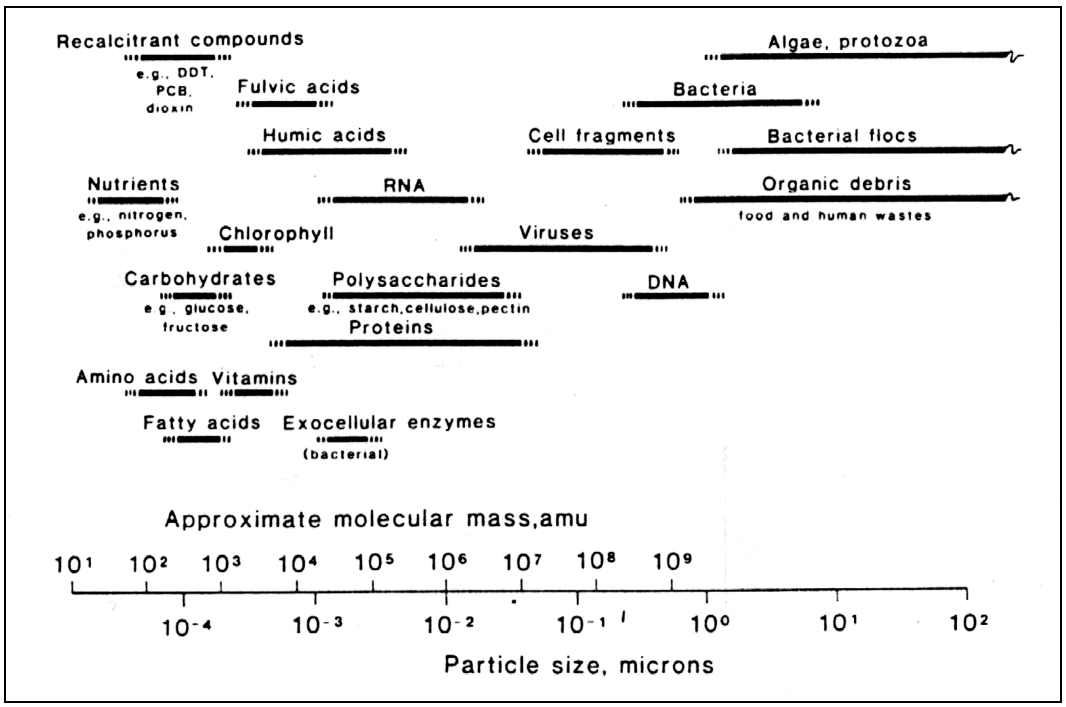

Figure 2.28. Size range of organic constituents in settled municipal wastewater. Levine *et al.*, 1985.

Despite that most organic matter in wastewater (~75 %) is made up of non-soluble material (Henze *et al.*, 1994; Levine *et al.*, 1985) and that hydrolysis often is the rate limiting step in biological wastewater treatment processes (Henze *et al.*, 1997), not much research has been directed at hydrolysis in biofilm reactors (Janning, 1998; Nielsen and Harremoës, 1995).

The many binding sites offered by the EPS matrix foresee high potentials of sorption of organic particles in biofilms (Flemming, 1995). An aspect, where this could cause problems would be in EBPR. A constant and significant release of easily degradable substrates from hydrolysis of sorbed particulate matter

during the aerobic/anoxic phase would hamper the competitive advantage of PAOs. Investigations have reported a significant detention of particulate organic matter in biofilters, this is resulting from a combination of sorption to the biofilm matrix and simple filtration (Boller *et al.*, 1997; Janning *et al.*, 1997). The influence and quantity of this particulate matter, depend on the filter backwash frequency relative to the hydrolysis rate. Reports on hydrolysis of particulate matter in biofilms are divided into 3 hypotheses, Fig. 2.29.

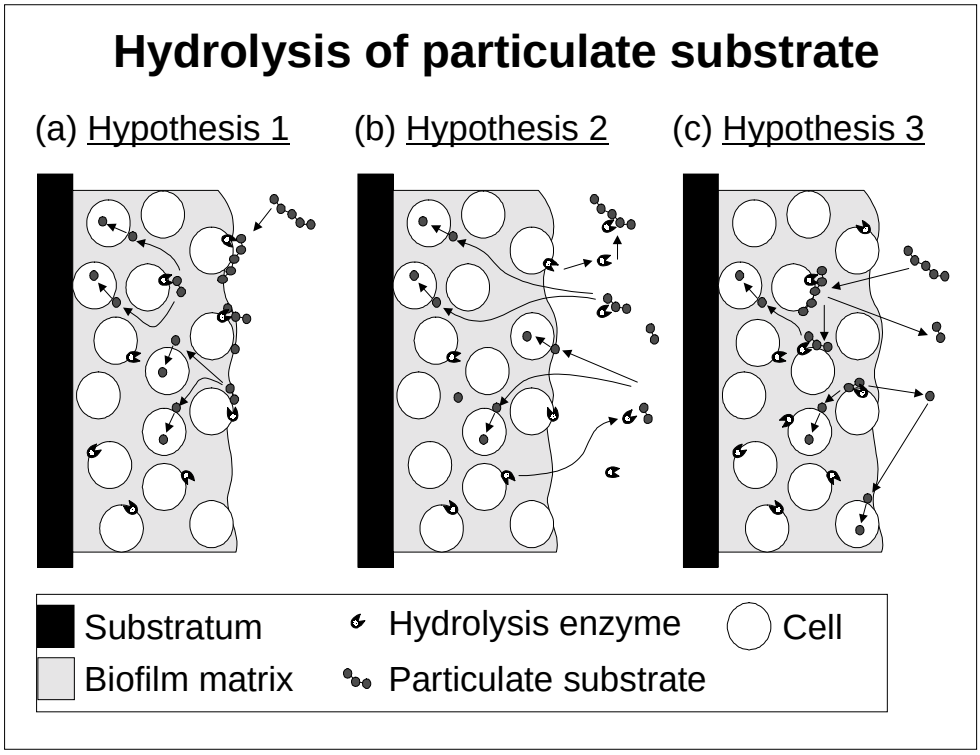

Figure 2.29. Different hypotheses for hydrolysis of particulate matter by biofilm bacteria.

(a) Macromolecules attach to the biofilm surface, hydrolysis takes place on the surface and the hereby formed hydrolysis products diffuse into the film to be degraded (Bouwer, 1987).
(b) Hydrolysis enzymes are released to the bulk water, hydrolysis take place in the bulk water and produces fragments that can diffuse into the biofilm for degradation (Larsen and Harremoës, 1994).
(c) Macromolecules attach to the biofilm surface or the interior of the biofilm matrix. Hydrolysis is cell associated and hydrolysis fragments might diffuse out into the bulk water. From here the cycle continues, until the fragments are small enough to be taken up by the bacteria (Confer and Logan, 1998).

The original perception was that macromolecules attach to the biofilm surface, hydrolysis takes place on the surface and the hereby formed hydrolysis products diffuse into the film to be degraded (Bouwer, 1987). Larsen and Harremoës,

1994, suggested a new hypothesis, where the main hydrolytic activity took place in the bulk water outside the biofilm and extracellular enzymes were released to the bulk water by the biofilm bacteria. They observed a decrease in the substrate degradation with an increase in the flow rate and attributed this to be caused by washout of extracellular enzymes. The most recent addition to these hypothesis was made by Confer and Logan, 1997, 1998. Based on experiments with fluorescent model substrates that made measurements of hydrolysis rate possible, they suggested a hypothesis where macromolecules attach to the surface or internal matrix of the biofilm. Hydrolysis is as in the model of Bouwer, cell associated, but as a difference to Bouwer, Confer and Logan predicted release of hydrolysis fragments back into the bulk solution. From here, the fragments continue the cycle of attachment and hydrolysis until they reach a size that can be taken up and degraded by the bacteria.
Confer and Logan, 1997, investigated the effect of different diversities of biofilm communities. The highest diversity, a wastewater biofilm, led to very low accumulation of hydrolytic fragments in the bulk water, probably caused by a rapid utilisation by the diverse microbial community, and it was concluded that consideration of this mechanism (release of hydrolytic fragments) is expected to have little effect on overall treatment kinetics in microbial diverse wastewater treatment reactors. Confer and Logan, 1998, disagreed with the hypothesis of Larsen and Harremoës, 1994, and stated that the observed reduced degradation by higher flow rate was due to washout of hydrolytic fragments.

BOX 3 Biofilm Models

The introduction of new methods for investigating fully hydrated biofilms in the early 90'es, such as the confocal laser scanning microscope (CLSM), revolutionised the perception of biofilms. Originally, biofilms were considered homogeneous, dense structures, but new observations showed that also heterogeneous structures with internal water channels and separated microcolonies of different microbial species exist. Different conceptual and computerised models of biofilm structures evolved in the search of universal factors that could identify the parameters determining biofilm morphology. No definite answer has been found, however, a connection to the substrate loading versus shear forces seem to be of major influence (van Loosdrecht *et al.*, 1995; Kwok *et al.*, 1998).

Biofilm bacteria are phenotypically, physiologically and ecologically different from their planktonic counterparts (Costerton *et al.*, 1994).

Complex 2- and 3-D models were presented in the late 90'es. Most of these were based on a cellular automaton principle, where space is divided into uniform, small squares (or cubes) that respond to environmental inputs according to a set of relatively few, simple mathematical rules. These models could predict biofilm structures ranging from very dense over channelised 'mushroom'- and 'stalk'-like structures when varying the external mass transfer limitation.

The best model for a given situation depends on the modelling objectives. A distinction is made between models used for practical engineering purposes, where simplicity is needed, and research purposes, where complexity is allowed.

Despite the very different kinds of models, one factor stands out as of common and all-determining influence: the transport via molecular diffusion. Whether this is from the surface and inwards trough a dense biofilm, or from an internal channel into a dense cluster. Zonated biofilms have been shown repeatedly in experimental investigations, e.g. anaerobic sulphate reduction in aerobic environments.

1-D models have been shown to reveal key aspects of biofilm processes, and when considering complicated processes, like EBPR, they have proved useful to enhance understanding of observed phenomena (Morgenroth, 1998).

Some open questions:

Are biofilm structures a result of 'divine intervention' where cells communicate to obtain a predetermined morphology, or do the structures evolve according to the principle of 'self-organisation' where the individual cell responds to local conditions following some rules of development?

Why are biofilm bacteria different from their planktonic counterparts? - What regulates these changes in behaviour? If cells communicate – then how?

Which are the main parameters determining biofilm structure - and detachment?

What determines the amount and composition of exopolymeric substances (EPS)?

How do biofilms adapt their strength/morphology to given shear forces?

How do biofilm bacteria respond to particulate matter – are hydrolysis enzymes cell/matrix bound or released to the bulk water? Is the response species dependent?

2.4 Biological Phosphorus Removal – in a Biofilm

2.4.1 Advantages of Biofilms over Activated Sludge

When upgrading existing wastewater plants to comply with increased treatment demands, the use of biofilters has the advantage of compactness. The small footprint area of biofilters is caused by two factors: 1) High volumetric biomass concentrations can be achieved (e.g. up to 16 gVSS/l in a BAS reactor, Kwok *et al.*, 1998) 2) The attached growth mode prevents washout of slow-growing organisms. In comparison, big tank volumes (to obtain high sludge retention times) are required in activated sludge plants to sustain slow-growing organisms such as nitrifiers (Boller *et al.*, 1994; Paffoni *et al.*, 1990). For many fixed-film processes, there is no need of a final clarifier, which makes up a relative high fraction of the total area of activated sludge plants (Borregaard, 1997) - settling of biomass removed by filter-backwash is a side-stream process with more compact clarifiers. Biofilters are characterised by less dependency of the sludge settle-ability and no problems related to secondary release of phosphate, as occasionally observed in final clarifiers of activated sludge systems due to the anaerobic conditions in the sludge blanket. The biofilm matrix provides protection against various toxins and different bacteria types can live in microenvironments within the film.

2.4.2 EBPR in a Biofilm versus Activated Sludge

2.4.2.1 Alternating conditions

When biomass is attached to a carrier material, the alternating conditions of the bio-P process have to be exerted on the biofilm reactor in contradiction to activated sludge where the biomass is circulated in the system. Alternation can be achieved in a continuous flow system by intermittent aeration or in a single reactor operated in a sequencing batch mode. A third alternative is the recently introduced floating bed reactors, where biomass is attached to floating carriers and circulated through the system analogous to AS plants (Ødegaard *et al.*, 1994). Plant configurations for EBPR are briefly discussed in the next chapter.

2.4.2.2 Removal of phosphate-rich excess biomass

For removal of phosphorus from a biofilm system, backwash of the filter must take place at a time where the internal storage of phosphorus in the bacteria is at it highest. In activated sludge systems this is achieved by settling after an aerobic phase.

2.4.2.3. Diffusion of substrates

Substances that are to be removed by biofilm bacteria have to diffuse into the film. Diffusion might also play a role in activated sludge systems, but due to the relatively small floc diameters, and diffusion from all sides, the problem of

diffusion is far less pronounced, Fig. 2.30. The sizes of activated sludge flocs have been investigated by several researchers reporting a size range of 10-1100 μm, however a typical floc diameter is less than 100 μm (Andreadakis, 1993; Levine *et al.*, 1985; Li and Ganczarczyk, 1991).

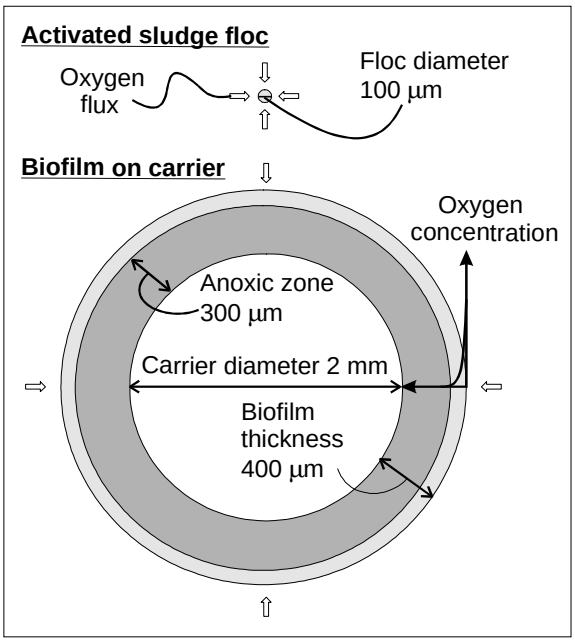

Figure 2.30. Schematic comparison of an activated sludge floc and a spherical carrier particle with attached biofilm. In this hypothetical example, oxygen penetrates 100 μm into the biomass. This induces a large, anoxic zone in the 400 μm thick biofilm, whereas the 100 μm thick sludge floc is completely aerobic. A sludge floc of up to 200 μm would remain aerobic, due to fluxes of oxygen from all sides. For biofilm on a carrier, oxygen penetrates only from the film surface.

Anoxic microniches in the centre of relatively thick flocs have been reported in several studies, verifying that diffusion limitation might be of importance in some activated sludge plants (Pochana *et al.*, 1999). Schramm *et al.*, 1999, investigated sludge flocs from 6 different activated sludge plants with microelectrodes. Anoxia was verified in flocs from 2 of the plants, apparently the densest flocs tested, but sulphate reduction could not be detected in any of the tested flocs, despite the presence of sulphate-reducing bacteria (SRB) as indicated by FISH with oligonucleotide probes targeting SRBs. For microelectrode measurements, Rasmussen and Lewandowski, 1998, evaluated oxygen fluxes measured with oxygen microelectrodes, and true oxygen fluxes as determined by the use of an electrochemical imitation of a biofilm. They found that oxygen fluxes based on microelectrode measurements were consistently higher than the true fluxes. The reason for this was hypothesised to be due to either simplifying assumptions accepted in computational procedures

employed to calculate oxygen fluxes, or the presence of the microelectrode in the mass boundary layer/the biofilm. Despite the very small tip diameters of usually a few microns, any change of biofilm structure or hydrodynamis caused by the tip might effect the results in an unpredictable way (Rasmussen and Lewandowski, 1998). For the relatively small, activated sludge flocs this consideration could be even more important than for biofilms. However, in the study by Schramm *et al.*, this uncertainty was considered by including batch experiments, where incubation with radioactively labelled $^{15}NO_3^-$ and $^{35}SO_4^{2-}$ was used to test denitrification and sulphate reduction, and qualitative agreement was in this study found between the two experimental procedures.
Biofilm thicknesses are normally much larger than activated sludge floc diameters. Many wastewater biofilms are 0.5-2.0 mm thick (Bishop, 1997). The problem, that significant masses of metabolic inactive biomass might dominate thick biofilms due to diffusion limitation, is generally acknowledged (Henze *et al.*, 1997, Lazarova and Manem, 1995).

2.4.3 Complications of Zonation in Regard to EBPR

When assuming diffusion as the main factor for transport of compounds into the biofilm, depending on biofilm thickness and bulk water concentrations this leaves the possibility of different zones inside the film as discussed in the previous chapter. Biological phosphorus removal is particularly interesting, however very complex, to look at when considering the diffusion/zonation aspect in a biofilm, since PAO's act differently, depending on whether they are exposed to anaerobic or aerobic/anoxic conditions. It might happen that e.g. nitrate during the anoxic phase only penetrates the outer part of the film leaving the inner part anaerobic. In this case there is the possibility of phosphorus release in the anaerobic zone deep in the biofilm at the same time as phosphorus is taken up by denitrifying PAOs in the outer part, Fig. 2.31. Since no easily degradable substrate is supplied during the anoxic phase of a denitrifying EBPR process, an internal production of a carbon source must take place inside the biofilm – e.g. via decay and hydrolysis - for significant release of phosphate (i.e. higher than simply due to cell lysis/maintenance) to occur in the bottom part of the film. The significance/possibility of simultaneous uptake and release of phosphate at different locations in a thick EBPR biofilm has never been investigated.
Morgenroth, 1998, and Morgenroth and Wilderer, 1998, 1999, studied some of the aspects of diffusion in an EBPR biofilm operated with oxygen as the electron acceptor. They used a sequencing batch reactor fed with synthetic wastewater (acetate/peptone as carbon source). Computer modelling with AQUASIM was used to qualitatively simulate concentration profiles of dissolved (oxygen, acetate and phosphate) and particulate compounds (PAO cells, poly-phosphate and PHB) inside the biofilm. Results of these simulations are shown in Fig. 2.32 I+II.

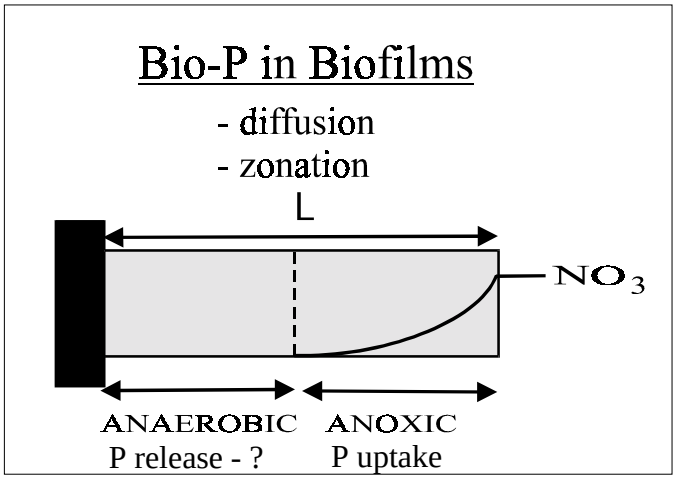

Figure 2.31. Diffusion might lead to zonation in a biofilm, which complicates the use of a biofilm for phosphate removal. Illustrated here is partly penetration of nitrate, leading to an anaerobic zone near the substratum. Uptake of phosphate (by denitrifying PAOs) in the outer, anoxic layer might happen simultaneously with phosphate release in the anaerobic zone.

Figure 2.32 I shows the concentrations of soluble compounds in the distances: 10, 100, 300 and 500 μm from the substratum of the simulated 500 μm thick biofilm, during the 8 hour alternating cycle. The deepest parts of the biofilm are not penetrated with oxygen at the beginning of the cycle, but as the cycle proceeds, oxygen penetrates further into the film and by the end of the phase, the whole film is aerobic. The reason for the increased penetration depth of oxygen, is that the oxygen utilisation rate in the outer layers decrease gradually due to depletion of the internal organic storage pools of these bacteria. Hence, since aeration is continuous, the lower utilisation rate in the outer layers permits oxygen to penetrate the biofilm further. Acetate only penetrates the biofilm fully during the first 20 min of the anaerobic phase (I b). As oppose to oxygen, acetate is only added to the system during the fill phase, whereby the acetate concentration in the bulk water (and hence also the penetration depth) decreases over time. Phosphate is present in the total depth of the film during the full cycle. The equivalent internal storage pools and the bacteria concentration during the cycle are illustrated in Fig. 2.32 II. The internal pool of PHB increases during acetate uptake, and poly-P is simultaneously reduced – as expected from the PAO metabolism. The concentration of bacteria cells vary during the cycle (II c), however, this is mainly because the porosity of the biofilm is set constant in the simulation, hence the volumetric concentration changes of stored polyphosphate or PHB are reflected in the volumetric concentration of PAOs. The biofilm thickness increases during accumulation of storage compounds, whereby the *mass* of PAOs does not decrease, only the volumetric concentration. Some PAOs die/lyse, but growth causes a net increase of the PAO mass over time.

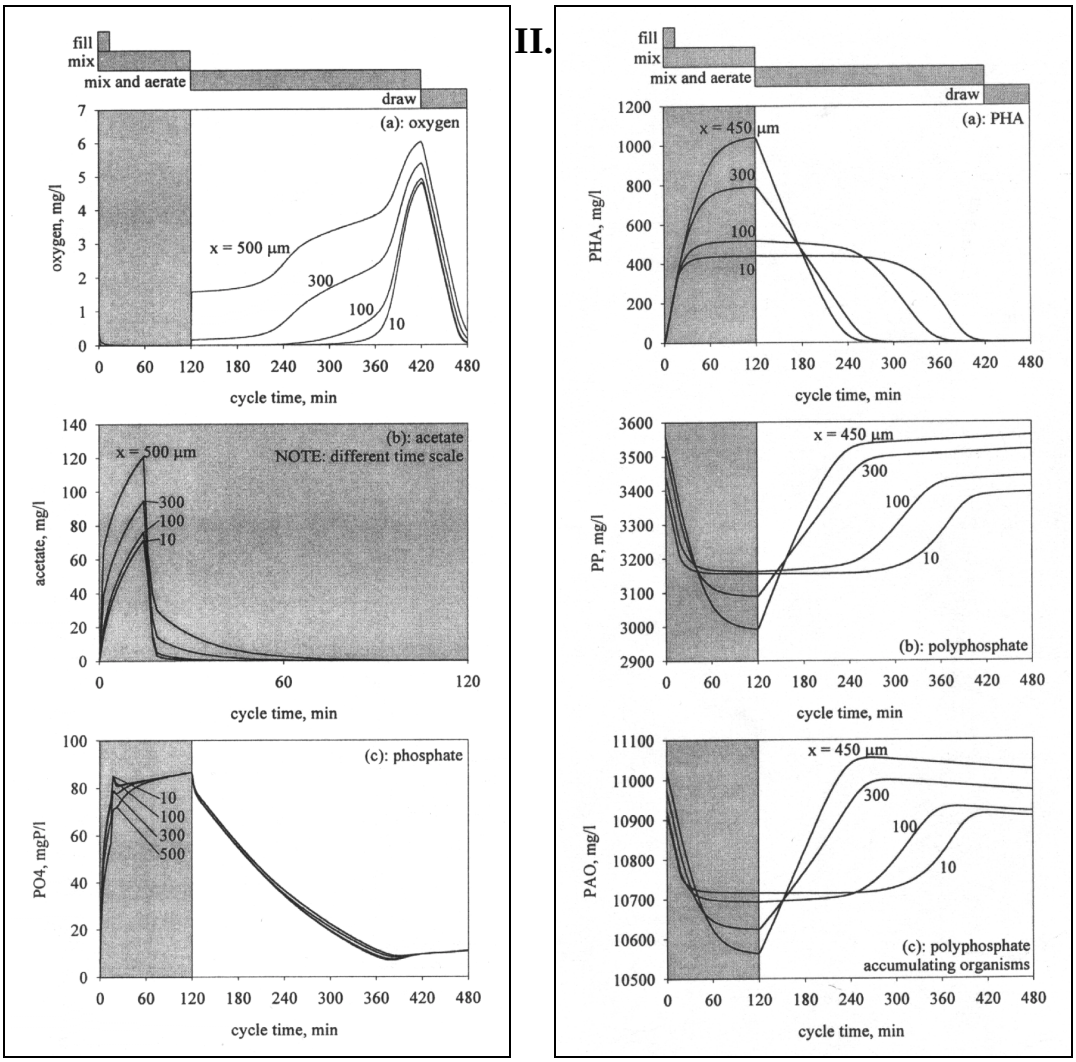

Figure 2.32. Simulated concentrations of soluble (I) and particulate (II) compounds inside an EBPR biofilm during an anaerobic/aerobic sequencing batch cycle. Morgenroth, 1998.

Ia: Oxygen does not fully penetrate the biofilm at the beginning of the aerobic phase, but as the utilisation rate in the outer most layers gradually decreases due to depletion of internal PHB pools (IIa), oxygen penetrates deeper and by the end of the phase, the biofilm is fully aerobic. *Ib:* Acetate fully penetrates the film during the first 20 min of the anaerobic phase, hereafter penetration decreases with time due to a decreasing bulk water concentration. As oppose to oxygen, acetate is only added in the fill phase. *Ic:* Phosphate fully penetrates the biofilm throughout the cycle. *IIa:* The internal storage pools of PHA increase in all depths of the biofilm during the anaerobic phase and are used up in the full length of the biofilm by the end of the aerobic phase. The degradation of PHA in the deeper layers begins when oxygen penetrates into these layers (Ia). *IIb:* The internal polyphosphate pools vary according to the phases of release or uptake of soluble phosphate in the anaerobic and aerobic phase, respectively. *IIc:* The concentration of bacteria cells vary during the cycle, however, this is mainly because the porosity of the biofilm is set constant in the simulation, hence the volumetric concentration changes of stored polyphosphate or PHB are reflected in the volumtric concentration of PAOs.

Morgenroth, 1998, concluded from the simulation results, that transport limitations of soluble substrates into the biofilm (for the given SBR cycle) had only a very minor effect on EBPR, since bacteria in the full depth of the film to some extent all were exposed to alternating conditions and hence stored polyphosphate. However, as is evident from the simulation results, this conclusion is very situation specific and depends on a set of parameters, especially: concentrations, phase lengths and biofilm thickness of a given system.

2.4.4 Effect of Cell Residence Time and Backwash

Regarding mean cell residence time (MCRT), biofilms are completely different to activated sludge systems. Actually, it is almost impossible to talk about a mean cell residence time of bacteria situated in biofilms. Cells stay in the system, until they are removed from the biofilm matrix via detachment. Detachment processes vary significantly from biofilm to biofilm as discussed in chapter 2.3.5. If erosion or abrasion at the biofilm surface is the dominant detachment process, then bacteria in the bottom of the film stay attached until they via the growth process slowly are pushed forward to finally reach the surface exposed to detachment. The movement of bacteria cell due to growth is defined as advective displacement (Wanner and Reichert, 1996). In this case, one can predict a mean cell residence time based on the advective velocity of the biofilm matrix, u_F, and the steady state biofilm thickness, L_{steady}. However, as illustrated by Morgenroth and Wilderer, 1999, the advective velocity depends on the distance from the substratum, whereby an integration of the velocity expression is necessary for calculating MCRT. If detachment, contrarily, is dominated by stochastic sloughing of the biofilm, bacteria residing in the deep part of the film are also removed via detachment and the mean cell residence time distribution becomes more unpredictable.

Morgenroth and Wilderer, 1999, discussed the mean cell residence time of a system where biomass detachment was controlled by regular backwash. It was assumed that backwash removed biomass above a certain, constant biofilm thickness (500 μm). The mean cell residence time distribution for different distances from the substratum was predicted. They found that cells close to the substratum had significantly longer MCRTs, up to 80 days, compared to the top. For cells more than 200 μm from the substratum, the MCRTs were below 20 days, decreasing with the distance, which is comparable to activated sludge plants. Bacteria cells that are not removed by backwash will not contribute to a net phosphate removal from the system, however they might still perform the process of release and uptake and hence utilise organic matter, which often constitutes a limited resource in wastewater. Phosphate taken up by bacteria in the bottom of the film that are not removed from the system shall eventually be released due to bacterial lysis and endogenous respiration (Morgenroth and

Wilderer, 1999). It was pointed out that the prerequisite for achieving efficient EBPR with a biofilm is frequent backwash in order to maintain a thin, active biofilm. Regarding diffusion limitation of soluble substrates, an advantage of sequencing batch reactors over continuous systems in general was postulated. The inherent transient operation mode of SBRs, where high substrate concentrations are present at some point of the cycle, makes it more likely that even thick biofilms shall be exposed to substrate to some extent. However, the situation for EBPR cannot directly be extrapolated to e.g. COD removal since transport limitation still might happen, even at high initial concentrations, depending on the internal removal rates. EBPR is special due to possible depletion of internal storage compounds, which may lead to deeper penetration of substrate later during a single cycle.

2.4.5 Other Investigations of EBPR in Biofilms

A wide range of reactor types and carrier materials have been used for EBPR in biofilms, Table 2.11. Almost no investigations by different researcher, applying the same carrier and reactor types, have been reported. The interest in EBPR with biofilm reactors has gained significant popularity within the last couple of years as evident from Table 2.11. However, as of yet only one investigation with a semi full-scale plant (17 m^3) has been reported, and this is still in the experimental phase, Arnz *et al.*, 2000b. The main focus of all investigations has been removal capacity as defined by percentage P removal. Generally neither biofilm thickness nor biomass characterisation of EBPR biofilms are reported, and also no discussions of the complexity of diffusion (except for the one of Morgenroth discussed above). Due to the importance of biofilm thickness and structure (diffusion coefficient) it is difficult to directly compare the different investigations.
Some results of different investigations were already mentioned in chapter 2.1, such as obtained phosphate contents for several reactor types, refer to Table 2.4b (p. 12), and investigations of different combinations of phase lengths, chapter 2.1.8.4 (p. 15).

González-Martinez and Wilderer, 1991, were among the first to report investigations of EBPR in biofilms. A laboratory, sequencing batch biofilm reactor (SBBR) with alternating anaerobic/aerobic conditions was used. The fixed bed reactor was operated with synthetic wastewater with acetate/peptone/glucose as carbon sources. A relatively long start-up of 17 weeks was reported, where good P removal was achieved after ‘a thinner biofilm’ developed. A very low stoichiometric coefficient of 0.09 C-mol acetate/mol P released was found (theoretical: 0.26-0.75 according to Smolders *et al.*, 1994a), pH was not controlled but stayed close to 7 during anaerobic phases. P content of the biomass reached 4.5 % for 6 h anaerobic phase length and 6.1 % during operation with 12 h anaerobic phase length.

Shin and Park, 1991, used a hybrid between activated sludge and biofilm in a PBCSBR. 'PBC' refers to the carrier: Porous biomass carrier. The carrier was polyurethane foam pads with a porosity of 98% and a specific surface area of $3.5*10^4$ m^2m^{-3}. 15% reactor volume was carrier-filled. For comparison, a SBR without added foam pads was operated in parallel. The removal (COD, nitrification and denitrification) in the PCBSBR was consistently higher than the AS SBR and attributed to the significantly higher biomass concentrations in this reactor. Biomass hold-up in the PBC carriers was a mixture of attached growth and entrapped biomass in the porous channels. A clear dependence of the COD/P ratio in regard to P removal was observed with almost no removal for COD/P = 20, but steadily increasing for COD/P up to the last tested ratio of 80. Obtained P content of the sludge was (for COD/P >= 40) 4.5 %. No information or discussion of backwash (frequency or method) were supplied. Backwash is assumed to be of major importance for the described process, since the diffusion limitations will increase dramatically with clogging of the porous channel structure of the foam pads.

Goncalves and Rogalla, 1992ab, used a continuous process, where 2 up-flow pilot-scale reactors were alternated. Presettled wastewater was fed to the reactor in anaerobic status, while the other reactor was aerated. After a time period, the filters were reversed whereby the alternating conditions of the biomass of both reactors were achieved. Different anaerobic phase lengths were tested in regard to EBPR and nitrification. The phosphate content of the biomass reached 4-5 % of the total dry weight.

Goncalves *et al.*, 1994ab developed the continuous process concept further. They used 5 alternating reactors and included denitrification by aerating only the top part of the upflow floating bed reactors, according to the Biostyr-ND-principle (Rogalla *et al.*, 1992; Borregaard, 1997). Nitrified water was recirculated to the inlet of the reactors in N removal mode. While one reactor was anaerobic, the others were used for nitrification/denitrification. Phosphate contents of the biomass varied between 2.1 and 4.1 %.

Kerrn-Jespersen *et al.*, 1994, operated a fixed-film reactor with alternating anaerobic/anoxic conditions by adding either acetate (anaerobic) or nitrate (anoxic) in the inlet. Good denitrifying, phosphorus removal was obtained with phosphate content of the sludge between 8 and 10 %. This is the highest content reported for EBPR processes with biofilms. Stoichiometric coefficients were found in agreement with dentrifying PAOs of Kuba *et al.*, 1993 (refer to chapter 2.1.6, p. 9-10).

Sieker, 1999, also exploited simultaneous denitrification and phosphorus uptake. She used a pilot-scale sequencing batch reactor cycle with a separate step (trickling filter) for nitrification, i.e. two filling phases were included in

each SBR cycle: 1) filling with presettled wastewater 2) anaerobic reaction phase 3) emptying the reactor 4) filling with nitrified wastewater 5) anoxic P uptake phase 6) emptying cleaned water. The advantage of an SBBR compared to AS SBR is no need for settling of biomass before emptying and the possibility of 100 % exchange ratio of water. Frequent backwash (every 2-3 days) was applied to keep the biofilm thin. Phosphate contents of the biomass was 3.5-4.5 %. The stoichiometric coefficients were approximately half of the ones found by Kerrn-Jespersen *et al.*, 1994, and Kuba *et al.*, 1993, for denitrifying PAOs (chapter 2.1.6, p. 9-10).

Castillo *et al.*, 1999a, used a sequencing batch biofilm membrane reactor. Biofilm grew on the outer surface of the membranes, in contact with the wastewater, and alternating anaerobic/aerobic conditions were established by purging either N_2 or O_2 through the inner volume of the membranes. For this system, significant simultaneous nitrification and denitrification was possible, since oxygen was supplied from the deep part of the biofilm (attached to the membrane) whereas organic matter was supplied from the biofilm surface (in contact with the wastewater), as observed and discussed in the study. The stoichiometric coefficients for g P released/g COD taken up were extremely low, from 0.014-0.025 g P/g COD (theoretical 0.48 g P/g COD, Smolders *et al.*, 1994a) and depended strongly on the influent COD, higher COD influent caused higher stoichiometric ratios. This was explained by ‘ required energy for the C-uptake is less when low organic loading rates are applied’, i.e. a shift in the metabolic energy requirements. This author questions this explanation. Perhaps, the observed phenomena could instead be explained by some changed interactions between direct utilisation of COD by either oxygen or nitrate and the phosphate metabolism. Or by competition phenomena between traditional denitrifying, GAOs and PAO bacteria? The acclimatisation periods to the tested different phase lengths and COD loadings were not described. Despite the low anaerobic coefficients, relatively high phosphate contents of the biomass were found: 4.2-5.2 %. In another publication from Castillo *et al.*, 1999b, the presence of GAOs and the possibility of competition with PAOs were recognised. Also the importance of not too high organic loading rates due to out-competition of slow-growing PAOs in the biofilm was empathised.

Gieseke *et al.*, 1999, were the first to report microsensor and some microbial investigations with FISH of a biofilm operated for combined nitrification and EBPR with oxygen as the electron acceptor. The findings with an oxygen microelectrode supported the modelling of Morgenroth, 1998, that the entire biofilm was penetrated during some point of time during the aerobic phase of a SBBR. However, significant higher activity of bacteria (detected by FISH) was found in the top layer of the film, indicating activity decrease with depth possible caused by transport limitation in part of the SBBR cycle. Biomass from this reactor was analysed further in the current study – see later.

Helness and Ødegaard, 1999, and Pastorelli *et al.*, 1999, used sequencing batch moving bed biofilm reactors (SBMBBR). Good EBPR was established provided high enough easily biodegradable COD in the inlet. Pastorelli *et al.* found P content of up to 9 %.

Table 2.11. Different reactor types and carrier materials applied in studies of EBPR in biofilms.

Reference	Year	Reactor Type	Carrier Material
González-Martinez and Wilderer	1991	SBBR (Sequencing Batch Biofilm)	Bio-Net, plastic cylinders in anet like structure, 155 m^2/m^3
Shin and Park	1991	PBCSBR (Porous Biomass Carrier Sequencing Batch Reactor)	Polyurethane foam pads, 15% filling, $3.4*10^4$ m^2/m^3
Goncalves and Rogalla	1992	Continuous upflow, , alternating	Granular polystyrene beads, 2.2 mm
Goncalves *et al.*	1994	Continuous upflow, alternating, Biostyr-ND	Granular polystyrene beads, 3 mm, 1050 m^2/m^3
Kerrn-Jespersen *et al.*,	1994	Continuous fixed-film, alternating	Plastic-Bio-Rings, 15 mm
Rovatti *et al.*	1995	SBBR, fluidized bed	Sand, 360 µm
Garzón-Zúñiga and González-Martínez	1996	SBBR, packed bed	Pall-Rings, 9 cm
Morgenroth *et al.*	1998 1999	SBBR	Biolith clay beads, 4-8 mm
Castillo *et al.*	1999	SBBR, membrane reactor	Accurel™ tubular gas permeable membranes
Pastorelli *et al.*	1999	SBMBBR (Sequencing Batch Moving Bed Biofilm Reactor)	KMT, polyethylene, 10 mm, cylinders with a cross inside
Gieseke *et al.*,	1999	SBBR	Biolith clay beads, 4-8 mm
Helness and Ødegaard	1999	SBMBBR	KMT, polyethylene, 10 mm cylinders with cross inside
Sieker	1999	SBBR, with separate nitrification step	Biolith/Blähton beads, 5-8 mm
Arnz *et al.*	2000b	SBBR	Biolith clay beads, 4-8 mm

A student project made at the Department of Environmental Technology and Engineering, Technical University of Denmark by Nielsen, 1993, was the main inspiration for initiating the current study. The results, Fig. 2.33, strongly indicated possible zonation in an EBPR biofilm, and that the 1-D diffusion model was a good approximation.

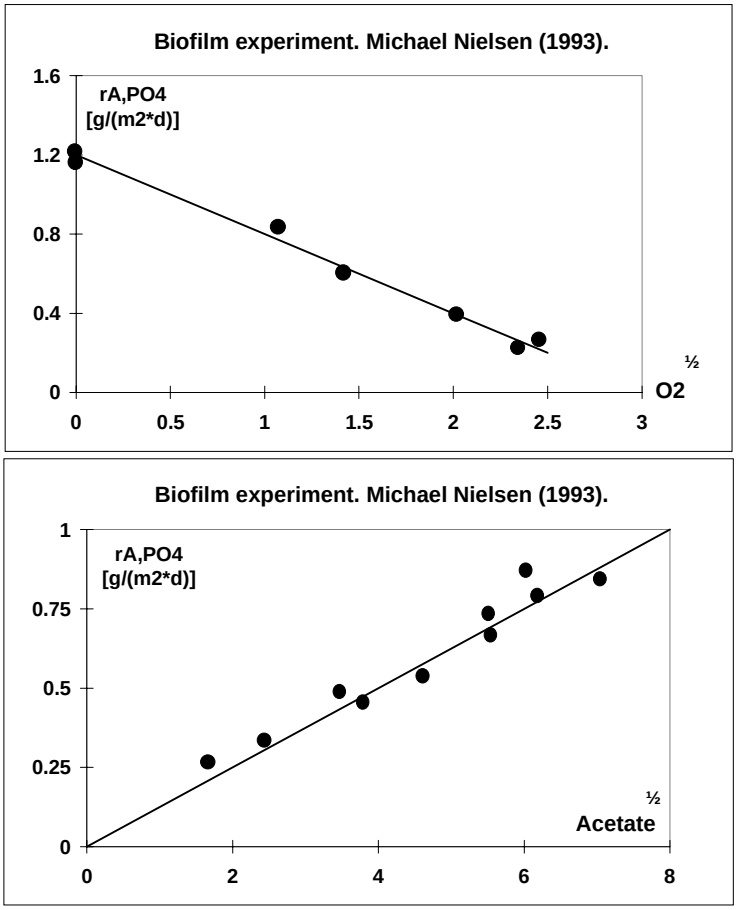

Figure 2.33. Results of a student project by Nielsen, 1993. Anaerobic P release was shown to decrease proportionally to the square root of the oxygen concentration in the bulk water, whereas a proportional increase was observed for the square root concentrations of the bulk acetate concentration.

Anaerobic P release was shown to decrease proportionally to the square root of the oxygen concentration in the bulk water, whereas an increase proportional to the square root of the acetate concentration was observed, when no oxygen was present. However, the experimental conditions were ill defined, and reproduction of the results was not provided, hence the results were never published further than an internal report and as a note in a newsletter (Harremoës, 1994?), despite of their significant news-value.

BOX 4 EBPR in Biofilms

The first investigations of EBPR with biofilms were reported in the early 90'es and still only a limited publication list exists. Advantages might be offered by biofilters: High biomass concentrations, no washout of slow-growing organisms, small footprint area, no dependence on sludge settle-ability, no danger of secondary P release since final settlers often are unnecessary, and higher resistance to toxic compounds. A wide range of reactor types and carrier materials have been tested, mainly SBBRs. As of yet, only one investigation with a semi full-scale plant (17 m^3) has been reported, Arnz *et al.*, 2000b.

The main focus has been removal capacity. Generally neither biofilm thickness nor biomass characterisation of EBPR biofilms are reported, and also no discussions of the complexity of diffusion (except for Morgenroth, 1998). For thick films, the possibility of a zonated biofilm structure with anaerobic bottom and anoxic or aerobic top makes biofilm thickness and structure (diffusion coefficient) of crucial importance, whereby it is difficult to directly compare the different investigations.

Morgenroth, 1998, emphasised, based on experimental and modelling results, the importance of keeping the biofilm thin, since only biomass removed by backwash contributes to net P removal. Morgenroth concluded that transport limitation of soluble compounds was insignificant, since all parts of the biofilm were penetrated to some extent during the SBBR cycle. However, as illustrated by Gieseke *et al*., 1999, deep layers of a relatively thick film might be penetrated with e.g. oxygen by the end of the aerobic phase, but the activity of the deeply situated cells was significantly reduced.

The maximum P content of biofilms for P removal was reported by Kerrn-Jespersen *et al*., 1994: 10 %. For most investigations, P contents are below 6 %.

Some open questions:

How stable is EBPR with a biofilm over longer time periods?

Is a zonated biofilm structure a reasonable approach for EBPR in biofilms? And what is the significance of zonation?

Will P contents of sludge from thick biofilms be low?

Do cells in the bottom of thick films stay active during periods of no substrate supply?

If thin biofilms are a prerequisite for good EBPR in biofilters – is the recommendable biomass concentration then still higher than in activated sludge systems? What other consequences does this demand have for the overall treatment process?

Is diffusion limitation in a continuous flow system more significant than in sequencing batch reactors, since bulk concentrations in continuous flow do not vary as much?

Are some reactor types and carrier materials better than others for EBPR?

2.5 Biological Phosphorus Removal – Plant Designs

Detailed practical design of wastewater treatment plants for EBPR is outside the scope of this thesis. Design considerations and guidelines can be found elsewhere (Henze *et al.*, 1997; Pitman, 1991; Wentzel and Ekama, 1997). However, different process configurations are briefly introduced below.

2.5.1 Single-Sludge Activated Sludge EBPR Processes

Figure 2.34 gives an overview of activated sludge plants for EBPR. The technology of the different trademarks are basically identical with some differences in the recycle patterns, selected in order for each of the processes to hold their own patent (Henze, 1996b).

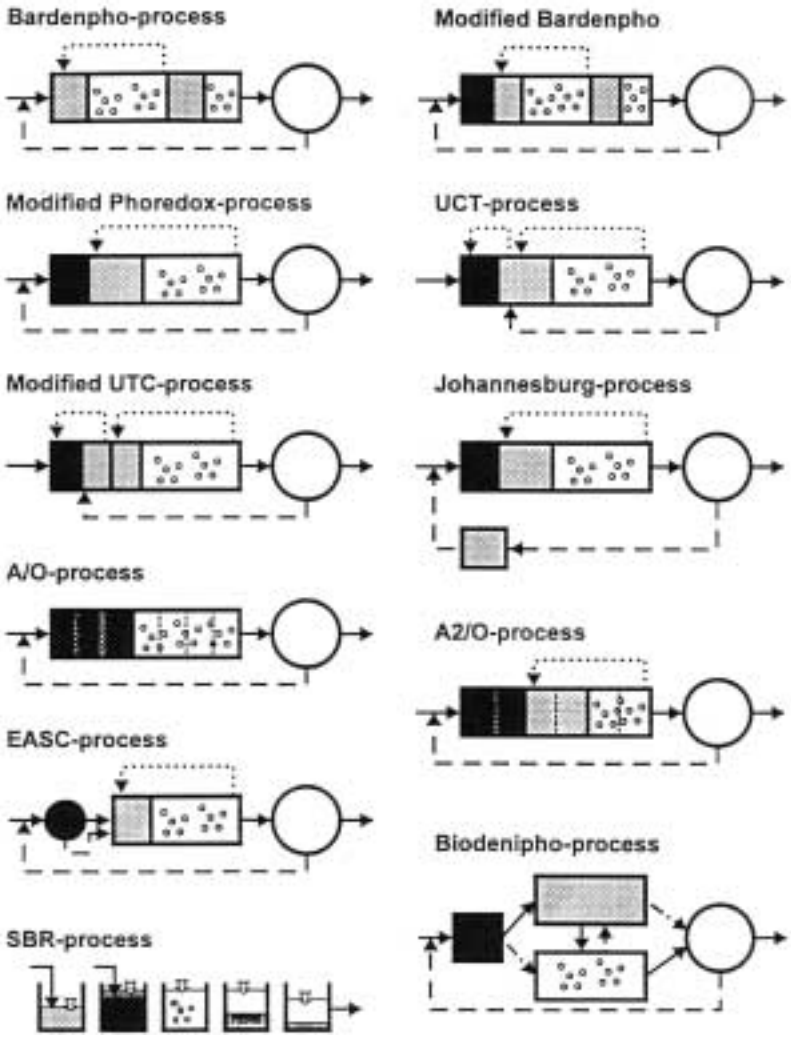

Figure 2.34. Single-sludge activated sludge processes for EBPR. Black: Anaerobic; Grey: anoxic; and White with bubbles: Aerobic. The circular white tank represents the final clarifier. Recycle of water and sludge are illustrated by arrows. Henze, 1996b.

The simplest process configuration is obtained, when no N removal is demanded: the A/O process, since then water is first passing an anaerobic tank for P release and then an aerobic for P uptake. This process is, however, not much in use except for laboratory scale for research purposes. Most typically, water enters an anaerobic phase, moves on to an anoxic and finally passes an aerobic tank. Nitrate rich water from the aerobic tank is recirculated to the anoxic tank. One of the main challenges of good EBPR is to prevent recirculation of electron acceptor into the anaerobic tank. The major source of such a feedback is the return sludge from the final clarifier. In this respect, processes such as the UCT ('University of Cape Town'), the modified UCT and the Johannesburg process are superior to the other processes, since the recycled sludge is passed through an anoxic zone to create a barrier (Pitman, 1991).
Processes most commonly in use today are the UCT, BARDENPHO, PHOREDOX and BIODENIPHO (Henze, 1996a).

In all the common single-sludge technologies for EBPR, Fig. 2.34, pre-denitrification is applied in order to exploit the internal carbon source of the wastewater. This procedure shall at the same time enhance the possibility of denitrifying PAO occurrence since internal PHB in this way is available in the anoxic reactor (Kuba *et al.*, 1997a).

As discussed in chapter 2.1.8.2 incorporation of a fermentation step is a frequently applied method to enhance the characteristics of the influent wastewater for EBPR. Different process designs for fermentation are given by Pitman, 1991.

2.5.2 Two-Sludge Denitrifying EBPR Processes

To exploit the possibility of simultaneous denitrification and phosphate uptake, two-sludge systems with separate nitrification is recommended to avoid competition with non-denitrifying PAOs (chapter 2.1.5). This can be done either by a nitrifying filter, according to the DEPHANOX process described by Bortone *et al.*, 1996, or by a separate nitrification activated sludge tank as described by Kuba *et al.*, 1996b, Fig. 2.35. The use of a filter saves one settling tank. The aerobic tank of the DEPHANOX process as illustrated in Fig. 2.35a, is included as an extra safety to avoid any phosphate leakage, but is not strictly necessary and not included by Kuba *et al.*, Fig. 2.35b. A final aeration step (by stirring) might improve the sludge settling properties by removing any entrapped nitrogen gas bubbles.
An additional advantage of separating the nitrifying sludge from the EBPR sludge is, that prolonged sludge ages in order to sustain the slow-growing nitrifiers have an adverse effect on the bio-P bacteria as discussed in chapter 2.1.7.3.

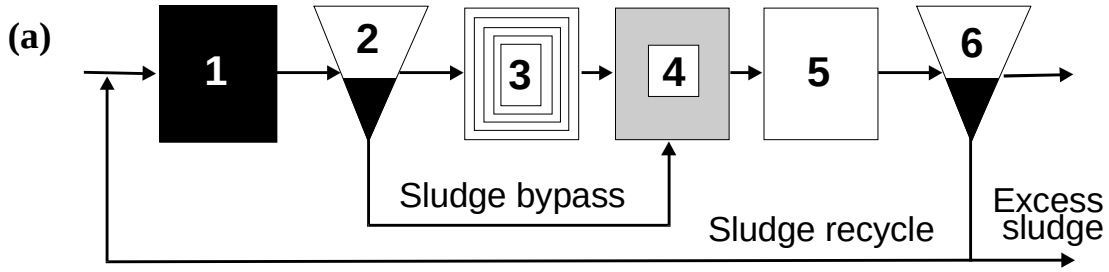

1) Anaerobic AS; 2) Settling; 3) Nitrification filter; 4) Anoxic AS; 5) Aerobic AS; 6) Settling

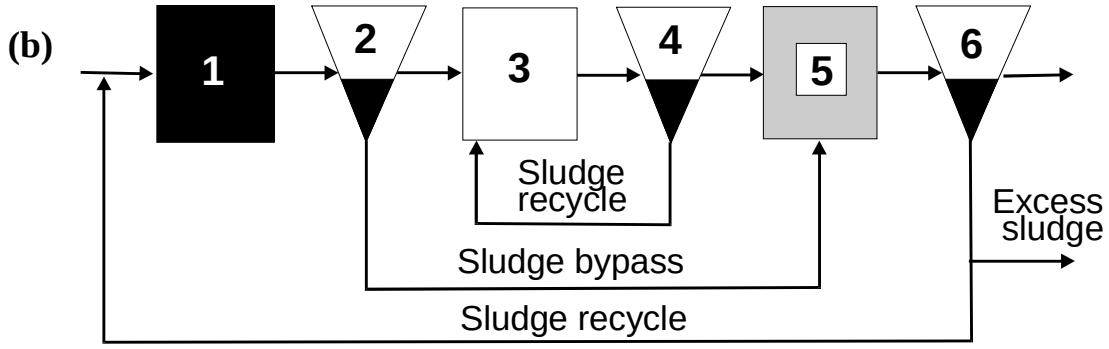

1) Anaerobic AS; 2) Settling; 3) Nitrification AS; 4) Settling; 5) Anoxic AS; 6) Settling

Figure 2.35. Two-sludge systems to achieve EBPR with denitrifying PAOs. (a) The DEPHANOX process by Bortone *et al.*, 1996, use a separate nitrification filter. (b) Kuba *et al.*, 1996b, suggest a separate activated sludge tank for nitrification.

2.5.3 Combined Biological and Chemical Phosphorus Removal

2.5.3.1 Addition of precipitation chemicals.

A thorough description of chemical phosphate removal technologies can be found in Henze *et al.*, 1997. They are all based on the same principle: addition of iron, aluminium or calcium in concentrations that cause the solubility product of the added ion and orthophosphate to be exceeded whereby precipitation occurs. For Ca^{2+}, pH of the water has to be elevated. The precipitation chemical can be added at different points along the mainstream process. If chemicals are added in the inlet, and COD/phosphate removal by precipitation is the only treatment objective, it is termed direct precipitation. This is not a common process, except for in Norway. Most widespread is simultaneous precipitation where chemicals are added into the aeration tank. Ferrous sulphate is here, due to its low cost, the preferred precipitant. Fe^{2+} is oxidised to Fe^{3+} before precipitation starts. Pre-precipitation, where chemicals are added to the inlet and precipitation takes place in the primary clarifier is the second most popular method of chemical P removal. In cases where extremely low effluent concentrations (< 0.5 mg P/l) are demanded, contact filtration may be applied as a post treatment process. Here, precipitants are added by the end of the

mainstream process, and subsequently the water is send through a filter. In this way, dissolved phosphate components are precipitated, but also remaining particles are held back. Often organic particles may constitute a substantial part of the remaining total phosphate content in the effluent from the final clarifier.
Typically, chemical precipitation is used as a polishing mechanism in combination with biological phosphate removal if the COD/P ratio of the wastewater is below 40-50. In such cases, simultaneous precipitation with 20-30 % of the normal precipitation dose for purely chemical treatment is normally used. The use of chemicals generally does not inhibit the biological process, provided that overdosing is prevented (Henze, 1996b). A problem that might arise with addition of chemicals to the biological process is concerned with nitrification. Addition of chemicals in the main sludge line lead to increased sludge production with a reduction of the aerobic sludge age as a consequence. As alternative, a side-stream process may be used (van Loosdrecht *et al.*, 1997a). One process is based on a combination of chemical and biological P removal as the main principle: the PHOSTRIP process (Levin *et al.*, 1972), Fig. 2.36. A fraction of the return sludge is passed through a separate anaerobic tank ('stripper'), where easily degradable organic matter is added to induce phosphate release. After sludge/water separation, the phosphate-rich water can be treated with chemicals, and the sludge is recycled to the plant inlet.

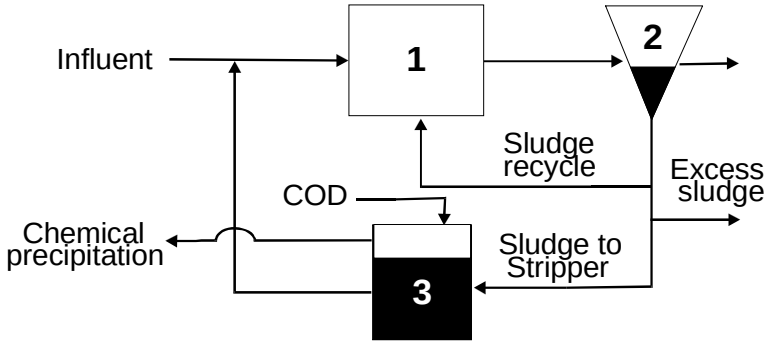

Figure 2.36. The PHOSTRIP process is based on precipitation of phosphate-rich sludge obtained by biological phosphate release.

2.5.3.2 Biologically induced precipitation

In the early years of EBPR, some confusion of the reason for excess phosphate contents of the sludge prevailed. It was not clear, whether phosphate was internally stored in the bacteria cells, or if the biological activity caused chemical phosphate precipitation. After the biological uptake has been verified, there still exists the possibility of also some biologically induced precipitation of phosphate. Biologically induced precipitation results from the elevated phosphate concentrations in the anaerobic tank due to release from PAOs, and additionally it might happen in denitrifying biofilms and flocs, due to internal elevated pH (Arvin, 1983).

The extent of biologically induced precipitation depends on the wastewater composition. High concentrations of especially calcium are favourable along with relatively low alkalinity (bicarbonate), and pH higher than 7.5. A recent discussion of chemical precipitation in EBPR plants was provided by Maurer and Boller, 1999.
For practical purposes, the precipitation can only be termed an extra profit, however, it might be problematic regarding research of biological process, where e.g. measured stoichiometric coefficients may be affected.

2.5.4 Biofilm Plants for EBPR

The one semi-full-scale plant that is investigated for EBPR with a biofilm is a sequencing batch reactor (Arnz *et al.*, 2000). Other plant designs that might be used for up-scaling to full-scale can be deduced from the many laboratory and pilot-scale experiments described in chapter 2.4.5.
The use of alternating anaerobic/anoxic conditions in tanks filled with a fixed carrier material is a process patented by the company Krüger. The design was inspired by the investigations of Goncalves *et al.*, 1994ab, but includes a separate nitrifying filter to optimise denitrifying PAO activity. A simplified illustration of the process is given in Fig. 2.37. Here only 2 tanks are included in the alternation, but to increase the flexibility of the process, more tanks may be included with the possibility of running different numbers in anaerobic, respectively, anoxic mode according to the wastewater characteristics. The inlet water is sent to a (currently) anaerobic tank, from here on to a (currently) anoxic tank (i.e. nitrate present) and finally through an aerobic tank for nitrification. Nitrate rich water from the aerobic tank is recirculated to the anoxic tank. The anaerobic and anoxic tanks alternate by shifting the inlet and recirculation flows from one tank to the other. As of yet, no experimental data or investigations of the process have been reported.

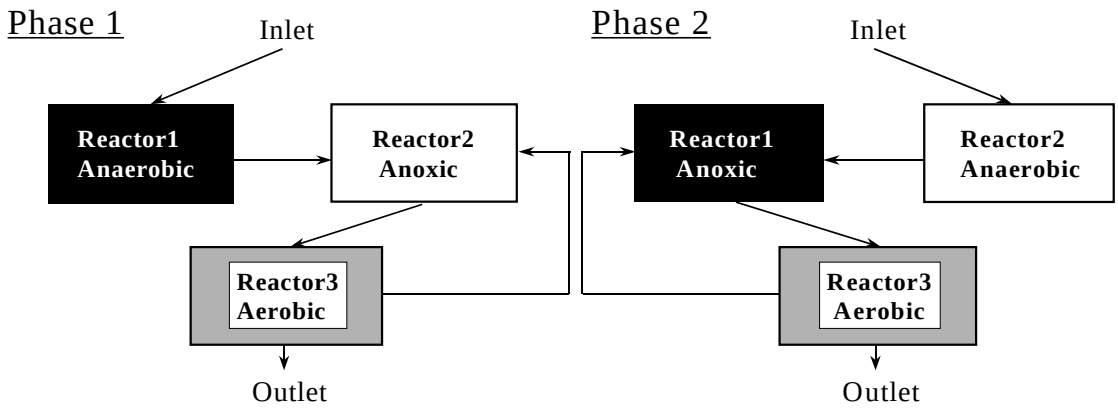

Figure 2.37. Principle of the Krüger process for simultaneous denitrification and phosphate removal in a biofilter plant. Reactor1 and Reactor2 alternate by shifting the inlet and recirculation flows.

2.5.5 Sludge Treatment

The fact that PAOs release phosphate when exposed to anaerobic conditions might cause secondary P release in the final clarifier, if anaerobic conditions arise in the sludge blanket. Another problem is the sludge treatment of EBPR processes as discussed by several authors (Banister *et al.*, 1998; Jardin and Pöpel, 1994; Wild *et al.*, 1996). Anaerobic digestion lead to re-release of phosphate. Large proportions of this is precipitated with simultaneously released metal-ions, and other ions present in the sludge, whereby anaerobic digestion generally does not lead to significant amounts of net phosphorus release according to Henze, 1996a. If sufficient magnesium or calcium is not present in the sludge for the precipitation, e.g. iron salts could be added, which often is done in any case to control sulphide levels in the produced methane gas (van Loosdrecht *et al.*, 1997a).
Pitman, 1999, listed recommendations for treatment of EBPR sludge:

1) Sludge should as far as possible be kept aerobic during handling. This includes minimum delay in the thickening and dewatering processes to avoid anaerobic storage.

2) Sludge from the primary clarifier (COD-rich) and sludge from the final clarifier (PAOs with high internal phosphate storage) should be treated separately to avoid excessive P release during any anaerobic conditions favoured by high COD concentrations.

3) Anaerobic digestion should be avoided, and sludge stabilisation should instead be made via aerobic composting.

4) Thickening and dewatering liquors should be pre-treated in a dedicated side-stream treatment process to avoid overloading of the mainstream process.

5) Waste activated sludge should preferentially be drawn from the aerobic reactor instead of from the final clarifier underflow as has been the traditional praxis.

BOX 5 Plant Designs for EBPR

All full-scale plants for EBPR are activated sludge. The only semi-full-scale investigation (17 m^3) with biofilms is still in the experimental phase (Arnz *et al.*, 2000).

A series of different single-sludge AS plants for EBPR exists, however they are all based on the same principle: first an anaerobic tank for P release, then an anoxic for denitrification and finally an aerobic for nitrification. Nitrified wastewater is recycled to the anoxic tank. One of the major challenges of good EBPR is to avoid recycling of electron acceptor into the anaerobic tank. Processes such as the UCT, modified UCT and the Johannesburg process are in this regard superior in that return sludge passes through an anoxic step.

Processes most commonly used are the UCT, BARDENPHO, PHOREDOX and BIODENIPHO.

Denitrifying PAO activity can be optimised in two-sludge systems with separate nitrification. The nitrification can be via a filter as in the DEPHANOX process, or via a separate AS system.

Polishing with chemicals might be necessary for wastewater with COD/P ratios lower than 40-50. 20-30 % of the normal precipitation dose for purely chemical treatment is needed.

The side-steam process PHOSTRIP is based on a combined chemical and biological process. The mainstream contains an aerobic tank and a final clarifier. Part of the sludge from the final clarifier is sent through a side-stream anaerobic tank where COD is added to induce P release. After sludge/waste separation, the phosphate-rich water is subjected to chemical precipitation, and the sludge returned to the plant inlet.

One biofilm plant design based on simultaneous denitrification and phosphate uptake has been patented by the company Krüger, but operational data have not been reported. The process is based on tanks alternated between anaerobic conditions fed with wastewater, and anoxic conditions fed with nitrate-rich water recirculated from a downstream nitrifying filter.

Handling and treatment of EBPR sludge is complicated since PAOs re-release the stored phosphate, if they are subjected to anaerobic conditions. As far as possible, the sludge should be kept aerobic. Sludge from the primary clarifier (COD-rich) and waste activated sludge (P-rich) should be treated separately. Liquor from sludge treatment should be pre-treated in a dedicated side-stream treatment process to avoid overloading of the mainstream process.

3. Focus, Tools and Structure of This Study

3.1 Focus of This Study

From the previous sections, it is clear that many open questions regarding EBPR in biofilms remain. Some of these were the inspiration and focus of this study. The main questions addressed are listed in BOX 6 below. The answering of, or the hypotheses arisen during the attempt to answer these questions shall bring the understanding of EBPR in biofilms one step further.

BOX 6 Open Questions in Focus

1. Is continuous alternation with nitrate as only electron acceptor possible with a biofilm over a longer time period, and how stable is the process?

2. How long time does it take to build up a denitrifying EBPR biofilm?

3. Is induction of denitrification possible in an EBPR biofilm acclimatised with oxygen as the electron acceptor, and how long time does such an induction take?

4. Can zonation be demonstrated with an EBPR biofilm? Is zonation of importance?

5. Does a thick biofilm lead to simultaneous release and uptake of phosphate inside the film?

6. Do cells in the bottom of a thick film stay active during periods of no substrate supply?

7. Are denitrifying PAOs different from PAOs using oxygen as the electron acceptor?

8. Are biofilm PAOs different from activated sludge PAO cultures?

9. Are low average P contents of excess sludge from thick EBPR biofilms found - due to inactivity of cells deep in the film?

10. Do GAOs accumulate in the bottom of thick EBPR biofilms, if phosphate is the limiting substrate, i.e. phosphate penetrates shorter into the biofilm during anoxic phases, than COD during anaerobic phases?

3.2 Tools of This Study

In order to address the questions in focus, a set of tools was selected:

1. A continuous laboratory-scale experimental setup
2. On-line measurements of bulk concentrations of phosphate and nitrate
3. Batch experiments with the experimental setup
4. Gene probes for in situ fluorescent hybridization
5. A confocal laser scanning microscope
6. The computer program AQUASIM for 1-D biofilm modelling (Reichert, 1994)

The individual tools shall be described in more details in the following chapters.

3.3 Structure of This Study

The structure was divided into 3 parts with different sub-focuses (Table 3.1):

PART A: 'Zonation and Stability of a Denitrifying EBPR Biofilm'
Tools: Continuous and batch lab-scale setup, on-line measurements.

PART B: 'Investigations of an Aerobic versus Denitrifying EBPR Biofilm'
Tools: Continuous lab-scale setup, gene probes, confocal laser scanning microscope.

PART C: 'Modelling of an EBPR Biofilm'
Tools: The computer program AQUASIM (Reichert, 1994) for 1-D biofilm modelling.

The different parts were performed on two different universities determined by the tools offered by these, respectively. PART A was made at the Department of Environmental Science and Engineering, Technical University of Denmark (Feb.'96-Dec.'98). PART B was made at the Institute of Water Quality Control and Waste Management, Technical University of Munich, Germany (Jan.'99-Dec.'99). PART C was made throughout the study.

PART A Technical University of Denmark (DTU)	**'Zonation in and Stability of a Denitrifying EBPR Biofilm'**	
	(Feb'96-Apr'97)	Idea, development and testing of the experimental setup.
	(May'97-Nov'97)	Testing carrier material. Modifications of the reactor. Building up a biofilm.
	(Dec'97-Dec'98)	Continuous run and batch tests.
	(Oct'98)	pH control is implemented.
PART B Technical University of Munich (TUM)	**'Investigations of an Aerobic versus Denitrifying EBPR Biofilm'**	
	(Jan'99-Apr'99)	First run for induction of denitrification in an aerobic bio-P biofilm.
	(May'99-Dec'99)	Second run for induction of denitrification in an aerobic bio-P biofilm. Microbial investigations.
PART C Both Universities	**'Modelling of an EBPR Biofilm'**	
	(Sep'96-Dec'99)	AQUASIM computer modelling

Table 3.1. Overview of the 3 parts that this study was divided into.

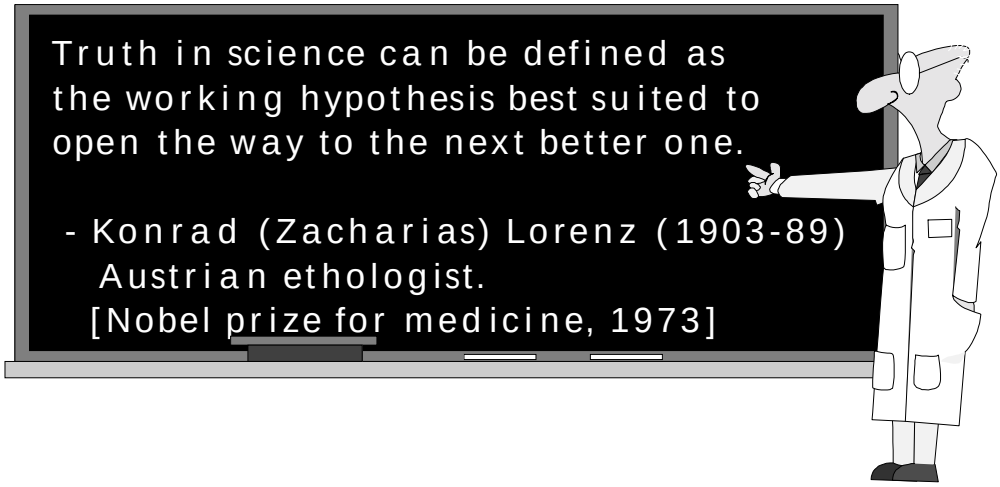

4. Experimental Setup

4.1 Choice of Reactor Setup

4.1.1 Automation and On-line Measurements

Previous student projects made at the Technical University of Denmark regarding biological phosphorus removal in biofilms have suffered from the lack of process monitoring and control (Bønlykke and Kristensen, 1995; Christiansen and Hollesen, 1994; Nielsen, 1993; Møller, 1994). The inherent non-steady state characteristics of the biological phosphorus removal process makes it of crucial importance to keep constant track of what is going on and record the process history. This can only be achieved by automatic operation and on-line measurements with data logging (Harremoës, 1997). For this reason, significant consideration and time was spent on developing and testing an automated experimental setup with on-line measurements of phosphate and nitrate. pH control was incorporated later in the study.

4.1.2 Reactor Scale

A laboratory fixed bed reactor was chosen for this study. This reactor type has frequently been used for research purposes at the Department of Environmental Science and Engineering, Technical University of Denmark. Toettrup *et al.*, 1994, provided evidence of the high potential of small-scale experiments for evaluating up-scaling. However, findings in laboratory-scale reactors cannot always be transferred to full-scale operation due to the inevitable differences, such as flow characteristics, backwash procedures, biofilter stratification and channeling, wall effects etc. For the focus of the present study, that was directed more towards fundamental biofilm research than practical studies, the simplification of the system by the use of a laboratory-scale reactor with well-defined conditions and synthetic wastewater was considered beneficial.
A granular media was chosen as the carrier material. This made it possible to test different carrier materials, but most important, in this way, it was possible to use the reactor also during PART B of the study, where a biofilm on granular carriers was taken from an existing EBPR plant and transferred to the lab-scale setup for investigation.

4.1.3 Components of the Lab-Scale Setup

The main components of the setup were:

- The reactor
- De-oxygenator system

- Inlet and recirculation pumps
- 200 L tank for synthetic micro-nutrients solution
- 10 L tank for anoxic substrate (KNO_3)
- 10 L tank for anaerobic substrate ($NaCH_3COO$)
- Two Tetlar bags for nitrogen gas
- 3-way magnetic valve
- Measurement equipment (PO_4-P, NO_3-N, O_2, pH)

Figure 4.1 shows a schematic illustration of the experimental setup as it looked by the end of the experimental period. Minor adjustments were made during the study. Detailed descriptions of the individual components follow below.

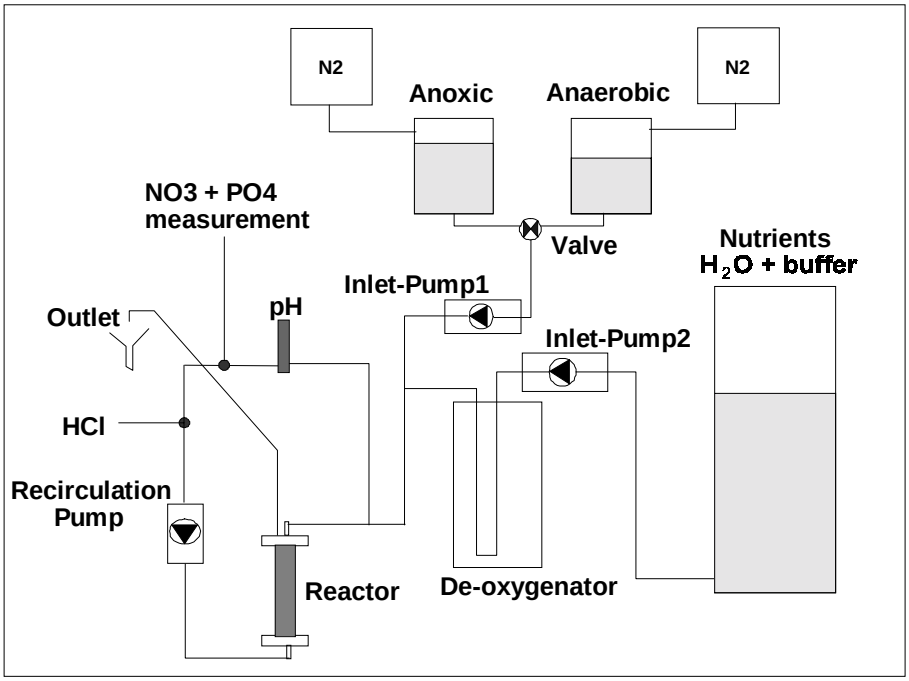

Figure 4.1. Schematic illustration of the experimental lab-scale setup.

4.2 The Reactor

A cylindrical plexi-glass reactor with a total inner volume of 0.41 L was used, a photo and a schematic illustration are seen in Fig. 4.2. The internal diameter was 44 mm, and the height 310 mm. In one end of the reactor was a perforated metal plate (hole diameter: 3 mm), that held the carrier material in place. Depending on whether it was floating or settling carrier material, this plate was in the out-, respectively, inlet of the reactor. The maximum volume of the carrier material was reduced compared to the total volume due to the metal plate and also for the purpose of backwash, so the maximum height of carriers was ~240 mm. The height of the carriers expanded with biofilm growth. The height after backwash

varied in the range 200-215 mm equivalent to a carrier volume of 0.30-0.33 L. The volume was calculated for individual batch experiments.

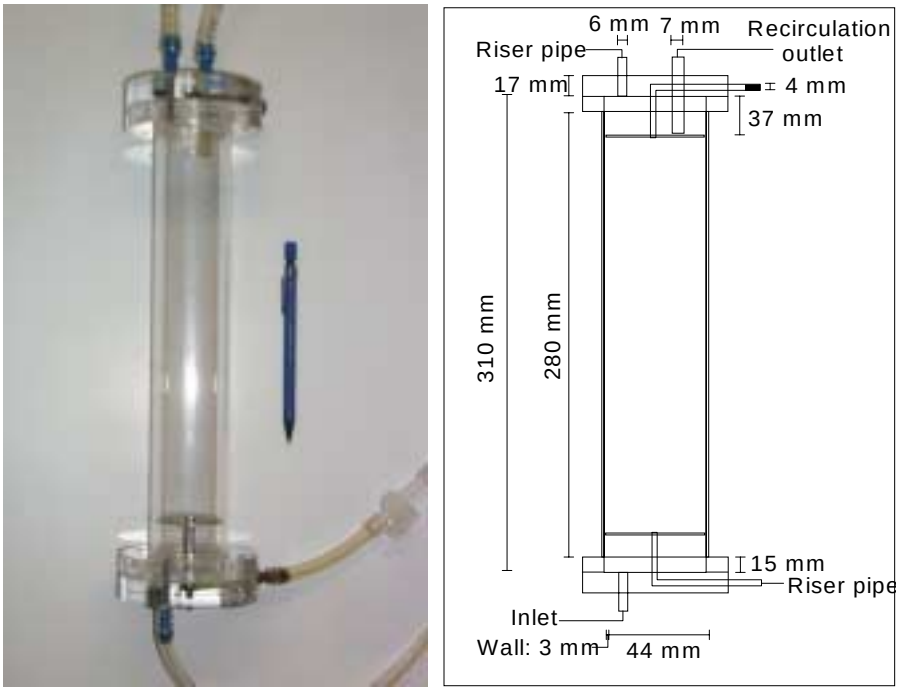

Figure 4.2. The reactor.

Upflow was used to facilitate transport of produced nitrogen gas out of the reactor. A small gas-trap was made in the top of the reactor by extending the recirculation outlet tube deeper into the reactor interior than the riser pipe connection, as illustrated in Fig. 4.2. Riser pipes were connected to the top and bottom of the reactor to indicate head loss and hence the need for backwash. However, these riser pipes were removed after the shift to Biolith® (see later) as carrier, since clogging of the reactor hereafter no longer was a problem. The outlet from the setup was then shifted to where the riser pipe in the reactor top at first was, whereby the effect of the gas trap was preserved.

4.3 The Carrier Material and Backwash Procedure

In the start-up phase, two commercially used granular carrier materials were tested: Biocarbon® and Biostyr®. Biocarbon® is granular expanded clay particles with sharp edges, a specific surface area of 1000 m^2/m^3, grain size of 3-6 mm and a density higher than that of water. Full-scale Biocarbon® biofilter plants have been in use since the early 80's and are found in many parts of the world, mainly Europe, North America and Japan. Biostyr® is granular floating polystyrene balls with a diameter of 3-5 mm and a specific surface area of 1050

m^2/m^3. The first full-scale Biostyr® biofilter plants were build in the late 80's, and today plants can be found in many European countries, especially in France and Denmark (Borregaard, 1997; Lacamp *et al*., 1993).

In full-scale biofilter systems, growing biomass attached to the carriers and suspended solids deposits are the main reasons of filter clogging. In this study synthetic wastewater without particulate matter was used, hence only biomass was responsible for clogging and in this way determining the so-called "run-time" of the filter. Boller *et al*., 1997, compared Biocarbon® and Biostyr® in regard to solids and gas accumulation. They investigated one Biocarbon® filter for treatment of primary effluent (secondary treatment) and one for treatment of secondary effluent (nitrification). Biocarbon® comes in different sizes for these different purposes. For nitrification, smaller grain sizes (2.5-3.5 mm) are used to increase the specific surface area. The investigated Biostyr® plant was for nitrification. It was found that the biofilm thickness after backwash was much lower for the Biocarbon® material, which was assumed to be caused by the intense scouring effect of the rough clay particles. This finding corresponds to an earlier investigation by Boller *et al*., 1994. Considerably higher amounts of biomass remained in the Biostyr® filter after backwash due to the less efficient backwash of these light, rounded particles. However, due to the easy expandability of the Biostyr® material, the headloss of this filter increased moderately also for high masses of accumulated solids – more than 1600-2500 $gTSS/m^3$ – whereas a sudden exponential increase in the headloss of the Biocarbon® filter was observed. For the bigger Biocarbon® grain size (3-6 mm) this sudden headloss appeared at solids concentration up to 3500-5000 $gTSS/m^3$ and for the lower grain sizes at solids concentrations of only 600-700 $gTSS/m^3$. Entrapment/hold-up of produced gas bubbles was highest in the Biocarbon®.

In the current study, a manual backwash procedure was applied due to the simplicity of this strategy for the small lab-scale reactor. During the initial experiments, it turned out to be difficult to backwash the Biocarbon® material. Biocarbon® particles quickly and strongly cemented together by the biomass and would have required a more efficient/strong backwash than the manual one. This was the main reason for choosing Biostyr®for future experiments.

During PART B of the study, another carrier was used: Biolith®. This is granular, round, clay balls with a diameter of 4-8 mm and a specific surface area of 500 m^2/m^3. The reason for using this carrier was, that it was used in the industrial pilot plant (Arnz *et al*., 2000ab) and the bench scale reactor (Gieseke *et al*., 1999) that supplied the biofilm for the investigations.

Backwash was done by shaking the reactor vigorously and turning it up and down in order to mix the carrier balls. During PART A with Biostyr®, the reactor was never exposed to air, because the detached excess sludge was pumped out of the reactor. Backwash was necessary 2-3 times a week. For PART B with Biolith®, it was chosen to empty the entire reactor into a glass beaker, stir it and remove the detached biomass before returning the carrier

particles to the reactor. This method was very quick and easy. Backwash was necessary once a week. Figure 4.3 illustrates the appearance of the investigated carrier materials, and Table 4.1 summarises the carrier characteristics.

Figure 4.3. The lab-scale reactor filled with the 3 tested carrier materials:
1) Floating Biostyr®, used during PART A of the study.
2) Biocarbon®, tested during start-up of the experimental period.
3) Biolith®, used during PART B of the study.

Table 4.1. Overview of main characteristics of the used carrier materials

Carrier name	Biostyr®	Biocarbon®	Biolith®
Producer	OTV France	OTV France	Phillip Müller, Germany
Material	Polystyrene	Expanded porous clay	Expanded porous clay
Form	Granular	Granular	Granular
Grain size [mm]	3-5	3-6	4-8
Specific surface area [m2/m3]	1050	1000	500
Shape	Round	Different, sharp edges	Round
In water	Floating	Settling	Settling

4.4 Synthetic Wastewater and Inlet Flow

Synthetic wastewater was used. As illustrated in Fig. 4.1, the setup had 2 inlets: 'Basic substrate' containing micronutrients was stored in a 200 L tank and send through a de-oxygenator system (see below) before entering the reactor. The other type of substrate was phase dependent, anoxic (nitrate) and anaerobic (acetate), respectively. This was kept in two separate 10 L bottles, stripped with nitrogen gas and kept free of oxygen by closing the bottles using a rubber stopper with an attached Tetlar bag filled with nitrogen. Addition of phase dependent substrate was regulated by a 3-way-valve. The reason for having two inlets was first of all to avoid bacterial growth in the substrate by separating the micro-nutrients from the carbon source and electron acceptor. Second, the use of the de-oxygenator system was very simple and economical for the significant volume of basic substrate needed during continuous operation, but due to a hydraulic residence time in this system of approximately ½ hour, it was not suited for the desired quick shifts of the phase dependent substrate.

Inlet flow: The basic substrate was added with a flow rate of 1035 ml/h. This flow rate was regularly tested and varied a little during the experimental period, but never more than 7 % from the average. The flow rate of the phase dependent substrate was 64.5 ml/h. This was also regularly tested and stayed very constant with a maximum deviation of less than 5 %. The total inlet flow to the reactor was the sum of the two: 1100 ml/h.

Basic substrate: The recipe of the basic substrate was taken from Baetens and Hosten, 1996. In addition to micro-nutrients, the basic substrate contained: Sodium bicarbonate, ammonium, phosphate, EDTA and yeast extract, Table 4.2. During PART A, the phosphate concentration of the basic substrate was 15.0 ppm P. Additional phosphate was added via the anoxic substrate to give a final concentration of 44.4 ppm P in the inlet during anoxic phases. Due to the dilution effect, the inlet concentration of phosphate during anaerobic phases was 14.1 ppm P. During PART B, a concentration of 30.0 ppm P was used in the basic substrate, and no additional phosphate was added to the anoxic substrate, hence the inlet concentration to the reactor was 28.2 ppm P during the entire phosphate cycle. This change was made to facilitate mass balance calculations of the system. The concentration was regularly measured and could vary up to 10 % from the average (a combination of the uncertainty introduced by the measuring equipment and by the substrate mixing).

Basic substrate was prepared in a 200 L tank once a week. Stirring was used during the mixing, but considered unnecessary once the compounds had been dissolved. Precipitates were never observed. The same strategy was used for the phase dependent substrate, however this was prepared in 5000 ml measuring bottles.

Anaerobic substrate: Acetate was used as the only carbon source throughout the study. The concentration of acetate in the anaerobic substrate was 6,6 g $NaCH_3COO$/l added in the form of $NaCH_3COO*3H_2O$, equivalent to an inlet concentration of 387 mg $NaCH_3COO$/l or 302 mg COD/l = 302 ppm COD.

Anoxic substrate: The anoxic substrate contained both nitrate and phosphate during PART A. The composition of the anoxic substrate was:

258 ppm P in the form of KH_2PO_4
258 ppm P in the form of $K_2HPO_4*3H_2O$
900 ppm N in the form of KNO_3

With the average flow rates given above, this gives inlet concentrations of 44.4 ppm P and 52.8 ppm N during anoxic phases. During PART B, no phosphate was added to the anoxic substrate as discussed above. The concentration of nitrate remained unchanged.

Table 4.2. Composition of synthetic wastewater, basic substrate – before addition of nitrate (anoxic phase) or acetate (anaerobic phase)

Compound	Concentration	Equivalent to	Addition to 200 L
$NaH_2PO_4*2H_2O$	75.5 mg/l [1)]	15 mg P/l [1)]	15.1 g
$MgSO_4*2H_2O$	90 mg/l	-	18.0 g
$CaCl_2*2H_2O$	14 mg/l	-	2.80 g
KCl	36 mg/l	-	7.20 g
NH_4Cl	107 mg/l	28 mg N/l	21.4 g
$NaHCO_3$	275.4 mg/l	-	55.08 g
Yeast extract	1 mg/l	-	200 mg
Nutrient solution	0.3 ml/l	-	60 ml

1) In PART A of the study. During PART B: 30 mg P/l.

Nutrient solution (0.3 ml/l added to basic substrate)	
Compound	Concentration (g/l)
$FeCl_3*6H_2O$	1.5
H_3BO_3	0.15
$CuSO_4*5H_2O$	0.03
KI	0.18
MnCl2*$4H_2O$	0.12
$Na_2MoO_4*2H_2O$	0.06
$ZnSO_4*7H_2O$	0.12
$CoCl_2*6H_2O$	0.15
EDTA	10

4.5 The De-oxygenator System

A de-oxygenator system according to Arcangeli and Arvin, 1995, was used to remove oxygen from the basic substrate. The principle of this was very simple, Fig. 4.4. 40 m of silicone tubing was immersed into a strong solution of $NaSO_3$ (100g/l) stored in a 20 L glass bottle with a tight rubber stopper. Gas penetrates the silicone tube wall whereby oxygen of the water inside the tube diffuses into the sulphite solution and oxidises sulphite into sulphate. $CoCl_2*6H_2O$ (200 mg/l) was used as a catalyst. The sulphite solution was continuously stirred and recirculated (~10 l/h) to avoid stagnating water or precipitates clogging the silicone surface. The silicone tube had a wall thickness of 1 mm and an inner diameter of 4 mm.

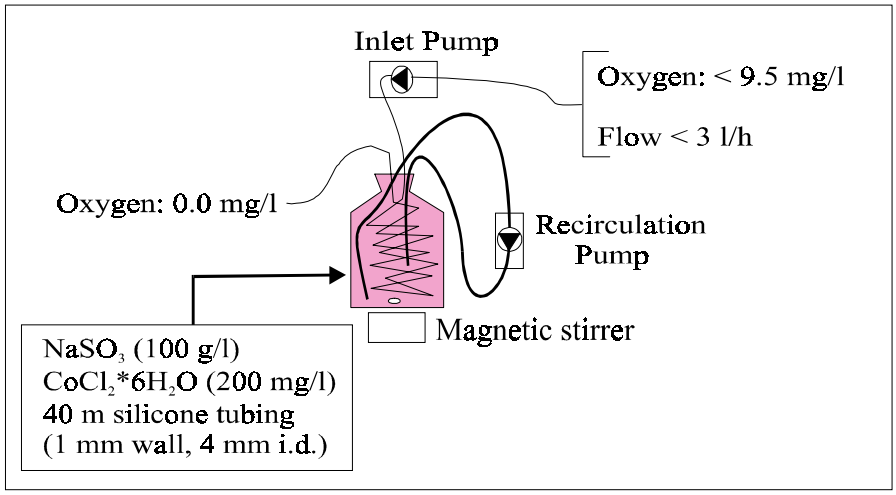

Figure 4.4. De-oxygenator system.

The system can remove oxygen up to 9.5 mg/l for a flow rate of up to 3 l/h (Arcangeli and Arvin, 1995). 9.5 mg/l is the saturation coefficient of oxygen in distilled water at 18 ^oC, the saturation concentration is lowered by higher temperatures and higher salt concentrations (Harremoës *et al.*, 1989), i.e. the saturation concentration of the basic substrate (room temperature) was below this concentration. The inlet flow was 1 l/h, which is well below the capacity of the de-oxygenator. The dissolved oxygen concentration in the outlet of the de-oxygenator was regularly controlled with an oxygen electrode, WTW microprocessor Oximeter, and no problems with the capacity were ever encountered. The sulphite solution was exchanged approximately every 3 months.

Oxygen in the setup: Tygon tubes with a wall thickness of 25 mm were used in the setup to minimise in-diffusion of oxygen from the surrounding air. PVC

tube connectors were used. Tygon or Marprene tubes were used in the recirculation pump. Silicone was used in the pump for the phase dependent substrate due to the low and accurate flow rate needed. Silicone was also used in the pump for basic substrate, but this pump was placed before the de-oxygenator. Glass holders with tight rubber stoppers were used for electrodes placed in the setup.
An oxygen electrode was included in the recirculation stream during the first year of operation as a control, but no problems with oxygen were encountered, so the electrode was removed when a pH electrode instead was included (the two signals interfered).
A test was made regarding in-diffusion of oxygen when the system outlet was closed and no biofilm/carrier was in the reactor, i.e. recirculation over the empty, clean reactor in a closed system. For an oxygen concentration of 0.0-0.1 mg/l, no in-diffusion could be detected over a 15 hours observation period.

4.6 On-line Phosphate Measurements

4.6.1 Principle of The Method

A photometric reaction was chosen for the on-line measurements of phosphate. As oppose to nitrate, no commercial phosphate electrode is presently available. The principle of the chosen method was to mix a colour reagent (Appendix 4.1) with the sample, let the two solutions react and measure the absorbance at a wavelength of 400 nm (ASTM D 515-68 non referee method B). The absorbance (A) is directly proportional to the phosphate concentration (C):

$$C = \text{Constant} \cdot A \qquad (4.1)$$

Figure 4.5 shows a schematic illustration of the measuring equipment that was developed and used. A spectrophotometer, a phosphate pump and 6 magnetic two-way valves were connected to the control computer. During a single measurement, a sample from the recirculation stream of the setup was first pumped to the flow cell in the spectrophotometer (pumping time set at e.g. 80 s). Reagent was pumped in with the same flow rate. 7 times higher flow rate was used for distilled dilution water. A short time for reaction was allowed (~20 s), and the electronic signal from the spectrophotometer was logged by the computer. A blank sample (distilled water) was hereafter run identically, and the phosphate concentration was calculated from the difference between the two signals. By always running a blank sample, the problem of a sliding base line was avoided. Higher dilution was used in some batch tests to increase the measuring range.
4 standards were used for the calibration and these were chosen according to the desired measuring range, for the continuous operation mainly 10-50 ppm P.

Linear regression was made according to Montgomery, 1991. A control standard (standard 2) was regularly run during continuous operation. In case of deviation, either an adjustment of the standard curve was made in order to match the new value, or for higher deviations a new, complete standard curve was run. The criteria for running a new standard curve in respect to allowed deviation could be defined in the user interface of the computer program. However, the stability of the measuring equipment was very good with no necessity of automatic runs of standard curves.

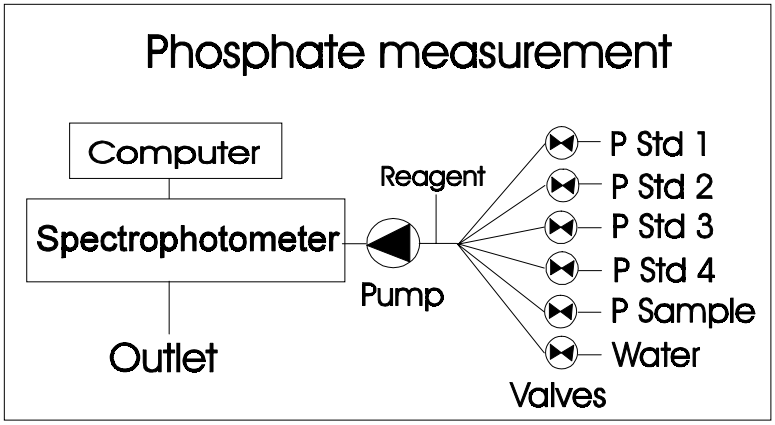

Figure 4.5. Principle of the phosphate on-line measuring device.

4.6.2 The Spectrophotometer

2 different spectrophotometers were used. First (March'96-April'97) a rather old one of the mark Gilford, but in the main part of the study (April'97-Dec'99) this was replaced by a newer model: Spectronic 20D.

The flow cell for the Spectronic 20D had both the outlet and the inlet in the top. To avoid short circuiting of the incoming water, this was changed by inserting a tiny Teflon tube via the inlet into the bottom of the flow cell, so that water came in by the bottom of the cell and out by the top, Fig. 4.6. This also prevented entrapment of air bubbles.

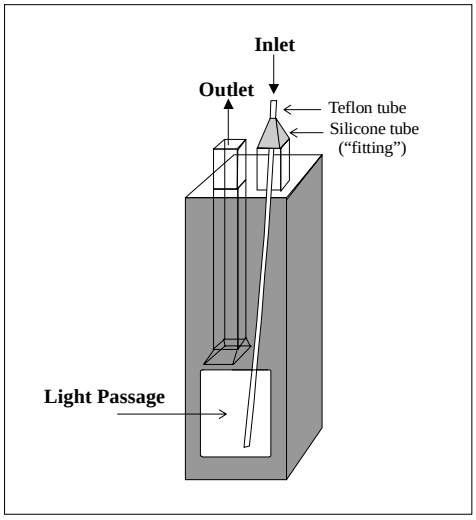

Figure 4.6. Flow cell for the Spectronic 20D spectrophotometer

The electrical signal from the Spectronic was based on the light intensity through the flow cell. The relationship between light intensity, I, and absorbance, A; is:

$$A = -\log_{10}\left(\frac{I}{I_0}\right) \tag{4.2}$$

- I_0 is the light intensity for the blank sample.
The absorbance is 1 for a 90 % reduction of the transmitted light ($I = 0.1*I_0$)

4.6.3 The Phosphate Measurement Setup

Figure 4.8 illustrates the total setup for phosphate measurements. 1 L glass bottles were used for the phosphate standards. These were prepared from dried KH_2PO_4 in distilled/Milli-Q water. A 5 or 10 L bottle was used for distilled dilution water. The phosphate reagent was stored in a 10 L glass bottle.

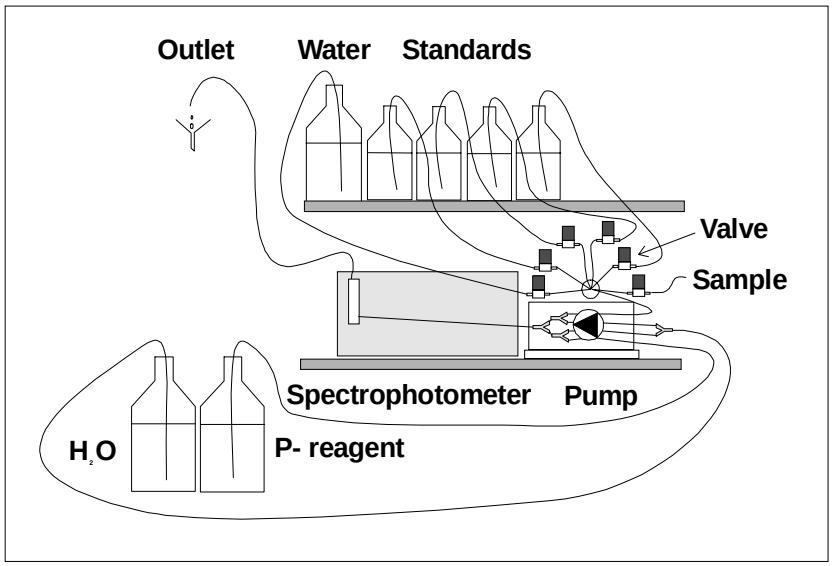

Figure 4.8. Phosphate measurement setup with Spectronic 20D spectrophotometer.

Teflon tubes with an inner diameter of 1 mm were used, in combination with silicone tubes in the pump. A round tube connector was used for combining the Teflon tubes from the standards and sample. This was made of a small, round acrylic block with 7 conical holes all meeting in the centre, Fig. 4.7. Small pieces of PVC tubes were glued in every hole, so that Teflon tubes could be connected. The connection was tight, when the Teflon tube was pressed firmly into the PVC tube. The dead volume of water was negligible, and the residence time in the entire system was approximately ½ min with a sample flow of 5 ml/min.

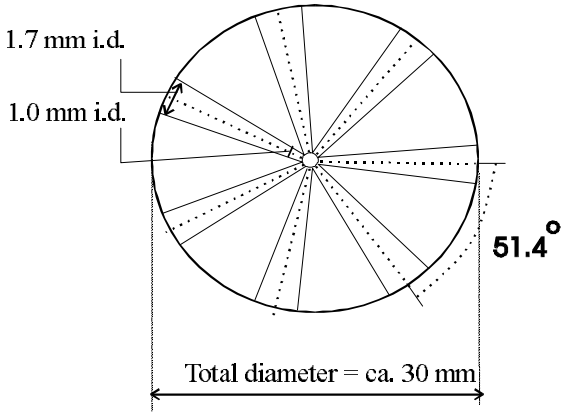

Figure 4.7. Tube connector for 7 tubes in the phosphate setup.

4.6.4 Linearity of The Phosphate Measurements

Without diluting more than the normally 7 times, a linear standard curve could be obtained up to phosphate concentrations around 90 ppm P, Fig. 4.9. The base line and the standard curve were very stable without much drift over time (time-scale: months). The standard curve could change slightly upon change of reagent (new reagent was made twice a month), change of bulb (about once a month) or change of pump tubes (about every 2 months), hence a new standard curve was always run upon any change in the setup. Correlation coefficients of the 4 point standard curves were always very close to 1.

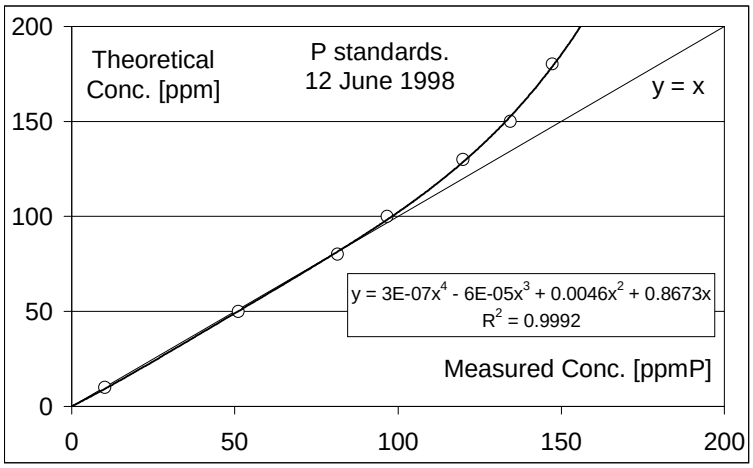

Figure 4.9. Liniarity of the phosphate measurements.

When moving the setup to TUM during PART B of the study, some problems occurred with the phosphate measurements. This problem turned out to be related to the ion-exchanged water. For some reason, still unknown, the ion-exchanged water contained one or more interfering compounds. Using Milli-Q water for standards, dilution and blank samples solved the problem.

4.7 On-line Nitrate Measurements

4.7.1 Principle of The Method

Several commercial nitrate electrodes exist and one of these (see later) was chosen for the on-line measurements. Some advantages of an electrode over a photometric reaction are no chemicals needed and larger measuring interval.

The Nernst equation: Many different ion-selective electrodes exist. An ion-selective electrode is an electrochemical half-cell responding to a specific ion and obeying the Nernst equation (Malmvig, 1996):

$$E = E_0 + \frac{R \cdot T}{z \cdot F} \cdot \ln(a_x) \qquad (4.3)$$

E = Electrode potential of the half-cell
E_0 = Standard electrode potential for the half-cell (a = 1)
R = The Gas constant (8.3143 joule * $^oK^{-1}$ * $Mole^{-1}$)
T = Absolute temperature ^oK
F = Faraday's constant (96487 coulomb $equiv.^{-1}$)
z = Charge number of the ionic species
z is positive for cations and negative for anions (for NO_3^-, z = -1)
ln = The natural logarithm
a_x = the activity of the ion species X (here NO_3^-)

All electrochemical cells consist of two half-cells. One of these can be a reference electrode (half-cell) and have a constant potential, E_{ref}, which can be subtracted from E_0 in the equation, giving E'. E then simply denotes the potential of the whole electrochemical cell. Calculating R/T and changing to normal logarithm then gives:

$$E = E' + z^{-1} \cdot T \cdot 0.1984 \cdot \log_{10}(a_x) \qquad (4.4)$$

For 25 ^oC (298.15^oK) and z = -1 (NO_3^-) $\rightarrow$ z^{-1}*0.1984*T = -59.16 mV.

In this way, there is a logarithmic relationship between the measured potential and the concentration (activity) of the considered ion:

$$\begin{gathered} Potential\,[\mathrm{mV}] = \alpha - 59.16\mathrm{mV} \cdot \log_{10}(\mathrm{Concentration}\,[\mathrm{ppmN}]) \\ \Updownarrow \\ \mathrm{Concentration} = \exp\left[\frac{\mathrm{Potential} - \alpha}{59.16}\right] \end{gathered} \qquad (4.5)$$

α is the intercept with the y-axis and –59.16 mV is the slope of a plot of the potential against the logarithm of the nitrate concentration, Fig. 4.10.

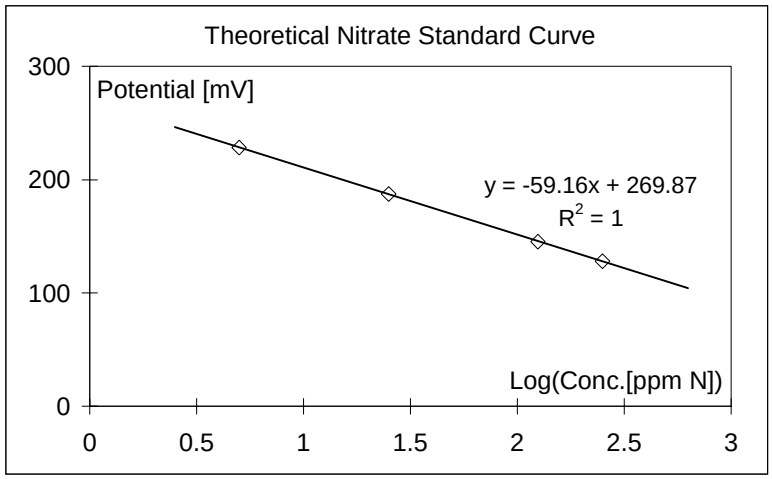

Figure 4.10. Theoretical standard curve for a nitrate electrode.

Activity of nitrate ions in the synthetic wastewater:

$$\left\{NO_3^-\right\} = \gamma_1 * \left[NO_3^-\right] \tag{4.6}$$

- { } is the activity
- γ_1 is the activity coefficient
- $[NO_3^-]$ is the concentration

The activity coefficient is calculated:

$$-\log \gamma_1 = 0.5 * z_i^2 \frac{\sqrt{I}}{1+\sqrt{I}} \tag{4.7}$$

- z_i is the charge of the considered ion, for nitrate = -1
- I is the ion strength of the solution calculated from all the ions present

The ion strength is calculated:

$$I = \frac{1}{2} * \sum_1^N C_j * z_j^2 \tag{4.8}$$

- C_j is the concentration of an ion and z_j is the charge of this.
- N is the amount of dissociated components in the solution, anions and cations.

The ions strength of the basic substrate was calculated from the molar concentrations of the ingredients, I = 6.62 * 10^{-3}, and this corresponded to an activity coefficient of nitrate, γ_1 = 0.92 (with a phosphate concentration of 15 ppm P). By including the acetate in the anaerobic inlet, I = 8.06 * 10^{-3} and γ_1 = 0.91. By including the nitrate and phosphate in the anoxic substrate, I = 12.1 * 10^{-3} and γ_1 = 0.89. The difference in activity coefficient is very small between anoxic and anaerobic inlet solution, since the basic substrate constitutes the

major contribution to the ion strength. It was therefore considered acceptable to prepare nitrate standards from basic substrate and ignore minor changes in the ion strength during a phosphate removal cycle.
Figure 4.11 shows a schematic illustration of the measuring equipment that was developed and used. A nitrate and reference electrode, a potentiometer, a nitrate pump and 5 magnetic 2-way valves were connected to the control computer. The electrodes were placed in a 10 ml glass beaker (see below). The sample was pumped into this beaker at the same time as the previous sample was pumped out. Constant stirring by a magnet was arranged in the beaker. The flow was stopped, before the computer registered the electrical signal.
4 standards were used for the calibration. These were chosen according to the desired measuring range, for the continuous operation mainly 4-60 ppm N. Nitrate concentrations high above the relevant ranges could be measured without dilution (up to ~1000 ppm N). Concentrations below 0.1-0.2 ppm N could not be measured exact due to the logarithmic nature of the method and the influence of other anions. Linear regression was made according to Montgomery, 1991. Automatic run of standard curves was implemented in the same manner as for the phosphate measuring equipment.

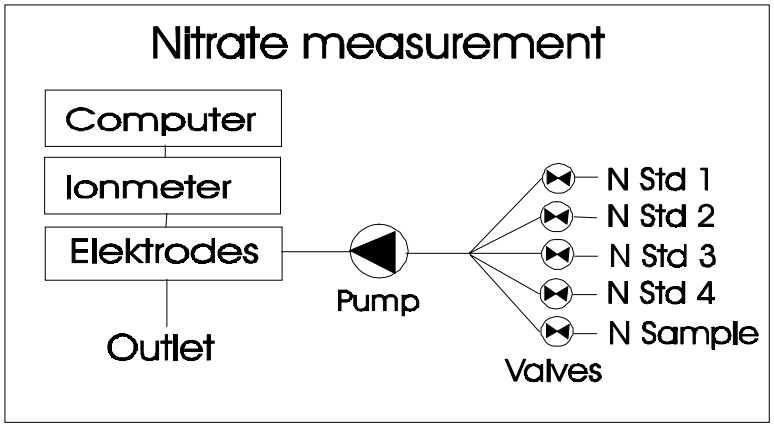

Figure 4.11. Principle of the nitrate on-line measuring device.

4.7.2 The Nitrate Electrode

The nitrate electrode was of the type: ISE25NO3 manufactured by Radiometer Copenhagen, Radiometer Analytical S. A., Lyon France. The reference electrode was from the same supplier and of the type: REF201 Ag/AgCl reference electrode with a salt-bridge solution of saturated KCl. Also the potentiometer, PHM64-ionmeter, was from Radiometer Copenhagen. For specific operating instructions and information regarding competing ions is referred to the user manuals.
Several arrangements of the nitrate electrode in a 10 ml measuring beaker were tried out. Figure 4.12 shows the optimised version that was used in the main

part of the study. The sample dripped into the beaker – the dripping was needed in order to disconnect the solution inside the beaker with the water stream in the setup due to static electricity (caused by the pumps) that otherwise disturbed the electrode signal. A glass tube was secured at a certain level just allowing the electrode to be under the solution surface. The glass tube served as the level control in the beaker, since the outlet flow was pumped via this tube. The same pump was used for the in- and outlet, however, a greater diameter of the pump tube was applied for the outlet to avoid water accumulation in the beaker in case of a slight deviation of in- and outlet flow. The water volume was kept as small as possible to minimise the hydraulic retention time of the system. A flow rate of approximately 15 ml/min was used, which demanded for a pumping time of 2-3 min to avoid carry-over between samples.
The electrode had to be cleaned very regularly (preferably every 2-3 day) due to biomass growth of the membrane surface. A new standard curve had to be run after each cleaning. The membrane of the electrode had to be shifted approximately every 3-4 month to maintain a good sensitivity (as indicated by the slope of the standard curve).

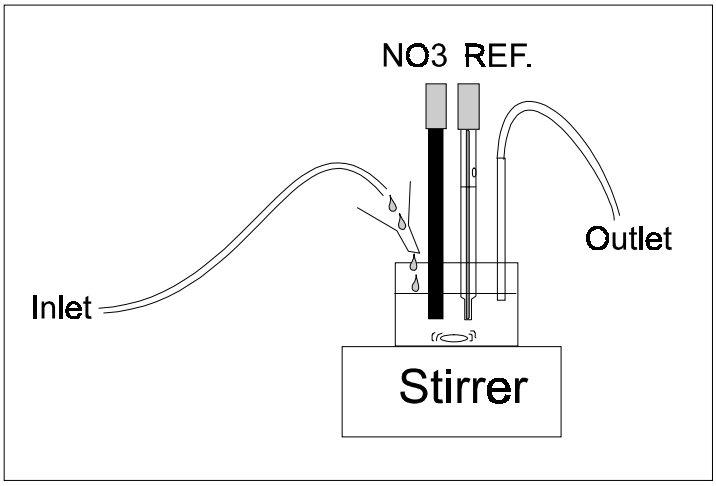

Figure 4.12. The nitrate and reference electrode setup in a 10 ml glass beaker.

4.7.3 The Nitrate Measurement Setup

Figure 4.13 illustrates the total setup for nitrate measurements. 1 L glass bottles were used for nitrate standards and these were prepared once a week. Teflon tubes and silicone pump tubes were used, equivalent to the phosphate measuring setup. A 6-way tube connector was constructed according to the same principle as the one used in the phosphate setup.

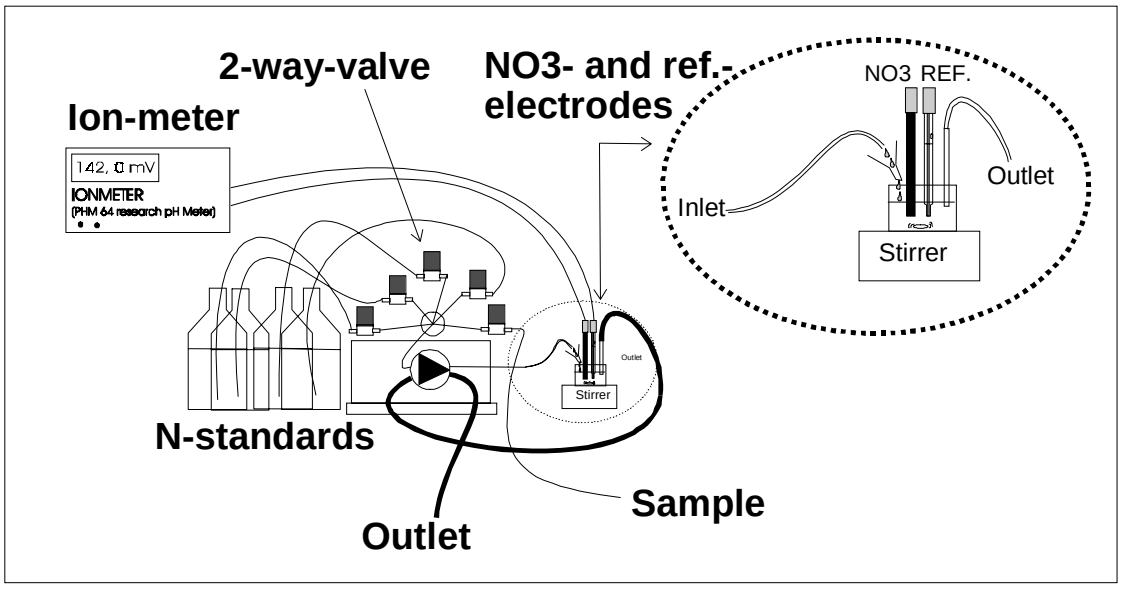

Figure 4.13. The nitrate measurement setup.

4.8 Sampling

Samples for phosphate or nitrate measurements were taken from the recirculation stream of the setup via a Teflon tube inserted in a PVC T-tube connector as illustrated in Fig. 4.14. The sampling frequency was defined in the user interface of the computer program, but samples for phosphate and nitrate measurements could not be taken simultaneously. For continuous operation, sampling intervals were typically 4 min for nitrate and 8 min for phosphate.

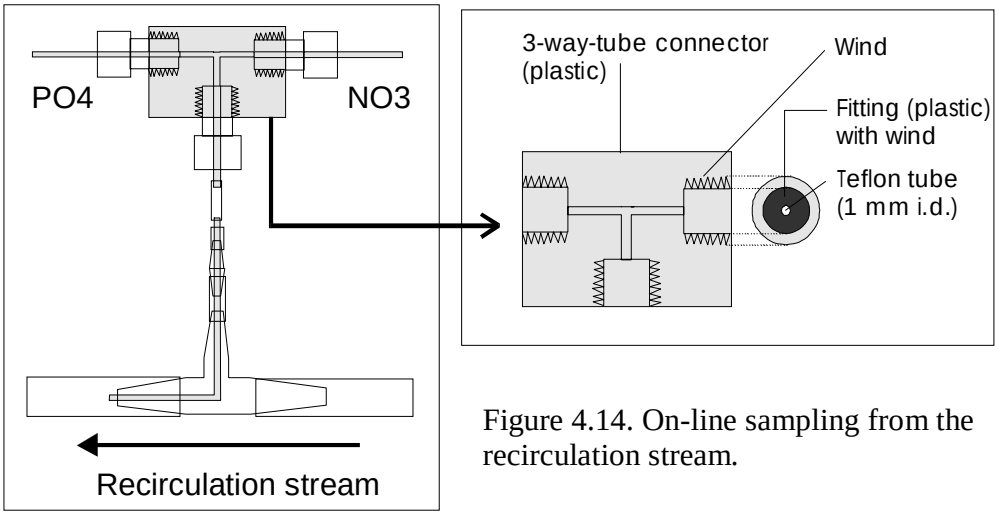

Figure 4.14. On-line sampling from the recirculation stream.

4.9 pH Control

pH control was implemented by the end of PART A (Sep.'98), by inserting a pH electrode, HI1910B Hanna instruments, and a Teflon tube (same principle as for sampling, Fig. 4.14) in the recirculation stream. The Teflon tube was via a pump connected to a 0.3 M HCl solution. The electrode and pump were coupled to the control computer and a small program was developed for pH control. pH was measured every minute and acid was added if necessary. pH was in this way kept at 7 ± 0.2 during the continuous operation. 1 L of 0.3 M HCl solution was used up in ~10 days. The HCl solution was kept anaerobic in a bottle identical to the one used for batch experiments (Fig. 4.15).
A semi-automatic pH control was used during batch experiments. Relatively high amounts of acid could be needed in the beginning of experiments with simultaneous presence of nitrate and acetate, which demanded for a higher flow rate of the acid pump in the beginning (or longer addition time) than by the end, which was adjusted manually.

4.10 Batch Experiments

The experimental setup could be used for batch experiments by inserting a batch bottle in the recirculation stream, closing the outlet and riser pipes and stopping the inlet pumps. Fig. 4.15 illustrates the experimental batch setup from Nov. 1997, and the batch bottle. This principle, and the same batch bottle was used throughout the study, however minor differences of the placing of the batch bottle in the recirculation stream occurred.

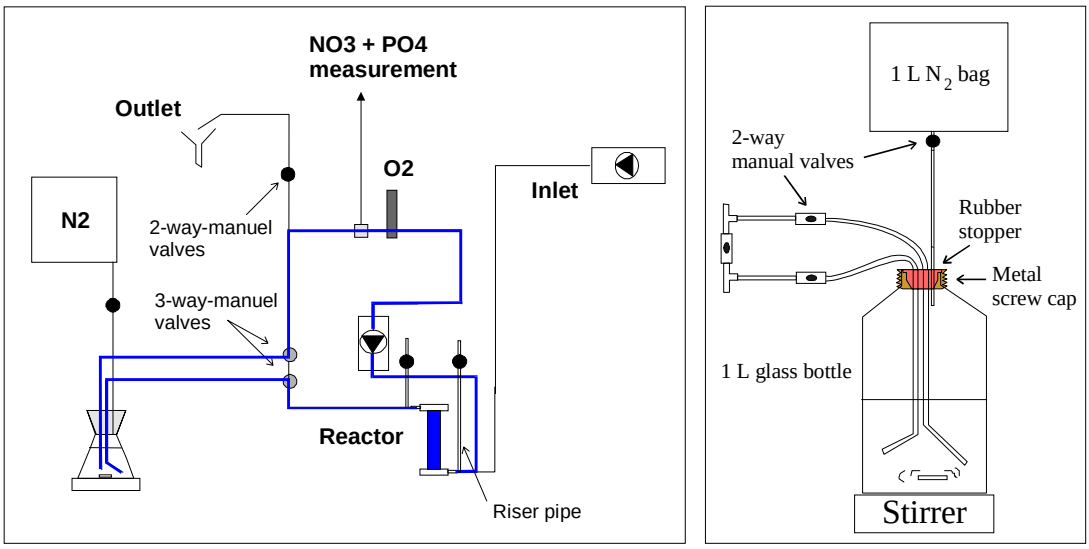

Figure 4.15. Experimental setup for batch experiments (Nov. 1997), and the batch bottle.

The volume of the batch bottle was 1 L. It was closed tightly by a combined rubber stopper and screw cap. A nitrogen-filled Tetlar bag was attached to the bottle to replace the water that was removed for sampling during an experiment. Batch experiments were performed by first sending only basic substrate through the reactor until all nitrate or acetate had been washed out. Then the tubes to the batch bottle were slowly filled with basic substrate (passed through the reactor) by opening the manual valves. The batch bottle was filled with the desired batch solution, stripped with nitrogen gas and the stopper was fixed. Then the batch experiment was started by: closing the riser pipes, closing the outlet, stopping the inlet pump, starting the magnetic stirrer of the batch solution, shifting the manual valves to direct the recirculation stream through the batch bottle, and finally start the recirculation pump. The start of recirculation was defined as time zero of the experiment.

4.11 The Total Experimental Setup

Figure 4.16 illustrates the total experimental setup (4 m length, 1 m width and 1.8 m height). It was placed in a laboratory at room temperature.

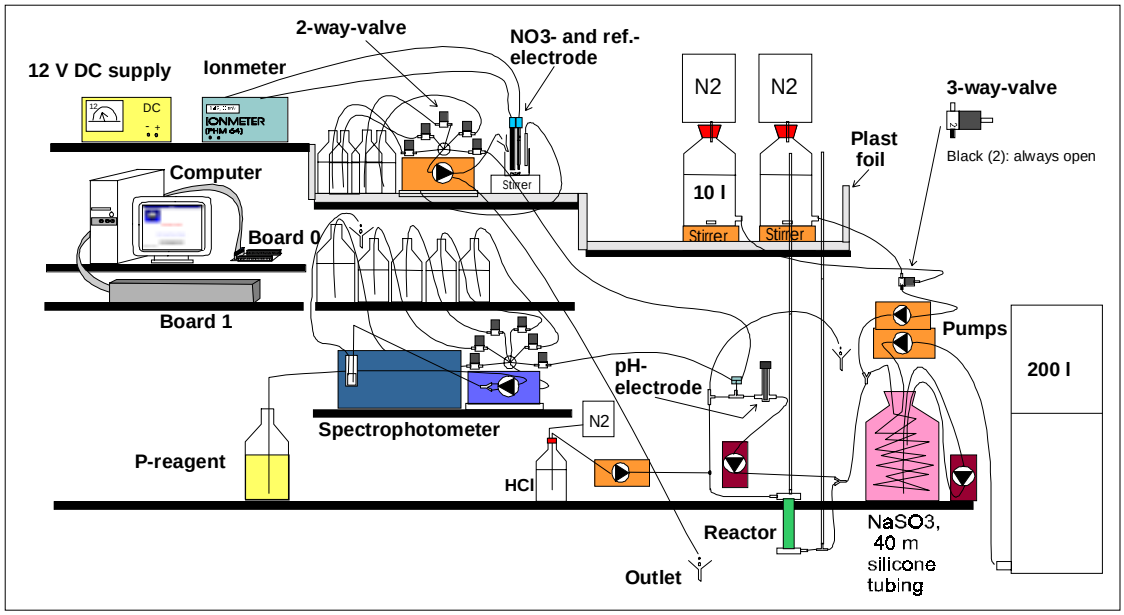

Figure 4.16. The total experimental setup (Nov. 1998).

4.12 Computer Program and Electronics

A 486, 33 MHz, computer was used as control computer. The following equipment was connected:

Sensors (convert physical variables, e.g. temperature and concentration, into electrical signals that can be measured directly in the form of electrical potential, resistance etc.):

- The spectrophotometer for phosphate measurements
- The ionmeter for nitrate measurements
- The oxymeter for oxygen and temperature measurements
- The pH electrode

Actuators (convert electrical signals into physical actions):

- The two inlet pumps
- The recirculation pump
- The nitrate pump
- The phosphate pump
- The pH pump
- The anaerobic/anoxic 3-way valve
- 6 valves in the phosphate measurement setup
- 5 valves in the nitrate measurement setup

Computerboards and electronics: The sensors send out analogue (continuous) signals, which have to be converted to digital (discrete) signals to be read by the computer. This was done via an A/D converter computer board: CIO-DAS801 from Computer Boards Inc., USA.

The actuators can be controlled directly by the computer (digital signal: on/off, 0/1), but an external power supply has to be connected. 12 V DC was used for all valves and for relays connected to any 220 V AC equipment.
A relay board with 24 relays that could be switched on by the 5 V internal power supply of the computer was used for controlling the actuators: CIO-ERB24 (external) in combination with CIO-DIO24 (internal), Computer Boards Inc. The relays on the board are so-called normally open, meaning that there is only electrical connection through the relay when a signal is written to it by the computer, Fig. 4.17.

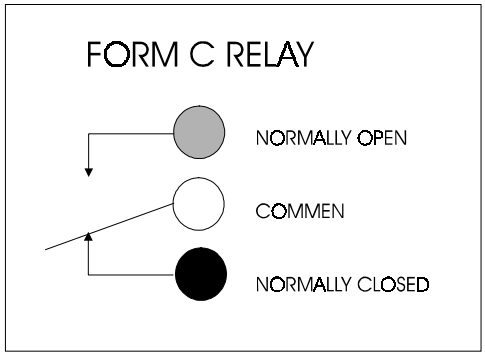

Figure 4.17. Relay type of CIO-ERB24, normally open. The connector is shifted when a signal is written to the relay.

Figure 4.18 illustrates the principle of connecting a 12 V DC power supply to a relay, and Fig. 4.19 illustrates how to turn on a 220 V AC device via a 12 V DC relay. The power supply can be connected in parallel to all the devices via a screw terminal (Fig. 4.20) whereby more than one device can be switched on simultaneously.

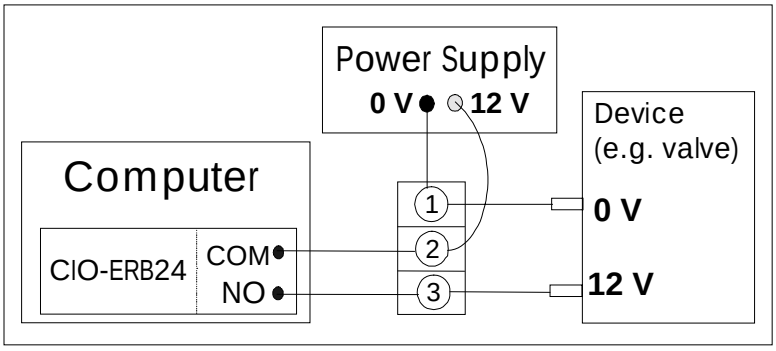

Figure 4.18. Voltage over the device (e.g. a valve) is obtained by establishing electrical connection between the COM and NO-poles of the CIO-ERB24 relay.

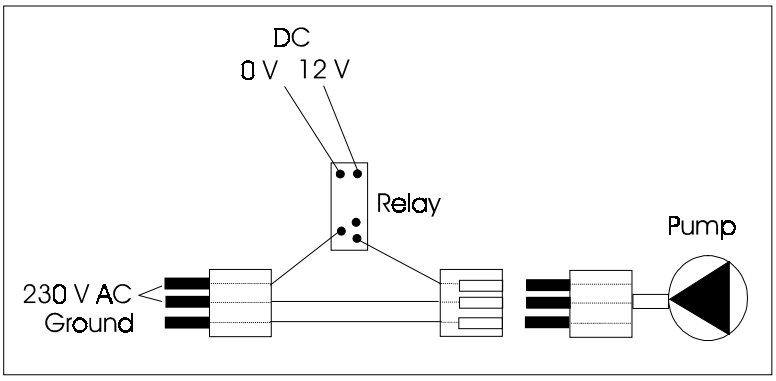

Figure 4.19. Voltage over a 220 V AC device (e.g. a pump) via a 12 V DC relay.

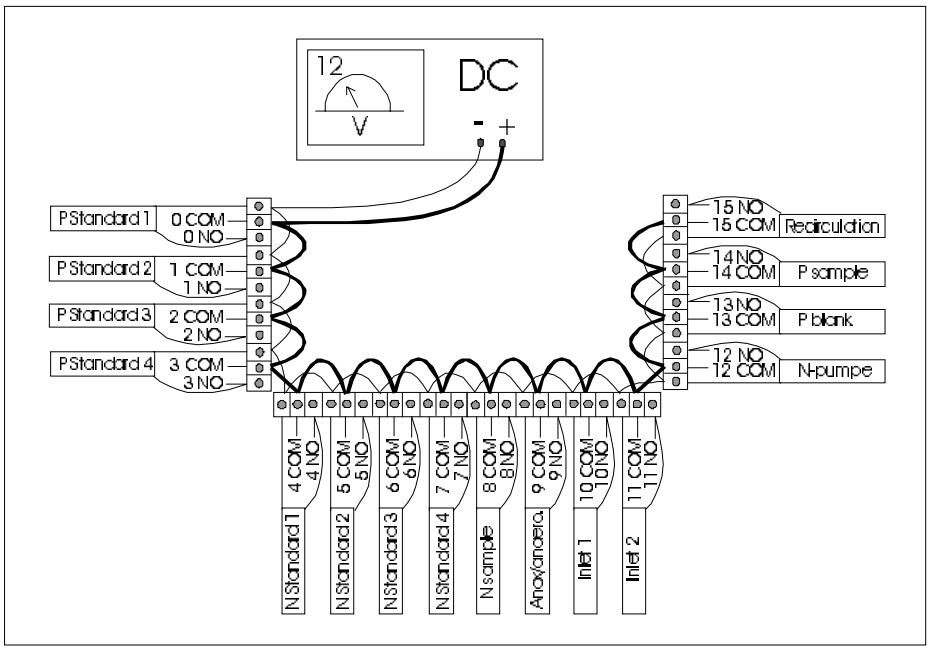

Figure 4.20. Parallel connection of a 12 V DC power supply to the screw terminal of CIO-ERB24. Once, the COM and NO ports are in connection, 12 V DC voltage is established over the actuator according to the principle illustrated in the close-up detail-picture in Fig. 4.18.

Computer program: Visual Basic was the programming language. For a description of Visual Basic is referred to the manual. Programming code and structure of the developed program shall not be included here. Two examples of the program windows are given to illustrate the idea. The interface during continuous operation is shown in Fig. 4.21a, and Fig. 4.21b shows the window for defining different operating parameters (these could be changed any time during operation). All data were stored in files that could be read by e.g. Excel.

(a)

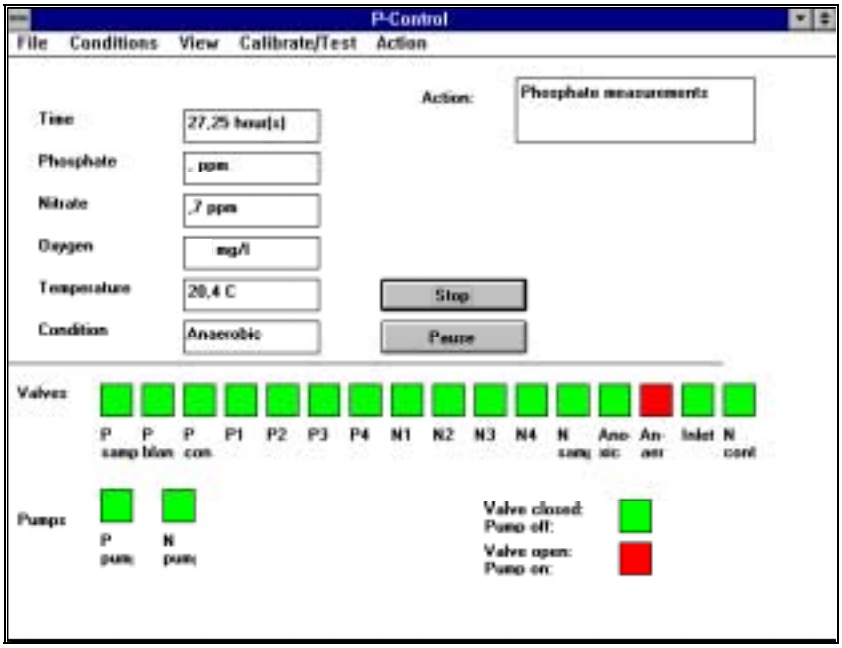

(b)

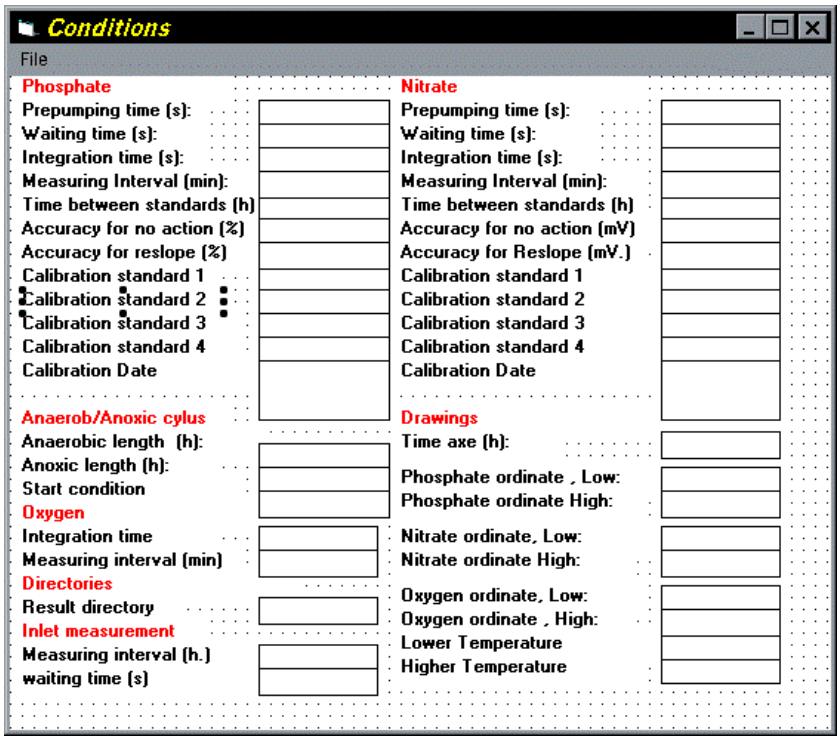

Figure 4.21. a) Program window during continuous operation. b) Program window for user definable parameters.

5. Calculations with the Experimental Data.

5.1 The Continuous Operation

5.1.1 Mixing Conditions and Theoretical Output Data

A high recirculation flow was applied over the reactor to establish mixing conditions close to ideal mix. PART A used a flow rate of ~15 l/h, i.e. 15 times the inlet flow, until Feb. '98 and hereafter ~20 l/h. The recirculation flow during PART B (new pump) was ~25 l/h. To evaluate the assumption of ideal mixing, an experiment was carried out where clean Biostyr® was placed in the clean reactor, and substrate was sent through. The measured and theoretical concentrations of nitrate are shown in Fig. 5.1. Figure 5.2 illustrates the theoretical outlet concentrations of NO_3-N, PO_4-P and COD in the continuous setup in case of no biological activity. The inlet concentration of phosphate was varied between the anaerobic (14.1 ppm P) and anoxic (44.4 ppm P) phases during PART A. PART B used a constant inlet concentration of phosphate throughout the cycle (28 ppm P) to facilitate mass balance calculations. The computer program AQUASIM (Reichert, 1994) was used to simulate the theoretical outlet concentrations of an ideally mixed reactor. Theory of ideally mixed and plug flow systems can be found elsewhere, e.g. Harremoës *et al*., 1989.

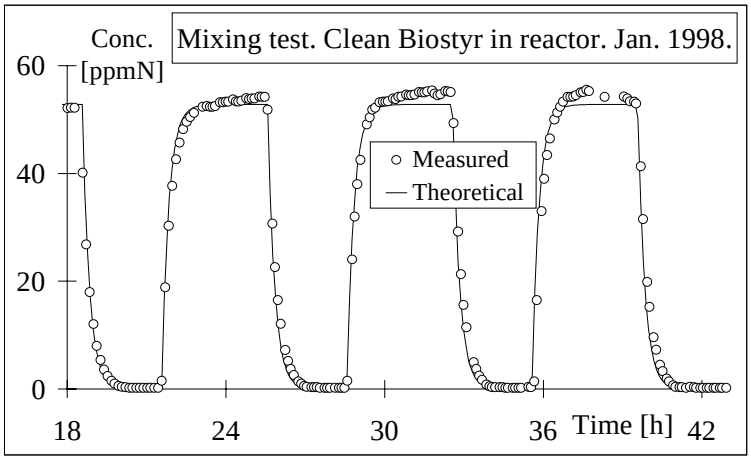

Figure 5.1. 'Tracer' experiment with the continuous operation. Nitrate is added as during normal operation, but clean BIOSTYR is placed in the reactor.

The experimental outlet data during operation with an active EBPR biofilm in the reactor reflect a combined effect of hydraulic mixing and biological activity. Figure 5.3 illustrates typical outlet data (nitrate and phosphate) from the continuous operation during PART A.

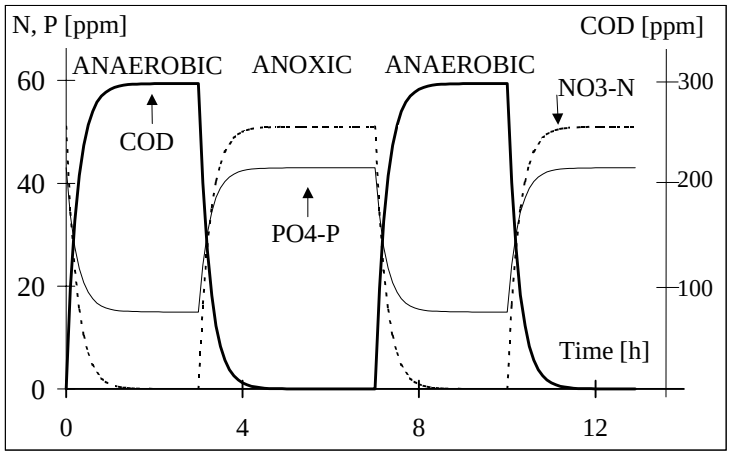

Figure 5.2. PART A: Expected continuous outlet concentrations in case of no reactions. The curves go up and down due to the changing inlet concentrations.

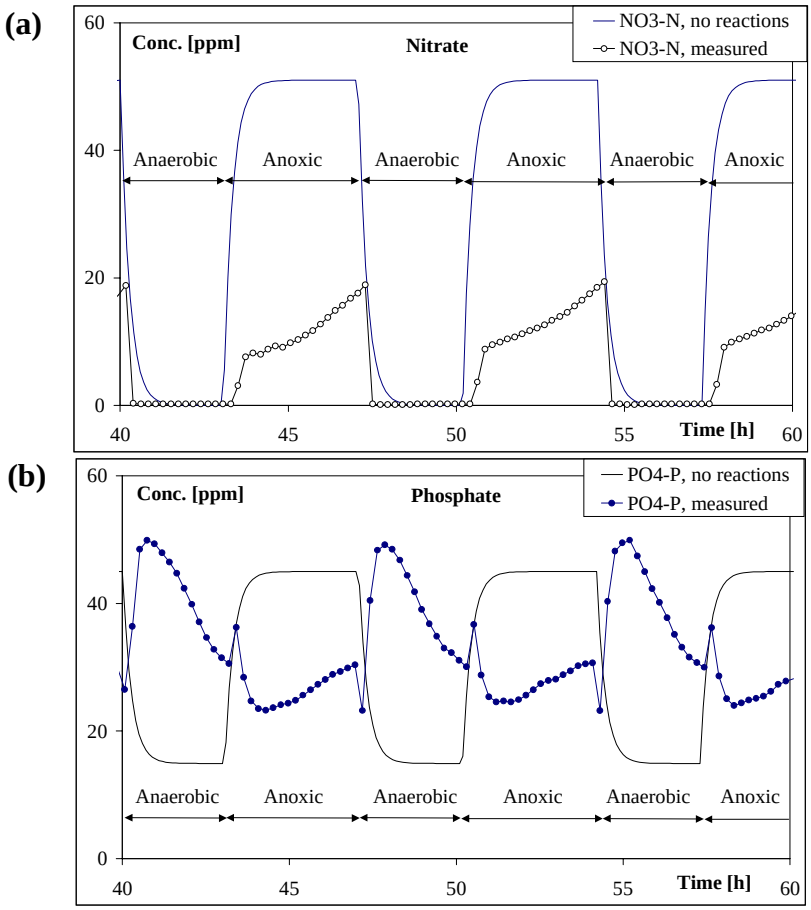

Figure 5.3: Typical data from the continuous operation during PART A: (a) Nitrate (b) Phosphate. The curves in case of no removal have been included. During the continuous run, the inlet concentrations are shifted according to the phases. The difference (area) between the curves for no removal and the measured curves illustrates the mass of phosphate that was taken up/released by the biofilm. For phosphate, (b), the combination between mixing and biological activity is particular evident.

5.1.2 Mass Balance Calculations for The Continuous Operation

5.1.2.1 Phosphate

The only source of phosphate is the addition via substrate. P can be removed from the system either via the outlet or via backwash. During backwash, 3 different types of accumulated phosphate can be removed along with the material flushed from the system:

1. P incorporated in the biomass as building blocks of the bacteria cells.
2. P incorporated in the bio-P-bacteria cells as poly-P-storage.
3. P in the form of chemical precipitates in the biofilm.

If *precipitation* occurs in the system, it will manifest itself in increased amount of P removed in the system compared to the biological removal. Precipitated P will add to the accumulation of 'biofilm' mass in the system and shall be removed along with biomass during backwash. If precipitation happens during the anoxic phase, the biological P uptake estimated from a mass balance based on phosphate in the in- and outlet will be overestimated. If precipitation happens during the anaerobic phase, the biological P release will be underestimated.
Possibly, precipitated phosphate may *dissolve* again. If e.g. phosphate has precipitated during the anoxic phase and is dissolved during the anaerobic, then both the anoxic biological P uptake and the biological P release are overestimated. If phosphate precipitates during the anaerobic phase and dissolves during the anoxic, the biological P release and P uptake are both underestimated. The result of precipitation and dissolution will be erroneous calculated coefficients for the biological P process and instead, the calculated coefficients will be for the combined chemical/biological P removal process.
Chemical precipitation can be verified by chemical analysis of the biofilm composition as discussed by Arvin, 1983.

The area between an AQUASIM-curve for no removal and the measured phosphate concentrations, Fig. 5.4, multiplied with the flow (Q, [m^3/h]) was used as an estimate of the mass of P taken up or released by the biomass. The area was approximated by numerical integration where the area was divided into trapezes according to the measuring points.

Ex. P release, Fig. 5.4:

P-area-2: - ½ * (t_2 - t_1)*((Measured1 - AQUASIM1) + (Measured2-AQUASIM2))

$$P_{released-Anaerobic1} = Q \cdot \sum_{1}^{n} P_{area,n} \qquad \text{(On Fig. 5.4, n = 9)} \qquad (5.1)$$

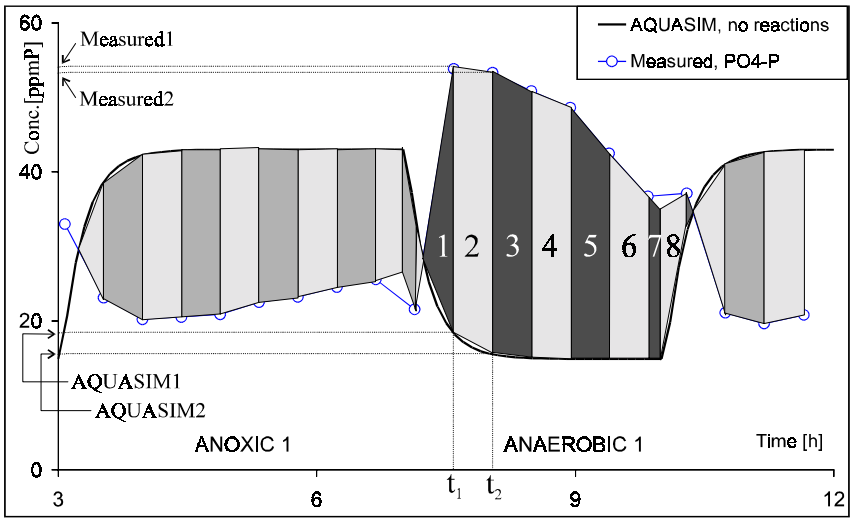

Figure 5.4. Area between an AQUASIM curve for no P reactions and a measured P curve.

A relatively small error is introduced with this calculation due to the fact, that the concentrations in the system by the end of a phase, when biological reactions take place, is not the same as simulated by AQUASIM for no reactions taking place. As an example, by the end of an anoxic phase AQUASIM uses 44.4 ppm P, whereas the actual concentration might be around 25 ppm P (Fig. 5.5). Hence, the starting point for the mixing curve by the beginning of an anaerobic phase is in the simulation 44.4 ppm P instead of the actual 25 ppm P. The same considerations apply for the end of an anaerobic phase and mixing curve for the start of the anoxic phases. The error seems small when looking at Fig. 5.5, where the correct AQUASIM curves have been included. The error is almost outbalanced, since the mistakenly calculated P release areas are almost same sizes as the mistakenly calculated P uptake areas.
The net P removal during one complete cycle is calculated from the area below the outlet curve (estimated in a similar numerical way as above, Fig. 5.4), multiplied with the flow rate to give the phosphate mass. The phosphate added via the inlet during the total cycle is subtracted from this area to give the net mass of phosphate taken up by the biomass:

$$M_{P,removed} = Q*\{(Pcycle,area) - (C_{PO4,ana,in}*T_{ana} + C_{PO4,ano,in}*T_{ano})\} \quad (5.2)$$

$M_{P,removed}$: The net mass of P taken up by the biofilm during one cycle
Q : The inlet flow
$P_{cycle,area}$: The area of the phosphate outlet curve during a cycle
$C_{PO4,ana,in}$: The inlet concentration of phosphate during the anaerobic phase
$C_{PO4,ano,in}$: The inlet concentration of phosphate during the anoxic phase
T_{ana} : The anaerobic phase length
T_{ano} : The anoxic phase length

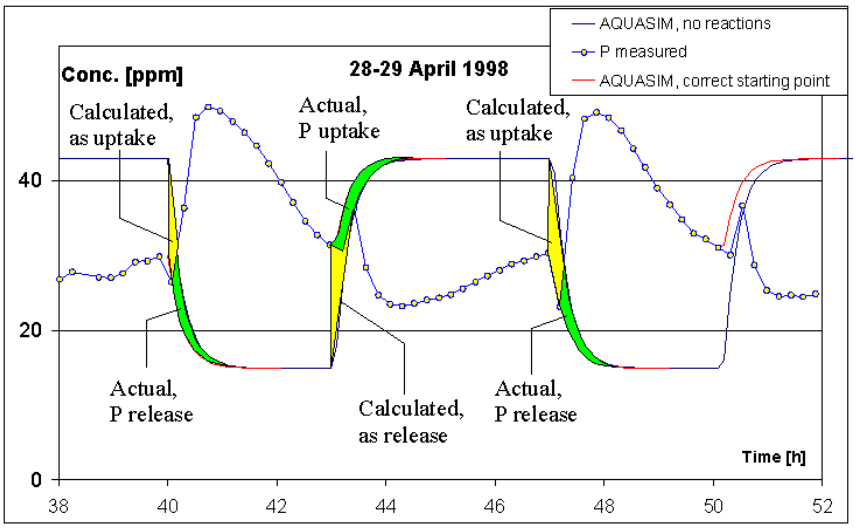

Figure 5.5. Calculation of areas between curves with different fix points in the mixing phases.

For the data from PART B of the study, the mass balance calculations of phosphate were very simple due to the constant inlet concentration. Fig. 5.6 illustrates the principle in this case. Phosphate released or taken up was simply the area between the outlet curve and a horizontal line by 28 ppm P.

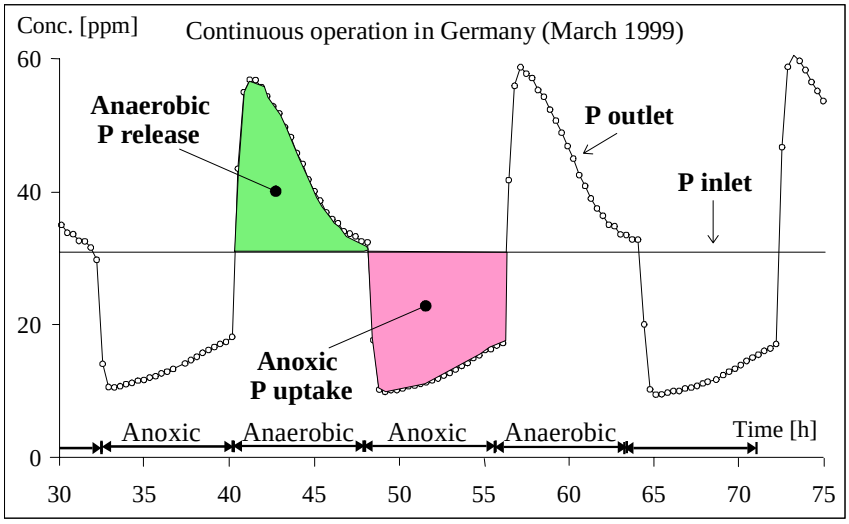

Figure 5.6. Mass balance calculations of P for constant inlet concentration – PART B of the study.

5.1.2.2. Nitrate-N and Acetate

The only source of nitrate is the nitrate content of the inlet during anoxic phases. No nitrification can take place in the system since no aerobic phase is included.

Nitrate is removed from the system either via the outlet or by denitrification where it is transformed to free nitrogen gas that leave the system in the form of gas bubbles.

The only external source of organic matter is the acetate added via the inlet during anaerobic phases. Organic matter is removed from the system either: Via the outlet, taken up and stored by the bacteria or by biological transformation to inorganic carbon and biomass that afterwards is removed from the system via either the outlet or backwash, respectively. Organic matter removed from the system via backwash can be divided into 2 fractions:

1. Organic C incorporated as building blocks of the bacteria cells.
2. Stored compounds in the bacteria cells.

Essentially 4 different types of denitrification can take place in the system:

1. Denitrification by bio-P bacteria, using stored organic matter.
2. Denitrification by bio-P bacteria, using organic matter present in the bulk water.
3. Denitrification by non-bio-P denitrifying bacteria, using organic matter from the bulk water.
4. Denitrification by non-bio-P denitrifying bacteria capable of storing, using stored organic matter.

Due to the way the system is operated, the transition from one phase to another gives a situation where both acetate and nitrate are present simultaneously. This leads to the possibility (likelihood) of denitrification using part of the acetate directly with nitrate as electron acceptor as discussed in chapter 2.1.9.

The mass balances of nitrate and acetate are simpler than for phosphate because the inlet concentrations are varied between zero and a constant value. The mass removed by the biofilm is calculated as the difference between the added amount (Q * inlet concentration * time) and the amount that exits the system via the outlet (Q * area under the outlet curve).

5.1.3 Reaction Rates in The Continuous Operation

Due to the mixture of hydraulic mixing and biological activity, it is difficult to calculate e.g. P release and uptake rates. Removal rates depend on the concentration in the bulk water as well as the internal storage pools of the bacteria. Both of these parameters change constantly as a function of time. The simultaneous presence of nitrate and acetate during transition from one phase to the other complicates the calculations additionally. For this reason batch experiments were used for more detailed analysis of process kinetics.

5.2 Batch Experiments

5.2.1 Mixing Conditions and Theoretical Output Data

Mixing: Same recirculation flow was used during batch tests as for the continuous operation and the solution in the batch bottle was additionally stirred by a magnetic stirrer. The batch system is schematically illustrated in Fig. 5.7.

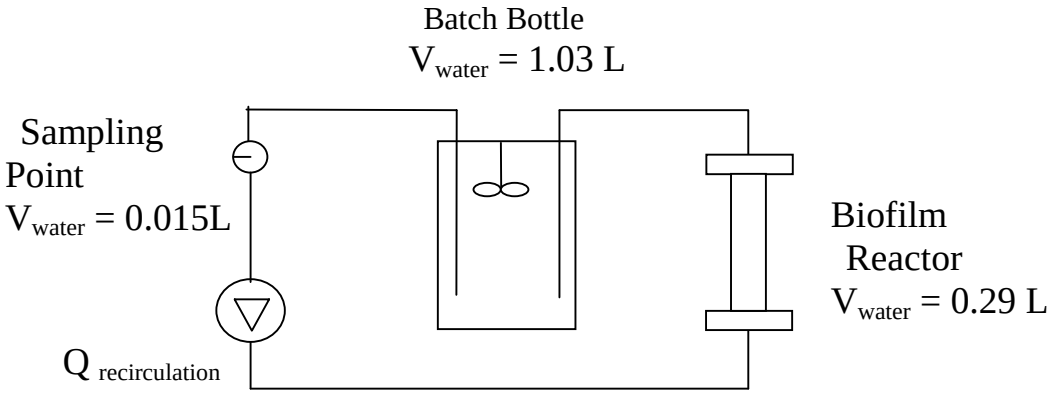

Figure 5.7. Schematic illustration of the batch setup.

An example of theoretical outlet concentrations for a start concentration of 150 mg/l in the batch bottle and 0 mg/l in the rest of the system (sampling point and reactor) is illustrated in Fig. 5.8 for different recirculation flows. It is here assumed, that the individual compartments can be considered as ideally mixed and that no reactions are taking place. The actual flow used was 15-20 l/h, and as it can be seen, it takes ~0.08 h = 5 min to reach equilibrium when $Q_{recirculation}$ = 15 l/h. AQUASIM (Reichert, 1994) was used for the simulation.

Output data: Figure 5.9a shows a theoretical curve for an anaerobic batch experiment. The phosphate concentration in the bulk water increases, and the concentration of organic matter decreases, as a function of time. The tangent of the P curve at time zero is shown. Similarly, Fig. 5.9b shows the theoretical concentration curves during an anoxic batch experiment, where nitrate and phosphate are removed from the bulk water.

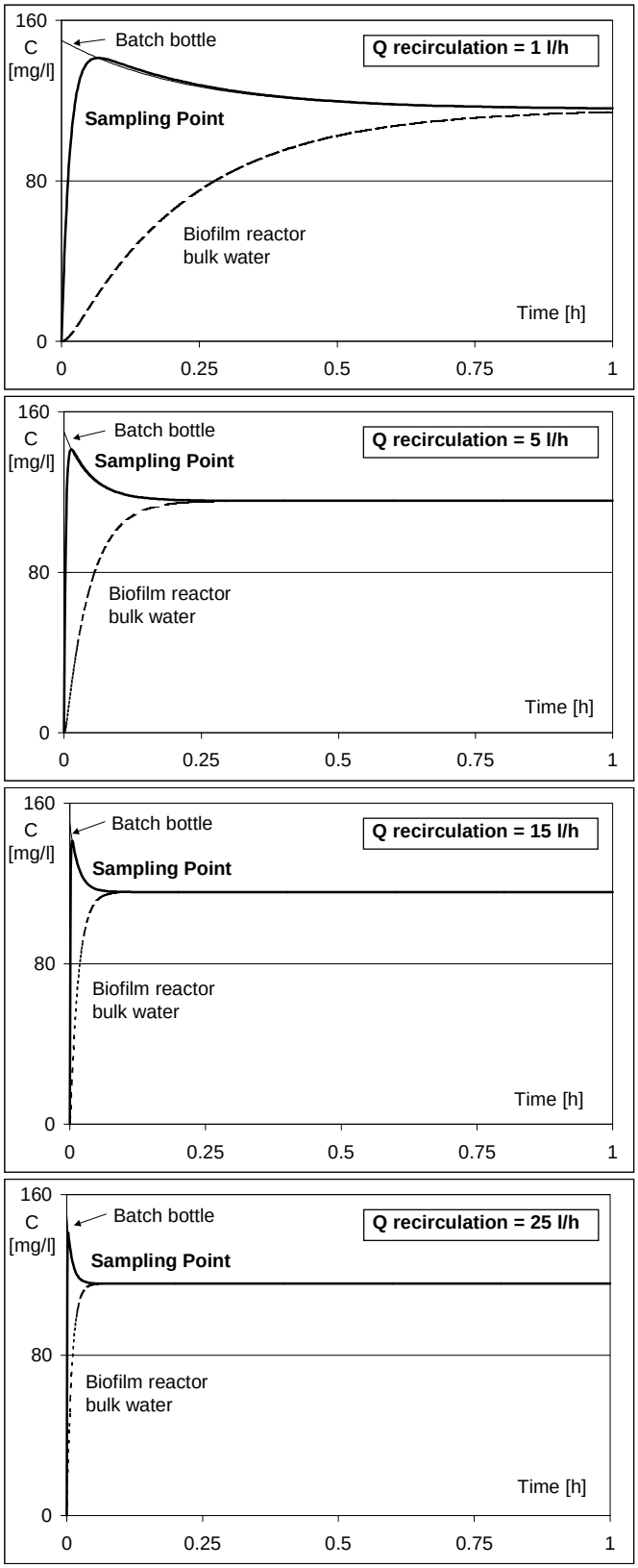

Figure 5.8. Modelled mixing in the batch system for different recirculation flows. Assuming no reactions. The start concentration was 150 mg/l in the batch bottle, and 0 mg/l in the rest of the system.

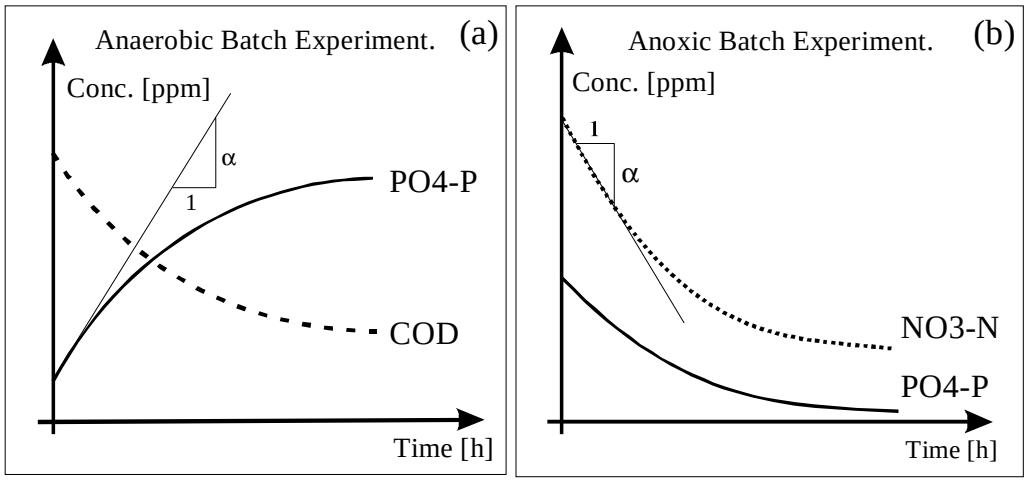

Figure 5.9. Curves illustrating the hypothesised principle of: (a) Phosphate release and COD uptake during an anaerobic batch experiment (b) Nitrate removal and phosphate uptake during an anoxic batch experiment. The slope of the initial tangent (t = 0) is used for calculating the initial release or uptake rate.

5.2.2 Mass Balances and Reaction Rates in Batch Experiments

The mass balance of a batch experiment is given by:

PRODUCED = ACCUMULATED

$$\boxed{r_A \cdot A^* = V_{bulk} \cdot \frac{dS}{dt}} \qquad (5.3)$$

r_A : removal rate pr. surface area [g/m^2*d)]
A : surface area [m^2]
V_{bulk} : bulk volume of the batch system [m^3]
dS/dt : change in substrate concentration pr. time [g/d]

The mass balances during batch experiments were calculated from the differences in the start and final concentration of the considered substrate(s).

In a single batch experiment transition between different reaction orders will often occur since the bulk water concentration decreases during removal and additionally, the removal rate is depending on the amount of internal storage compounds.

The removal rate at any given time can be calculated via the tangent to the curve (Fig. 5.9), since it will be proportional to the slope (α). Other parameters that are included in the calculation are: the total water volume (V_{water}) and the biofilm surface ($A_{biofilm}$):

$$r_A = \alpha \cdot \frac{V_{water}}{A_{biofilm}} \qquad [g/(m^2 \cdot d)] \tag{5.4}$$

Since removal rates change during a batch experiment, it is necessary to select a well-defined point, if different batch experiments are to be compared. This point could conveniently be the starting point, which was chosen in this study. When evaluating experimental curves, it was chosen to fix the initial tangent (tangent for $t \rightarrow 0^+$) at the theoretical start concentration and neglecting the first 1-2 measuring points (the first 5 minutes) to account for the uncertainty caused by the hydraulic mixing.

The water volume of a batch experiment decreased as a function of time due to sampling. This made a restriction on the amount of samples during an experiment. However, all batch experiments had the same initial water volume, and since the initial tangent was used, the decrease of water volume could be disregarded. During a typical batch experiment, a total of approximately 10-15 % of the water volume was removed.

By varying the start concentration in different batch experiments, it is possible to establish a relationship between bulk concentration and phosphate release or uptake rate. However, it should be noticed, that batch experiments can not be performed directly after each other. The biofilm needs a "normalisation" period, where it is exposed to normal conditions (continuous operation), to assure that the start conditions in respect to the biomass (storage etc.) will be the same for each batch experiment. Backwash was performed prior to batch experiments as an attempt to establish similar biofilm thickness for different batch tests.

The removal/release rates of different compounds found at the same moment (e.g. by the tangent slope) can be used to calculate stoichiometric relationships.

For different orders of reaction rate in the bulk liquid, the mass balance equation (5.3) can be solved:

$$0\,\text{order:}\quad k_{0A} \cdot A^* = V_{bulk} \cdot \frac{dS}{dt} \rightarrow S = \frac{k_{0A} \cdot A^*}{V_{bulk}} \cdot t + K \tag{5.5}$$

$$\tfrac{1}{2}\,\text{order:}\quad k_{\frac{1}{2}A} \cdot S^{\frac{1}{2}} \cdot A^* = V_{bulk} \cdot \frac{dS}{dt} \rightarrow S^{\frac{1}{2}} = \frac{k_{\frac{1}{2}A} \cdot A^*}{2 \cdot V_{bulk}} \cdot t + K \tag{5.6}$$

$$1\,\text{order:}\quad k_{1A} \cdot S \cdot A^* = V_{bulk} \cdot \frac{dS}{dt} \rightarrow \ln(S) = \frac{k_{1A} \cdot A^*}{V_{bulk}} \cdot t + K \tag{5.7}$$

From the equations 5.5-5.7, the following can be predicted (Fig. 5.10):
By plotting the concentration as a function of time, a 0 order reaction will give a straight line with the slope: $(k_{0A}*A^*) / V_{bulk}$. If plotting the square root of the concentration as a function of time, a ½ order reaction will give a straight line with the slope: $(k_{½A}*A^*)/(2*V_{bulk})$. And finally a 1 order reaction will lead to a straight line if plotting the logarithmic concentration as a function of time.

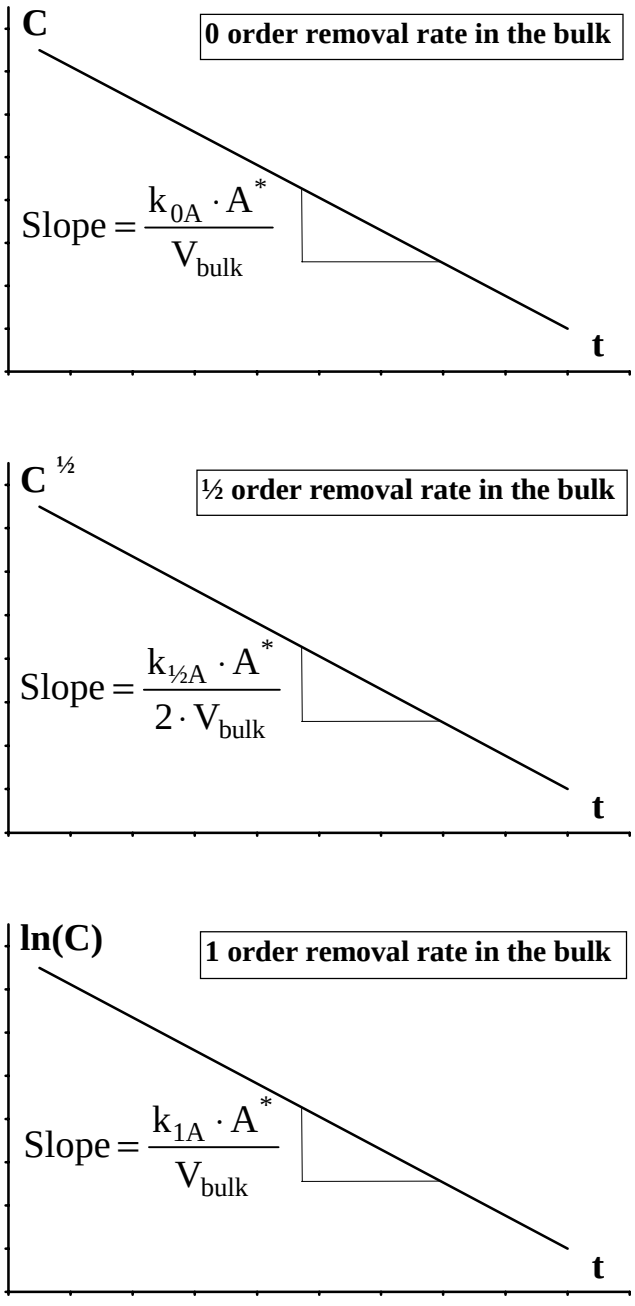

Figure 5.10. Illustration of how different removal rates during a batch experiment can be plotted as a straight line by using different plot definitions.

6. Hypothesis of Diffusion Limitation

6.1 Conceptual Biofilm Model of This Study

The 1-dimensional model, where molecular diffusion is considered as the only transport process, forms the basis of this study. It was used for evaluating hypothetical concentration profiles inside the biofilm, for investigating zonation in the biofilm and for modelling of the process. The complexity and uncertainties regarding EBPR in biofilms was one of the reasons for choosing this simplified transparent model. The 1-dimensional approach is an appropriate approximation for dense biofilms with no significant internal channel structure. Based on the current state of knowledge (chapter 2.3), the following experimental conditions support the hypothesis, that a dense, compact biofilm would evolve in this study:

- Use of high nutrient availability
- High shear forces due to a relatively high flow rate in the reactor
- A mixed bacteria culture
- Low growth rate of PAOs

Transport limitation in a liquid boundary layer by the biofilm surface was not considered. Christiansen *et al*., 1995, showed that the effect of liquid film diffusion was insignificant for evaluations based on the 1-D model approach, when using a reactor type (submerged, granular filter) and flow rates comparable to this study.

6.2 Concentration Profiles Inside the Biofilm

6.2.1 Quasi-Steady State

In the following, it is assumed that diffusion inside the biofilm is a fast process in comparison with the changes in the bulk water concentrations. This is supported by the findings of Picioreanu *et al*., 1999, refer to Fig. 2.17 (one cycle in the continuous operation is ~8 hours = 28.800 s), and also by the findings and thorough discussion provided by Morgenroth, 1998. In this way, it is possible to consider diffusion profiles to be in *quasi-steady states*. A quasi-steady state can be defined: In case, the bulk concentrations, internal storage concentrations, reaction rates and biofilm thickness would stay unaltered from this point on, the diffusion profiles would stay unaltered as well.
Non-steady states are equivalently defined: In case, the bulk concentrations, internal storage concentrations, reaction rates and biofilm thickness would stay

unaltered from this point on, the diffusion profiles would change to obtain steady-state. This could be the case if e.g phosphate release (or another production process) only takes place in the middle of a biofilm. Before equilibrium is reached, the concentration is highest in the middle of the film, but as release continues, the concentration by the bottom will increase via diffusion of the product, until reaching the same concentration as in the release zone in the middle.

6.2.2 Profile Assumptions - for The Sake of Simplicity

A set of concentration profiles, that can form the basis for understanding and discussion, are illustrated below. In order to simplify the profiles and thereby facilitate the identification of major phenomena, the profiles were made according to a list of assumptions:

1) Only PAOs and their reactions are considered
2) No depletion of internal storage pools
3) Uptake of phosphate in the presence of nitrate and no acetate
4) Release of phosphate in the presence of acetate (also when nitrate is present)
5) No reactions, if neither nitrate nor soluble COD (acetate) are available

The assumptions imply that an internal COD production by decay and hydrolysis is not considered. Internal COD production seem likely for a real system where e.g. particulate organic matter is present, and it would bring about some phosphate release. The same holds for anaerobic maintenance/endogenous respiration that generally is observed to involve slow phosphate release (~1 order of magnitude smaller than anaerobic P release with COD present, Kuba *et al*., 1993, 1997b).

6.2.3 The Two Phases

6.2.3.1 The Anoxic Phase

Figure 6.1 illustrates the three possible situations during anoxic phases:

(1) Full penetration with both nitrate and phosphate, where phosphate is taken up simultaneously with denitrification (via internally stored COD) in the full depth of the biofilm.
(2) Phosphate only partly penetrates the biofilm. Nitrate is present in the full depth of the biofilm, but not removed beyond the penetration depth of phosphate.
(3) Nitrate only partly penetrates the biofilm. Phosphate is present in the full depth, but not taken up beyond the penetration depth of nitrate.

A situation where both nitrate and phosphate are partly penetrating would occur only if the bulk concentrations of these compounds exactly matched the stoichiometric relationship between the two.

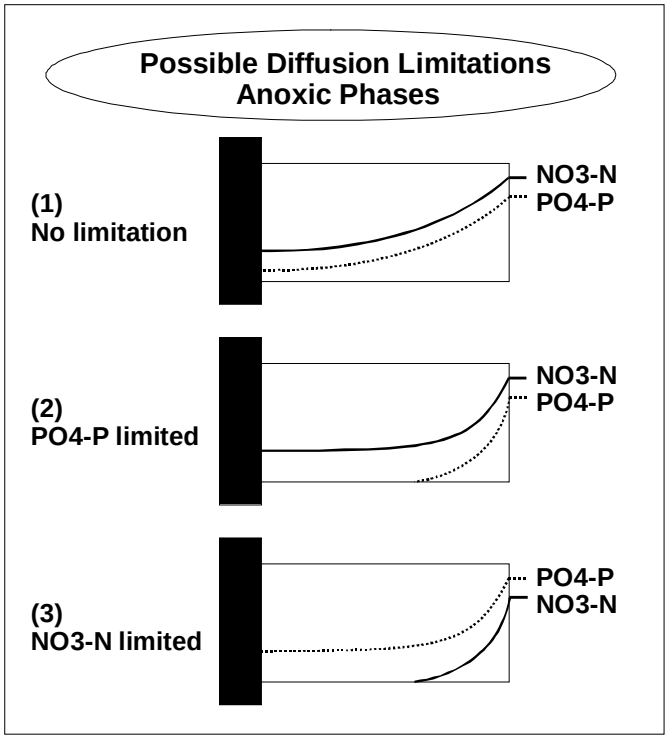

Figure 6.1. Possible diffusion limitations during anoxic phases of EBPR cycles.

6.2.3.2 The Anaerobic Phase

During anaerobic phases, only one substrate is supplied in soluble form via the bulk water: COD (acetate). Hence, only one diffusion limitation situation is possible: COD does not fully penetrate the biofilm, Fig. 6.2 (2). Phosphate concentrations in the biofilm are higher than in the water due to phosphate released from the internal polyphosphate pools of the bacteria, however no phosphate is released beyond the penetration depth of COD.

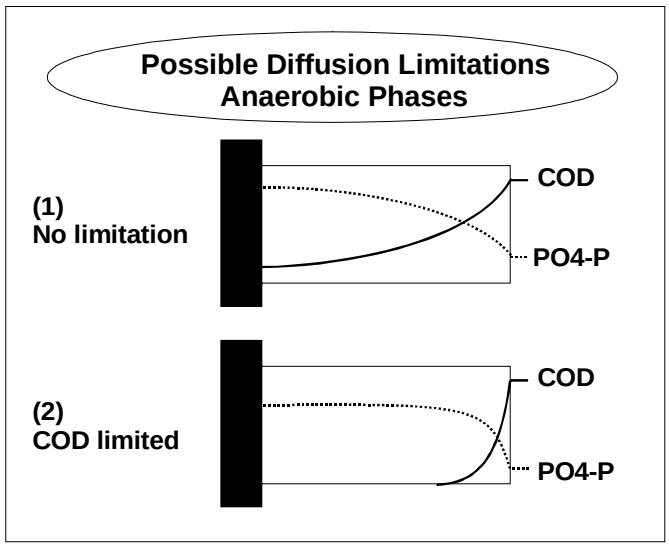

Figure 6.2. Possible diffusion limitations during anaerobic phases of an EBPR cycle.

6.2.4 Transition Between Phases

Figure 6.3 shows hypothetical concentration profiles during transition from anoxic to anaerobic phase (a) and transition from anaerobic to anoxic phase (b). It is here assumed that there is no diffusion limitation during the individual phases. If diffusion limitation exist in one or the other or both phases, transition series shall be derivatives of the illustrated ones.

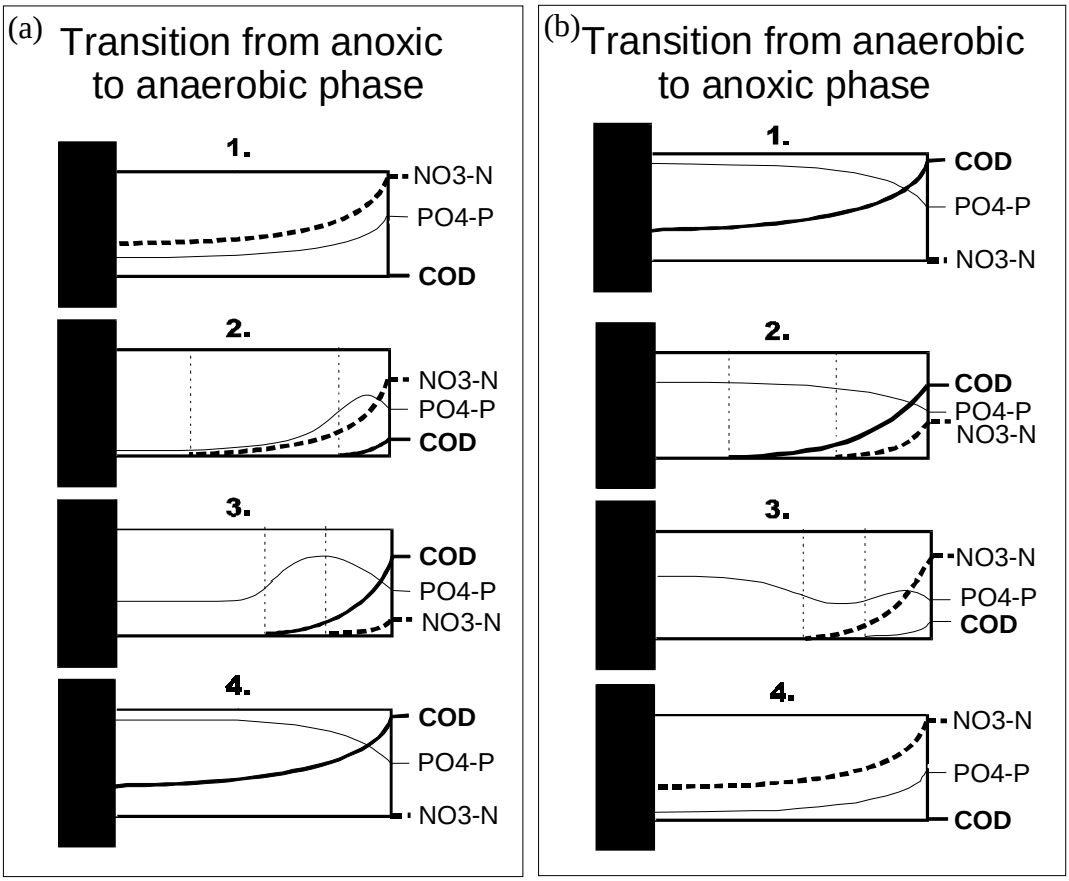

Figure 6.3. Hypothetical concentration profiles in the biofilm during transition from one phase to the other – see text for explanation.

Fig. 6.3a: During transition from anoxic to anaerobic phase, the biofilm is initially penetrated with nitrate and phosphate (a1). COD is then added via the inlet to the system, and the bulk concentration starts to rise. As soon as COD starts to penetrate the film, phosphate uptake is replaced by phosphate release (a2). However, in the deeper part of the biofilm, where nitrate still is present but no COD, phosphate uptake continues (a2), until COD penetrates deeper into the film than nitrate (a3). By the end of the transition, nitrate is flushed from the bulk water, and COD penetrates the total depth of the biofilm, leading to phosphate release (a4).

Fig. 6.3b: During transition from anaerobic to anoxic phase, the biofilm is initially penetrated with COD and phosphate is released in the full depth of the film (b1). The nitrate concentration in the bulk water rises at the same time as COD is being flushed from the system. As long as nitrate penetrates shorter into the film than COD, phosphate release continues in the COD penetrated part (b2), but when nitrate penetrates deeper into the film, phosphate uptake is initiated in the COD-free zone (b3). By the end of the transition, COD is flushed from the bulk water, and nitrate fully penetrates the biofilm, leading to phosphate uptake (b4).

6.3 Effect of Diffusion Limitation on Outlet Concentrations

For simplicity reasons a continuous system with a constant inlet concentration of phosphate is considered. This system was used in PART B of the study. For a stationary situation *without backwash*, the phosphate outlet curves can look in two ways depending on whether the biofilm is partly or fully penetrated, Fig. 6.4. Phosphate is here used as the example, assuming full penetration of acetate and nitrate in the anaerobic and anoxic phases, respectively. The considerations would be similar, if instead one of these substrates limited the process.

If the biofilm is only *partly* penetrated with phosphate, a constant amount of P (M_P) will be taken up during an anoxic phase and released again during the following anaerobic due to the diffusion limitation of the available mass of phosphate (Fig. 6.4, left), i.e. the *active* biofilm thickness stays constant. M_P depends on the anoxic phase length for a constant inlet concentration of phosphate. Phosphate might penetrate the biofilm deeper as a function of anoxic time, if bacteria in the outmost layer stop taking up phosphate due to empty internal storage pool (Morgenroth, 1998). Whether this happens depends on the anoxic phase length, maximum storage capacity of the individual bacteria cells and cell density in the film.
Slightly less amounts of P are released during the anaerobic phases due to the P incorporated in the growing biomass. The outlet concentration will vary according to the phases, but the peak height of the curve (anaerobic P release) will stay at a constant level and similar to the anoxic phosphate “valley”.
If the biofilm is *fully* penetrated, the growing biomass results in an increasing mass of P taken up for each cycle and released in the subsequent anaerobic phase (Fig. 1, right) due to an increasing active biofilm thickness – until the biofilm gets too thick for full penetration to continue.
For each cycle with a fully penetrated biofilm, a net P uptake is observed: mass of P released < mass of P taken up. This is an oppose to the partly penetrated biofilm, where the mass of P released and the mass of P taken up during one cycle are identical (except for the normal biological P uptake due to incorporation in the growing cell mass).

For phosphate mass to be removed from a system operated with a partly penetrated biofilm, backwash must occur after each anoxic phase (to remove phosphate rich biomass), otherwise no net removal of P takes place. A problem in this regards is, that backwash not necessarily removes the *outer* phosphate rich layers of the biofilm. It is possible that biomass is not removed in layers from the top and inwards during backwash, but more in a clump like manner with the *thickest* parts of the film first falling off. In this way, a low average phosphate content of the removed biomass shall be observed. Imagine, that the top 100 micrometer has a 10 % P content and the underlying 600 microns 1.2% (no poly-P storage left) then the total biomass will have an average of ~2.8 % P.

The situation *around backwash* is different than the hypothesis in Fig. 6.4. Both for a partly and a fully penetrated film, an increasing anaerobic outlet peak and accordingly decreasing anoxic phosphate valley shall be observed following backwash. For the fully penetrated biofilm, the active biofilm thickness (equal to the thickness) decreases by removal of biomass during backwash. For a partly penetrated biofilm, some biomass from the deep inactive layers are laid open by the backwash. The bacteria residing in these layers have empty storage pools and need time to recover their activity levels.

Excess amount of phosphate taken up during the aerobic phase is reported for several investigations of biological phosphate removal with biofilms. Most of these investigations have been made with sequencing batch reactors, where the excess uptake is easily seen by a final phosphate concentration in the batch reactor smaller than the concentration in the wastewater added (Gieseke *et al*., 1999; Castillo *et al*., 1999; Morgenroth, 1998). An explanation of these observations can be either a fully penetrated (thin) biofilm as explained above, or a biofilm with a penetration depth of COD during anaerobic phases smaller than the penetration depth of phosphate during aerobic phases. The relative penetration depths of the different compounds depend on the bulk concentrations, phase lengths and biofilm properties. Fig. 6.5 illustrates the last possible explanation, where part of the phosphate taken up stays in the deep part of the biofilm due to COD limitation during the anaerobic phase. This case would also for a continuous operation lead to relatively higher amounts of phosphate taken up than released during a cycle. For this hypothesis to hold, the release of phosphate from bacteria during anaerobic conditions without COD (maintenance) should be small.

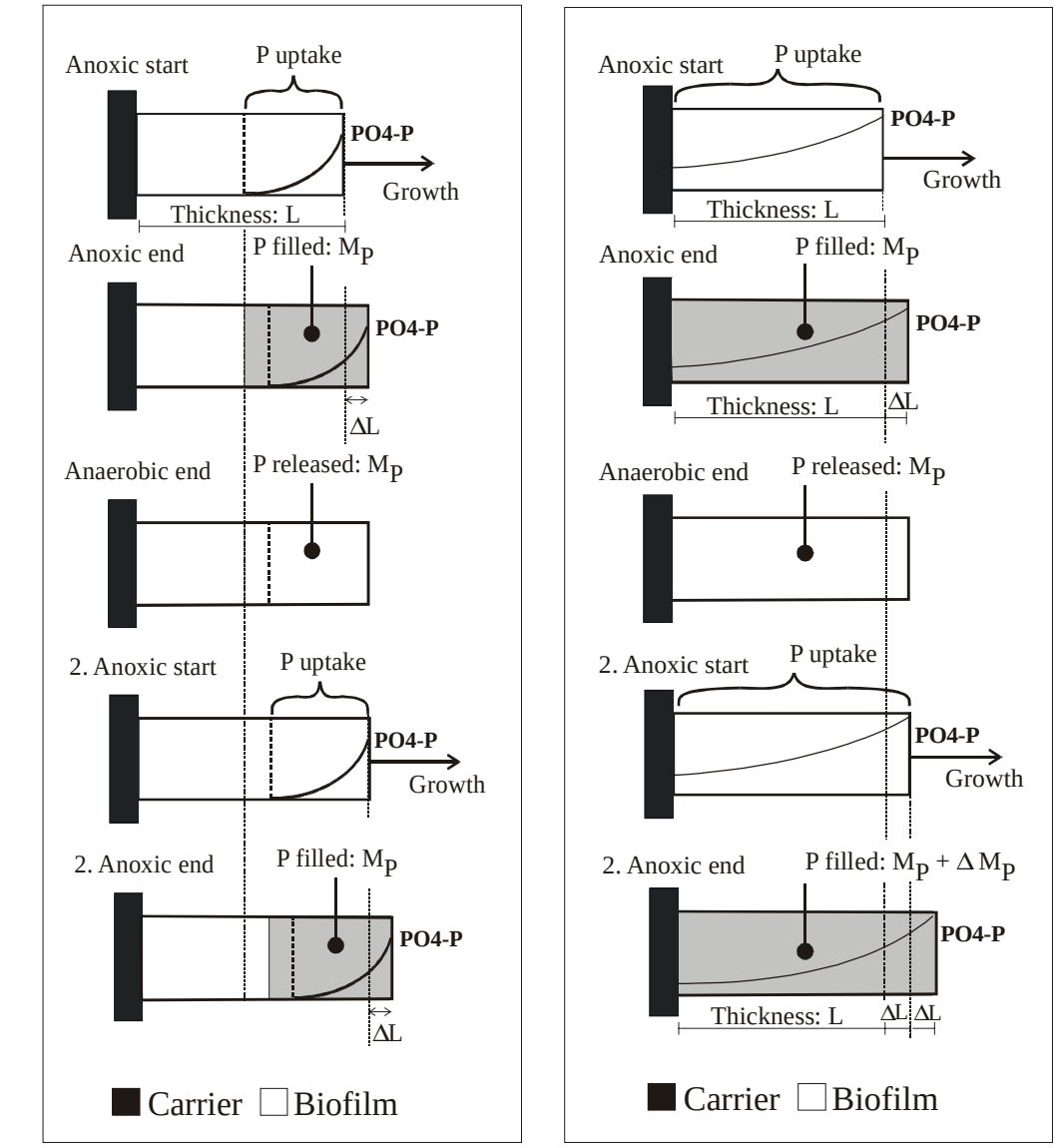

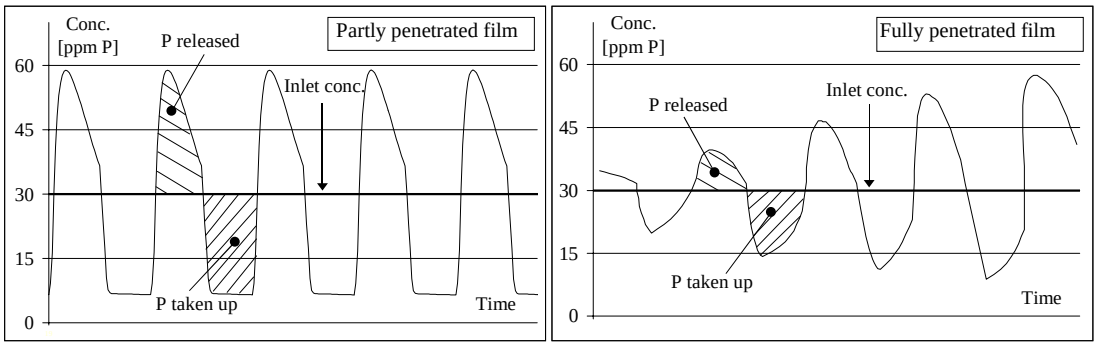

Figure 6.4. Hypothesis regarding the outlet concentrations of phosphate in the continuous operation in case of (a) phosphate only partly penetrates the film and (b) phosphate fully penetrates the film. In case of partly phosphate penetration, the same amount/mass of P shall be taken up and released during all the cycles, but for a fully penetrated film, the amount of P taken up and released increase with time due to increased active biofilm thickness. Only for full penetration, a net P uptake is seen (mass of P taken up > mass of P released).

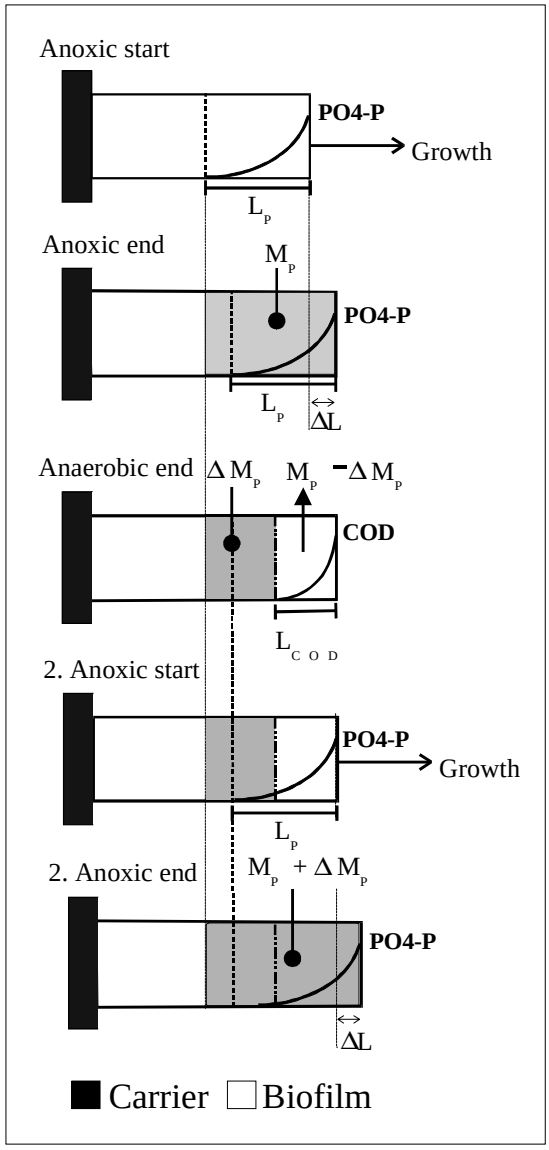

Figure 6.5. Hypothesis of excess phosphate removal with a COD-diffusion-limited biofilm. In case the organic substrate during the anaerobic phases penetrates the biofilm less than the phosphate during the aerobic/anoxic phase, a net P removal shall be observed on the premise that phosphate release during anaerobic conditions without COD is relatively small.

6.4 Other Consequences of Diffusion Limitation - ?

The term **'EBPR'** is in this study used for the process of excess phosphate uptake during anoxic conditions *given* phosphate is available, with subsequent anaerobic phosphate release. For a biofilm, situations of diffusion limitation might lead to low P contents in the biomass, but the process as such is still termed EBPR.

Apart from the serious problem of possibly no net removal of phosphate with a partly penetrated EBPR biofilm, other problems might occur in a diffusion limited EBPR

biofilm. First, what happens to bacteria cells residing in the deep layers of the film and not subjected to substrate? Can these cells start to metabolise as soon as they are fed again, e.g. following backwash? Second, if a biofilm is phosphate limited during anoxic phases, the deep part of the biofilm is not accumulating phosphate. What if COD penetrates this part during anaerobic conditions – shall GAOs start to flourish in the deep layers, since this situation is similar to the way of cultivating GAOs by feeding low P/COD wastewater. Whether GAOs shall accumulate will be a question of the time periods that these bacteria have advantageous conditions over PAOs. This is a balance between growth rates of the two bacteria groups, biofilm thickness and backwash frequency. These questions were already formulated in BOX 6 as part of the questions in focus of this study.
To avoid diffusion limitation, a thin biofilm is required. However, how much biomass can in this case be accumulated in the filter – will it still be more than in activated sludge parts or does this advantage no longer hold?

BOX 7 Hypothesis of Diffusion Limitation

The 1-dimensional model approach shall be a good approximation in the current study due to a high probability of a relatively compact biofilm –according to the environmental conditions of: High nutrient availability, high shear forces, mixed culture bacteria and low growth rate (PAOs). For this reason, it is expected to observe ½ and 0 order removal rates (phosphate release or uptake rates) in the bulk water for a partly versus fully penetrated biofilm.

No net phosphate removal shall be seen for a biofilm where COD during the anaerobic phase penetrates the film deeper than phosphate during the anoxic phase – unless the biofilm is backwashed following each anoxic phase to remove phosphate-rich biomass.

Low average phosphate contents shall be observed for diffusion limited EBPR biofilms - unless backwash removes only the outer, active layer of the biofilm.

7. PART A - Results and Discussion

7.1 Start-up: Building up The Biofilm

7.1.1 Inoculation

Biocarbon® was tested during start-up before Biostyr® was chosen for further experiments. The Biocarbon® was taken from a denitrification tank at Hundested wastewater treatment plant, Denmark (Janning *et al.*, 1995), which was operated for nitrification and denitrification, but not for biological phosphate removal. It was speculated that part of the denitrifiers would possess the metabolism for anoxic phosphate removal and that this could be relatively quickly induced. It has previously been shown that non-bio-P sludge can be adapted for aerobic bio-P removal, Table 7.1. The up-start periods that have been reported in the literature vary significantly and no consistency has been seen regarding faster start-up for reactors inoculated with bio-P sludge compared to conventional activated sludge. Generally a start-up time of 1-2 months must be expected.

A few experiments of up to 10 days were carried out with the Biocarbon® biofilm, however no sign of bio-P activity could be detected, so it was chosen to add a thin solution of sludge taken from a bio-P activated sludge plant. In retrospect, EBPR activity could possibly have appeared, had the experiments been continued. However, problems with clogging of the Biocarbon® material additionally favoured the start of new experiments with Biostyr® as the carrier instead.

In the first run with Biostyr®, the reactor was fed for 18 hours with a solution of bacteria taken from a BIO-DENIPHO pilot-plant. The principle of the BIO-DENIPHO (Einfeldt, 1992) is based on aerobic P uptake but an anoxic phase for denitrification is included in the cycle. The operation of a BIO-DENIPHO plant can be characterised as a mixture of a continuous flow system and a sequencing batch reactor (Isaacs, 1997). Turning on or off aeration alters the conditions in the nitrification/denitrification-tanks according to a fixed cycle, but the anaerobic tank receiving the incoming wastewater is kept anaerobic.
During the inoculation period, the system was otherwise run under normal conditions. The anoxic phase was 3½ h and the anaerobic 2½ h. The reactor construction gave some problems with entrapment of flocs, but this problem was solved and a second run started. All flocs were flushed from the system and almost no significant bio-P activity remained. The reactor was then fed with bacteria for 6 hours. The anoxic phase was changed to 4 h and the anaerobic to 3 h. Backwash was performed every 2-3 day.

Table 7.1. Time required for induction and stabilisation of EBPR as stated in the literature. AS: Activated sludge. BF: Biofilm.

System	Scale	Start-up [weeks]	Organic substrate	Reference
AS,Continuous	Full	7-8	Wastewater	Lindrea et al., 1994
AS,Continuous	Pilot	24	Presettled wastewater	Jardin and Pöpel, 1994
AS,Continuous	Lab	2 [P]	Acetate	Christensson et al., 1998
AS, SBR	Lab	7 [P]	Acetate	Smolders *et al.*, 1994a
AS, SBR	Lab	6 [P], 6 [C]	Acetate, glucose	Appeldoorn *et al.*, 1992
AS, SBR	Bench	1 [P], 8 [C]	Acetate	Belia and Smith, 1997
BF, SBBR	Semi-Full	2-3	Wastewater	Arnz *et al.*, 2000b
BF, SBBR	Lab	17 [P]	Acetate, peptone, glucose	González-Martinez and Wilderer, 1991
BF, SBBR	Bench	3-5 [C]	Acetate, peptone	Morgenroth, 1998
BF, Alternating	Lab	4-5 [P]	Acetate	This study

[P] Inoculated with bio-P activated sludge
[C] Inoculated with conventional activated sludge

7.1.2 Biofilm Development - The Continuous Operation

Figure 7.1 illustrates data from the continuous setup. (a) and (b) are from shortly after start of the first run. (a) shows nitrate and phosphate measurements and (b) shows the phosphate measurements and the theoretical curve for this concentration if no reactions were taking place (P as conservative element).
The bio-P activity manifests itself in a P-curve lower than the conservative curve during the anoxic phase due to the P uptake and a P-curve higher than the conservative one during the anaerobic phase due to the P release. The combination of mixing and biological activity is evident during the shifts from one phase to the other. For shifts from anoxic to anaerobic phase, the concentration in the outlet first goes down caused by the lowered P concentration in the anaerobic substrate, but increases shortly after due to the biological release of phosphate. The release of P is limited by the stored amount, and this is the reason that the phosphate outlet curve decreases again during the anaerobic phase as a result of depletion of the internal P pool. (c) and (d) show the same curves for Day 28 of run 2. The higher activity at this stage is evident by the higher phosphate concentrations in the outlet during the anaerobic phases and the lower concentrations during the anoxic phases.

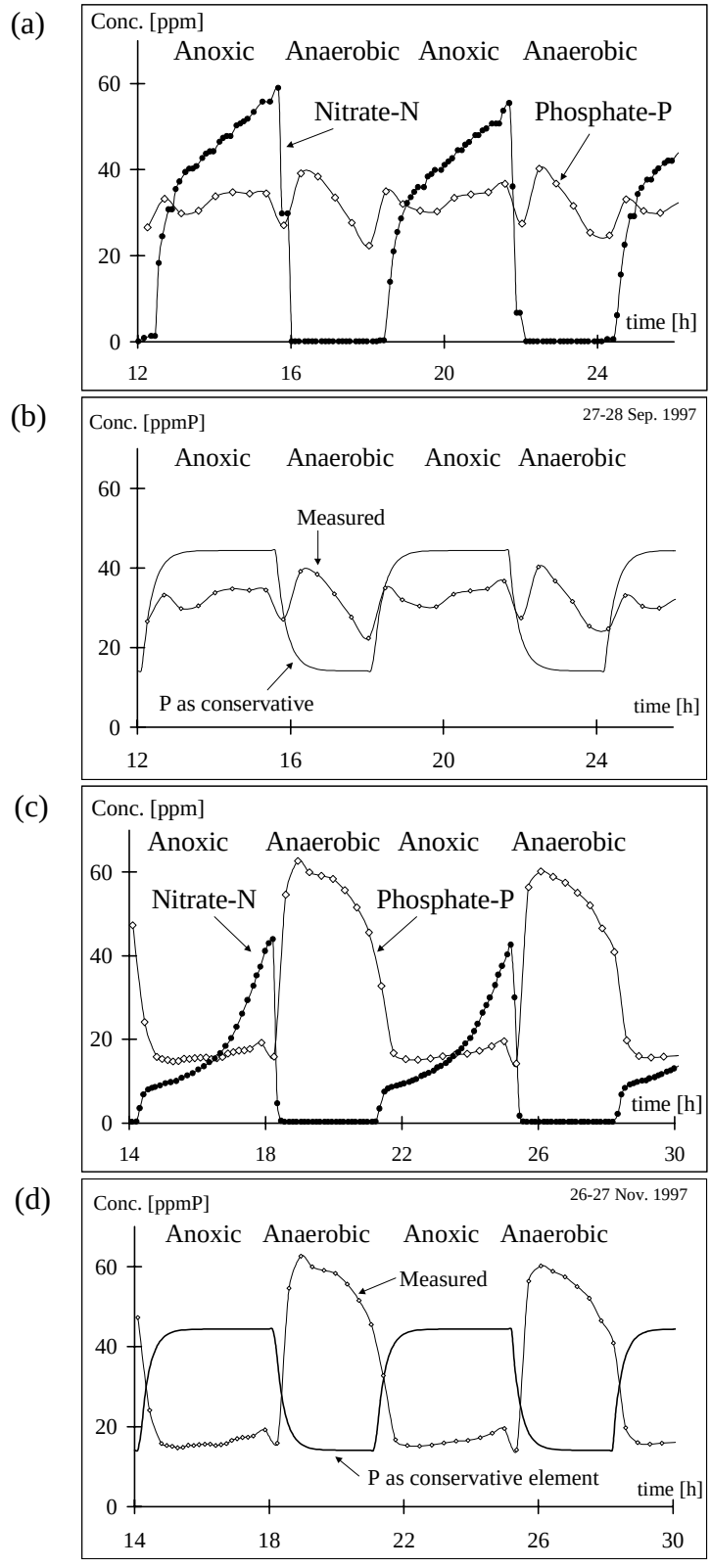

Figure 7.1. Outlet concentrations of phosphate and nitrate from the continuous setup. (a) and (b): First run, shortly after inoculation. Low bio-P-activity. (c) and (d): Second run, Day 28. High bio-P-activity. (b) and (d) include a curve for no reactions with P.

7.1.3 Biofilm Development - Anaerobic Batch Tests

Day 0 in the following is the day of inoculation for the second run.
Figure 7.2a shows anaerobic batch tests with identical start concentration of COD: 196 ppm. The phosphate concentration in the bulk water is shown as a function of time. Curves from Day 5, 8, 19 and 30 are included. The initial slope of the curves increases with the days. Several of these batch tests were performed over a period of 37 days. The result of these is summarised in Fig. 7.2b where the initial P release rate is plotted against the days. An exponential increase in the rate appear until a constant level is reached after ~1 month. The increase is less than what is generally seen for denitrifying bacteria which out rules that the increase simply is due to a growing biofilm. Besides, the biofilm was regularly backwashed to control the thickness. The reason that no additional points are included after the stabilisation occurred is due to problems with the setup, where almost no acetate was added for 3 days, which subsequently required time in order for the biofilm to return to previous activity levels.

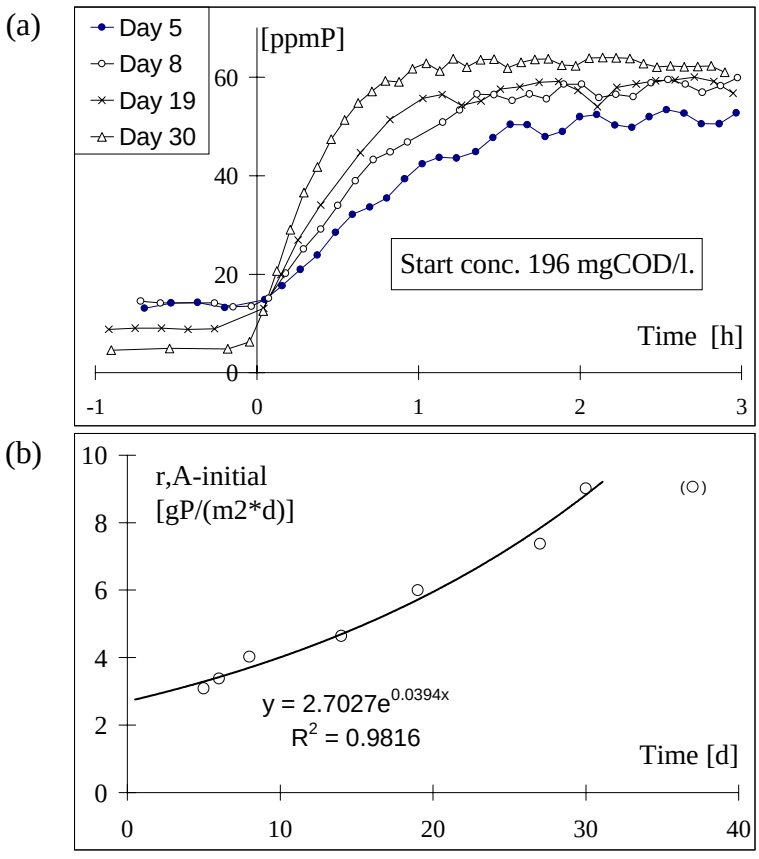

Figure 7.2. (a) Anaerobic phosphate release batch tests. The initial (at time zero) tangent slope is increasing as a function of days from inoculation, indicating an increasing activity. (b) Initial area specific release rate (r,A-initial) as a function of days, calculated from the initial tangent slope of individual batch tests. The exponential increase is speculated to be caused by enrichment of the denitrifying PAO's in the biofilm.

Around Day 20, a series of anaerobic batch experiments with different start concentrations of acetate were performed (chapter 7.2). These revealed partly penetration of the biofilm for COD concentrations below 256 ppm COD. The COD concentration used in the tests of Fig. 7.2 was 196 ppm COD. Hence the biofilm was only partly penetrated at least around day 20.
The increase in the initial P release rate over time is for these reasons speculated to be caused by an increased density of the denitrifying bio-P bacteria in the film, i.e. an enrichment of the bacteria type favoured by the given operational conditions. Since space in a biofilm is limited, the bacteria density is limited, which suggests reaching a constant (maximum) level in time.

7.2 Batch Experiments - Zonation

7.2.1 Anaerobic Batch Experiments

Biofilm characteristics: Over a period of 5 days (Day 19-23, Nov.'97) several anaerobic batch tests with different start concentrations of acetate were carried out. These tests were performed on the biofilm starting at the moment of transition from anoxic to anaerobic conditions, i.e. the bacteria had high amounts of internally stored poly-P (and glycogen) and low amounts of internally stored PHB. The bacteria were allowed to replenish their internal storage pools between two subsequent batch experiments by running the reactor in a continuous mode for at least 2 cycles. Figure 7.3 illustrates three of the anaerobic batch experiments.

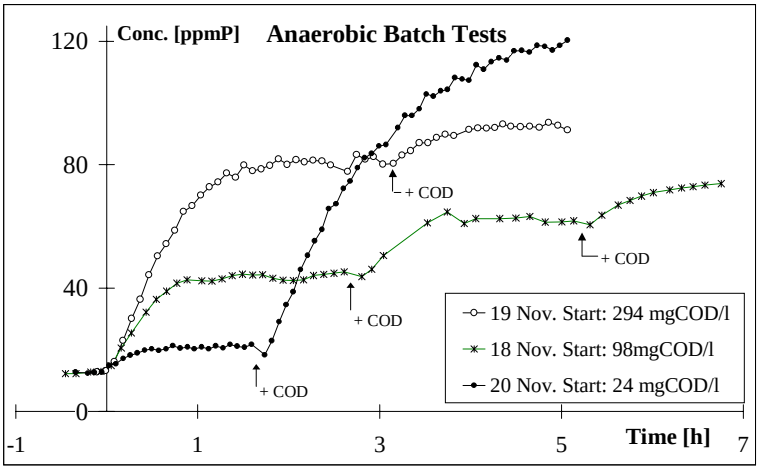

Figure 7.3. Anaerobic batch experiments with different acetate start concentrations.

In activated sludge, the same initial P release rate would appear in the different experiments. The curves would reach a horizontal plateau after different time

periods depending on the depletion of acetate in the water phase or the depletion of internally stored phosphate (or glycogen) (Meinhold *et al.*, 1999). By comparison, the characteristic of the biofilm is indicated in the figure by the different initial P release rates (slope of the curves at time zero) – the higher the initial acetate concentration, the higher the release rate due to higher penetration of the film. Later in the experiments, more acetate was added. In this case, the influence of the internal phosphate storage (or glycogen) plays a role, since some bacteria might have emptied their storage. For the experiment with the lowest start concentration (20 Nov), the later addition of acetate led to a release rate equal to the one found as the initial release rate in the experiment of 19 Nov. This was the maximum initial release rate of the film, i.e. the film was fully penetrated.

½ and 0 order of reaction: For a series of batch tests, the initial release rate has been plotted as a function of the square root of the acetate concentration, Fig. 7.4a. A straight line indicates a half-order reaction and a horizontal line indicates a zero-order reaction (full penetration). For the removal rates, the unit per m^2 is used. This m^2 refers to the carriers surface area. On the figure is included a similar series of batch tests performed Feb.'98. The figure demonstrates the theory of ½ and 0 order kinetics in the bulk water outside the film, i.e. molecular diffusion as the major transport mechanism of soluble compounds into the biofilm. Figure 7.4b shows the same data, but removal rate is here plotted against the concentration of acetate. The data from Feb'98 are more scattered than from Nov.'97. This could be due to an increased heterogeneity of the biofilm thickness/structure for the "older" biofilm, which was noticed by looking at the biofilm with the naked eye (Fig. 7.5), however, no microbiological investigations were performed.
It is actually surprising to find such an "ideal" ½ and 0 order reaction for Nov.'97, since backwash was performed prior to each experiment, which would make some differences in the biofilm thickness to be expected and hence give a more smooth transition from ½ to 0 order of reaction. Also, the biofilm thickness appeared rather inhomogeneous from looking at the carriers where some of these seemed almost naked whereas others were completely covered (Fig. 7.5). During backwash, it appeared as if the biofilm mainly detached in "clumps" that laid the surface bare. Perhaps this is the reason for the nice appearance of the points – biofilm detached after having reached a certain thickness, whereby the remaining biofilm had a relatively homogeneous thickness despite no even coverage of the carriers.
The nice appearance of ½ and 0 order reaction rates additionally imply that bacteria cells in the deep parts of the biofilm are capable of optimum acetate uptake/phosphate release when met with acetate. This is despite that they might not be exposed to alternating conditions during the continuous operation, where diffusion limitation possibly plays a role (see later sections).

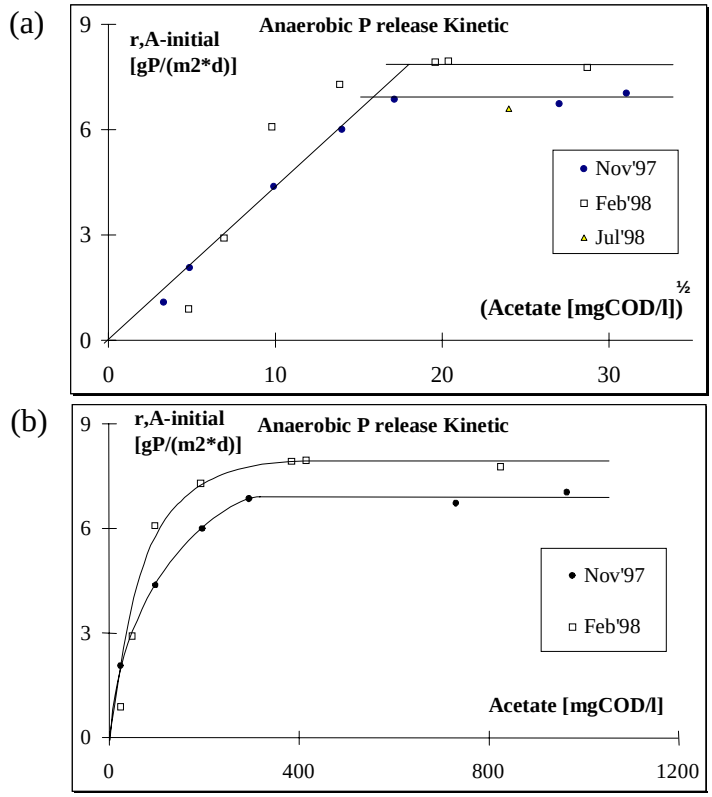

Figure 7.4. Anaerobic batch experiments with different acetate start concentrations.

Calculated biofilm thickness: The concentration leading to transition from half to zero order of reaction was 256 ppm COD (Nov.'97). The maximum release-rate for a fully penetrated film was 6.9 g P/(m^2*d). Assuming a diffusion coefficient of $83*10^{-6}$ m^2d^{-1} for acetate (Wanner and Gujer, 1984) and a stoichiometric relationship of 0.25 g P/g COD for the anaerobic P release (see below), the calculated biofilm thickness is 1.5 mm. This value seems reasonable from looking at the biofilm with the naked eye.

Stoichiometry: That further release of phosphate was observed upon the extra addition of acetate served as an indication that all of the initially added acetate had been taken up. This assumption was used for making the mass balances and calculating the stoichiometry between acetate taken up to phosphate released. This was found to be within the range: 0.22-0.32 g P/g COD with an average of 0.25 g P/g COD and it did not change during the build up period, Fig. 7.6. This coefficient is low compared to the coefficients cited in the literature. This could indicate that other bacteria compete with the bio-P bacteria for organic substrate during the anaerobic phase. Since neither oxygen nor nitrate was present during the anaerobic batch tests these competing bacteria would be capable of storing. However, it is noticeable that the coefficient did not change with time, which would indicate an unchanged ratio between the two bacteria groups and hence identical growth rates. Another explanation of the low coefficient could be a

different metabolism of PAOs in biofilms compared to previously studied activated sludge PAO cultures.

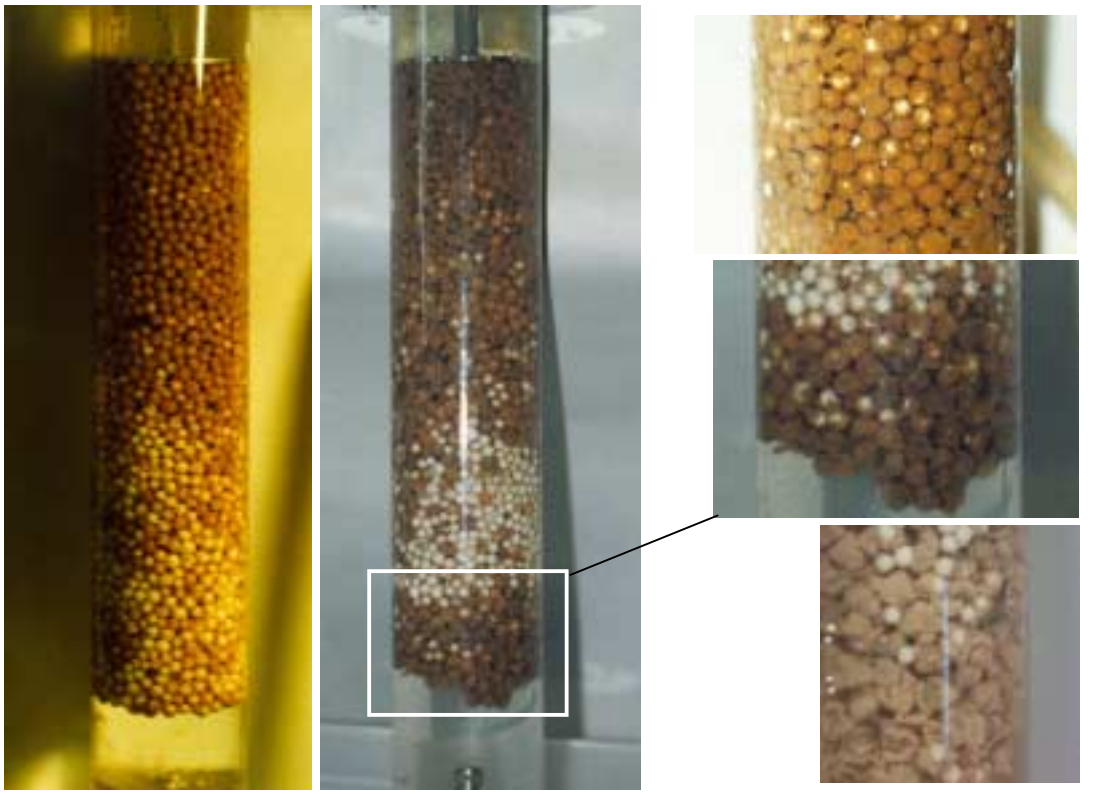

Reactor, Nov. 1997 *Reactor, Apr. 1998* *Close-ups, from the top: Dec.'97, Apr.' 98 and Dec. '98.*

Figure 7.5. Illustration of the uneven coverage of the BIOSTYR carriers, white balls: no biofilm. The Dec'98-close-up image on the left was taken March 1999 after storage of the reactor in the refrigerator for 3 months, so some biofilm detachment had occurred, but the image still illustrates the uneven coverage and the very thick biofilm that developed during the study.

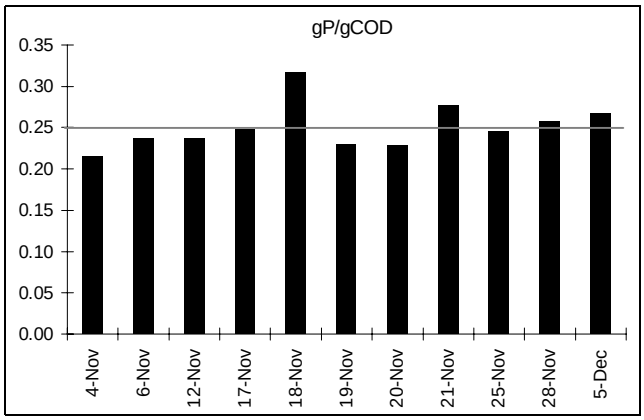

Figure 7.6. Stoichiometric coefficients during anaerobic batch experiments in the up-start period, Nov.-Dec. 1997, calculated by mass balances of added acetate and released phosphate.

For a series of batch experiments performed Feb.'98, the stoichiometric coefficient had decreased to 0.18-0.23 g P/g COD with 0.21 g P/g COD as the average, and in Dec'98: 0.12-0.15 g P/g COD. For Dec'98, pH regulation had been included, which lowered pH with approximately one unit (from ~8 to 7), which might account for the significantly lower coefficient at this point of time. Figure 7.7 summarises the measured stoichoimetric coefficients (some points calculated from the continuous operation are included). A third explanation of measuring the low coefficients could be a physical binding/adsorption of acetate to the biofilm matrix. However, it would seem unlikely that the bound acetate could not be released and available for the bacteria as the concentration in the bulk water decreases. Also, the stoichiometric coefficients that were calculated for successive additions of acetate during a single batch experiment (Fig. 7.8) were not different from calculations of coefficients based on initial addition. Differences would be expected, if the biofilm matrix initially bound a certain amount of the added acetate and reached "saturation" in regard to adsorption.

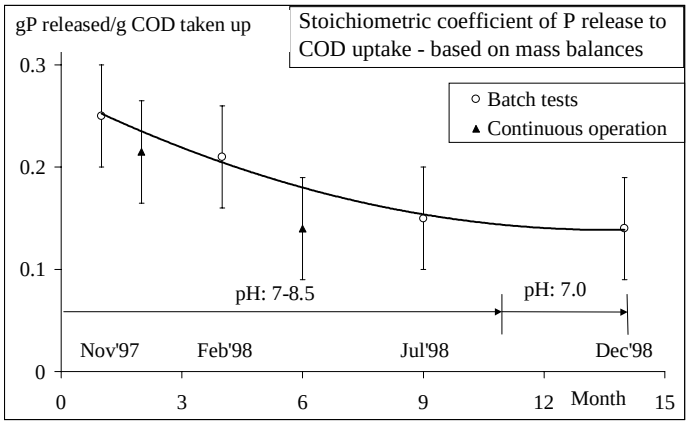

Figure 7.7. Stoichiometric coefficients of released P to COD taken up. Plotted against the month of operating the reactor during PART A, Nov.'97-Dec.'98.

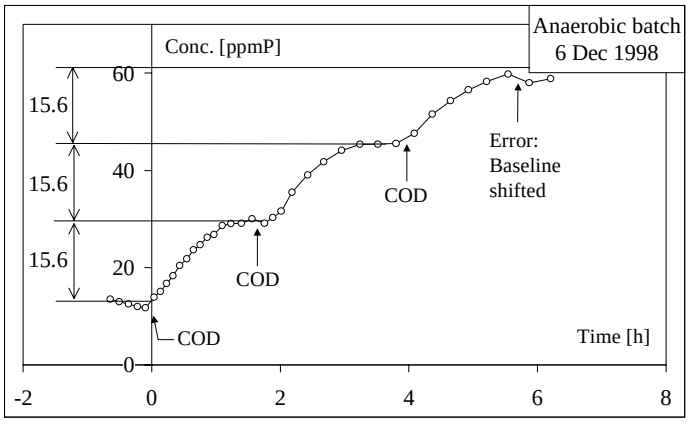

Figure 7.8. Successive addition of 112 ppm COD to an anaerobic batch experiment, Dec.'98. The stoichiometric coefficient did not change during the batch test: 0.14 g P/g COD.

7.2.2 Anoxic Batch Experiments

Reproducibility: Figure 7.9 shows 2 anoxic batch experiments made on Day 16 and 18 (Nov.'97). Phosphate is taken up along with removal of nitrate as a function of time. The reactor was backwashed before each experiment. The figure illustrates the reproducibility of the experiment and as such the stability of the biofilm in the considered short time perspective. The first point for the nitrate curves falls outside of the curve due to insufficient mixing within the first couple of minutes, so for insertion of an initial tangent, this point was excluded. The same was the case for the phosphate curves, if the first point was outside of the curve trend.

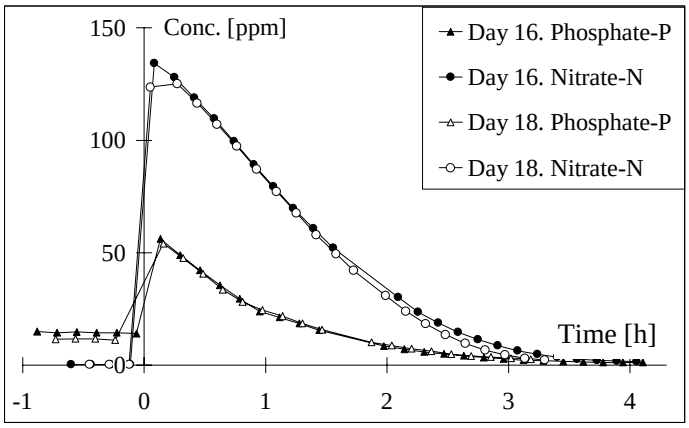

Figure 7.9. Decreasing nitrate and phosphate concentrations as a function of time for 2 anoxic batch experiments performed 2 days apart.

Stoichiometry: The ratio between the slope of the initial tangents for the phosphate and nitrate curve was used to determine the stoichiometric coefficient between phosphate uptake and nitrate removal (Fig. 7.12a). The coefficient varied in the range 0.51-0.75 gP/gN with an average of 0.65 gP/gN (Feb.-Jun. 1998). This can be recalculated to mol P/mol e^- : 0.046-0.068 and average 0.058, assuming nitrate is reduced all the way to nitrogen. Kuba *et al.*, 1993, found for enriched denitrifying cultures of phosphate accumulating organisms a stoichiometry of 0.19 mol P/mol e^-, in comparison the coefficient of the current study is very low. The reason for this could be a reduction of nitrate only to nitrite, which would convert the mol P/mol e- from 0.058 to 0.15 mol P/mol e^- (2 electrons for reduction of nitrate to nitrite, compared to 5 electrons for the full reduction of nitrate to dinitrogen). Nitrite was not measured in batch tests, only occasionally during the continuous operation. Up to 4 ppm NO_2-N could be observed during the transition from one phase to the other, but no nitrite was present apart from during the mixing phases. I.e. the bacteria were able to reduce nitrate completely to free nitrogen gas, however with a delay in the nitrite reduction compared to nitrate. As discussed below, phosphate release was

observed in the anoxic batch experiments upon depletion of nitrate in the bulk water. This indicates that the electron acceptors were depleted by the end of the experiments, i.e. also nitrite. Another explanation of the low coefficient is the use of nitrate by non-PAO's, which would agree with the also low coefficient of phosphate release to acetate uptake found during anaerobic batch experiments.

½ and 0 order of reaction: For anoxic batch tests, two soluble substrates can be limiting: nitrate or phosphate. A series of batch tests were made for both situations, i.e. in one case excess amounts of phosphate was added and different start concentrations of nitrate tested and vice versa. The results of both of these series of experiments are given in Fig. 7.10a and 7.10b, respectively. Numbers by each point indicate the day that the individual batch tests were made, the biofilm was subjected to normal continuous operation for minimum 2 cycles between each batch experiment.

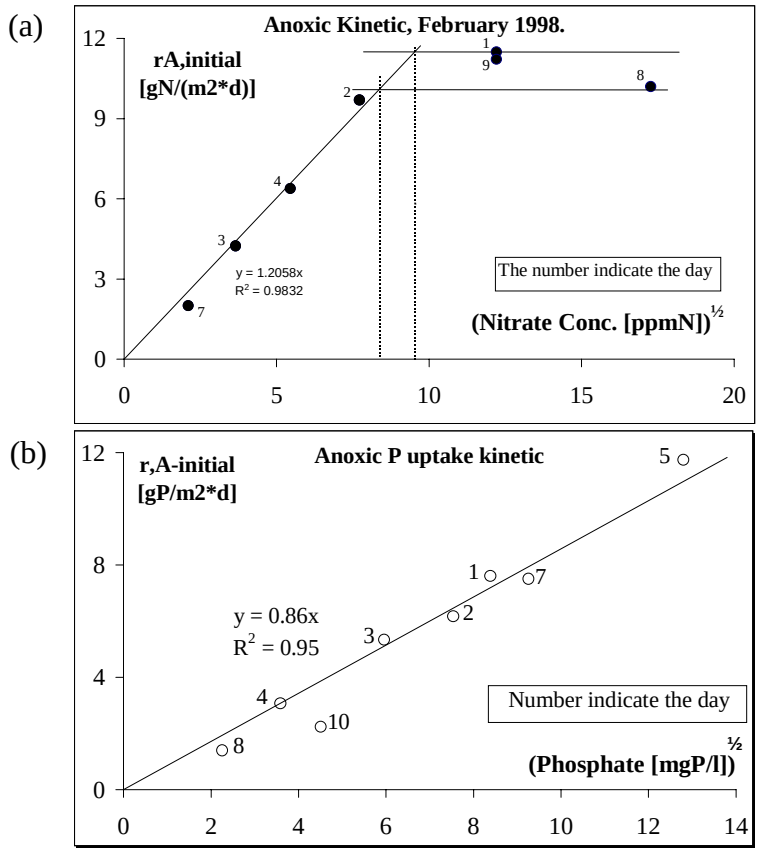

Figure 7.10. Anoxic batch experiments. (a) Excess phosphate was added to investigate the relationship between the nitrate concentration and denitrification rate. (b) Excess nitrate was added to investigate the relationship between phosphate uptake rate and phosphate concentration.

The theoretical start concentration of nitrate, respectively phosphate, was used as fix point for the intercept of the initial tangent with the y-axis. The first two

measuring points were in this way typically not included in the tangent, Fig. 7.11. These points were above the initial tangent, which was because the batch bottle was placed in the recirculation stream after the reactor and before the sampling point, whereby the nitrate rich batch solution passed the sampling point before being mixed with the nitrate free water in the reactor. The situation in Fig. 7.9 was opposite because the batch bottle at that time was placed before the reactor.

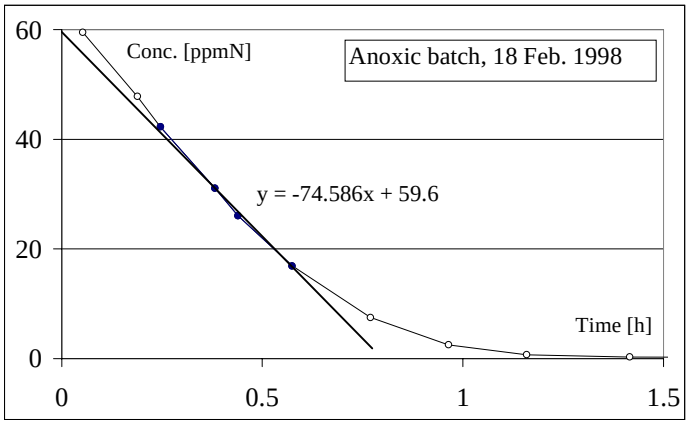

Figure 7.11. Example of insertion of the initial tangent during an anoxic batch experiment. Interception with the y-axis is fixed according to the theoretical start concentration.

Transition to 0 order removal of nitrate was found at a concentration around 70-91 ppm N with corresponding maximum removal rates of 10.1-11.5 gN/(m^2*d). The uncertainty on the 0 order level was relatively high, possibly due to variations in the biofilm thickness after back-wash and also caused by the uncertainty on inserting the initial tangent. By using a diffusion coefficient of $1.28*10^{-4}$ m^2/d (Henze *et al.*, 1997) for nitrate, the calculated biofilm thickness is 1.8-2.0 mm (Feb.'98). This is higher than a thickness of 1.1 mm that was calculated same month by the use of anaerobic batch experiments. The deviation might be due to uncertainty of the diffusion coefficients and initial tangents.
For the test with phosphate, no horizontal level could be reached, i.e. no 0 order of reaction rate for the tested phosphate range up to 164 ppm P. This should be attributed to a very thick biofilm and a limited capacity of the on-line phosphate measuring equipment for high phosphate concentrations (maximum: ~160 ppm P). For 164 ppm P, an uptake rate of 11.8 g P/(m^2*d) was found. By using the diffusion coefficient of phosphate $9.7 * 10^{-5}$ m^2/d (Edwards and Hoffmann, 1959) reduced by a factor of 0.8 for diffusion in biofilms compared to water (Henze *et al.*, 1997), the calculated biofilm thickness is > 2.2 mm (Jun.'98).

Phosphate release upon depletion of nitrate in the bulk water: The figures above illustrate the importance of diffusion for the process of phosphorus

removal in a biofilm. The deep part of a thick biofilm might never be exposed to the alternating conditions, either because bulk concentrations do not allow for full penetration, or the oscillation time is too short. Release of phosphate from the deep part of a biofilm may occur simultaneously with uptake of phosphate in the outer layers, if the biofilm is only partly penetrated with nitrate. The measured bulk concentration will be the net result. Figure 7.12 illustrates two anoxic batch experiments where P release was seen immediately upon depletion of nitrate in the bulk water. The release seems too significant to be due to maintenance/endogenous respiration only, especially when comparing with Fig. 7.9 where a relatively horizontal plateau of phosphate is observed prior to an anoxic batch experiment, before the electron acceptor is added. Also during anaerobic batch tests, a horizontal plateau was reached upon depletion of COD in the bulk water, despite additional phosphate release capacity – Fig. 7.3. Since no easily degradable substrate was added to the batch, an internal production of a carbon source must have taken place inside the biofilm – e.g. via decay and hydrolysis. Or the reason for release of phosphate *after* an anoxic batch experiment (Fig. 7.12) compared to before (Fig. 7.9) could be related to the higher internal glycogen levels produced during the experiment. The higher glycogen levels might induce more P release due to utilisation of glycogen.

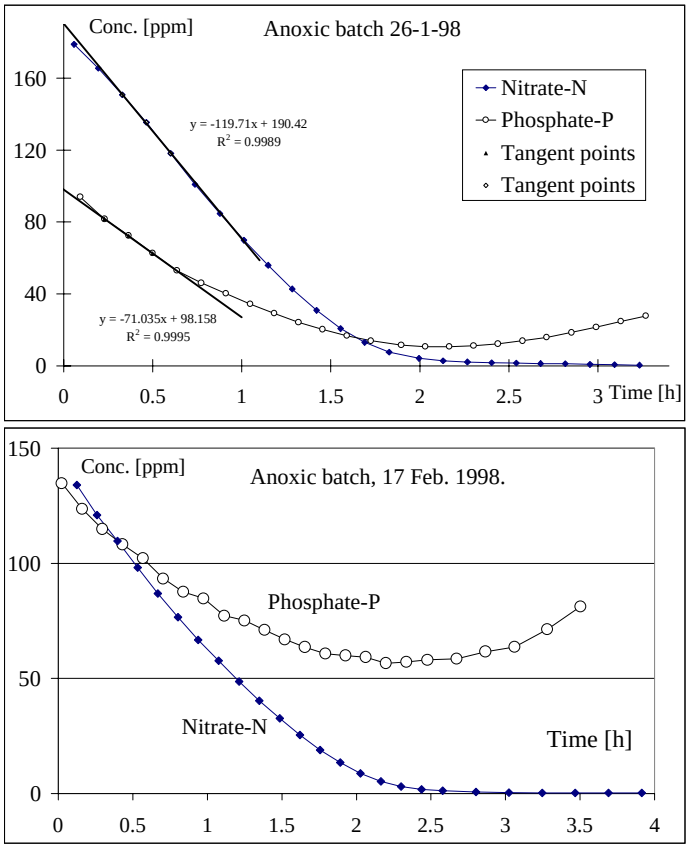

Figure 7.12. Anoxic batch experiments. Phosphate is released upon depletion of nitrate in the bulk.

The time at which phosphate release was initiated, cannot be seen from the results. It is likely that release starts in the deep part as soon as nitrate no longer fully penetrates the film. However, the released phosphate is taken up in the outer, anoxic layer and only when the whole biofilm is anaerobic does phosphate penetrate all the way out into the bulk water.
The concentration of nitrite should have been measured in the anoxic batch experiments. It cannot be ruled out, that the high amount of nitrate and hence possible accumulation of nitrite might have stressed the bacteria during the batch experiments leading to release of phosphate as a stress response.

Continued denitrification upon depletion of phosphate in the bulk water: Continued denitrification was consistently observed upon depletion of phosphate in the bulk water during anoxic batch experiments. Figure 7.13 shows an example. This indicates that oxidation of internally stored organic matter can occur also without simultaneous phosphate uptake. This is in agreement with previous findings and supports the recommendation of avoiding extensive aeration in EBPR plants after complete phosphate removal has been achieved, to avoid non-EBPR utilisation of internal organic matter. That the denitrification rate decreases as a function of time (reduced slope of the curve tangents) due to decreased/depleted internal organic storage pools.

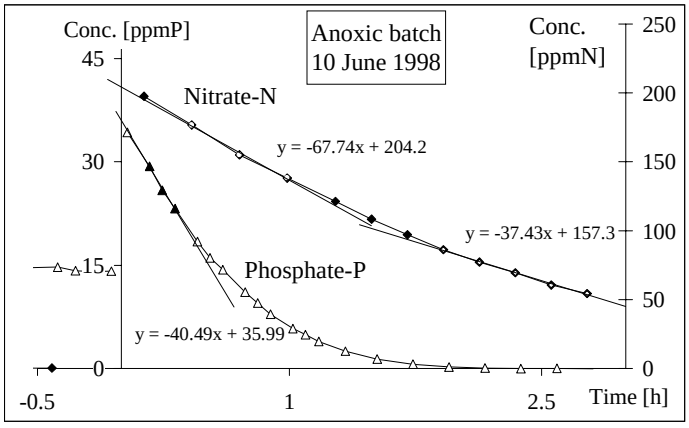

Figure 7.13. Anoxic batch experiment. Denitrification continues upon depletion of phosphate in the bulk.

7.2.3 Summary of Anaerobic and Anoxic Batch Experiments

Anaerobic and anoxic batch experiments illustrated the characteristics of removal of compounds with a biofilm, where the removal rate is depending on the substrate concentration in the bulk water and hence the penetration of this substrate into the biofilm. ½ and 0 order of reaction rate could be verified for anaerobic phosphate release and nitrate removal, but only ½ order of reaction

for phosphate uptake due to limitation of the phosphate measuring equipment for high phosphate concentrations. Table 7.2 summarises stoichiometric coefficients deduced from batch experiments. Both the values for anaerobic P release and for anoxic phosphate uptake were low compared to the literature for enriched denitrifying bio-P cultures. This could be an indication of the presence of competing bacteria with the capacity of storing organic substrate and good survival in the continuous alternating operation, or a different metabolism of biofilm PAOs compared to activated sludge PAO cultures.
Maurer and Boller, 1999, discussed the possibility of 'natural' chemical precipitation induced by the high phosphate concentrations under anaerobic conditions, even at pH below 8. Arvin, 1983, discussed the enhanced possibility of phosphate precipitation inside denitrifying biofilms due to the pH gradient inside the film. For the synthetic substrate used (chapter 4.4) the likelihood of precipitation is minimal. Calculations have shown that precipitation of calcium and hydroxy phosphates (apatit, the most likely phosphate precipitation compound) should not occur for pH below 9. However, it cannot be excluded that chemical precipitation and pH may have influenced the found stoichiometric coefficients.

Table 7.2. Stoichiometric coefficients calculated from batch experiments.

Stoichiometry	Unit	Interval	Average	Literature
P-release, Nov.'97 (mass balance)	g P/g COD	0.22-0.32	0.25*	0.4 Henze *et al.*, 1995
P-release, Feb.'98 (mass balance)	g P/g COD	0.18-0.23	0.21*	0.4 Henze *et al.*, 1995
P-release, Dec.'98 (mass balance)	g P/g COD	0.12-0.15	0.14**	0.4 Henze *et al.*, 1995
P-uptake, Nov'97 -Jan'98 (tangent slope)	g P/g N	0.51-0.75	0.65	2.1 Kuba *et al.*, 1993
P-uptake, Nov'97 -Jan'98 (tangent slope)	mol P/mol e^-	0.046-0.068	0.058	0.19 Kuba et al., 1993

* pH not regulated, ~ 8.0 ** pH regulated at 7.0

Table 7.3 summarises the reaction rates etc. for series of batch experiments. Reasonable agreement was found for the anaerobic batch tests performed in Nov.'97 respectively Feb.'98 in regard to removal rate and acetate concentration leading to transition from ½ to 0 order of reaction rate in the bulk water. The stoichiometry for phosphate release to acetate uptake decreased slightly between the two experiments (Table 7.2) and also the maximum phosphate release rate. Both phenomena could indicate increased dominance of non-PAO bacteria in the biofilm taking up acetate under anaerobic conditions. The biofilm thickness calculated for the different series vary significantly (1.1-2.2 mm), also for series made in the same month (Feb.'98). This is possibly the result of several

uncertainties related to: Variances in the actual biofilm thickness after backwash, insertion of initial tangent, diffusion coefficients etc. Caution is suggested for using this way of calculating the average biofilm thickness, however a rough indication can be obtained. As may be seen in Fig. 7.5, the biofilm thickness actually did increase during the experimental period, which necessitated the removal of some carrier beads in Dec. 1997 (~ 25 %).

Table 7.3: Overview of kinetic experiments with the bio-P biofilm.

Kinetic	$S_{transition}$	$k_{½A}$	$r_{A,max}$	L
Anaerobic, Nov'97	256	0.11	7.9	1.6
P release, Acetate	ppm COD	$gCOD^{½}\,m^{-½}\,d^{-1}$	$gP\,(m^2*d)^{-1}$	mm
Anaerobic, Feb'98	234	0.14	6.9	1.1
P release, Acetate	ppm COD	$gCOD^{½}m^{-½}d^{-1}$	$gP\,(m^2*d)^{-1}$	mm
Anoxic, Feb'98	71	1.21	10.2	1.8-2.0
N removal, Nitrate	ppm N	$gN^{½}\,m^{-½}\,d^{-1}$	$gN\,(m^2*d)^{-1}$	mm
Anoxic, Jun'98	> 164	0.83	> 11.8	> 2.2
P uptake, Phosphate	ppm P	$gP^{½}\,m^{-½}\,d^{-1}$	$gP\,(m^2*d)^{-1}$	mm

7.2.4 Simultaneous Presence of Acetate and Nitrate

Batch tests with simultaneous presence of acetate and nitrate were made Jul.-Dec. 1998. The batch tests were made after the biofilm had gone through an anoxic phase in the continuous operation, i.e. similar to the anaerobic batch tests described above. It was expected to see a decrease in the phosphate release rate with the addition of nitrate, since the bacteria would oxidise part of the acetate directly via nitrate according to the theory of Kuba *et al.*, 1994. Figure 7.14 shows one result of such an experiment. An anaerobic batch test was performed (start concentration of acetate: 576 ppm COD) 2 Jul'98 and a similar experiment was carried out the following day, but this time with addition of nitrate (37 ppm N). Surprisingly, no difference in the phosphate release rate could be observed. The removal of nitrate seemed to follow a ½ order removal kinetic, since a straight line appeared when plotting the square root of nitrate over time, Fig. 7.15. No full penetration with this nitrate concentration agrees with the need of more than 70 ppm N for full penetration during anoxic batch tests (Table 7.3).
The plateau of phosphate reached on 3 July was 20 ppm P lower than for the 2 July, which corresponds well with the COD used for denitrification: 0.19 gNO_3-N is used per g CH_3COO denitrified, hence 37.3 ppm N demands 196.3 ppm CH_3COO = 214 ppm COD. For a stoichiometry of 0.21 g P/g COD, a start concentration of 576 ppm COD can support up to 121 ppm P. 100 ppm P was observed on 2 July, which might be due to empty P (or glycogen) storage. On 3 July (576-214) ppm COD = 362 ppm COD was available for phosphate release, which is equivalent to up to 76 ppm P. An end concentration of 80 ppm P was observed. However, for this batch test no pH control was implemented and the

pH rose tremendously (up to 9.2) due to the denitrification directly with acetate, Fig. 7.16. The necessity of introducing pH control was evident.

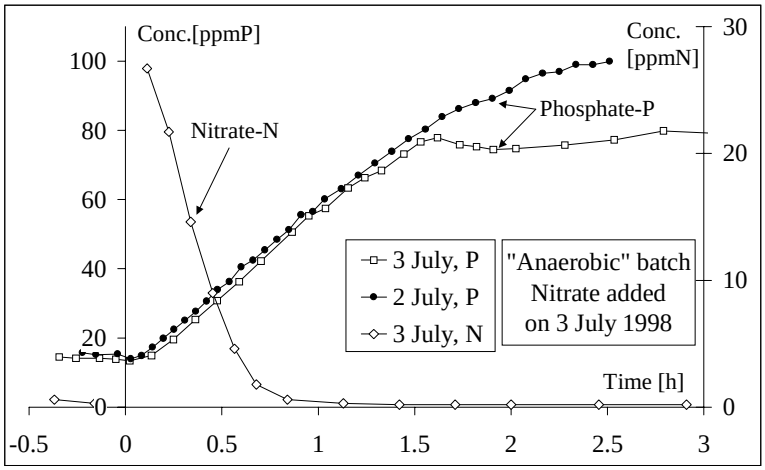

Figure 7.14. "Anaerobic" batch tests (performed after an anoxic phase in the continuous operation) with and without addition of nitrate (37 ppm N). No difference in P release rate is observed.

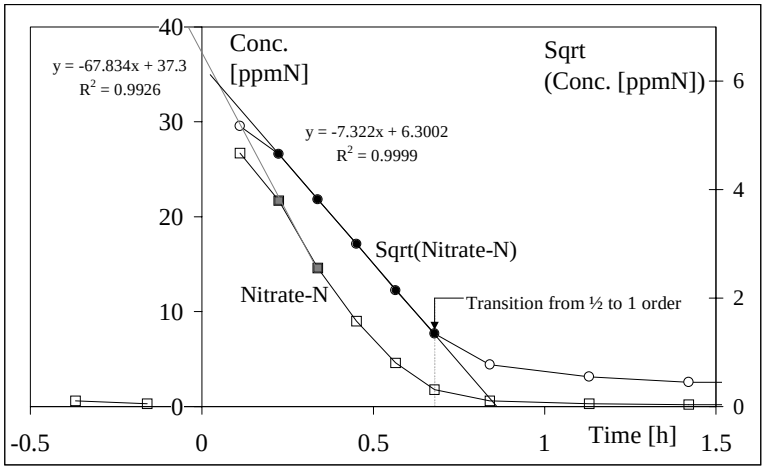

Figure 7.15. ½ order nitrate removal rate during "Anaerobic" batch test 3 Jul'98.

After pH control had been implemented, new batch tests were performed for pH = 7.0 ± 0.3. Figure 7.17 illustrates three of these. The phosphate release rate was reduced by the presence of 75 ppm N nitrate for acetate concentrations below a certain level. For an initial COD concentration of 1754 ppm COD (24 Nov.), the phosphate release rate was identical to the release rate observed in another experiment upon depletion of nitrate and addition of additional COD (4 Nov.) This indicates that the release rate only decreased in case of a limitation in the available amount of COD. The bare presence of nitrate apparently did not disturb the phosphate release.

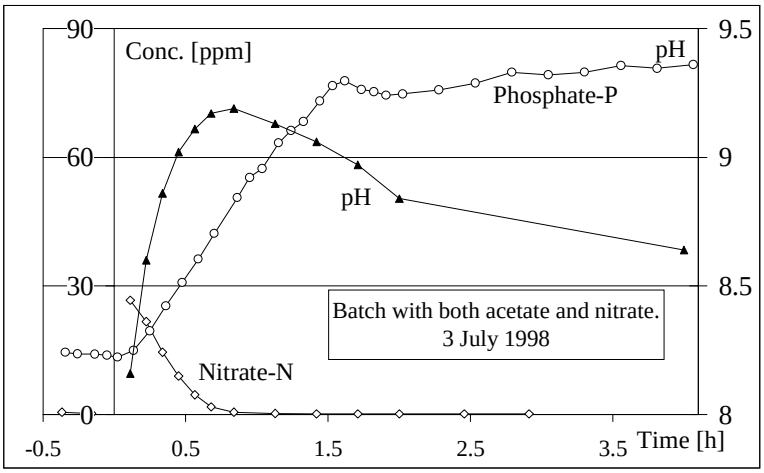

Figure 7.16. pH during "Anaerobic" batch test (nitrate added) 3 Jul'98.

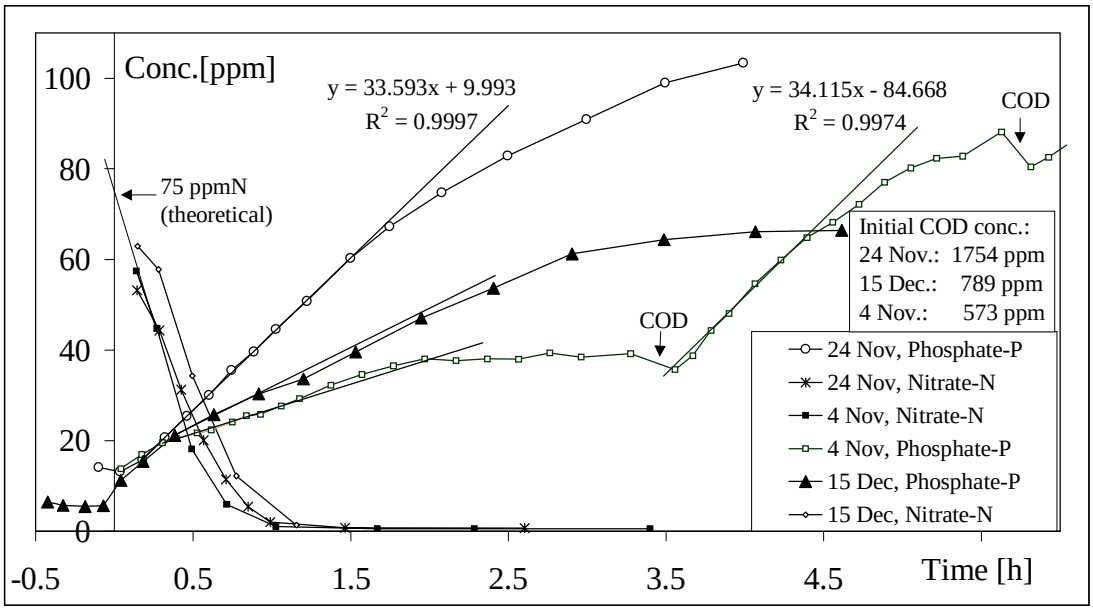

Figure 7.17. Batch tests with simultaneous presence of nitrate and acetate, Nov.-Dec.'98.

7.3 Continuous Operation

7.3.1 Stability of The Process

7.3.1.1 Long time stability

Outlet concentrations: The continuous outlet concentrations of phosphate during a 7 months period, Nov'97-Jun'98, is illustrated in Fig. 7.18. Figure 7.19 shows the same data with nitrate measurements included, and data from the single months are plotted on separate charts. pH was not controlled and varied

in the interval 7.0-8.5 during a cycle. However, since identical synthetic wastewater composition was used in the entire period, the effects of pH were expected to remain uniform. The highest activity in terms of maximum phosphate concentrations during the anaerobic phases and accordingly lowest phosphate concentrations during the anoxic phases were found in the first months of operation. Hereafter, the activity declined and later increased again, but was always lower than initially.

A significant change in the nitrate outlet concentrations took place 3 months after start-up, from Dec.'97-Jan.'98. Significantly more nitrate was removed from this time on, despite of the decrease in the phosphate removal activity, which indicated that nitrate was used for other purposes than phosphate release – possibly by other bacteria.

The nitrate measurements were not as reliable as the phosphate measurements, the electrode had to be cleaned and calibrated every second day, which was not always obeyed, hence the exact values should be taken with some reservations, but the trend is clear. Calibrations were always made prior to batch tests and mass balance calculations.

The reason for the differences in activity is not known. Changes in the microbial community are speculated to be the reason. As previously discussed, it appears from the calculated stoichiometric coefficients that not only PAOs are present in the reactor, but also other bacteria capable of storing. The variations in the activity might be an expression of a competition between these organisms. Microbial characterisation methods would have been valuable tools in order to support the assumptions.

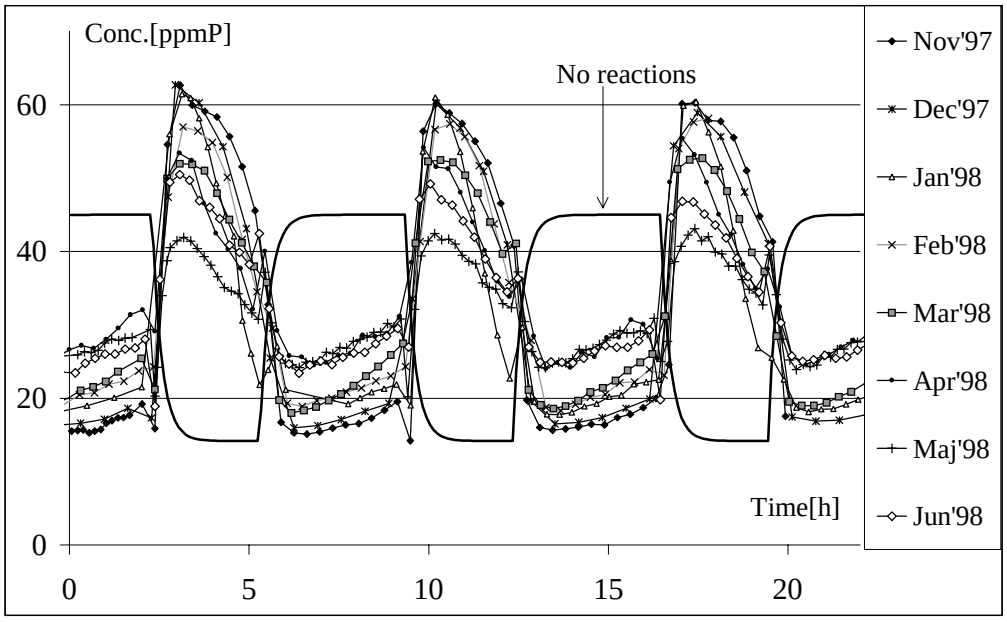

Figure 7.18: Outlet concentrations of phosphate during a 7 months period, Nov'97-Jun'98. Inlet of phosphate was varied between anoxic (44 ppm P) and anaerobic (14 ppm P) phases.

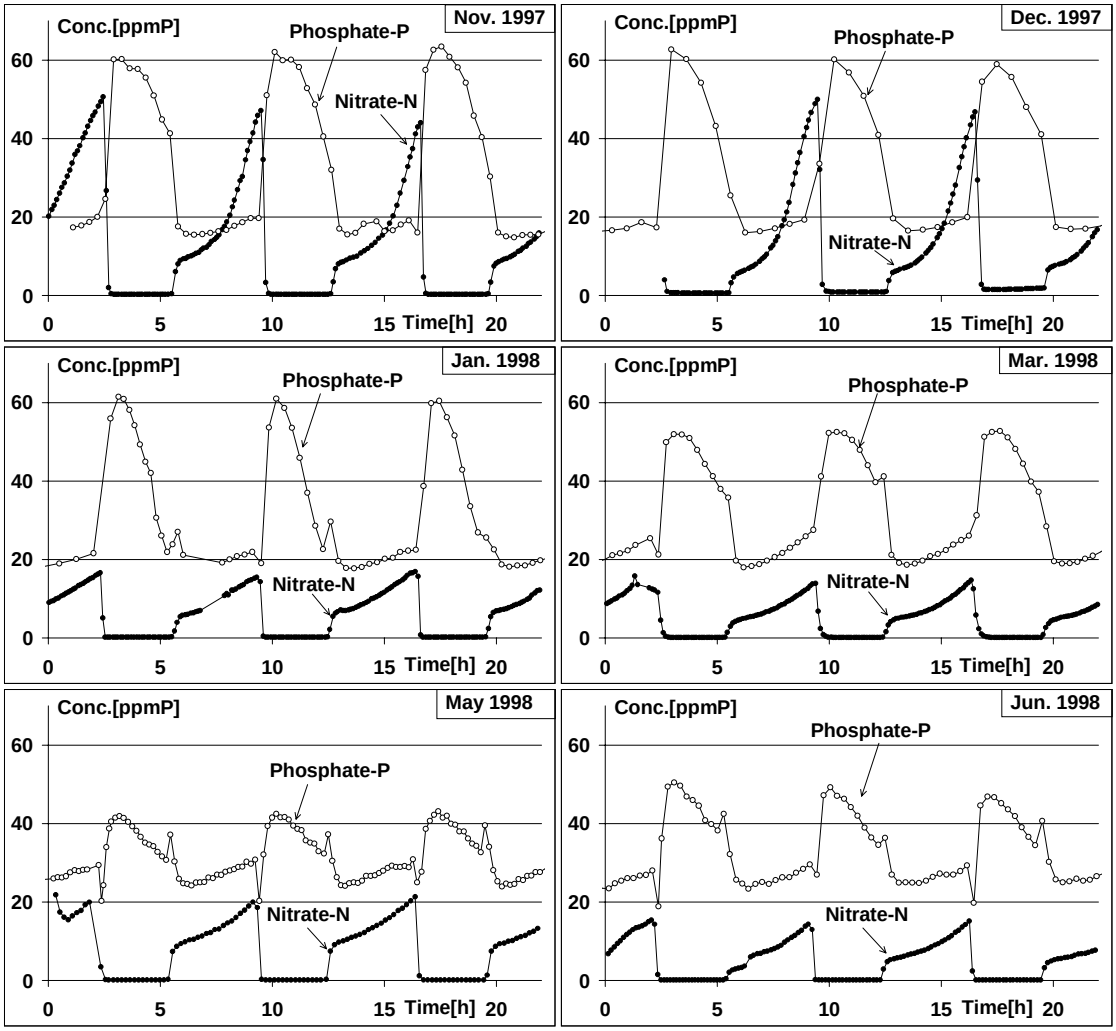

Figure 7.19. Typical outlet concentrations from the continuous operation for different months in the period: Nov. 1997 – Jun. 1998 (read from the top left corner to the right). The phosphate activity, in terms of maximum P in the anaerobic outlet and minimum P in the anoxic outlet, were highest in the first months of operation. The nitrate removal increased (decreased outlet concentrations) despite of the lowered bio-P activity.

Phase lengths: The phase lengths in the continuous operation were:

Oct'97-Jul'98	: 3 hours anaerobic and 4 hours anoxic
Jul'98-Sep'98	: 8 hours anaerobic and 8 hours anoxic
Sep'98-Dec'98	: 5 hours anaerobic and 8 hours anoxic
Dec'98	: 4 hours anaerobic and 8 hours anoxic

After the change to longer phase lengths Jul'98, the bio-P activity declined and stayed at a considerably lower level than for the previous period. The change back to shorter phase lengths in Dec'98 improved the activity again, leading to a

final activity similar to the previously measured activities. However, it was in the period with longer phase lengths, that also batch tests with simultaneous presence of acetate and nitrate were performed. The latter might have given competing non-PAO bacteria advantages, whereby it cannot be concluded that the deterioration of the phosphate activity was caused by the changed phase lengths. Figure 7.20 illustrates anaerobic release rates from the different periods. The figure is the same as Fig. 7.4a, but including data from the periods with longer phase lengths. The release rates from batch experiments after the shift to longer phase lengths, Jul'98, are significantly below the previous findings.

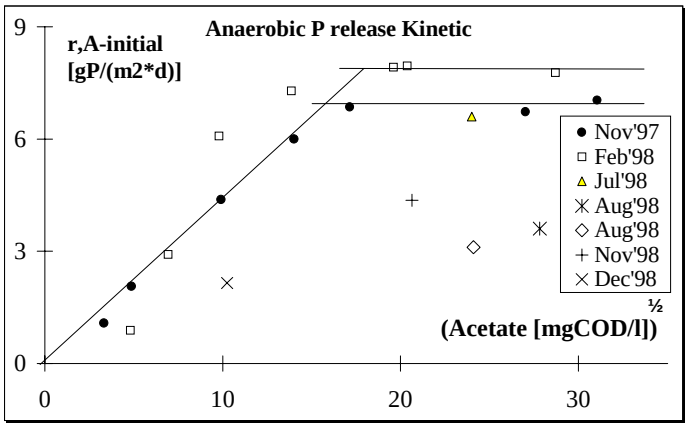

Figure 7.20. Anaerobic batch tests. Longer phase lengths (7 hours, against earlier 4 hours) were used from mid Jul'98 until end Sep'98. Oct-Dec'98 used 5 and 4 hours phases. The long phase lengths appeared to be disadvantageous for the phosphate release rate (the PAOs), but batch experiments with simultaneous presence of acetate and nitrate were performed in the same time periods which possibly influenced the microbial population.

During the continuous operation, the declined activity was evident from a lower phosphate peak during anaerobic phases and equivalently higher phosphate concentrations in the outlet during anoxic phases. Figure 7.21a+b gives some examples that can be compared with Fig. 7.18.

Storage at 4-5 ^{o}C: During periods where the continuous setup could not be maintained, the reactor was kept in the refrigerator. The activity upon returning the reactor to the setup was very close to the activity before storage, indicating good survival of the bacteria in the biofilm. Figure 7.22 shows an example of the outlet concentrations before and after one of these storage periods. The reactor was here stored for 3 weeks (Apr.-May'98). Whether storage periods might have had some influence of a more long-time character, cannot be excluded. The reactor was stored in the periods: 18 Dec'97-16 Jan'98; 7-16 Apr'98; 29 Apr-20 May'98; 22-26 Oct'98 and 8-14 Nov'98.

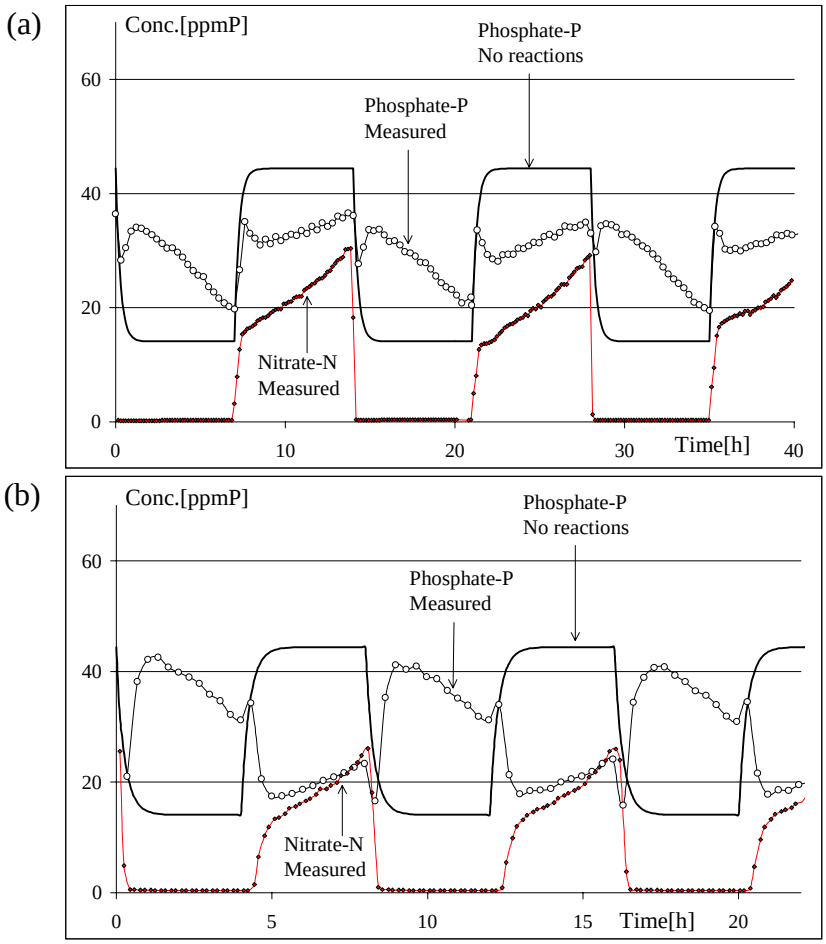

Figure 7.21. (a) Example of activity during 7 hours phase lengths (Aug'98). (b) Example of activity during 4 hours phase lengths (Dec'98).

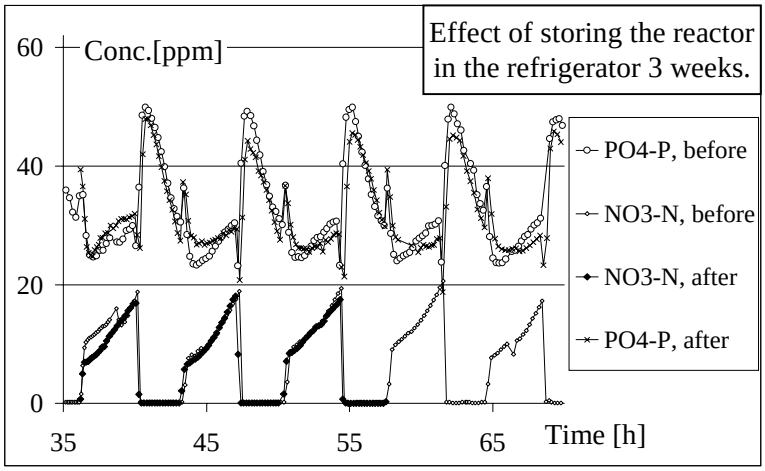

Figure 7.22. The reactor had to be kept in the refrigerator a few times during operation. An example of the only small influence this had on the bio-P activity is illustrated in this figure for a situation where the reactor was stored over a 3 weeks period.

Appearance of the biofilm: The appearance of the biofilm shifted over time from a relatively smooth biofilm to a more heterogeneous, rugged structure, refer to Fig. 7.5, and black precipitates appeared by the bottom of the film. These black precipitates were assumed to be caused by consistent anaerobic conditions by the bottom of the film with formation of precipitates e.g. FeS, if this assumption is correct, it would be a verification of an only partly penetrated biofilm during the anoxic phases. The sulphate concentration in the in- and outlet was measured over one cycle Apr.'98. The inlet concentration was measured to 17.5 ± 0.1 ppm S (by HPLC) and the outlet to 17.4 ± 0.4 ppm S. The measured inlet concentration was in agreement with the theoretical value. Hence, no sulphate precipitation could be measured by the outlet concentrations, but since the black precipitates appeared slowly over time, it is still likely that it anyway could be FeS precipitates, since sulphate was not regularly measured. The black layer was not easily removed during backwash, apparently it attached strongly to the Biostyr surface.
The increased removal of nitrate observed in the continuous operation as a function of time (Fig. 7.19) could perhaps be attributed to utilisation by a sulphur cycle in the bottom of the thick film. The action of a sulphur cycle cannot always be identified by sulphate measurements in the bulk water, since no precipitation necessarily is involved (refer to chapter 2.3.9).

Microscopy: The biomass was not investigated with microbiological method. However, a few transmission images was taken of the biomass removed by backwash May'98. These showed the dominance of two morphological bacteria types: a large coccoid and a smaller short rod, Fig. 7.23. These were arranged in dense, separate colonies. No cells arranged in the typical tetrads reported for GAOs were observed.

7.3.1.2 Short time stability

Over shorter periods of time (time-scale: days), the biofilm could be considered in a quasi-steady state. During such periods, different batch experiments could be performed and compared as done in chapter 7.2. An example of start-up of the system following different batch experiments is shown in Fig. 7.24. The first phase is different for the different batch tests due to different storage, but already the second phase is very similar in the different runs. In order to be able to compare different batch experiments it is essential to know that the biofilm can be considered quasi-steady. For this reason the history of the biofilm need to be known, which can only be obtained by continuous on-line measurements.

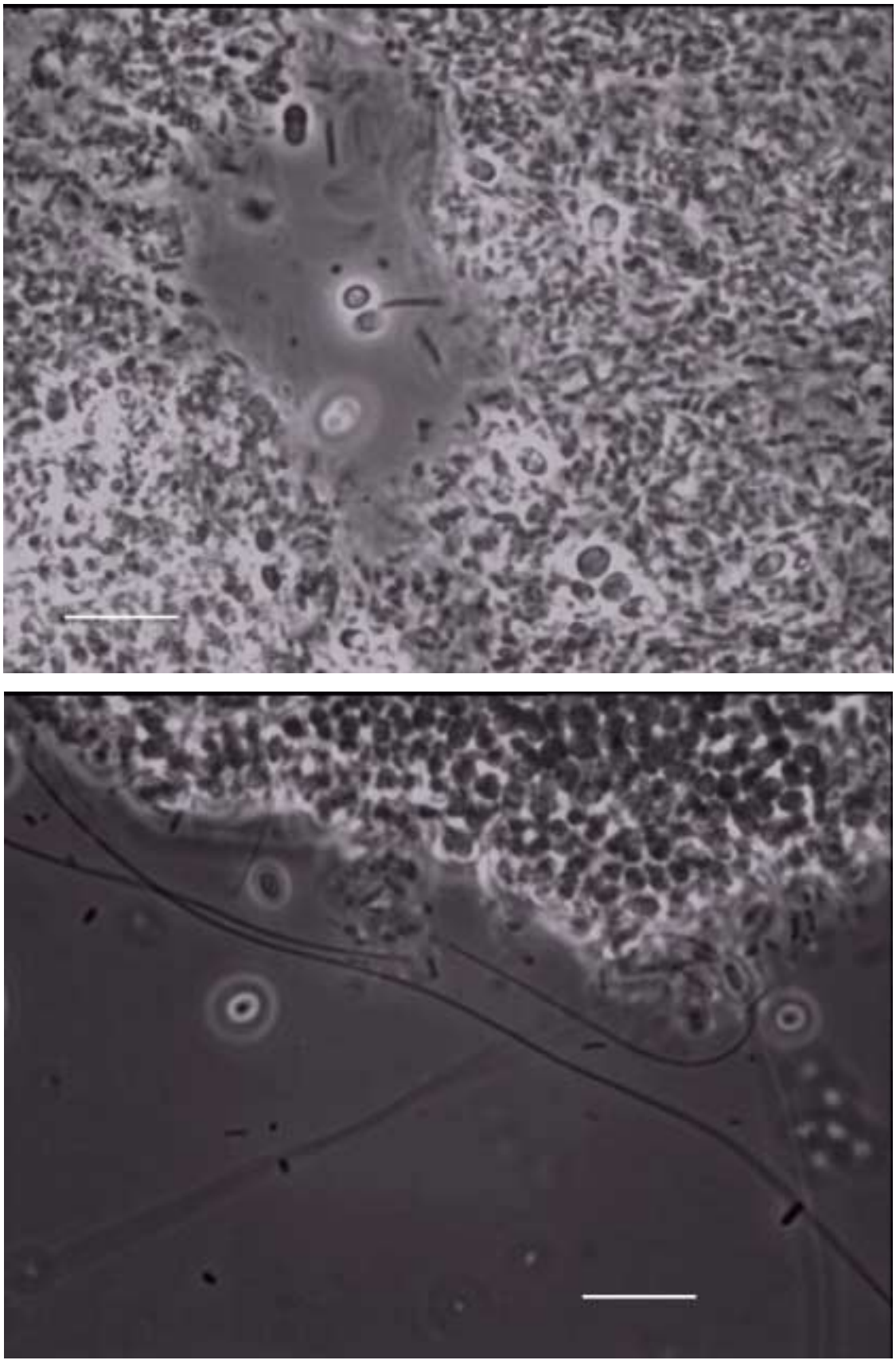

Figur 7.23: Material flushed from the reactor 24 May 1998. Bar: 10 µm.

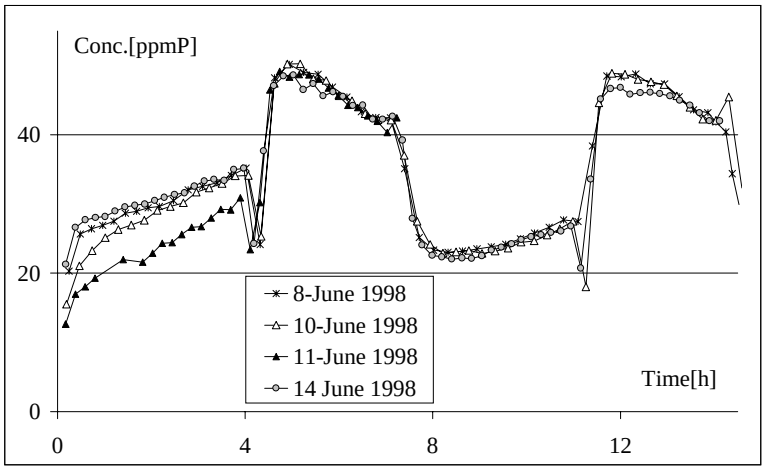

Figure 7.24. Start-up of the continuous system upon different anaerobic batch experiments.

7.3.1.3 Effect of backwash on the outlet concentrations

The outlet curves from the continuous operation did not change over shorter periods of time (time-scale weeks) which according to the hypothesis outlined in chapter 6.3 indicates that the biofilm was only partly penetrated. However, the hypothesis of decreasing amplitude of the outlet concentration of phosphate following backwash was not demonstrated. The outlet concentrations typically seemed unchanged after backwash. Two examples of the outlet concentrations during continuous operation are given in Fig. 7.25. These are situations from the beginning of the experimental period, Nov'97 (3 days), and from the final period, Dec'98 (5 days). Backwash is for Dec'98 marked by a small star on the x-axis.

The reason for no significant effect of backwash on the outlet curves could be that the bacteria residing in the deeper layers might stay active and metabolise at maximum rates as soon as they again are exposed to substrate (after the outer layer is removed during backwash). However, this would demand them to maintain a significant level of internal poly-phosphate, PHB and glycogen levels while buried in the depth of the film. Another possibility is, that backwash does not remove the outer active layers of the film, but rather thick cohesive cloaks of the biofilm as discussed in chapter 7.2.1. In this way, no significant decrease of the activity of a partly penetrated biofilm would be expected after a backwash, as long as enough biomass remain in the reactor to preserve the bulk water removal level. This explanation agrees with the visual observations during backwash and the inhomogeneous appearance of the biofilm with naked carriers by the side of carriers with a very thick biofilm (Fig. 7.5).

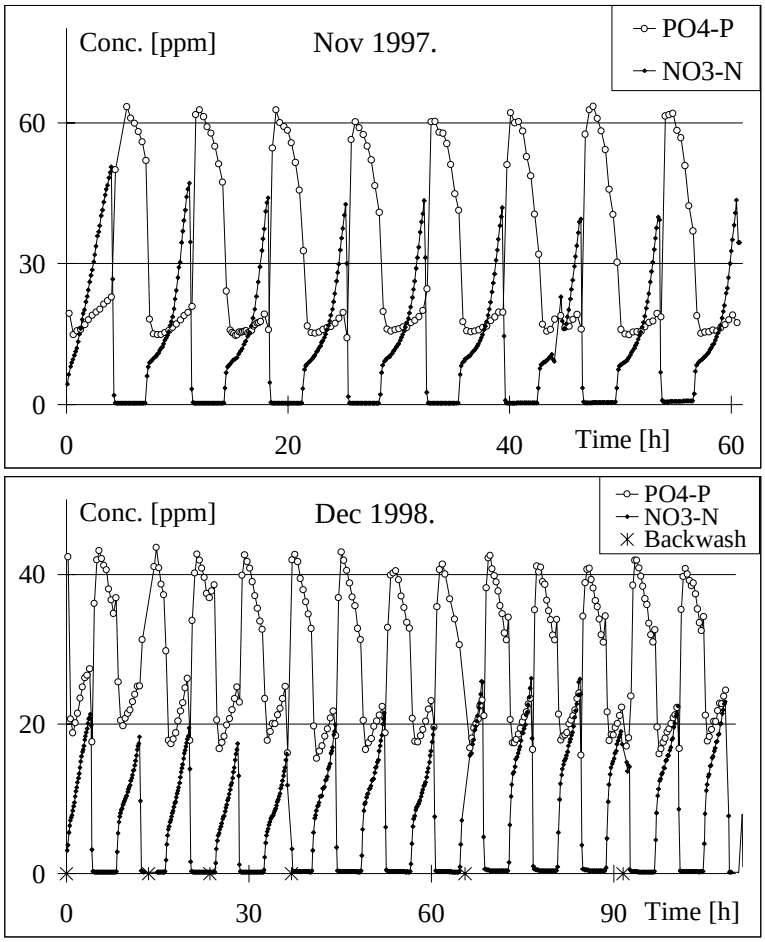

Figure 7.25. Outlet concentrations from the continuous operation, Nov'97 and Dec'98. In both cases a stable level is seen indicating an only partly penetrated film – a growing biomass would result in a growing amplitude of the outlet curves in case of no substrate limitations.

7.3.2 Mass Balances

Mass balances of phosphate for the continuous operation were complicated by a very high sensitivity of the calculations to the concentration measurements. In some cases, even a slightly higher mass of released phosphate than phosphate taken up was found... This is not possible (except for temporary un-steady state operation), and the error was attributed to measuring inaccuracy. A deviance of ~2 ppm P of the actual inlet concentration compared to the used theoretical one could in all cases account for the error. Measurements of the inlet concentrations were not made frequently enough to enable reliable mass balance calculations of the entire experimental period during PART A. Generally, mass balances showed approximately the same amount of phosphate (M_P) taken up during anoxic phases as what had been released during the previous anaerobic phase. As discussed in chapter 6.3, this was to be expected for a phosphate

diffusion limited biofilm where excess COD (as defined by deeper penetration into the biofilm) is added during anaerobic phases compared to phosphate during anoxic phases. Mass balance results from 3 time periods, chosen from the criteria of a steady outlet level, are summarised in Table 7.4. Fig. 7.26 illustrates one of the periods, Feb'98: (a) shows the 3 considered cycles (the average was used as result of the mass balance), and (b) shows the continued operation with very stable outlet level of both phosphate and nitrate. The mass of phosphate involved in EBPR activity (release and subsequent uptake) was 79-97 mg P during a cycle.

Table 7.4. Mass balances in the continuous setup. No significant difference of the amount of P taken up during an anoxic phase and released during the following anaerobic phase was found, indicating phosphate diffusion limitation in the biofilm during anoxic phases. All values refer to a single cycle.

Time ↓	M_P	N removed	P taken up / N removed	COD removed	P released / COD removed
	mg P	mg N	g P/g N	mg COD	g P/g COD
Feb'98	97 ± 2	174±2.2	0.56	-	-
Apr'98	79 ± 2	188±3.0	0.42	615	0.13
Jun'98	95	-	-	-	-

It was not possible to verify a slightly lower amount of phosphate released during the anaerobic phases that would have been expected due to the phosphate incorporated in the growing cell mass. This is likely due to the relatively small amount of P incorporated in the cell mass compared to the mass flux of phosphate caused by the poly-P-storage metabolism. Assuming a biomass production of 0.58 gTS/d = 0.17 gTS/cycle (see below), and a phosphate content of 15 mg P/gTS in the cell mass, the phosphate mass removed via incorporation in the growing biomass would be 2.5 mg P/cycle, i.e. 30 times less than the excess amount of phosphate taken up and released by the bacteria.
The stoichiometry of phosphate taken up to nitrate removed was slightly lower (0.42-0.56 gP/gN) than was found during anoxic batch tests (0.51-0.75 gP/gN). This is likely caused by direct denitrification of part of the nitrate during transition phases in the continuous operation where acetate and nitrate are present simultaneously as oppose to the anoxic batch tests.
A mass balance including COD was made Apr'98. COD was measured during an anaerobic cycle in the form of TOC by the use of an IO Model 700 TOC Analyser (Janning, 1995). The result is shown in Fig. 7.27 where TOC has been converted from mg C/l into mg COD/l (1 ppm C = 2.665 ppm COD). A background concentration of approximately 8 ppm COD is measured during anoxic phases. This might be due to detached bacterial cells or difficult degradable microbial polymers . By subtracting this background level, it is found that 615 mg acetate-COD is removed during one anaerobic phase.

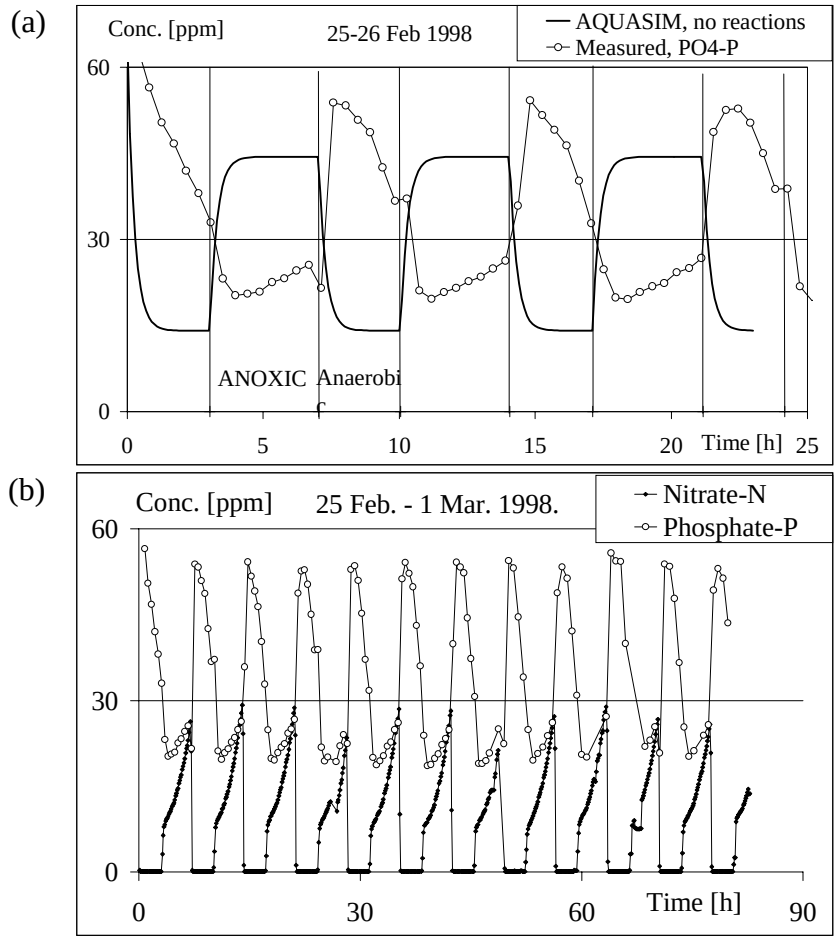

Figure 7.26. One period of which phosphate mass balances were calculated. (a) includes a curve for no reactions taking place in the reactor, and this was used for the mass balance. (b) shows the continued operation with stable outlet concentration levels of phosphate and nitrate.

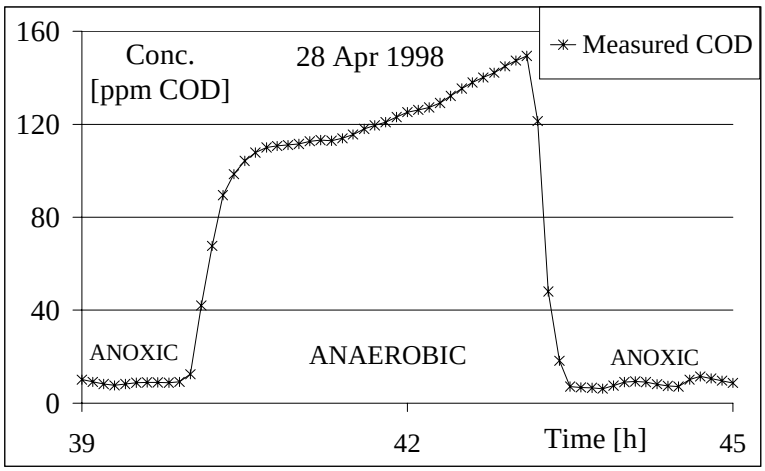

Figure 7.27. COD measurements during a cycle in the continuous operation, Apr'98.

7.3.3 Estimation of The Observed Yield Coefficient

The total mass of solids (TS) removed via backwash was measured over a period of 14 days, Feb-Mar'98. Figure 7.28a shows the removed mass for each backwash and it is noticed that more mass was removed via a backwash when more days had passed since the previous backwash. The cumulative curve for the data of Fig. 7.28a is given in Fig. 7.28b. The slope of this curve corresponds to the average daily amount of TS removed from the reactor: 0.58 g TS/d. By combining this value with measurements of the removed daily amount of COD, the observed yield coefficient of the bacteria can be calculated. It is in this calculation assumed that biomass removed during the continuous operation is negligible compared to during backwash. This assumption is based on always very clear outlet water from the continuous operation.

$$Y_{obs} = \frac{\text{Biomass produced}}{\text{COD removed}} \qquad (7.1)$$

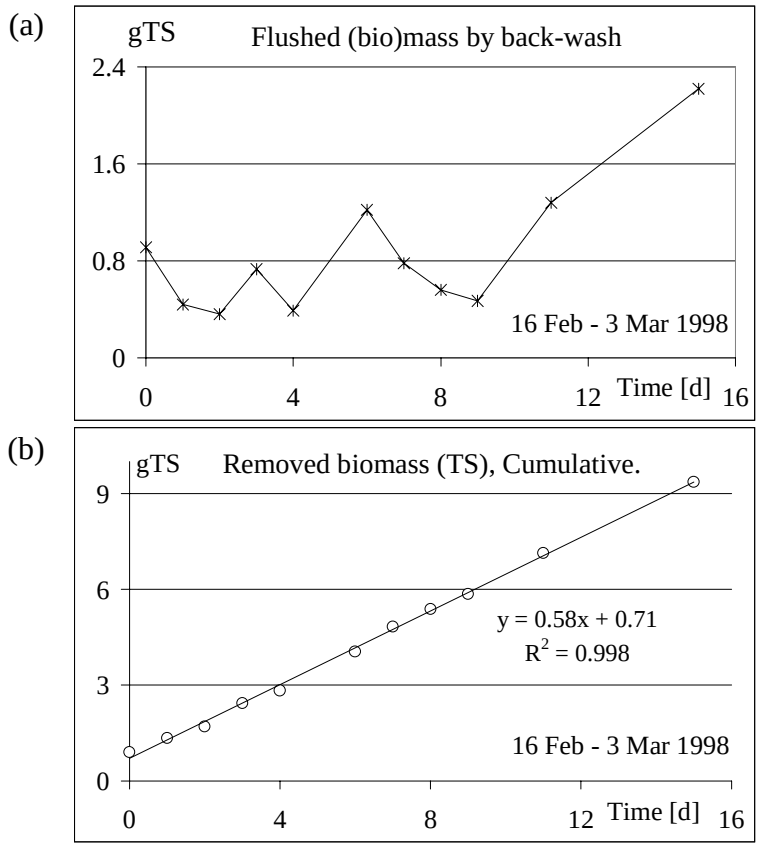

Figure 7.28. Removed mass during backwash. (a) Removal by a single backwash, notice the more days between the backwashes, the higher the amount removed. (b) Cumulative removed mass over a 2 weeks period. On average 0.58 g TS was removed daily.

Unfortunately, only COD measurements from Apr'98 are available (Fig. 7.27). The bio-P activity in Apr'98 was slightly lower than in Feb'98, see Fig. 7.28 below. In Apr'98 a COD removal during one cycle was measured to 615 mg COD/cycle. The cycle length was 7 hours, equivalent to 3.43 cycles/day and hence removal of 2.11 g COD/day. This value gives for the produced biomass daily in Feb'98 an observed yield of:

$$\mathbf{Y_{obs}} = (0.58\ \text{gTS/d}) / (2.11\ \text{g COD/d}) = \mathbf{0.27\ g\ TS/g\ COD}$$

Kuba *et al.*, 1993, report observed yield coefficients in the range 0.25-0.3 gSS/gCOD for a system operated with nitrate as the electron acceptor. In comparison they found a yield of 0.35-0.4 for a system operated with oxygen as the electron acceptor. The low yield indicates a lower sludge production when exploiting the potential of nitrate as electron acceptor.
If the assumption is made, that the mass of removed phosphate during the anoxic phases is proportional to the acetate taken up during anaerobic phases, a rough estimation of the actual COD removed in Feb'98 can be calculated. The removed mass of phosphate over a 2 hours period was calculated as indicated in Fig. 7.29 by linear regression of the outlet curves. The problem regarding the mixing phases was avoided by taking 2 hours in the middle of an anoxic phase. The ratio between the removed mass of phosphate in Feb'98, respectively Apr'98, was 1.22. If this coefficient is used for the COD removal (assuming higher COD removal in Feb'98), the observed yield coefficient is instead 0.23 gTS/gCOD. However, this correction is based on PAOs as the only growing/COD consuming organisms in the reactor.

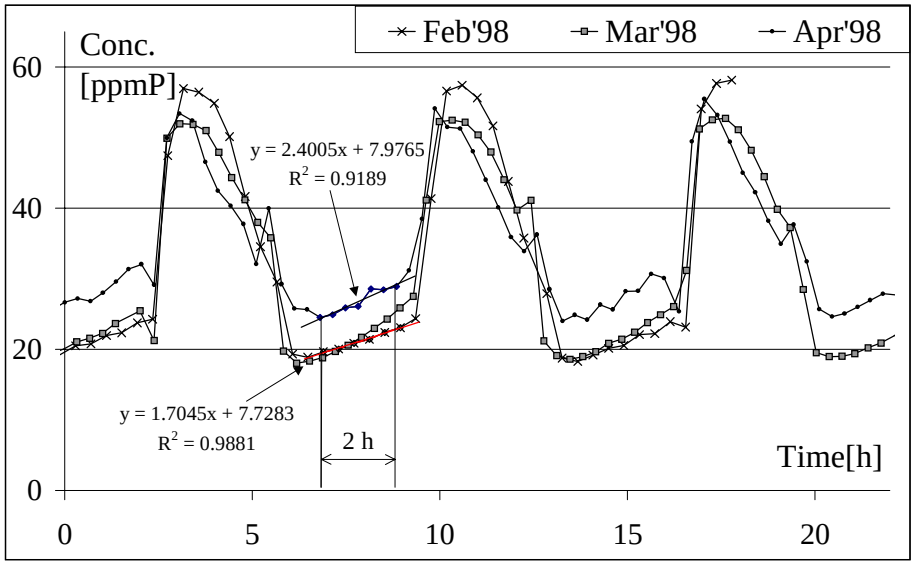

Figure 7.29. Continuous operation. Lower bio-P activity in Apr'98 compared to Feb'98. The tangents inserted during an anoxic phase were used to estimate the difference in removed mass of phosphate.

7.4 Key Results during PART A of The Study

1) Start-up of the biofilm system and induction of denitrifying bio-P activity took approximately 1 month after having fed the Biostyr system with activated sludge from an aerobic EBPR plant. The increased activity manifested itself in an exponential increase of the anaerobic release rate observed by batch tests.

2) Significant variation in the bio-P activity was observed over the 15 months period despite using well-defined operation and synthetic wastewater with acetate as the only carbon source. Highest activity levels appeared during the first months of operation. Microbiological investigations would have been valuable in order to investigate population shifts.

3) The biofilm could be considered quasi-steady-state over shorter time periods (weeks).

4) ½ and 0 order removal rate were verified by the use of anaerobic phosphate release and anoxic phosphate uptake batch tests. This indicated a zonated biofilm structure with molecular diffusion as the major transport mechanism of soluble compounds into the film.

5) The stoichiometry of phosphate released per COD taken up was low: 0.25 g P/g COD in Nov'97 and decreased during the study to a final value of 0.14 g P/g COD in Dec'98. However, this might be due to lower pH (regulated to 7) in the latest part of the study.

6) A relatively low coefficient of phosphate taken up per nitrate removed during anoxic batch tests was observed: 0.65 g P/g N = 0.058 (Nov'97-Jan'98). Low coefficients during both anaerobic and anoxic phases could indicate the presence of other bacteria with the capacity of storing COD under anaerobic conditions and degrading it via nitrate during anoxic periods, or a different phosphate metabolism of PAO biofilm bacteria compared to previously studied activated sludge cultures.

7) Some batch experiments with simultaneous presence of nitrate and acetate were made on the transition from anoxic to anaerobic phase. The results indicated no effect of the presence of nitrate on the phosphate release rate for high enough acetate concentrations to avoid COD limitations. However, more tests should be carried out in order to make a final conclusion.

8) The outlet curves stayed at a relatively constant concentration level between backwashes, which indicated an only partly penetrated biofilm. Backwash did not influence the concentration levels much. This indicated that the bacteria residing in the deeper layers were ready to perform immediately upon receiving

substrate, as also indicated via the series of batch test. Or backwash did not mainly remove the outer, active layer of the film, but rather big cloaks of thick biofilm as speculated based on direct visual observations during backwash.

9) The appearance of the biofilm shifted during the time of operation from a relatively smooth biofilm to a more thick and more heterogeneously looking film with black precipitates in the bottom. These black precipitates indicated an anaerobic bottom of the film and hence only partly penetration of nitrate during the anoxic phases.

10) The observed yield coefficient was estimated to 0.23-0.27 g TS/g COD from a mass balance of COD during continuous operation and measurement of the removed TS during backwash. This relatively low yield is in agreement with other investigations of anoxic yield (Kuba *et al.*, 1993) indicating a lower sludge production than for aerobic processes.

8. PART B - Results and Discussion

8.1 Induction of Denitrification

8.1.1 Origin of The Tested Biofilms

Two experimental runs were made. In the first run, a biofilm sample was taken from a semi full-scale sequencing batch biofilm pilot plant (17 m^3) in Ingolstadt, Germany (Arnz *et al.*, 2000ab). The plant had been operated for EBPR for 4 months (Arnz *et al*., 2000b). For the second start-up, a biofilm sample was taken from a bench-scale EBPR sequencing batch biofilm reactor that had been operated for 2-3 years (Gieseke *et al.*, 1999). Both of these SBBR plants were altered between anaerobic and aerobic conditions whereby initially only a fraction of the PAOs could denitrify. The biofilm samples were transferred to the lab-scale reactor with alternating anaerobic and anoxic conditions for investigation of the development of denitrifying bio-P-activity. The major differences between the bench-scale SBR and the lab-scale reactor are summarised in Table 8.1, both of these reactors were investigated with gene probes (FISH) during the second experimental run. Samples from the original SBBR reactor with oxygen as electron acceptor served as a reference of natural microbial fluctuations.

Table 8.1: Main characteristics of the two bio-P biofilm reactors analysed with FISH

	Denitrifying bio-P reactor	Aerobic bio-P reactor
Electron acceptor	NO_3-N	O_2
Carrier Volume	Lab-scale: 0.36 L	Bench-scale: 20 L
Phosphate in inlet	28 ppm P	~ 4-15 ppm P
Carbon source	Acetate (302 ppm COD)	Presettled wastewater (~100 ppm dissolved COD, ~200 ppm total COD)
Operation	Continuous flow	Sequencing batch
Carrier	Biolith (clay balls, 4-8 mm)	Biolith (clay balls, 4-8 mm)

8.1.2 Phosphate Removal Activity - The Continuous Operation

Figures 8.1 and 8.2 show the phosphate outlet concentrations during the two experimental runs. Each peak on the curve identifies one anaerobic phase. The area between the measured phosphate curve and the inlet concentration gives the amount of released phosphate during an anaerobic phase. The area between

the inlet concentration and the measured curve during the anoxic phases gives the amount of phosphate taken up by the bacteria (baseline of 28 ppm P, see Figs. 8.1 and 8.2).
Phosphate release during the anaerobic phases happened quickly, leading to a very high, but narrow peak. Phosphate uptake was slower, leading to a 'flat' valley. On the figures, it may be difficult to distinguish the separate cycles (first the curve goes up during the anaerobic phase, then down during the following anoxic, then up again during the next anaerobic phase etc.) due to the very compressed curve. However, the curve trend of a steep phosphate-release peak and a more flat phosphate-uptake valley is similar to the observations during PART A, see e.g. Fig. 7.18.

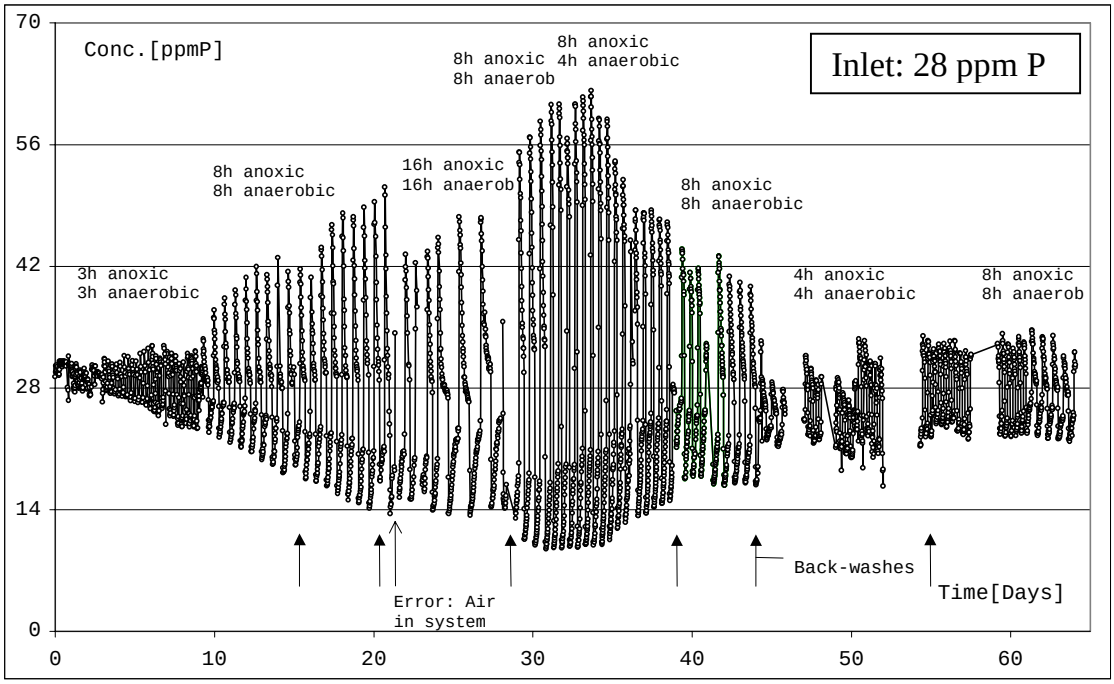

Figure 8.1. Phosphate outlet concentrations during the first experimental run. The original biofilm was taken from a semi-full-scale EBPR SBBR operated with oxygen as the electron acceptor. The inlet concentration was constant (28 ppm P). Each peak on the curve identifies one anaerobic phase, and each valley identifies one anoxic phase. It may be difficult to distinguish the separate cycles (first the curve goes up during the anaerobic phase, then down during the following anoxic, then up again during the next anaerobic phase etc.) on the figure due to the very compressed data-curve. The area between the outlet concentration curve and the inlet concentration (28 ppm P) during anaerobic phases equals the amount of phosphate released from the biofilm. The area between the inlet concentration (28 ppm P) and outlet concentration curve during anoxic phases equals the amount of phosphate taken up by the biofilm. Anaerobic and anoxic phase lengths were changed during the period as indicated on the figure. Maximum phosphate removal activity occurred around day 32.

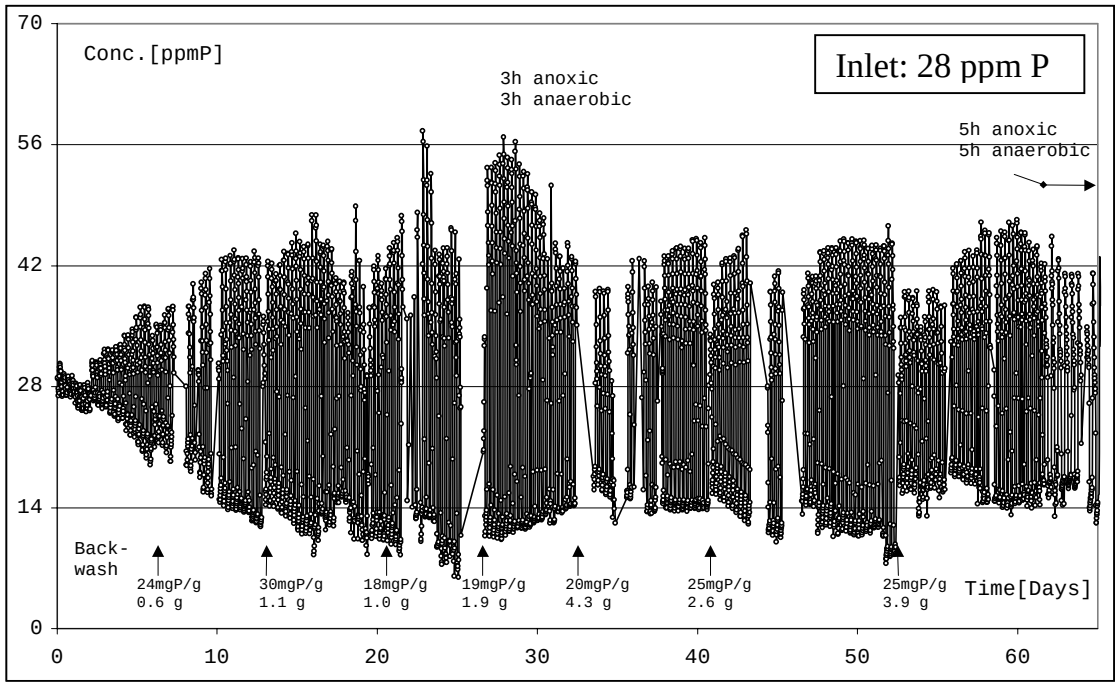

Figure 8.2. Phosphate outlet concentrations during the second experimental run. The original biofilm was taken from a pilot-scale EBPR SBBR operated with oxygen as the electron acceptor. The inlet concentration was constant (28 ppm P). Each peak on the curve identifies one anaerobic phase, and each valley identifies one anoxic phase (see text of Fig. 8.1). Anaerobic and anoxic phase lengths were not changed during the period, 3 hours each (4 cycles/day). Maximum phosphate removal activity occurred around day 28. The numbers by the arrows show the phosphate content and amount of detached biomass during the respective backwashes.

For the first run, the phase lengths were changed about every other week as indicated in Fig. 8.1. The activity declined after a change of the anaerobic phase length after 32 days, and this trend was apparently non-reversible despite returning to the previous cycle configuration. The reason for this deterioration was speculated to be a shift in the microbial population caused by the changed phase length, perhaps in favour of so-called glycogen-accumulating organisms. A new experimental run was started using a fresh inoculum from the aerobic bench-scale SBBR. This time regular biomass samples were collected and investigated with FISH. During the first 60 days the phase lengths were kept constant at 3 hours. However, in this run a build-up similar to the first run was seen during the first 28 days followed by a deterioration almost identical to the first run. In this case, the operating conditions had not been changed and hence the deterioration could not be explained in the way first assumed for the previous run. Furthermore, the loss of activity in the first run by the end of the period may have been due to a very rough backwash on day 45 where a lot of biomass was lost. A similar but less pronounced effect of a backwash is seen for the second run on day 52. For days 61 to 90, five-hour phase lengths were used

and for days 91 to 120 eight-hour phase lengths (Fig. 8.3). The amplitude of the phosphate outlet curve increased a little by the use of longer phase lengths, and the activity was stable.

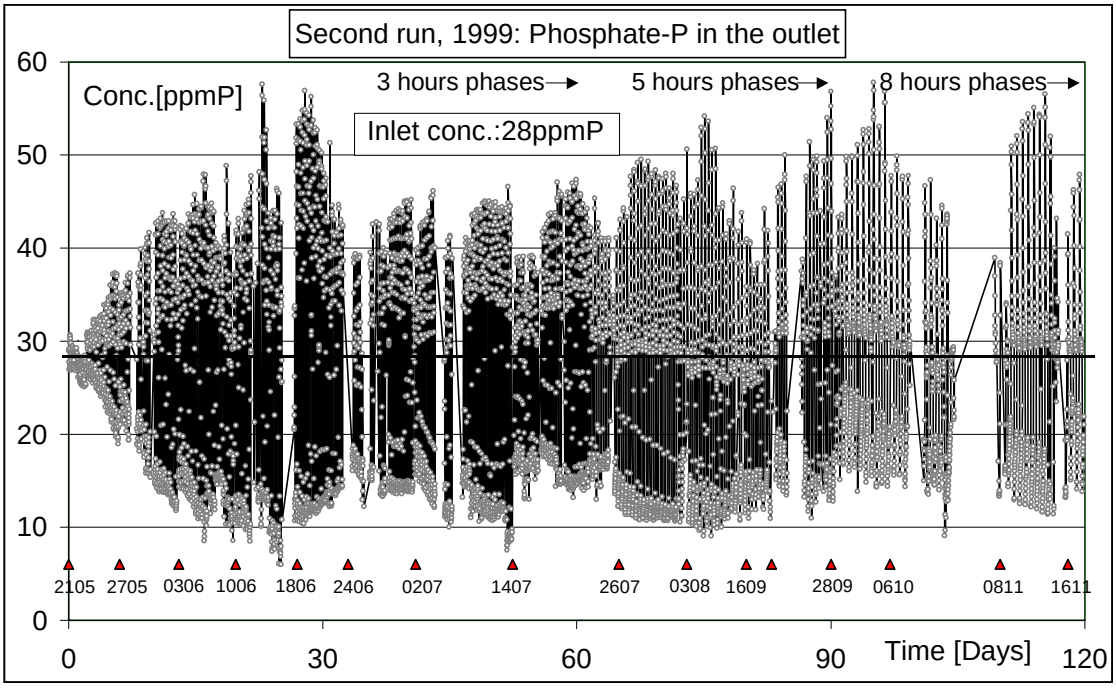

Figure 8.3. The second run, May-Nov'99. Days 0-65 are also shown in Fig. 8.2. The arrows and dates indicate backwash. The reactor was stored in the refrigerator twice: 0308-0909 and 1310-0211.

8.1.3 Effect of Backwash on The Outlet Concentrations

As it seen from the figures above, the amplitude of the phosphate outlet curve increased in both runs during the first month of operation. This is in agreement with the hypothesis of a fully penetrated biofilm/no substrate limitation. Increased amounts of phosphate was taken up for each cycle due to a growing biofilm or enrichment of denitrifying PAOs. As a function of time, this trend changed and a more constant level of the phosphate outlet curve was seen – at least for the second run, where the activity remained – indicating that substrate limitation influenced in the biofilm. A combined effect of biofilm thickness and increased density of the denitrifying PAOs in the biofilm is likely responsible for the development of diffusion limitation.

The typical picture around backwash was as hypothesised in chapter 6.3 that a decreased activity followed backwash due to a reduction in the amount of active biomass. A close-up of Fig. 8.2/8.3 is given in Fig. 8.4 to illustrate the phenomena of decreasing activity after backwash. (a) shows a backwash in the

very beginning of the run, Day 6, and (b) after the concentration levels were stabilised, Day 44. The activity decreased after backwash in both cases. Here it is assumed that the biofilm was fully penetrated during the start-up phase (Day 6) and partly penetrated after a stable outlet level was reached (Day 44).

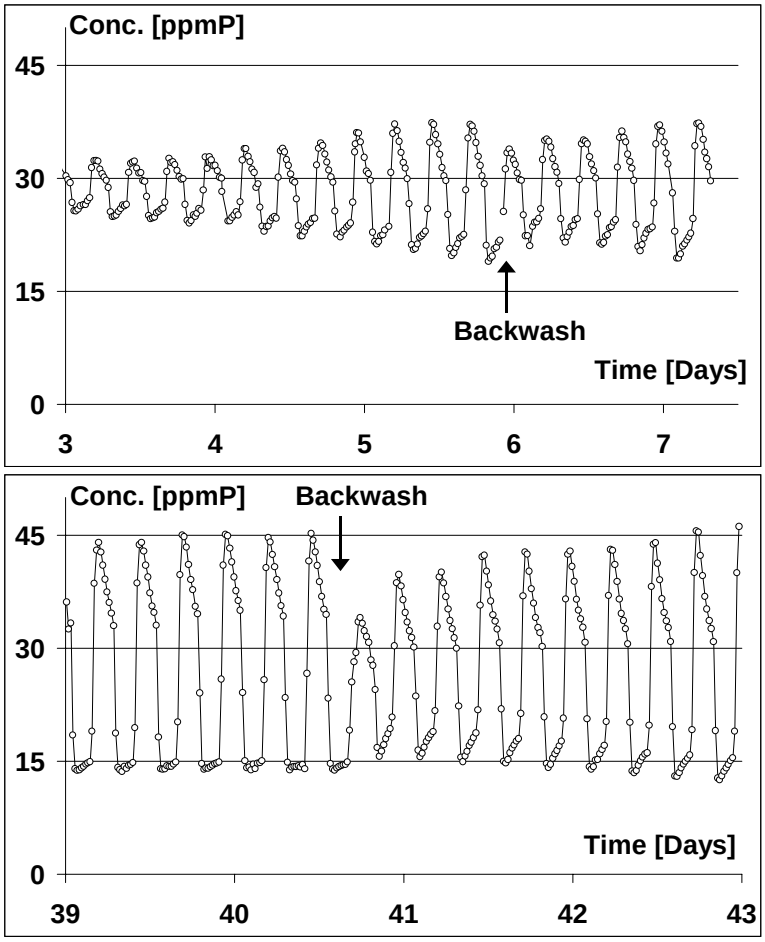

Figure 8.4. The activity decreased following backwash, both during the up-start phase and after a stabilisation of the outlet concentration level had occured. This agrees with the hypothesis of decreasing activity following backwash for both a partly and a fully penetrated biofilm due to a reduction of the active biomass.

8.1.4 Mass Balances

Due to the constant inlet concentration of phosphate throughout a cycle, the mass balance of phosphate was simpler than in PART A. Frequent inlet samples were collected during especially the first run to keep precise track of the added amount of phosphate to the system. Figure 8.5a illustrates the calculated amounts of phosphate released and taken up during 58 cycles of the first run. The equivalent outlet concentrations are found as Day 10-42 in Fig. 8.1. The

same data are shown on Fig. 8.5b where the phosphate taken up is plotted against the released amount of P. It can be seen, that a relatively higher amount of phosphate (15%) was taken up during the first 20 cycles compared to later in the experimental period (5%). This shift is likely due to a situation where parts of the biofilm is only partly penetrated with phosphate (leading to less net P removal). However, the points became more scattered as a function of time. The scatter could be caused by a more heterogeneous structure/thickness of the film, where part of it is fully penetrated and other parts only partly penetrated.

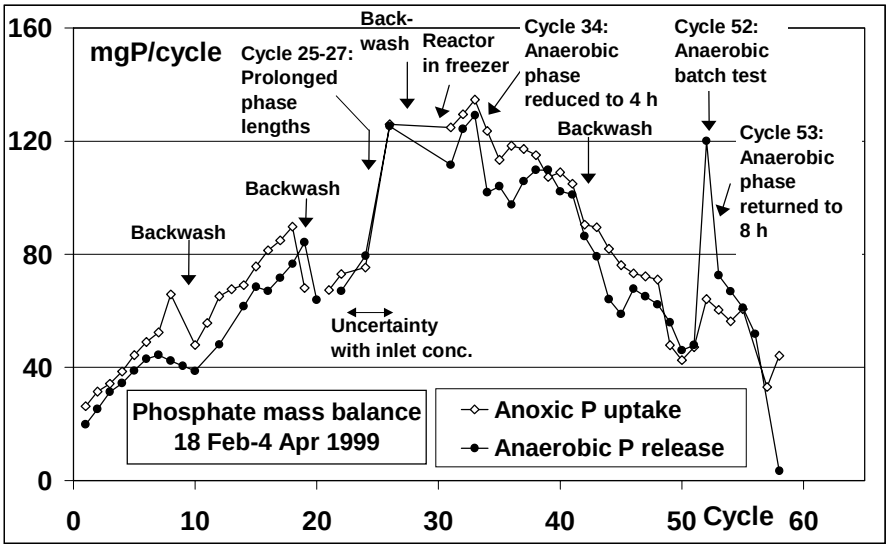

Figure 8.5a: Amounts of phosphate taken up and released during 58 cycles of the first experimental run, Day 10-42.

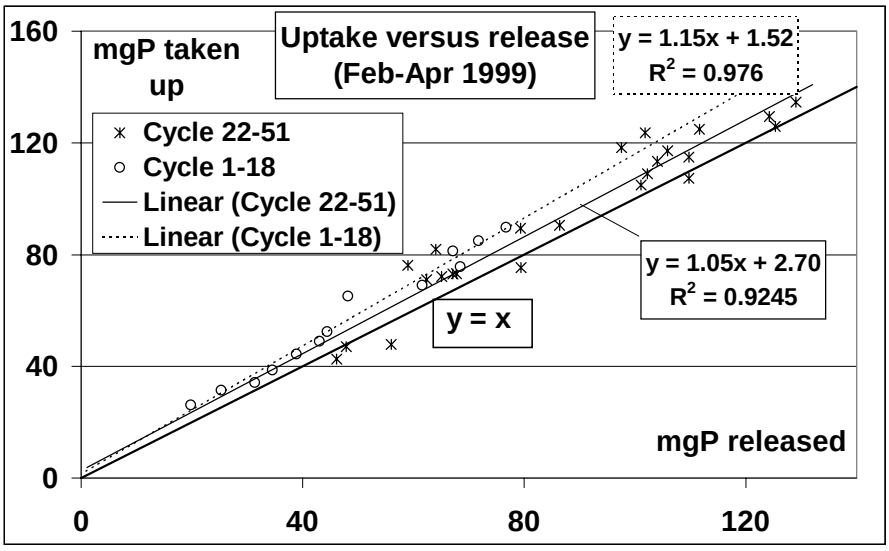

Figure 8.5b: The amount of phosphate taken up relative to the phosphate released in the preceding anaerobic phase. First run during PART B.

A mass balance of nitrate was made around the day of changing the anaerobic phase length from 8 to 4 hours in the first run (Day 29-34), the anoxic phase was kept at 8 hours, Fig. 8.6. Immediately, a significant increase in the outlet concentration of nitrate was noticed upon the reduced anaerobic phase length. The mass balance revealed the stoichiometry of phosphorus and nitrate for the three cycles before the change: 0.44 g P/g N. For the 3 cycles after the change (day 32-33.5), the stoichiometric coefficient was 0.57 g P/g N. Hence relatively more P was taken up per g of nitrate removed after the change. During PART A, a stoichiometric coefficient of 0.51-0.75 g P/g N was determined by anoxic batch tests. The changed coefficient could indicate that the reduced anaerobic phase length had a positive effect on the competitive advantage of the PAOs. If phosphate is the limiting substrate for PAOs, deeper penetration of nitrate during the anoxic phase is expected and of acetate during the anaerobic phases. Assume that competing organisms live as 'scavengers' in the depth of the film, and that these store acetate during anaerobic conditions without the use of phosphate. During anoxic phases, they degrade the stored acetate via nitrate (in principle a denitrifying GAO organism). In this case, it would not be surprising to observe a changed coefficient after reducing the anaerobic phase length – less time for these bacteria to store acetate and hence less consumed nitrate.

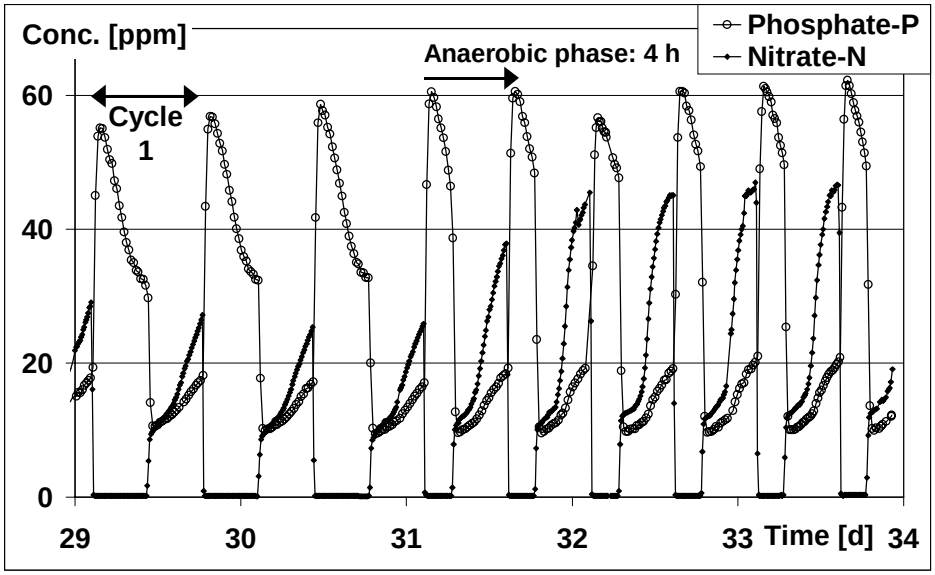

Mass Balance Cycle	1-3	4-5	6-8
gP taken up/gP released	1.07	1.15	1.12
Stdev.	0.04	0.09	0.08
gP/gN	0.44	0.52	0.57
Stdev.	0.01	0.03	0.01

Phosphate inlet = 29 ppmP. Anoxic nitrate inlet = 51 ppmN

Figure 8.6. Outlet concentrations of phosphate and nitrate before and after changing the anaerobic phase length from 8 to 4 hours. Mass balance of nitrate and phosphate in the table.

8.1.5 Phosphate Content of The Sludge

The phosphate content of the sludge removed after an anoxic phase by backwash was determined twice during the first run. After 10 days of operation with 8 hours phase lengths 40 mg P $(gTS)^{-1}$ was measured, Day 20. By the end of the experimental period after deterioration of the bio-P activity (and 4 hours phases), the content was 20 mg P $(gTS)^{-1}$, Day 56, which is not much more than for non-bio-P sludge (~15 mg P $(gTS)^{-1}$). For the second run, the phosphate content of the dried biomass was regularly measured. This varied in the range 18-31 mg P/g TS with an average of 24 ± 4 mg P/g TS (2.4 %). This is very low compared to what is cited in the literature for activated bio-P sludge (40-160 mg P/g TS). The reason for the low content is hypothesised to be diffusion limitation in the biofilm as discussed in chapter 6.3. No correlation could be found between the amount of removed biomass and the measured phosphate content, Fig 8.7. This indicates that backwash did not remove the top layers of the film (which would contain most phosphate), but more likely cohesive parts of the film (i.e sloughing). When investigating the biofilm from the Biolith® before backwash with a microscope (see below) it appeared that the biofilm was made up of two fractions: big "clumps" extending from a more smooth film covering the surface of the carriers. The clump-like structure could also be observed from looking at the reactor directly, Fig. 8.8. These clumps would possibly be most susceptible to detachment. By the end of an anaerobic phase, 1.2 % P was measured in the sludge.

Another explanation of the low phosphate contents would be the dominance of non-PAOs. The low stoichiometric coefficients determined also during PART A indicate the use of other metabolisms than the one based on poly-phosphate. According to the "survival of the fittest" theory, it appears likely that bacteria capable of storing COD without the use of phosphate would survive/invade a biofilm, which is only partly penetrated with phosphate and have a higher penetration of COD during the anaerobic phase and of nitrate during the anoxic phases. It can be speculated whether these bacteria are different *groups* or simply the *same* bacteria that can shift metabolism between the periods where phosphate is available or not? The fact that the system operated in a stable fashion over longer time periods with consistent P release and uptake could be taken as an indication of this. If other bacteria were in competition with the PAOs, this competition would most likely fall out in favour of one of the two due to different growth rates - ? Same bacteria shifting metabolism could also explain, why the PAOs in the depth of the film appear to stay active as indicated by the batch tests during PART A. The fact that the stoichiometric coefficient of COD uptake to phosphate release decreased over time during the experimental period of PART A could be due to an increasing biofilm thickness (as observed by visual evaluation). A relatively higher fraction of the bacteria would hence be employing the non-poly-P metabolism due to a relatively lower phosphate penetration depth of the biofilm.

The phosphate content of the aerobic SBR sludge varied in the range 20-28 mg P/g TS over the 2 month sampling period with an average of 24 ± 3 mg P/g TS (backwash after an aerobic phase once a week). However, the situation for this biofilm was different to the lab-scale continuous reactor, since it was operated in a SBR mode, and the phosphate concentration in the bulk water following an aerobic phase was very low (~1-2 mg P/l). Therefore, it was not possible for the bacteria to take up more phosphate – in this case, a limitation in the available mass of P was causing the low phosphate levels of the biomass, not diffusion limitation. This hypothesis was tested by increasing the phosphate content of the inlet from the normal ~5 ppm P to ~15 ppm P by external phosphate addition (KH_2PO_4) during 2 weeks of operation. The measured phosphate content of the sludge during these 2 weeks was consistently higher than normal with an average of 35 ± 2 mg P/g TS.

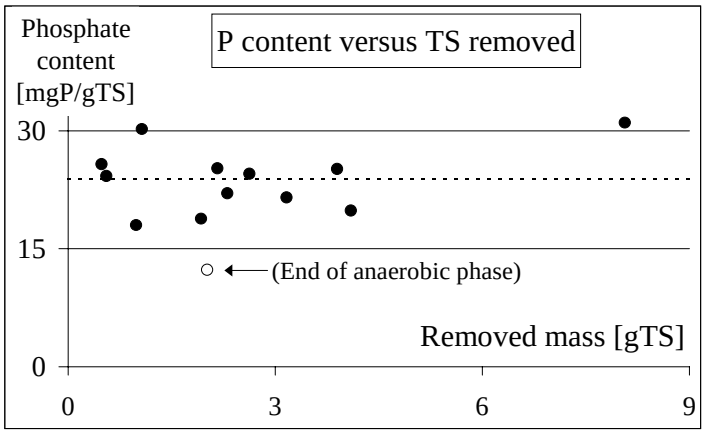

Figure 8.7. Relationship between phosphate content of the sludge and the total removed mass of sludge during backwash after anoxic phases - no correlation. May-Nov 1999.

Figure 8.8. Appearance of the biofilm on the Biolith® carriers (Jul'99). A clump-like, heterogeneous biofilm thickness is evident.

8.2 Microbiological Investigations

8.2.1 Microbiological Materials and Methods

Sampling and cell fixation: Samples were collected once every week from the reactors. The biomass that detached during backwash after an aerobic or anoxic phase was used for this purpose. Fixation was done with ethanol or

paraformaldehyde (PFA) according to the protocols described by Amann (1995). The fixed samples were stored at –20 ^{o}C.

Phosphate measurements: Phosphate was measured on-line in the lab-scale setup according to Standard Methods (ASTM D 515-68 non referee method B). Non-fixed biomass was kept aerobic, centrifuged and the pellets placed at 105 ^{o}C over night before measuring the phosphate content of the dry mass. The phosphate content of the dry mass was measured according to the German industrial norm DIN 38405-D11.

In situ Hybridization and Oligonucleotide probes: Fixed biofilm samples were immobilized on glass slides by air drying and dehydrated for 3 min in 50, 80 and 100 % (v/v) ethanol, respectively. After the dehydration step, the ethanol-fixed samples were treated by adding lysozyme (100000 U/mg) according to Beimfohr *et al.* (1993). These pre-treated samples were subjected to probes detecting the gram-positive bacteria with high G+C DNA content (HGC69a, lysozyme: 20 mg/ml, 15 min), the nocardioform actinomycetes (MNP1, lysozyme: 10 mg/ml, 20 min), and *Microlunatus phosphovorus* (MP2, lysozyme: 20 mg/ml, 30 min). The hybridization procedure was carried out as described by Amann (1995). The stringency in the hybridization buffer and washing buffer was probe dependent, and was adjusted by changing the formamide or NaCl concentration, respectively (Table 8.2).

Table 8.2: Oligonucleotide probes used for in situ hybridization.

Probe	Specificy	Formamide [%]	NaCl [mM]	Reference
EUB338	*Bacteria*	0-50	10-900	Amann et al., 1990b
Alf1b	Alpha subclass of the *Proteobacteria*	20	225	Manz et al., 1992
Bet42a	Beta subclass of the *Proteobacteria*	35	80	Manz et al., 1992
GAM42a	Gamma subclass of the *Proteobacteria*	35	80	Manz et al., 1992
CF319	*Cytophaga-Flavobacteria* group	35	80	Wagner et al., 1994a
RHC438	*Rhodocyclus*-like cluster	30	100	Hesselmann et al., 1999
RHX851	*Rhodocyclus*-like clone	30	100	Hesselmann et al., 1999
ACA23a	*Acinetobacter spp.*	35	80	Wagner et al., 1994a
HGC69a	Gram-positive bacteria with high DNA G+C content (GPBHGC)	20	225	Roller et al., 1994
MNP1	Nocardioforme actinomycetes	50	10	Schuppler et al.,1998
MP2	*Microlunatus phosphovorus*	10	490	Kawaharasaki et al., 1999

The ethanol-fixed samples frequently detached during the washing procedure, therefore a modified washing step was applied for these samples: Warm (48 °C) washing buffer was gently added via a pipette to cover the sample on the slide surface, and the slide was then incubated in a moisture chamber for 15 min at 48 °C. Afterwards the slide was rinsed with washing buffer, new washing buffer was added to the slide followed by another 15 min of incubation. This step was repeated twice. Care was taken that fluids from different wells of the slide (6 wells for individual samples on each slide) did not mix during the modified washing step. It was observed that mixing during the washing step of fluids from wells hybridised with the non-stringent EUB338 probe could result in binding of the washed off EUB probe to samples of other wells.

Table 8.2 presents an overview of the rRNA-targeted probes used. The probes were purchased from MWG Biotech (Ebersberg, Germany) and labelled with the sulfoindocyanine dyes Cy3 or Cy5. Due to only a single mismatch between the BET42a and GAM42a probes, the unlabelled probes (unlabelled GAM42a to labelled BET42a and vice versa) were added to prevent binding to non-target cells.

Staining with fluorescent dyes: For visualisation of the biofilm thickness, staining with Flourescein 5-isothiocyanate (FITC) was applied according to Schmid *et al.* (2000). FITC binds to amino groups whereby both cells and extracellular polymeric substances (EPS) of the biofilm are stained. A 0.01 % solution of FITC was used. The carrier was placed in this solution for 15 min and washed by immersing the carrier into a phosphate buffer (PBS) and transferring it to clean buffer 3 times.

Confocal laser scanning microscopy (CLSM): All confocal images were recorded using a 410 CLSM (Zeiss, Germany) including an Axiovert 135 microscope equipped with 100 x/1.3, 40 x/1.3 (both oil immersion type) and 10 x/0.3 plan neofluor objectives. The two internal helium-neon lasers (543 nm and 633 nm) were used as the excitation source for the Cy3- (at 543 nm) or Cy5- (at 633 nm) labelled oligonucleotide probes. The fluorescence of the FITC dye was detected with an external argon laser (488 nm). Image processing was carried out with the Zeiss software package. After in situ hybridization with rRNA-targeted oligonucleotide probes, an anti-fading agent AF1 solution (Citifluor Ltd., London, United Kingdom) was distributed onto the slides before analysis with the CLSM.

The FITC-stained carrier particles were cut into halves immersed into a phosphate buffer solution (PBS) and the peripheral biofilm along the diameter was analysed with the inverse CLSM, Fig. 8.9.

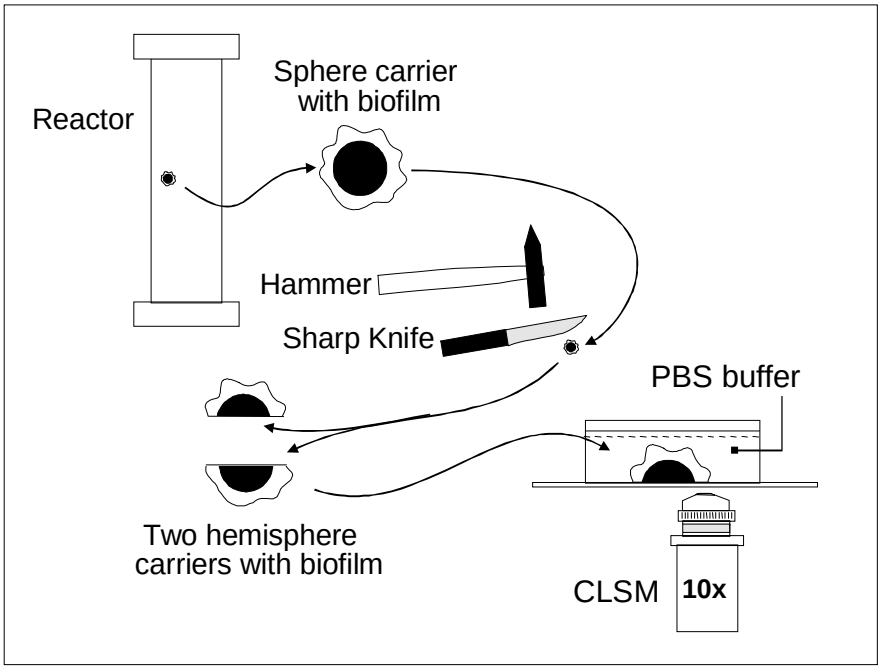

Figure 8.9. The biofilm thickness was investigated by removing a biofilm-coated carrier particle from the reactor, cutting this in two halves and investigating the perimeter of the hemisphere carriers with an inverse confocal laser scanning microscope.

8.2.2 Biofilm Thickness

An example of the appearance of carrier particles with the denitrifying biofilm before and after backwash are seen in Fig. 8.10.

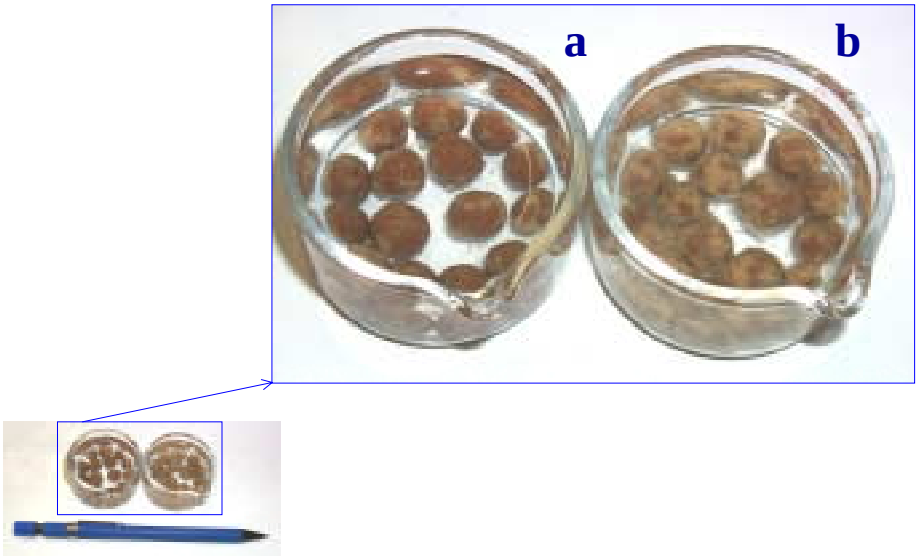

Figure 8.10. Appearance of the Biolith® carriers with the denitrifying biofilm after (a) and before (b) backwash.

The carrier particles with the aerobic biofilm had almost no biofilm on them that was visible to the naked eye neither before nor after backwash.

The denitrifying biofilm was very heterogeneous and it was not possible to determine an average thickness. For one spot sample before backwash, the thickness varied from 67 to 1096 μm along the carrier diameter, mainly above 400 μm, Fig. 8.11 (left). After backwash, the thickness varied from 0 to 469 μm, mainly above 100 μm, Fig. 8.11 (right). Different carriers were used for investigations of the biofilm thickness before and after, since the carrier particles could not be reused after having been cut in two halves. It appeared that the biomass evolved in a clump-like pattern with big clumps of biomass extending from a thinner smooth biofilm close to the carrier (Fig. 8.11 left, number 3 from the top). Some channels were seen in the biofilm, but mostly the biofilm appeared very dense with big, rounded biomass structures/colonies merging together.

The aerobic biofilm was thinner and with a more homogeneous thickness, Fig. 8.12. Before backwash, the typical thickness was 100-200 μm, and after 0-50 μm. The aerobic biofilm community was inhabited by many protozoans, Fig. 8.12 (right). Most of the protozoans apparently stayed attached during backwash, whereas bacterial cells between them detached. The stalks of e.g. ciliates were in this way more evident after backwash. No protozoans were seen in the denitrifying biofilm, which was to be expected due to the lack of oxygen, since most protozoans are aerobic.

The differences in the biofilm thickness and appearance may be attributed to several factors. First of all, the scale of the reactors makes a significant difference in the backwash mode. For the aerobic bench-scale, a more homogeneous and thorough backwash of the filter was applied by the use of a vigorous action by combined water flow and aeration, whereas manual stirring of the carriers was used for the lab-scale reactor.

Another difference was the microbial community, which was more diverse in the bench-scale reactor fed with wastewater and operated with oxygen. The substrate composition with higher COD load in the denitrifying reactor might be the reason for the thicker biofilm, but also the use of aeration with bubbles in the aerobic reactor might have caused a continuous detachment by erosion/abrasion from this biofilm. Grazing by protozoans in the aerobic biofilm also play a role. Different shear stress in the two reactors is another factor.
In the following when mentioning 'flocs', it is referring to the observations of the *detached* biomass, but it has to be borne in mind that these flocs originated from a biofilm matrix where they made up a cohesive structure.

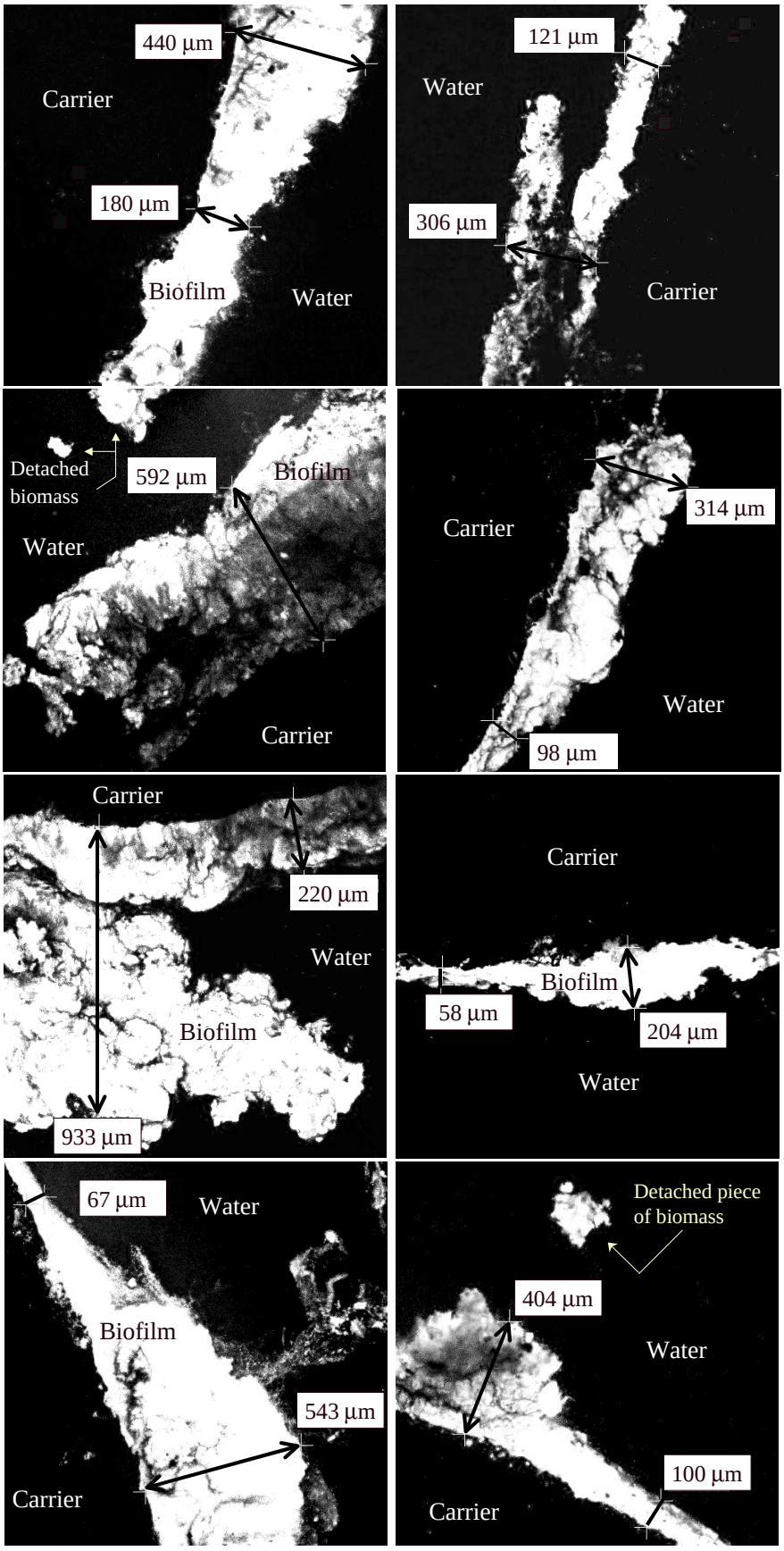

Figure 8.11. The denitrifying biofilm thickness before (left) and after (right) backwash.

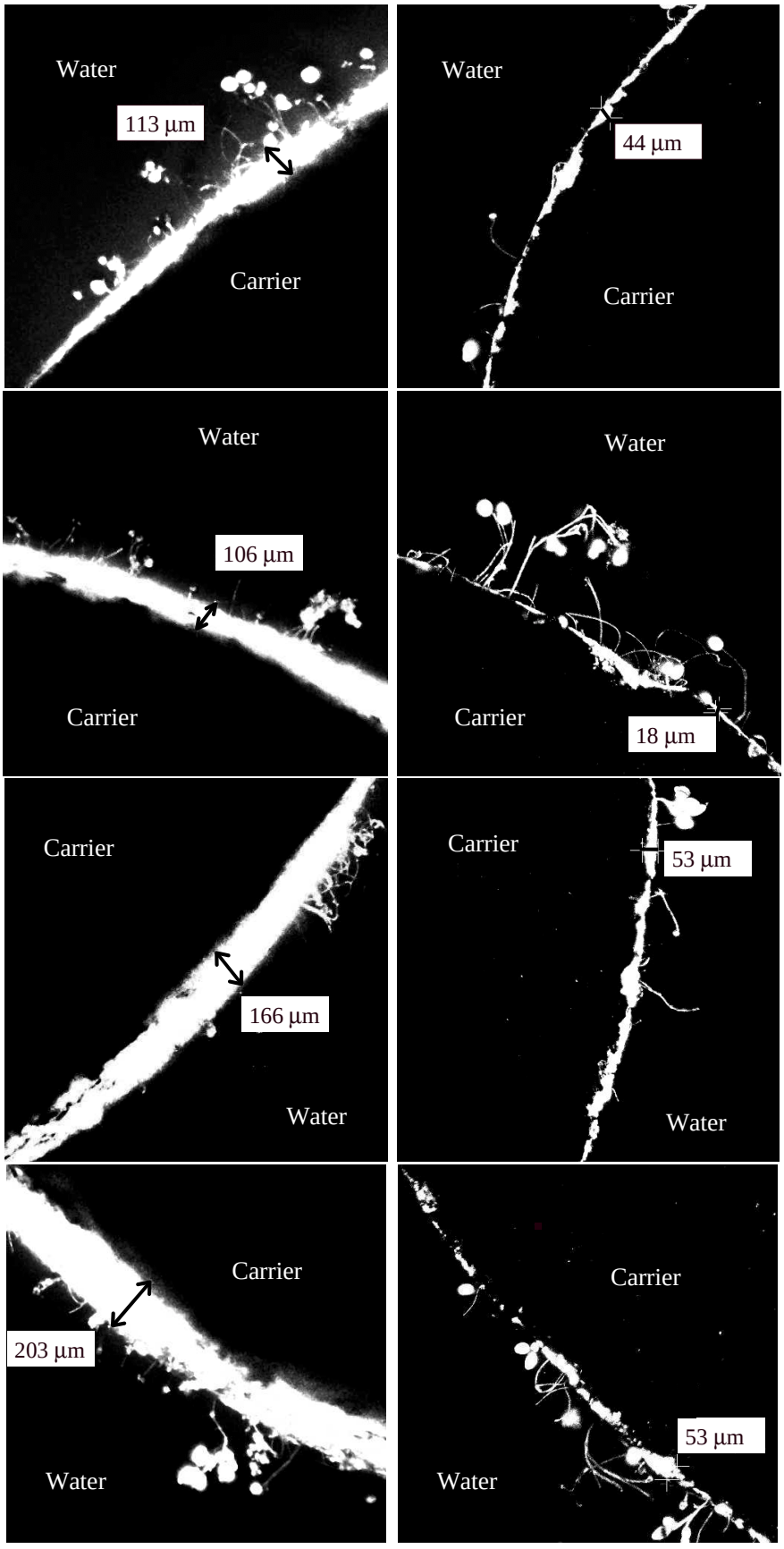

Figure 8.12. The aerobic biofilm thickness before (left) and after (right) backwash.

8.1.3 General Observations of The Biomass

Table 8.3 summarises some characteristics of the biomass samples from the two reactors.

Table 8.3. Observations of the biomass samples from the two investigated reactors.

Denitrifying bio-P biomass (Acetate)	**Aerobic bio-P biomass (Wastewater)**
Most changes in the microbial population were observed within the first 2 weeks of operation	No major changes in the population could be detected with gene probes or normal microscopy during the 2 month sampling period
Low autoflourescence	High autoflourescence
Almost no dark particles in transmission images	Dark particles in transmission images
More filaments appeared as a function of time.	Very few filamenteous bacteria
Low cell diversity	High cell diversity
Very slimy, light brown biomass	Non-slimy, dark brown biomass
Ethanol-fixed samples easily detached during the FISH washing step.	

From a direct visual look with the naked eye, major differences between the two sludges were their colour and slime content. The aerobic sludge was much darker brown than the denitrifying sludge (light brown). Much more slime (EPS) was associated with the denitrifying sludge than with the aerobic. From light microscopy, differences between the sludges were also visible. The aerobic sludge contained particles that appeared as black spots in transmission images (Fig. 8.13, Day 0), possibly particles (inorganic?) added via the wastewater feed. More filaments developed over time in the denitrifying biofilm, but otherwise, the biomass from this reactor looked less diverse.

8.1.4 Gene Probe Analysis

Major shifts in the microbial population were observed with FISH in the biofilm during the first two weeks following the transfer from the aerobic bench-scale SBR to the lab-scale reactor. Two weeks was also what was indicated by the outlet concentrations of phosphate as the time required for acclimatisation to nitrate as the electron acceptor. No significant shifts in the population could be verified with FISH around the time of the activity decline after 1 month of operation. No obvious changes in the aerobic sludge could be observed with FISH or normal microscopy during the sampling period. This indicated a stable microbial population in the aerobic SBBR and hence that the shifts observed in the denitrifying lab-scale reactor were significant and caused by the changed environment. Table 8.4 gives an overview of the results of the gene probe

analysis. In the following, Day 0 is the day of transferring the aerobic EBPR biofilm from the SBR reactor to the second run of the anoxic EBPR lab-scale system. Almost all cells were detectable with the *Bacteria* probe (EUB338). The good coverage with the EUB338 probe was verified by comparing with normal transmission images. Examples from the denitrifying biofilm are given in Fig. 8.13. Over time filaments became more numerous and appeared to serve as connectors between biomass colonies (the Day 73 image). However, the most dominant bacteria morphology throughout the period was a characteristic, short, oval rod (the images from Day 13 and 80).

Table 8.4. Main results of the FISH analysis. • : Very few cells. • • • • • : Most cells. As indicated by comparison with the EUB338 probe and a transmission image. The major shift happened within the first two weeks after transfer from the aerobic to the denitrifying setup. Bacteria belonging to the alpha subclass of *Proteobacteria* disappeared and characteristic round beta *Proteobacteria* clusters were replaced by single short rods identified as beta *Proteobacteria*. Characteristic small clusters of Gram positive bacteria with a high G+C DNA content (GPBHGC) decreased in numbers and were gradually replaced by filamentous GPBHGC.

Gene probe	**Denitrifying bio-P reactor**	**Aerobic bio-P reactor**
EUB338	• • • • •	• • • • •
ALF1b	•	• • •
BET42a	• • • •	• • •
GAM42a	• •	• • •
HGC69a	• • (small clusters → filaments)	• • •
ACA23a	•	•
MNP1	•	•
MP2	•	•
CF319	• •	•
RHC438	• • → •	• •
RHX851	•	•

There were significant differences in the properties of the two investigated sludges regarding the use of FISH. When investigating the denitrifying sludge, a lot of thick and very dense bacteria flocs were observed. It was difficult to obtain sharp images from these flocs and single cells were hard to distinguish. The best images were obtained by looking at less dense bacteria areas e.g. by the edge of the dense areas or after homogenisation of the sample. The samples from the aerobic bench-scale reactor were easier to treat and investigate. These had a lower slime content, which made the preparation of sample easier (easier to take out biomass with a pipette tip etc.). Also, the samples did not easily

detach from the microscopic slides during the FISH washing step as discussed for the samples from the denitrifying reactor before the modified, gentle washing method was used. The signals obtained with FISH were generally sharper than for the denitrifying sludge. Perhaps the high amount of EPS/slime in the denitrifying sludge caused the 'blurring' of the otherwise strong signals.
The bacterial biofilm community from the aerobic bio-P reactor consisted of a high number of alpha, beta, gamma *Proteobacteria* and gram-positive bacteria with a high DNA G+C content (GPBHGC), which were found in similar frequency. Many characteristic round clusters belonging to the beta subclass of *Proteobacteria* were found in the aerobic biofilm. These clusters were often surrounded by gamma *Proteobacteria* clusters that appeared to "fill in" space between the beta *Proteobacteria* cell clusters (Fig. 8.14).

Biofilm samples from the aerobic bench-scale reactor were previously investigated by Gieseke *et al.* (1999). They also observed these characteristic beta *Proteobacteria* clusters and these cells gave positive signals with a probe for *Nitrospira* (a nitrifying bacterium). The beta and gamma *Proteobacteria* clusters occurring in the aerobic biofilm became less abundant within the first few weeks of operation in the denitrifying lab-scale reactor and were replaced by many short oval rods belonging to the beta *Proteobacteria* giving rise to a cohesive layer (Fig. 8.15). Within this layer single gamma *Proteobacteria* cells were relatively evenly distributed, but at much lower abundance than the beta *Proteobacteria*.

Almost no bacteria belonging to the alpha subclass of *Proteobacteria* remained in the denitrifying biofilm after 2 weeks of start-up (Fig. 8.16) and they stayed absent.

Bacteria belonging to the C*ytophaga-Flavobacteria* group occurred only in a very small numbers in the aerobic biofilm and were more frequently found in the denitrifying biofilm. An interesting phenomenon was observed over the experimental period for the GPBHGC in the denitrifying biofilm. The small GPBHGC clusters in the beginning were during the 4 months experimental period gradually completely replaced by filamentous GPBHGC (Fig. 8.17). These filaments were situated inside flocs and looked like a "floc-skeleton". Other filaments were extending from the flocs and were detected with the BET42a probe (the ones also detected with the EUB338 probe, Fig. 8.13, Day 73). More filaments appeared as a function of time.

Both biofilms (aerobic and denitrifying) contained only small amounts of *Acinetobacter* spp. and bacteria identified as nocardiaform actinomycetes. Also the *Rhodocyclus*-like group (probe RHC438) did not seem to play a dominant role in the two investigated populations and not the recently by Hesselmann *et al.*, 1999, characterized *Rhodocyclus* like clone (probe RHX851).

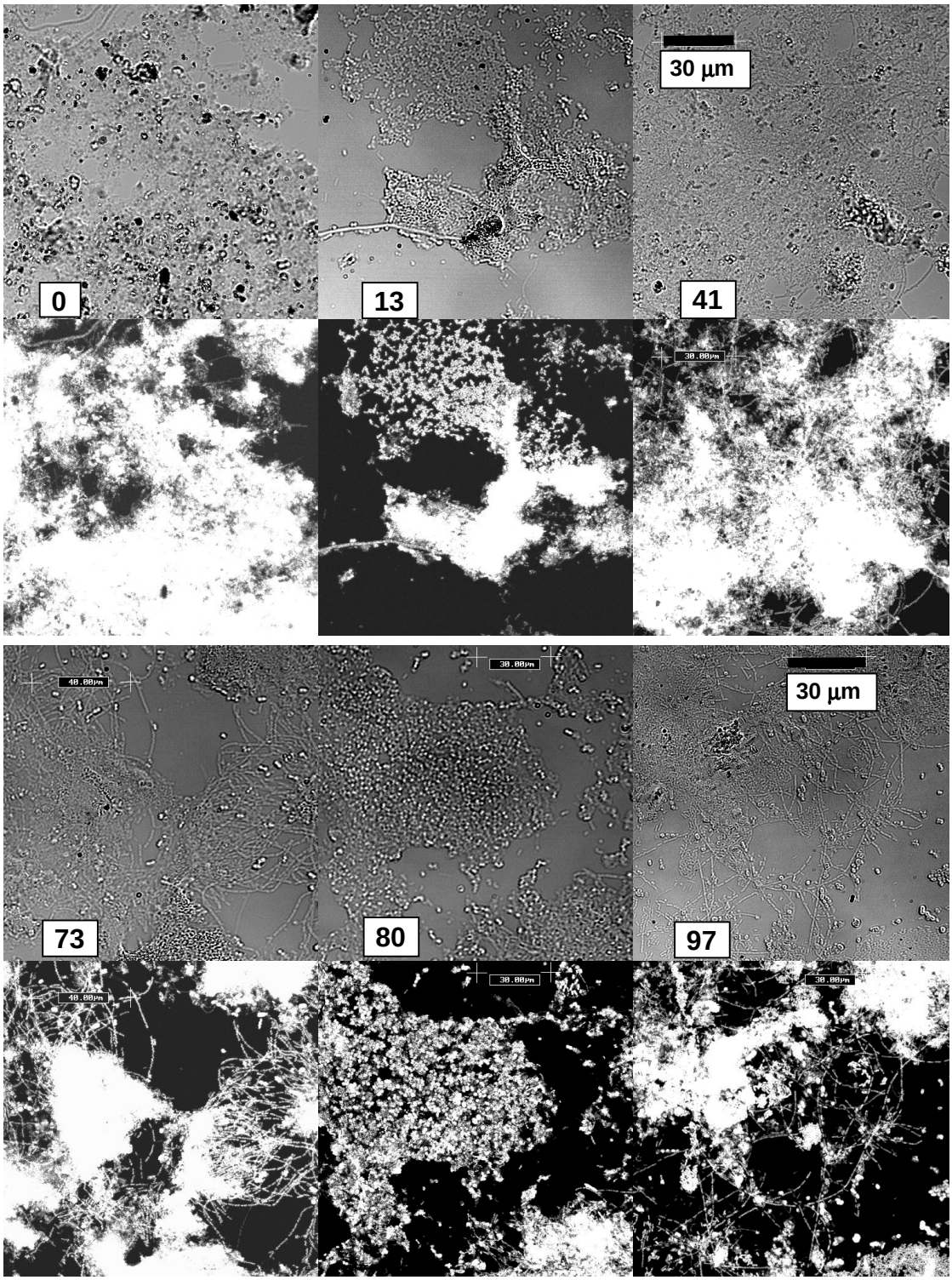

Figure 8.13. Analysis of the denitrifying sludge with the EUB338 probe. Transmission images are included above the EUB image to illustrate the good coverage of most cells with the probe. The number refer to the day after transfer of the aerobic biofilm to the denitrifying lab-scale reactor. The 30 µm bar apply to all images. The development of filaments with time is clear from the Day 73 and 97 images. The most typical morphology of the sludge was however a short, oval rod as seen especially in the images of Day 13 and 80.

a)

b)

20 μm

c)

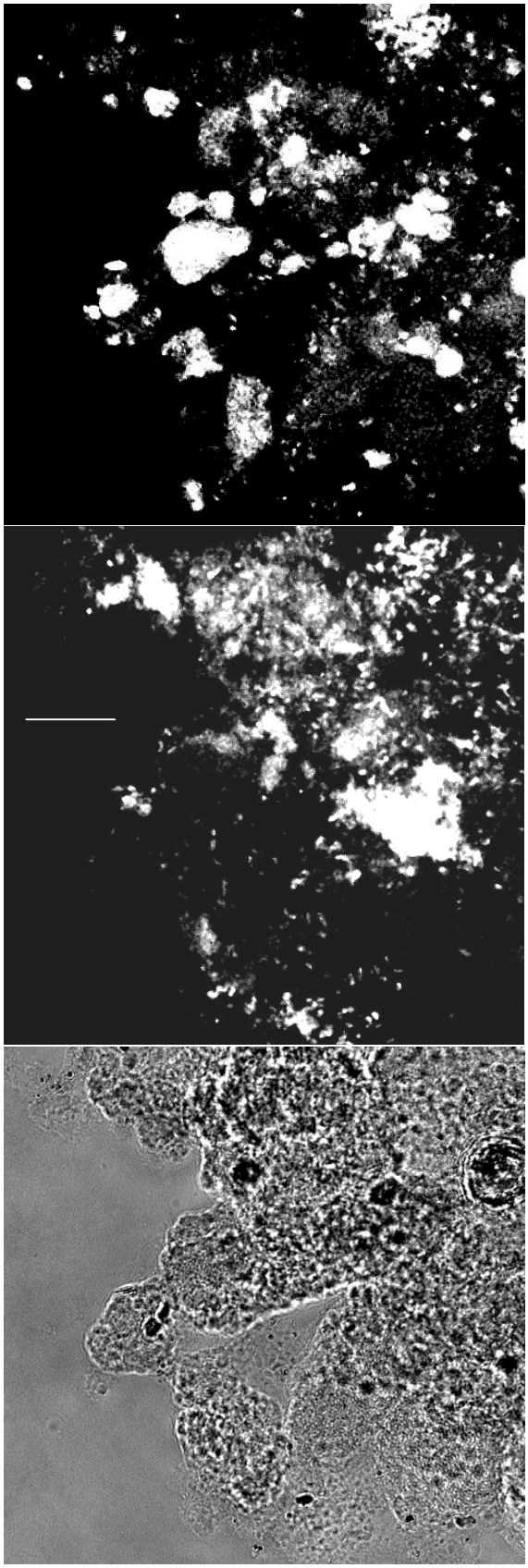

Figure 8.14. FISH of an aerobic biofilm sample (Day 41) with a Cy3-labeled BET42a probe (a) and a Cy5-labeled GAM42a probe (b). (c) is the transmission image of the sample. The beta *Proteobacteria* clusters were often surrounded by gamma *Proteobacteria* clusters that appeared to "fill in" the space between the beta *Proteobacteria* clusters.

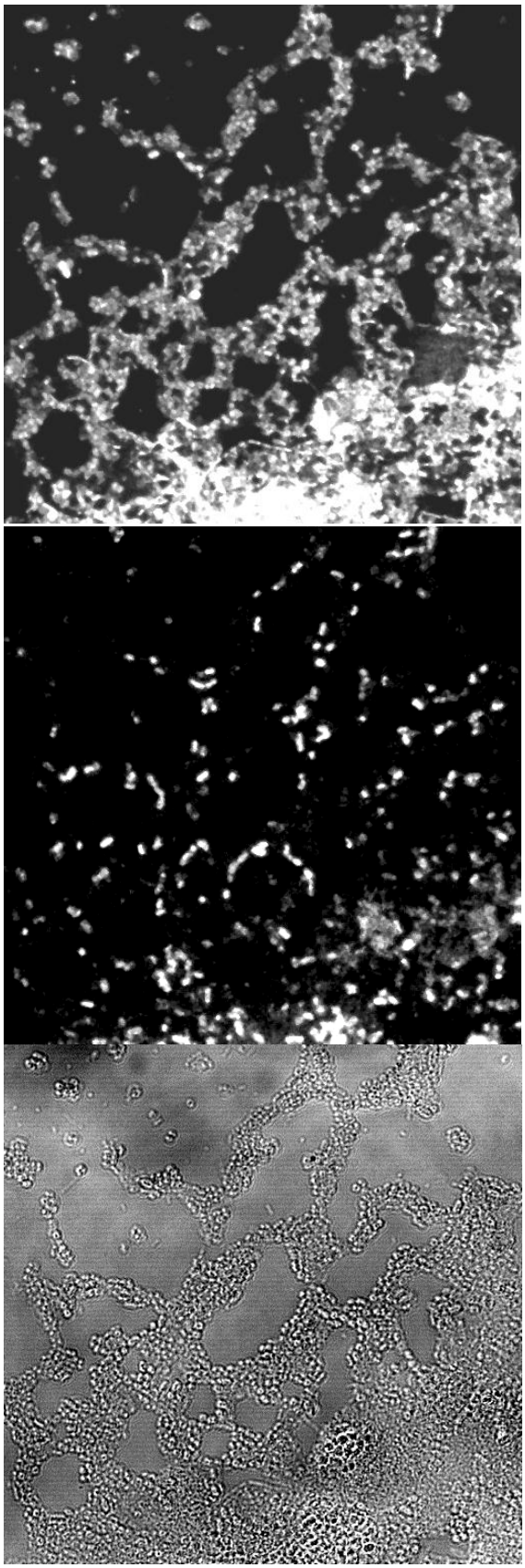

Fig. 8.15. FISH of a denitrifying biofilm sample (Day 52) with a Cy3-labeled BET42a probe (a) and a Cy5-labeled GAM42a probe (b). (c) is the transmission image of the sample. Single gamma *Proteo-bacteria* cells appeared relatively evenly distributed amongst the beta *Proteobacteria* cells. The beta bacteria were the major bacteria group of the denitrifying biofilm.

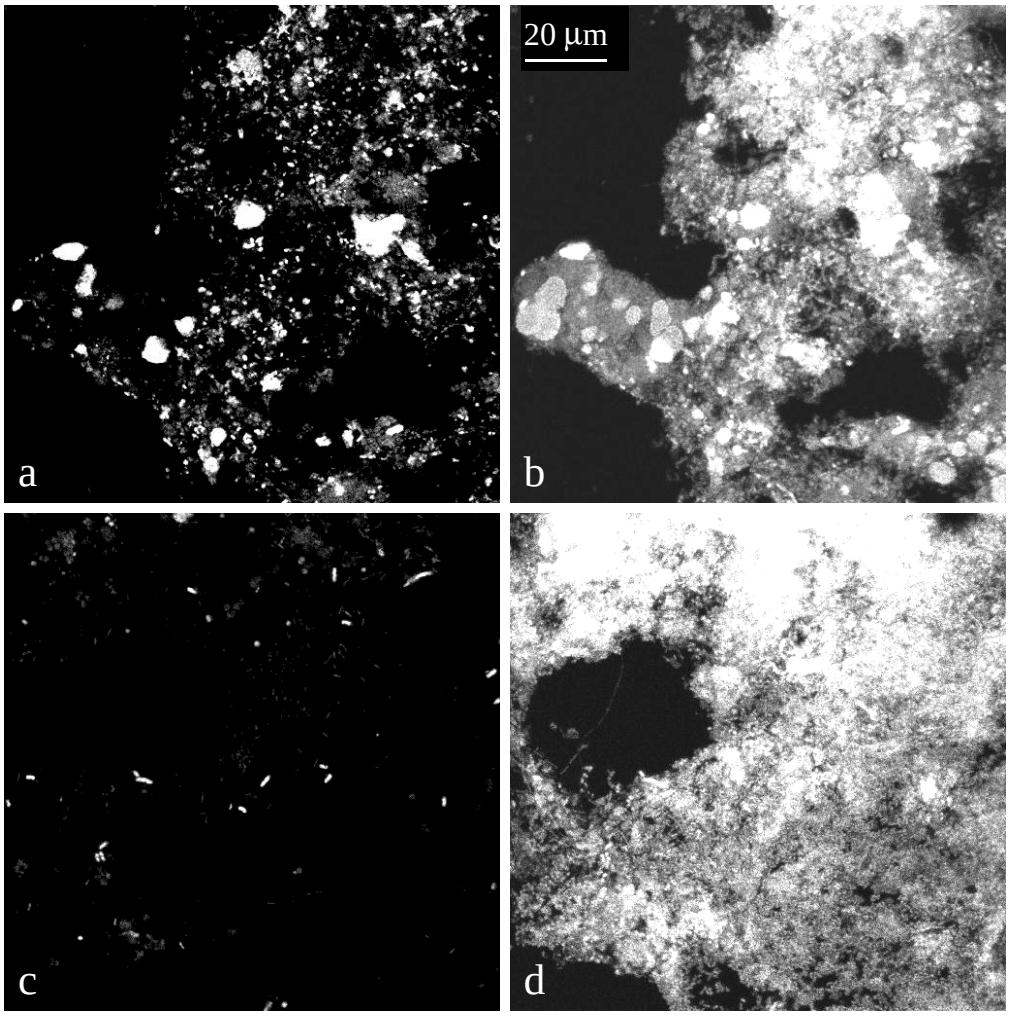

Figure 8.16. FISH with a Cy3-labeled ALF1b (alpha subclass of *Proteobacteria*) and a Cy5-labeled EUB338 (*Bacteria* domain) probe. The upper half shows images of the aerobic biomass 2 weeks into the sampling period, and the lower half shows images two weeks after start-up of the denitrifying biofilm in the lab-scale reactor. Almost all of the alpha bacteria disappeared within the first two weeks following transfer of the biomass to the denitrifying setup. a) ALF1b, aerobic sample. b) EUB338, aerobic sample. c) ALF1b, denitrifying sample. d) EUB338, denitrifying sample.

The denitrifying biofilm community was less diverse (e.g. no protozoa) than the aerobic one. This was to be expected due to the use of a single carbon source, acetate, and the use of nitrate as electron acceptor instead of oxygen. For example, nitrifying bacteria could not survive in the anoxic lab-scale reactor.

The fact that no significant change in the microbial population could be verified with the applied set of gene probes around the time of the peak activity after one month of operating the anoxic lab-scale reactor could require alternative explanations of the observed decrease in bio-P activity. One hypothesis is a

change in the biofilm structure, e.g. related to the EPS production. A reduced biofilm-specific diffusion coefficient (i.e. reduced penetration of the film) could account for the lower activity level. However, it should be stressed that the study applied mainly broad phylogenetic probes and only a few strain-specific probes. Hence, despite the fact that no significant changes in the microbial population were detected during the time of the activity decline, it cannot be excluded that changes possibly took place *within* one of the broad groups that were investigated.

The characteristic tetrad structure of cells reported for GAO organisms were not detected in any of the samples. For the denitrifying sludge, almost no signals with the ALF1b probe remained after 2 weeks. As typical GAO organisms have been reported to belong to the alpha subclass of *Proteobacteria* it can be concluded that if non-PAO COD-storing organisms were present in the biofilm biomass, these were different from the frequently observed GAOs. Blackall *et al*., 1997, also showed that these organisms were unable to reduce nitrate further than to nitrite, and no nitrite accumulated in the continuously operated system.

The results in this study demonstrated the potential of gene probes in the field of tracking microbial population shifts. It was shown that a combined study of microbial population changes and process performance is needed to understand the correlation between the two and avoid false conclusions based on only one of them. FISH was able to detect major changes in the population and these changes coincided with detection of denitrifying bio-P activity as indicated by the bulk concentration measurements of phosphate. For an improved practical use of gene probe analysis in regard to phosphate removal, more research is necessary regarding the organism(s) responsible for bio-P and as important also regarding the competing glycogen accumulating organism(s). Development of new probes for these organisms would enhance investigations of the dominance of the two groups in relation to different operation conditions.
In order to verify which bacteria do the phosphate removal (or other processes) it is necessary not only to show a high abundance of a certain bacteria group, but also to verify the metabolism by the use of innovative methods like MAR or NMR. Staining methods for specific storage compounds can be used as assisting tools in this process.

Some time (a few months) was required in order to train the engineer in this study to perform the microbial characterization methods. The protocols are relatively simple, but the complexity of mixed bacteria cultures, makes repeating the FISH analysis and experience by the microscope necessary before reliable and reproducable images/results can be obtained. For the promising microbiological methods to gain popularity and hence usefulness in improving operating conditions of e.g. wastewater plants, the understanding between the two different fields of science is essential.

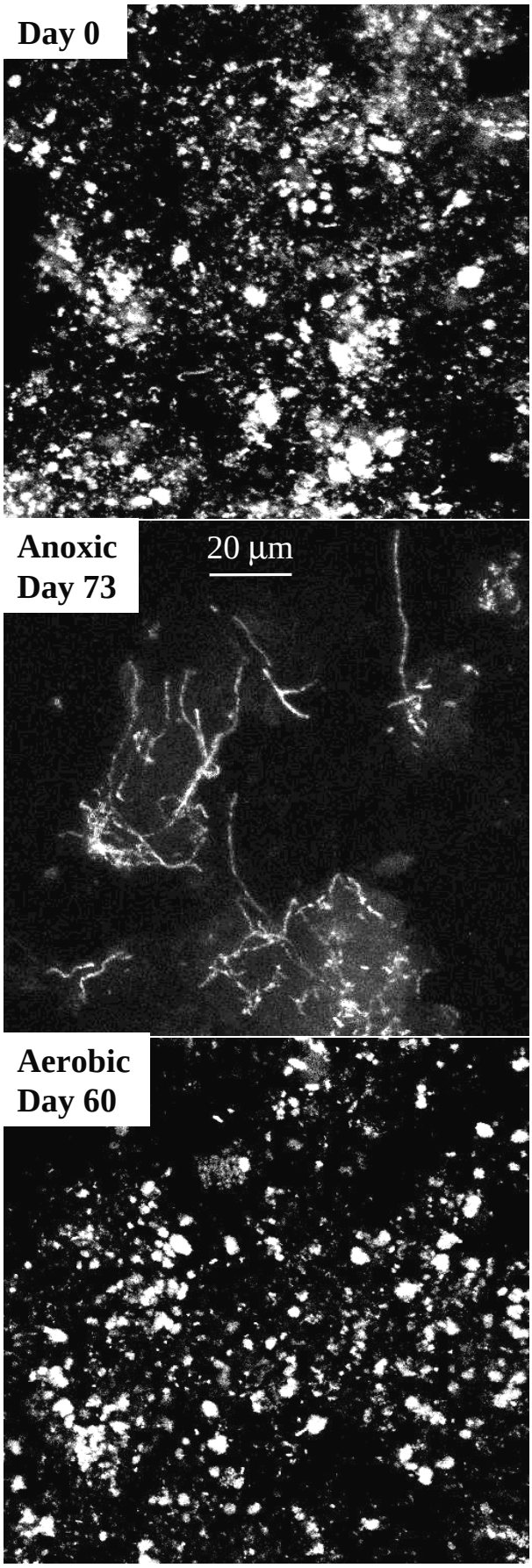

Figure 8.17. FISH with a Cy3-labeled HCG69a probe on day 0 (original biofilm from the aerobic bench-scale reactor), day 73 in the anoxic lab-scale reactor, and day 60 in the aerobic bench-scale reactor. The abundance of small clusters of gram-positive bacteria with a high DNA G+C content (GPBHGC) in the aerobic reactor decreased dramatically in numbers within the first few weeks in the anoxic reactor; they were gradually completely replaced by filamentous GPBHGC.
No noticeable change was detected in the aerobic bench-scale reactor during the sampling period.

8.3 Key Results during PART B of The Study

1) Acclimation of a phosphate-removing biofilm to nitrate instead of oxygen as terminal electron acceptor took approximately 2 weeks. This was tested via 2 separate experimental runs with the aerobic EBPR biofilm originating from a semi full-scale SBBR pilot plant and a bench-scale SBBR reactor, respectively.

2) FISH revealed a significant change in the microbial population during the acclimation. Bacteria belonging to the alpha subclass of *Proteobacteria* disappeared and characteristic round beta *Proteobacteria* clusters were replaced by single short rods. Characteristic small clusters of Gram positive bacteria with a high G+C DNA content (GPBHGC) decreased in numbers and were gradually completely replaced by filamentous GPBHGC

3) The biofilm needed 1 month to adjust to a stable activity level, since a steady rise in the activity was seen in this period followed by a sudden decrease. This phenomenon was seen in two independent runs and had nothing to do with the chosen phase lengths as first assumed. Instead, it must be attributed to a biofilm up-start stability phenomenon, perhaps related the diffusion coefficient in the biofilm matrix. FISH did not reveal any significant change in the microbial population around the time of the sudden activity decrease. The emphasis of the need for always repeating an experiment before concluding on an observed phenomenon has been illustrated via the two runs, along with the importance of combined studies of microbial population and process performance.

4) More filaments developed in the denitrifying sludge over time. FISH revealed that the filaments belonged to at least 2 different bacteria groups, HGC and BET.

5) The measured phosphate content of the detached biomass from the denitrifying EBPR biofilm was relatively low, 24 ± 4 mg P/g TS. The explanation is hypothesised to be due to an only partly phosphate penetrated biofilm and a detachment mode of the biofilm that removed the biofilm in a clump like manner and not in a layer wise manner with detachment of mainly the outer phosphate-rich layers. The characteristics of the measured outlet curves around backwash and during stable operation supported the hypothesis of an only partly penetrated biofilm. The observed phenomena emphasise the importance of strict biofilm thickness control to obtain successful EBPR in as biofilter.

6) The measured phosphate content of the detached biomass from the aerobic EBPR biofilm was also relatively low 24 ± 3 mg P/g TS. In this case, the outlet concentrations from the SBBR were always very low, whereby a limitation of the available mass of phosphate played a role. After applying elevated phosphate concentrations in the inlet for 2 weeks, the phosphate content of the sludge increased to 35 ± 2 mg P/g TS.

9. PART C - Modelling

9.1 Why make a model?

When looking at bio-P removal, different aspects appear more complicated than more traditional transformation processes like e.g. COD removal and nitrification. First of all, the biological phosphorus removal is a combination of 2 interdependent processes: the anaerobic phosphate release with storage of organics and the aerobic/anoxic process with degradation of the previously stored organics by the use of the available electron acceptor. Second, the rates of the 2 separate processes depend on the amount of internal storage. The amount of internal storage depends on wastewater composition and the length of the anaerobic and aerobic/anoxic phases. The internal storage, and hence the transformation rates, change throughout the whole phosphate removal cycle.
For a biofilm the additional complication regarding diffusion has to be considered. The diffusion causes the process to depend on also the concentration in the bulk water outside the film and the biofilm thickness.
In order to investigate the process regarding optimal process configuration (phase lengths, biofilm thickness, tank sizes etc.) and up-scaling, a mathematical model seems necessary due to the high degree of complexity. A model can also help with the illustration and understanding of what goes on inside the biofilm e.g. the penetration depths of the different compounds involved in the process and competition between different species of a multispecies biofilm.

9.2 Purpose of Modelling in This Study

The purpose of the developed model was to investigate specific phenomena inside the biofilm, such as penetration depth, effect of biofilm thickness/backwash frequency and competition between PAOs and normal denitrifying heterotrophs. The aim of the modelling was rather to illustrate the phenomena/principles, than to develop a calibrated model. A relatively simple and thereby transparent model is suitable for this purpose. The 1-D biofilm model supported by the software program AQUASIM (Reichert, 1994) was used. For a calibrated model, much more experimental data would be needed than was available. Development of a calibrated model applicable for up-scaling was beyond the scope of the study and would likely require a Ph.D.-study of its own.

9.3 The Model

9.3.1 Model Elements

The Activated Sludge Model No. 2d (Henze *et al.*, 1999) forms the basis of the developed model. The ASM 2d incorporates denitrifying PAOs as opposed to the previous ASMs.
The experimental setup allowed for several of the processes described by ASM2d to be excluded:

1) No oxygen was present in the system, i.e. no nitrification, no aerobic P uptake and no aerobic metabolisms.
2) Acetate was used as the only carbon source in the influent (anaerobic inlet), therefore hydrolysis and fermentation were ignored. Decay of bacteria was assumed to be converted directly into 90 % acetate and 10 % inert material.

Two bacteria types were included in the model: Denitrifying PAOs (X_{PAO}) and heterotrophic denitrifiers incapable of storing any compounds (X_D).
The following 8 processes were included (Table 9.1):

For the heterotrophic denitrifiers:
1) Anoxic growth of X_D on acetate
2) Lysis of X_D

For the denitrifying PAOs:
3) Storage of PHB from acetate with release of phosphate
4) Anoxic storage of polyphosphate (X_{PP})
5) Anoxic growth of X_{PAO} on stored PHB
6) Lysis of X_{PAO}
7) Lysis of polyphosphate
8) Lysis of PHB

The process equations were simplified from the ones given by ASM2d. Only 3 soluble components were included: Acetate (S_A), nitrate (S_{NO3}) and phosphate (S_{PO4}). 5 particulate variables were included: X_{PAO}, X_D, X_{PHB}, X_{PP} and X_I (inert particulates). Values for stoichiometry and kinetic parameters were taken from the Activated Sludge Model 2d (Henze *et al.*, 1999). Table 9.1 gives an overview of process reaction expressions and stoichiomety, and Table 9.2 lists values of the constant parameters.
Backwash was implemented like in the model developed by Morgenroth (1998), i.e. back-wash after a given time period with the assumption that the biofilm has a set biofilm thickness after each backwash, all overlaying layers are removed by the backwash procedure. A constant solid fraction of 0.36 was used. The density of solid matter was set at 70 kg TS m^{-3}, except for the poly-phosphate that was set at 2500 kg P m^{-3} according to Lide (1992). Masuda *et al.* (1991)

measured solid densities that varied in the range 37-102 kg m^{-3} within the biofilm, with the highest density closest to the substratum, however, a homogeneous density was assumed here.

9.3.2 Simplifications In The Model

The model is one-dimensional. It assumes a homogenous biofilm structure with a uniform biofilm thickness and transport into the biofilm only by diffusion. A real biofilm may contain pores and has a heterogeneous structure with a range of thicknesses. However, when looking at the average response of a biofilm to given operating conditions, the simplified model can give useful indications. The results of the batch experiments reported above indicate that the assumptions of a zonated biofilm and transport via diffusion are reasonable. One simplification of the model is not to include glycogen-accumulating organisms. However, very little is known about these organisms (growth rate, metabolism etc.), whereby this group was excluded from the model. The use of default values is always a severe simplification of a model, especially the use of values based on activated sludge for modelling of a biofilm system. However, for investigating the principles of a process and when no measured values are available, this is a practicable starting point.
As indicated by experimental observations, backwash might mainly remove the thickest parts of a biofilm instead of the top layers. However, for simplicity and due to a lack of knowledge of the real detachment mode, a layer-wise biomass removal was used in the model (refer to the next section).

9.3.3 Mode of Detachment - Phosphorus Content

Figure 9.1 illustrates 2 different extreme modes of biomass detachment that may happen during backwash of a biofilter. Left shows the modelled version where only the top layer above a certain thickness ($L_{backwash}$) is removed during backwash. Right shows the other extreme, where thick cohesive parts of the biofilm are removed (sloughing), exposing an almost naked carrier surface. For an only partly penetrated biofilm, the mode of detachment is determining the average phosphorus content of the excess sludge. The top layers contain in this case higher amounts of internally stored polyphosphate than the bottom layers. If only the top, active layers are removed by backwash, the average P content of the detached biomass shall be higher than if cohesive parts of the total depth of the film detach. In the following, two different average phosphate concentrations are therefore considered – the average P content in the biomass removed by backwash (thickness above $L_{backwash}$), and the average P content over the total depth of the film, i.e. the total biomass from substratum to surface. If backwash in practise removes mainly the thickest parts of the biofilm (sloughing), the measured P contents shall be most similar to the average P content of the total depth of the film compared to the top layer.

Table 9.1 Process expressions implemented in the AQUASIM model. Based on The Activated Sludge Model 2d (Henze *et al*., 1999). Symbols: see text and Table 9.2.

(1) Anoxic growth of heterotrophic denitrifiers (X_D) on acetate:

$$r_{Denitrification} = \mu_{H} \cdot \eta_{NO3\text{-}H} \cdot \frac{S_{NO3}}{K_{NO3} + S_{NO3}} \cdot \frac{S_A}{K_A + S_A} \cdot \frac{S_{PO4}}{K_P + S_{PO4}} \cdot X_D$$

Stoichiometry: S_A: -1.6; S_{NO3}: -0.21; S_{PO4}: -0.02; X_D: 1.

(2) Lysis of heterotrophic denitrifiers (X_D):

$$Lysis_{X_D} = b_D \cdot X_D$$

Stoichiometry: S_A: 0.9; X_I: 0.1; X_D: -1.

(3) Anaerobic uptake of acetate and storage in the form of internal PHB by denitrifying PAOs:

$$r_{PHB} = q_{PHB} \cdot \frac{S_A}{K_A + S_A} \cdot \frac{\frac{X_{PP}}{(X_{math} + X_{PAO})}}{\left(K_{PP} + \frac{X_{PP}}{(X_{math} + X_{PAO})}\right)} \cdot X_{PAO}$$

Stoichiometry: S_A: -1; S_{PO4}: Y_{PO4}; X_{PP}: $-Y_{PO4}$; X_{PHB}: 1.

(4) Anoxic uptake of phosphate and storage as internal poly-phosphate by denitrifying PAOs

$$r_{PP} = q_{PP} \cdot \eta_{NO3} \cdot \frac{S_{NO3}}{K_{NO3} + S_{NO3}} \cdot \frac{S_{PO4}}{K_{PS} + S_{PO4}} \cdot \frac{\left(\frac{X_{PHB}}{X_{math} + X_{PAO}}\right)}{\left(K_{PHB} + \frac{X_{PHB}}{X_{math} + X_{PAO}}\right)} \cdot \left(\frac{K_{MAX} - \frac{X_{PP}}{X_{math} + X_{PAO}}}{K_{IPP} + K_{MAX} - \left(\frac{X_{PP}}{X_{math} + X_{PAO}}\right)}\right) \cdot X_{PAO}$$

Stoichiometry: S_{NO3}: -0.07; S_{PO4}: -1; X_{PP}: 1; X_{PHB}: -0.2.

(5) Anoxic growth of PAOs:

$$r_{PAO\text{-}Growth} = \mu_{PAO} \cdot \eta_{NO3} \cdot \frac{S_{NO3}}{K_{NO3} + S_{NO3}} \cdot \frac{S_{PO4}}{K_P + S_{PO4}} \cdot \frac{\left(\frac{X_{PHB}}{X_{math} + X_{PAO}}\right)}{\left(K_{PHB} + \frac{X_{PHB}}{X_{math} + X_{PAO}}\right)} \cdot X_{PAO}$$

Stoichiometry: S_{NO3}: -0.21; S_{PO4}: -0.02; X_{PAO}: 1; X_{PHB}: -1.59.

(6) Lysis of PAOs: $Lysis_{X_{PAO}} = b_{PAO} \cdot X_{PAO}$

Stoichiometry: S_A: 0.9; X_I: 0.1; X_{PAO}: -1.

(7) Lysis of internal poly-phosphate: $Lysis_{X_{PP}} = b_{PAO} \cdot X_{PP}$

Stoichiometry: S_{PO4}: 1; X_{PP}: -1.

(8) Lysis of PHB: $Lysis_{X_{PHB}} = b_{PAO} \cdot X_{PHB}$

Stoichiometry: S_A: 1; X_{PHB}: -1.

Table 9.2. Overview over values of constants used in the AQUASIM model.

Constant	Description	ASM2d (Henze et al., 1999) (20°C)	AQUASIM Model
D_A	Diffusion coefficient of acetate	-	$3.5*10^{-6}$ m^2h^{-1} [1]
D_{NO3}	Diffusion coefficient of nitrate	-	$5.3*10^{-6}$ m^2h^{-1} [2]
D_{PO4}	Diffusion coeff. of phosphate	-	$3.2*10^{-6}$ m^2h^{-1} [3]
eps_PAO_ini	Initial volume fraction of PAO's in the biofilm	-	0.15
eps_D_ini	Initial volume fraction of X_D in the biofilm	-	0.15
eps_X_I_ini	Initial volume fraction of inert particles in the biofilm	-	0.001
eps_PHA_ini	Initial volume fraction of PHA in the biofilm	-	0.05
eps_PP_ini	Initial volume fraction of PP in the biofilm	-	0.002
b_{PAO}	Rate constant for lysis of X_PAO	0.008 h^{-1}	0.002 h^{-1} [4]
b_D	Rate constant for lysis of X_D	0.017 h^{-1}	0.010 h^{-1} [4]
K_A	Half saturation const. for acetate	4 gCOD/m^3	4 gCOD/m^3
K_{IPP}	Inhibition coefficient for PP storage	0.02 gPP/gPAO-COD	0.02 gPP/gPAO-COD
K_{MAX}	Maximum ratio of X_PP/X_PAO	0.34 gPP/gPAO-COD	0.34 gPP/gPAO-COD
K_{NO3}	Saturation/inhib. coeff. for nitrate	0.5 gN/m^3	0.5 gN/m3
K_P	Saturation coeff. for P (nutrient)	0.01 gP/m^3	0.01 gP/m^3
K_{PHB}	Saturation coeff. for PHA	0.01 gPHB/gPAO-COD	0.01 gPHB/gPAO-COD
K_{PP}	Saturation coeff. for poly-phosphate	0.01 gPP/gPAO-COD	0.01 gPP/gPAO-COD
K_{PS}	Saturation coeff. for P in PP storage	0.2 gP/m^3	0.2 gP/m^3
L_ini	Initial biofilm thickness	-	0.0003 m (typically)
μ_H	Max. growth rate of heterotrophs	0.25 h^{-1}	0.25 h^{-1}
μ_{PAO}	Max. growth rate of PAO's on PHB	0.042 h^{-1}	0.042 h^{-1}
η_{NO3}	Reduction factor for anoxic P uptake compared to aerobic	0.6	0.6
η_{NO3-H}	Reduction factor for anoxic growth of heterotrophs compared to aerobic	0.8	0.8
n_sp	Number of Biolith spheres	-	670
Q_{max}	Inlet flow to the system	-	0.00110 m^3/h
q_{PHA}	Rate constant for PHA storage	0.13 gPHA/(gPAO-COD*h)	0.13 gPHA/(gCOD*h)
q_{PP}	Rate constant for PP storage	0.063 gPP/(gPAO-COD*h)	0.063 gPP/(gCOD*h)
rho_P	Density of polyphosphate	-	2.500.000 gPP/m^3 [5]
rho_X	Density of organic components	-	70.000 gTS/m^3 [6]
S_A1	Acetate in anaerobic inlet	-	302 gCOD/m^3
S_A2	Acetate in anoxic inlet	-	0 gCOD/m^3
S_NO3_1	Nitrate in anaerobic inlet	-	0 gN/m^3
S_NO3_2	Nitrate in anoxic inlet	-	53 gN/m^3
S_PO4_inlet	Phosphate in the inlet	-	15 gP/m^3
Y_PO4	P released pr. COD taken up	0.4 gP/gCOD	0.4 gP/gCOD
z_sp	Radius of Biolith balls	-	0.0035 m
X_{math}	Included for numerical reasons	-	0.001 gPAO-COD/m^3

[1] Wanner and Gujer, 1984. [2] Henze *et al.*, 1997. [3] Edwards and Hoffmann, 1959 (reduced with a factor 0.8 for diffusion in a biofilm compared to water). [4] Wentzel *et al.*, 1989. [5] Lide, 1992. [6] Average from Masuda *et al.*, 1991.

If a sloughing-like detachment mode dominates, it can be modelled by choosing a very thin biofilm thickness after backwash and increasing the backwash interval compared to the actual interval. Assume that backwash is performed once a week, removing one third of the total amount of biomass in the reactor. If detachment mainly removes the thickest parts and remove them so that the carrier is left almost naked afterwards, this could be approximated by a simulation where $L_{backwash}$ is chosen very small (e.g. 15 μm) and the backwash interval is 3 times the actual interval, i.e. 21 days. However, the presence of different biofilm thicknesses would demand for a more dimensional model to make an exact calculation. This is beyond the scope of this study where focus is on the phenomenal /qualitative prediction.

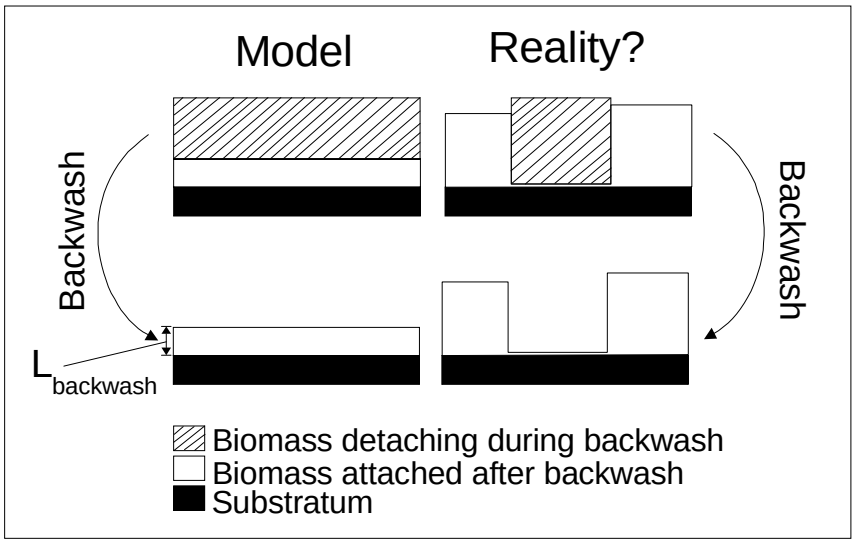

Figure 9.1. The detachment of biomass during backwash of a biofilter may appear in two distinctly different manners. The 1-D AQUASIM model assumes detachment of the top layer of the biofilm above a set thickness ($L_{backwash}$). However, it is not known exactly how the biofilm detach in reality. Experimental observations (naked carriers next to carriers covered with a thick biofilm, Fig. 7.5) could suggest a sloughinh-like detachment mode with removal of cohesive pieces of the thickest parts of the biofilm as illustrated above right.

9.4 Examples of Modelling Results

The experimental system of PART B was used as the model system.

9.4.1 Result of One Simulation – Particulate Components

Figure 9.2 shows an example of a modelling result. In this simulation, a biofilm thickness of 350 μm after backwash was used. The cycle length was 6 hours with 3 hours anaerobic and 3 hours anoxic phases. Backwash once a week after

an anoxic phase was used (equivalent to the experimental operation), i.e. 28 cycles between two backwashes. The figure shows the variations in the particulate compounds inside the biofilm at a distance of 300 µm from the carrier surface as a function of time. Similar plots could be shown for other distances from the carrier surface (substratum: x = 0). During one period between two backwashes, the biofilm thickness increased from 350 to 870 µm. The chosen initial conditions determine the starting point of the curves. An equal initial fraction of PAOs and denitrifying heterotrophs was used. The weekly backwash causes the wave-like appearance of the curves. Each individual peak on the curves identifies a single cycle. That the concentration of bacteria varies within a single cycle is caused by the use of a constant solid fraction as discussed in section 2.4.3. The mass of bacteria does not vary significantly during a single cycle, but the internal storage and subsequent degradation of PHB (less significant effect of the dense PP) makes the biofilm expand or shrink, respectively. As time progresses, the advantageous operation for the PAOs makes the fraction of denitrifying heterotrophs (X_D) decrease in the biofilm. However, for reaching a steady state biofilm composition, almost 1 month of operation (30 days) is required. The fraction of inert materials (X_I) rises as a function of time due to accumulation of inert material inside the biofilm originating from decaying bacteria. The poly-phosphate content, X_{PP}, is highest shortly after a backwash, and by the end of the 7 days, it is almost zero. The reason is diffusion limitation in the growing biofilm – soluble phosphate does not penetrate the film as it gets thicker, whereby the poly-phosphate storage pools cannot be replenished.

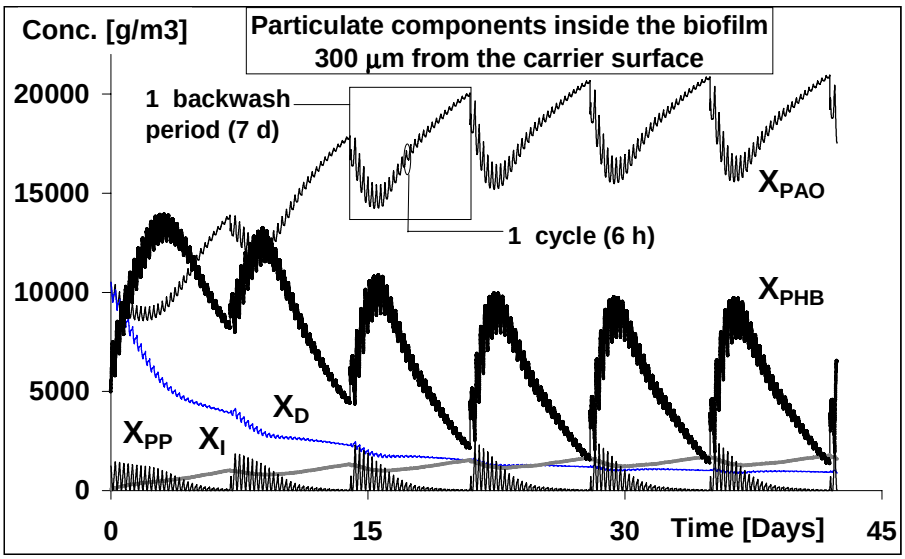

Figure 9.2. Modelled concentrations of particulate components inside the biofilm 300 µm from the carrier surface. Backwash interval: 7 days. Each 'wave' indicates one period between two backwashes. Each little peak on the curves indicates one cycle, 3 hour phase lengths were used, i.e. 28 cycles between each backwash. The biofilm thickness after backwash was set to 350 µm.

Figure 9.3 shows the poly-phosphate content in different depth of the biofilm between two backwashes (Day 28-35). The distances refer to the distance from the substratum surface. As time progresses, the biofilm thickness increases, hence the poly-phosphate contents can only be shown for the higher distances when the film has reached this thickness.

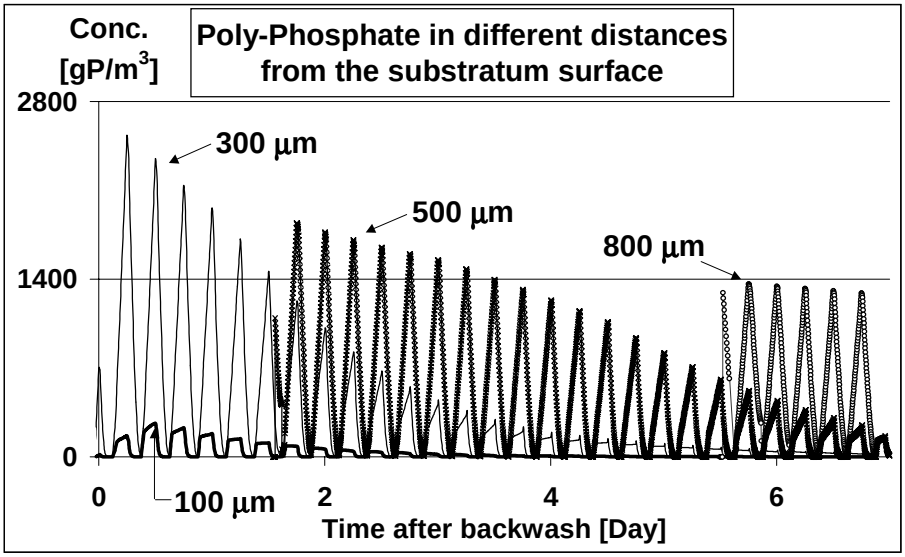

Figure 9.3. Modelled poly-phosphate storage pools inside the biofilm between 2 backwashes. 3 hours phase lengths were used, i.e. 28 cycles between each backwash. The biofilm thickness after backwash was set to 350 µm. As the biofilm thickness increases with time, soluble phosphate can no longer fully penetrate the biofilm whereby the storage pools in the deep layers of the biofilm (close to the substratum, e.g. 100 µm) cannot be replenished. By the end of the period, highest polyphosphate is found in the top layers (e.g. 800 µm).

By assuming 15 mgP/gTS in the cell biomass without PHB (X_{PAO} and X_D), the simulated poly-phosphate contents can be recalculated into the equivalent phosphorus content of the total dry mass. This is done simply by dividing the phosphate concentration with the total concentration of dry matter at a given distance:

$$\%\ P\ content\ = 100\% \cdot \frac{(X_{PP} + 0.015\ gP/g \cdot (X_{PAO} + X_D))}{X_{PAO} + X_D + X_I + X_{PHB} + X_{PP}}$$

Based on Henze *et al*., 1997, a stoichiometric factor of 1.42 g COD/g biomass is used – the biomass is in the ASM2d calculated in COD units, which need to be recalculated in order to calculate the phosphorus content of the dry biomass. Figure 9.4 shows the result of such a calculation in 3 different distances from the substratum.

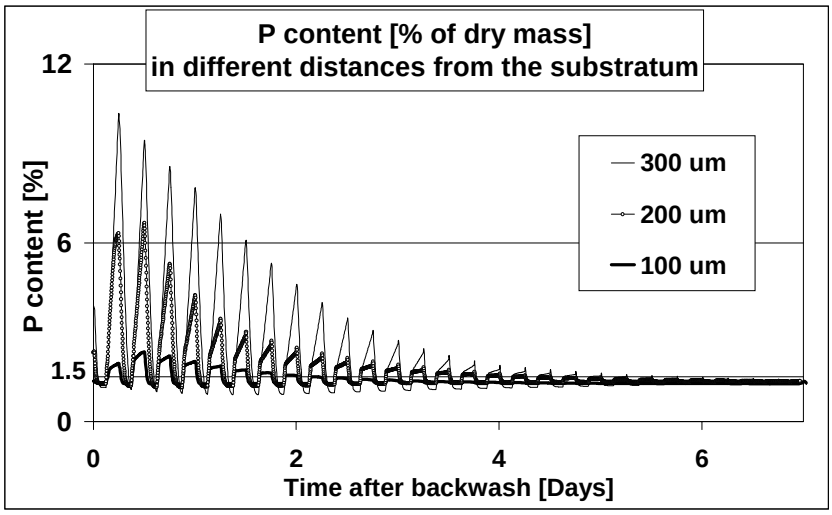

Figure 9.4. Modelled total phosphorus content [% of dry mass] at different distances [μm] from the substratum as a function of time after backwash. By the time of backwash (after 7 days) no excess P is stored in the shown layers (≤ 300 μm from the substratum).

An automatic calculation by the computer model can only be carried out for distances that are available for calculation throughout the backwash period, i.e. smaller than the biofilm thickness after backwash (here 350 μm). As seen in Fig. 9.4, by the time of backwash none of the layers below the distance of 300 μm from the substratum contribute to excess P removal. Figure 9.5 shows the distribution of particulate compounds inside the biofilm just before backwash on Day 35. By the top of the film, the PHB concentrations are very high, ~65% of the total mass of PAOs and PHB. Due to the constant solid fraction in the model, the PAO volume concentration decreases proportionally in the PHB-rich layers. As PHB storage pools are depleted, shrinkage of the film occurs, whereby the PAO concentrations in different layers are more uniform, as seen by the bottom of the film. No maximum PHB content of bacteria cells is included in the ASM2d as oppose to the maximum PP contents. The reason for this is a lack of knowledge of such an inhibition term and also that PHB saturation has not been reported for practical AS systems (Henze, 1999). Based on the simulation results here, a PHB inhibition term would be recommendable for biofilm modelling of EBPR. The reason that the PHB gets so high is, that when the biofilm grows then the layers in the bottom are no longer penetrated whereby stored PHB is not degraded, hence PHB accumulates. Growth of PAOs (i.e. use of PHB) is in the model assumed to take place only in the presence of phosphate. For a phosphate limited biofilm, where nitrate is available in the depth of the film, this assumption is questionable – it was actually experimentally observed, that denitrification continued also after depletion of phosphate, in agreement with general literature reports. More knowledge of the PHB degradation during periods where phosphate is not available is a subject

that could be investigated and included in the ASM model. The consequence of the very high PHB concentrations in the model is, that the biofilm thickness increases significantly and that the concentration of PAOs decreases in the PHB rich layers. If the content of PHB was lower then the biofilm would be thinner, but the penetration depth of phosphate would be equivalently smaller due to the higher concentration of PAOs in the top layer of the biofilm. Hence, phenomenological a model with lower PHB levels in the bacteria cells would predict similar trends as the here presented model.

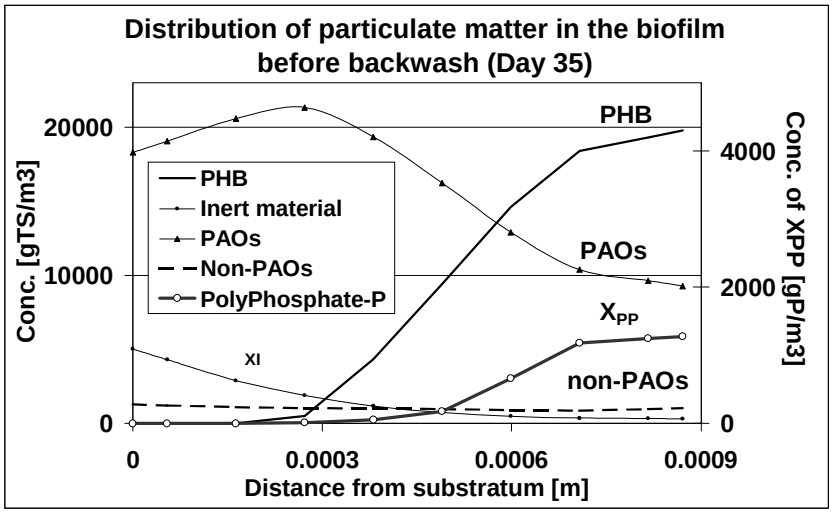

Figure 9.5. Modelled distribution of particulates inside the biofilm before backwash on Day 35.

A grid structure is applied by AQUASIM to divide the biofilm into separate layers for calculation purposes. In the shown simulation, 10 grid points were used, which divided the biofilm into 9 compartments/layers. The appearance of the simulated diffusion profiles depends on the number of grid points - the more grid points, the more smooth line. A real diffusion profile is a smooth curve, but due to the time required for calculation, a limited number of grid points was chosen. The phosphorus content in each of the grid points can be calculated, Fig. 9.6, and form the basis of a numerical integration to obtain the average P content at the time of backwash. The content varies from 1.2 to 4.5 % from the deepest to the top layer of the film. Layers below 500 μm do not contribute to excess P removal. The average P content, calculated as illustrated in Fig. 9.7, of the total biomass is 2.3 %. This low P contents is in agreement with the experimental findings (2.4 % ± 0.4 %). The average P content of the biomass that is removed by backwash (in the model), i.e. the biomass above 350 μm from the substratum, is 3.1 %. The low P content is a result of the diffusion limitation of phosphate and illustrates the problem regarding the use of a biofilm for EBPR. According to the illustrated modelling results, the biofilm thickness should be kept thin in order to maintain high phosphate levels. A thin

thickness can be obtained by regular and well-controlled backwash. As illustrated in Fig. 9.4, the phosphate levels in the top of the film were ~ 10 % right after backwash. By thinner biofilms after backwash and/or frequent backwash, it would apparently be possible to obtain high P contents of the biomass. However, as illustrated below, the biofilm thickness after backwash is also determining the competition between PAOs and non-PAO, denitrifying heterotrophs in the studied continuous system, where thicker biofilms are in favour of the slow-growing PAOs.

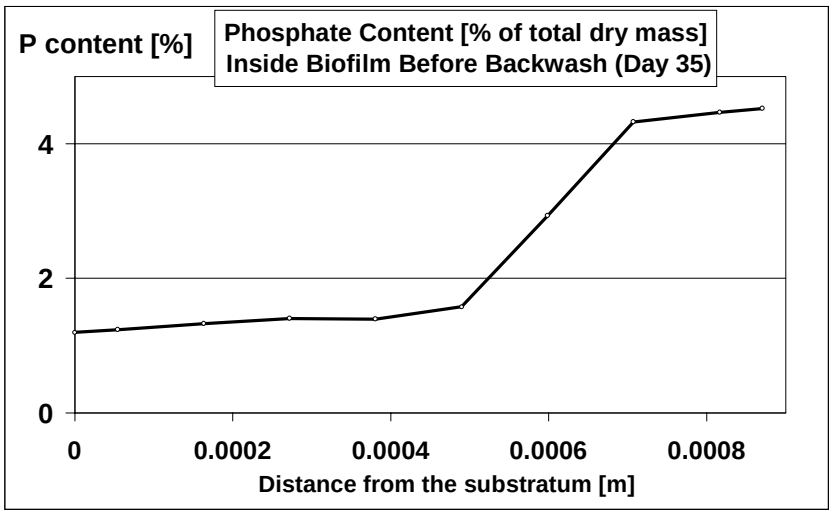

Figure 9.6. Average P content in different distances from the substratum before backwash. Weekly backwash with 350 μm biofilm thickness after backwash.

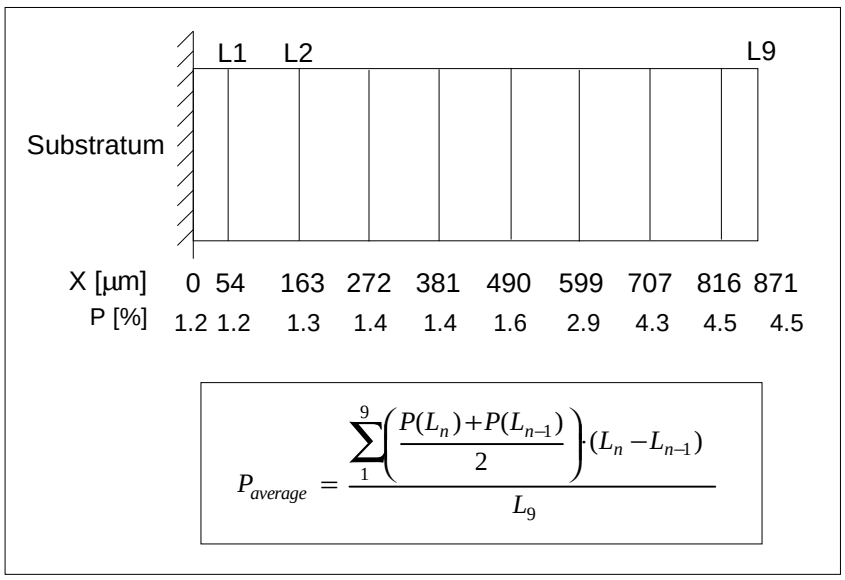

Figure 9.7. Numerical integration of phosphorus contents in different layers of the biofilm before backwash on Day 35. The calculation of the average P content over the *total* biomass is illustrated.

9.1.2 Diffusion Profiles of Soluble Compounds

Figure 9.8 illustrates concentration profiles of soluble compounds inside the biofilm during the last cycle before backwash on Day 35 – 'steady-state' operation according to Fig. 9.2.

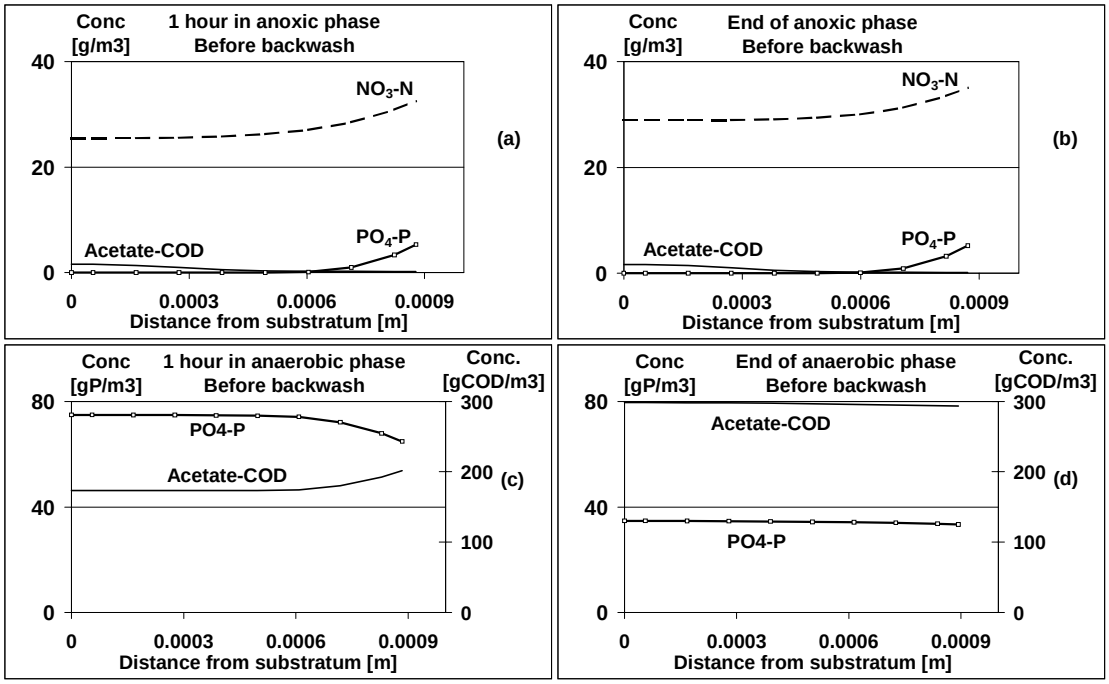

Figure 9.8. Diffusion profiles of soluble compounds in the biofilm. The last cycle before backwash on Day 35. (a) and (b) show profiles during the anoxic phase after 1 and 3 hours respectively (3 hours = end of the phase). Phosphate only penetrates the top 250 μm. An internal production of acetate takes place due to decay of bacteria. (c) and (d) show profiles during the anaerobic phase after 1 and 3 hours respectively (3 hours = end of the phase). Phosphate release accompanied by acetate uptake takes place in the top layers where internal phosphate pools are available, until the pools are depleted by the end of the phase.

Figure 9.8(a) shows the concentrations after 1 hour of the anoxic phase and (b) by the end of the 3 hours anoxic phase. In both cases, phosphate only penetrates the top 200-250 μm of the biofilm whereas nitrate fully penetrates the film. Inside the biofilm, some acetate is produced due to decay of bacteria, however all of this produced acetate is used up before penetrating to the bulk water. Possible release of phosphate due to the produced acetate by the bottom of the film is insignificant – too low for detection according to the phosphate profiles. (c) and (d) show the diffusion profiles of acetate and phosphate during the anaerobic phase before backwash, respectively 1 hour after start of the phase

and by the end of the 3 hour phase. Nitrate is not shown since no nitrate is present in the anaerobic phase except for the initial transition period (~20 min). Significant release of phosphate accompanied by uptake of acetate is evident in the top 200-250 μm of the film after 1 hour of anaerobic phase, however, since no polyphosphate pools are available below this thickness no reactions can take place here. By the end of the phase, almost no release or uptake takes place due to empty polyphosphate storage pools also in the top layers.

Figure 9.9 shows figures equivalent to Fig. 9.8, but after backwash has been performed on Day 35 – note the different scale of the x-axis due to the reduced biofilm thickness. Phosphate now fully penetrates the biofilm by the end of the anoxic phase, Fig. 9.9(b). Higher phosphate concentrations are seen by the end of the phase (Fig. 9.9b) than after 1 hour (Fig. 9.9a), which is caused by reduced uptake due to depletion of internal PHB pools. However, as also evident from the figures above, reaction rates in the biofilm during the very first cycle after backwash are reduced due to depleted storage pools in the previously 'buried' layers. Already cycle number 2 after backwash is phosphate diffusion limited in that phosphate throughout the anoxic phase only penetrates the top 150-200 μm layer, Fig. 9.10.

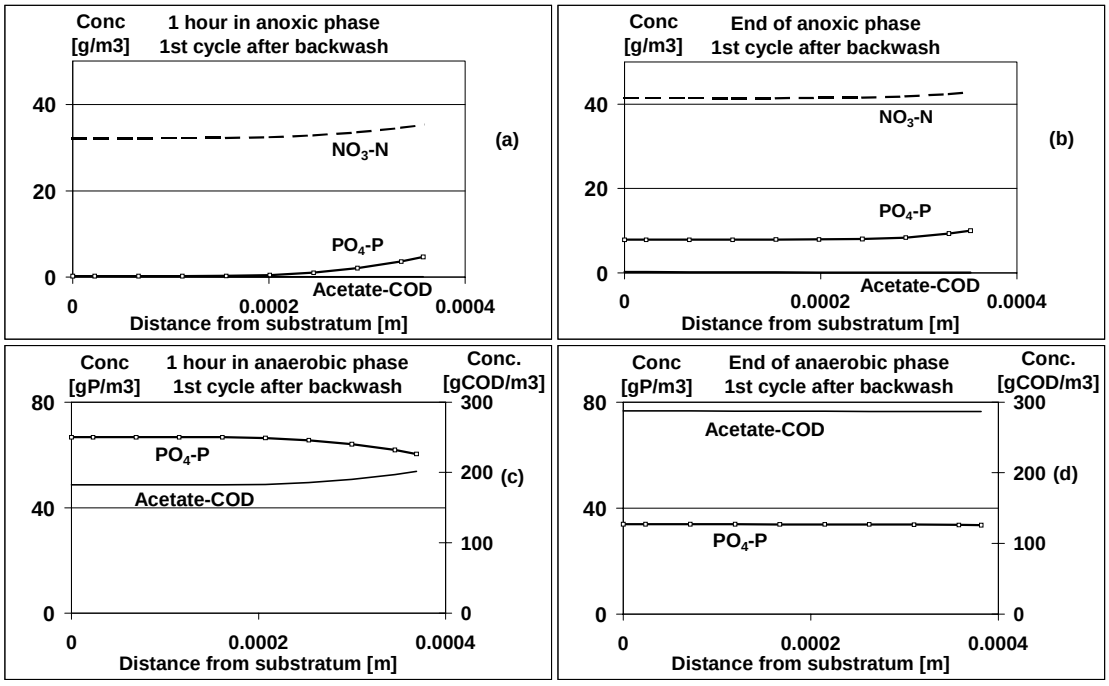

Figure 9.9. Equivalent to Fig. 9.8, but 1 cycle after backwash. Note the different scale of the x-axis due to the reduced biofilm thickness after backwash. See text for explanation

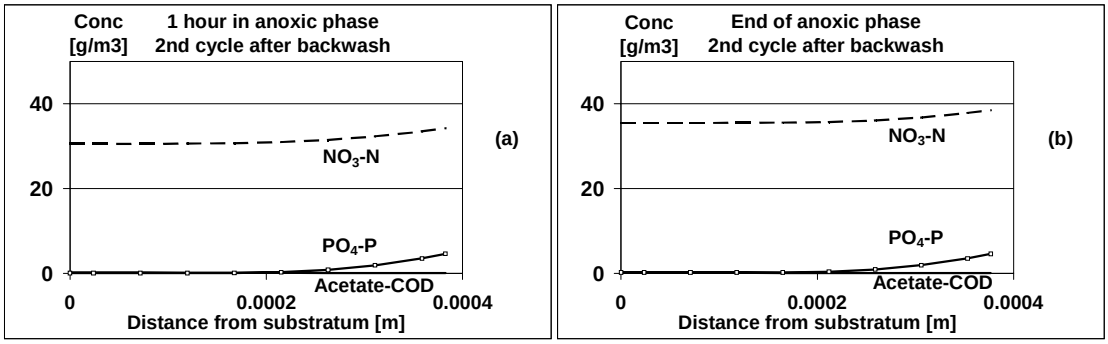

Figure 9.10. Equivalent to Fig. 9.9, (a) and (b), but 2nd cycle after backwash. See text for explanation.

9.1.3 Bulk Concentrations

Figure 9.11 illustrates the simulated bulk water concentrations of phosphate, nitrate and acetate during one period between backwash (Day 28-35).

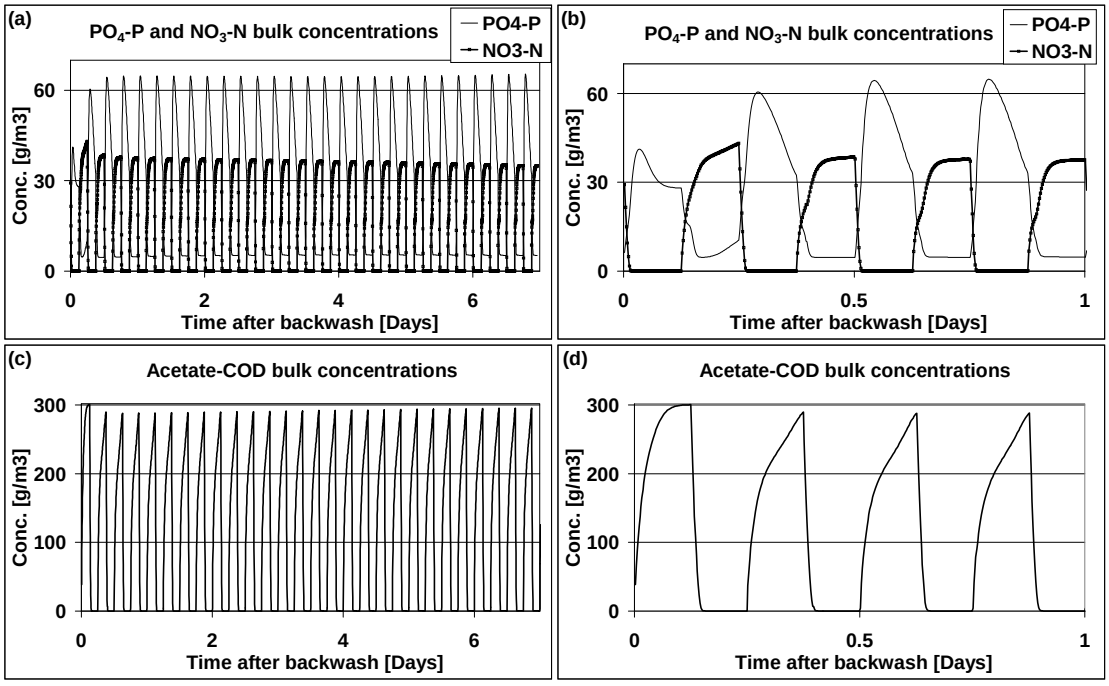

Figure 9.11. Simulated bulk concentrations. Backwash interval: 7 days. Biofilm thickness after backwash: 350 mm. 3 hours phase lengths. (a) and (b) Phosphate and nitrate, different scales on the x-axis (7 and 1 days. respectively). (c) and (d) Acetate-COD, different scales on the x-axis (7 and 1 days. respectively).

The bulk concentrations are not in numerical agreement with the observed concentrations, but qualitatively the curves resemble well the experimental data.

The simulated phosphate concentrations are a bit higher during anaerobic phases than what was observed experimentally: simulated ~64 ppm P and experimentally ~45 ppm P, and the concentrations during anoxic phases a bit lower than experimentally: simulated ~5 ppm P compared to measured ~14 ppm P, refer to Fig. 8.4. The simulated nitrate and acetate values were both a bit higher than actually observed - measured end-values during the respective phases were for anoxic phases ~30 ppm N against the simulated ~37 ppm N, and for anaerobic phases ~198 ppm COD against the simulated ~290 ppm COD. The lower experimental values of both nitrate and COD indicate either that other bacteria are involved in storage and degradation of these compounds, or different stoichiometric coefficients of the PAOs in the biofilm than what is given by the default ASM2d values. However, measurements of COD were only occasionally performed during the experimental runs and on-line measurements of nitrate were not consistently maintained during the second experimental run of PART B, so some care should be made in the comparison of these compounds with the simulation. For a non-calibrated model, the simulated results obtained by default values are in satisfactory qualitative agreement with the measured data.

9.1.4 Biofilm Thickness, Backwash Interval and Phase Lengths

9.1.4.1 Competition between PAOs and non-PAO heterotrophs

Figure 9.12 shows the P content in different layers of the biofilm just before the time of backwash, when different biofilm thicknesses after backwash were tested with the model. The phase lengths and backwash interval were as above, 3 hours and 7 days, respectively. One curve on the figure is the result of one simulation. The number by each curve indicates the biofilm thickness after backwash. The biofilm thickness before backwash can be read on the x-axis (the end point of the curve). The peak of the phosphate curve moves inwards for thinner films. This is the result of a balance between mainly two processes:

1) Diffusion and
2) Growth/death of the two types of organisms, PAOs and non-PAO denitrifying heterotrophs.

One characteristic feature of the considered continuous setup is the simultaneous presence of acetate and nitrate during transition from one phase to the other. This gives the possibility for traditional denitrifying heterotrophs (X_D) to survive in the system. For thin biofilms (<~50 μm after backwash), the film is fully penetrated, which would lead to a uniform distribution of the phosphorus content, i.e. a horizontal profile. However, for thin biofilms, faster growing non-PAO organisms dominate the film and especially the top part, whereby the maximum P content of the film is found in the deepest layers. For thicker biofilms, diffusion limitation sets in and only the top part of the film is

penetrated with phosphate, leading to a phosphate peak in the top layer of the film. Figure 9.13 shows examples of the ratio between the two considered organisms for different thicknesses after backwash. Phase lengths were 3 hours, and the backwash interval was 7 days. Figure 9.13a shows the distribution inside the biofilm before backwash, and Fig. 9.13b shows the integrated amount [%] over the total depth. The ratio was calculated as the percentile mass ratio of the two different bacteria types relative to the total mass of bacteria, i.e. the storage compounds PP and PHB, and inert material were not included in the calculation.

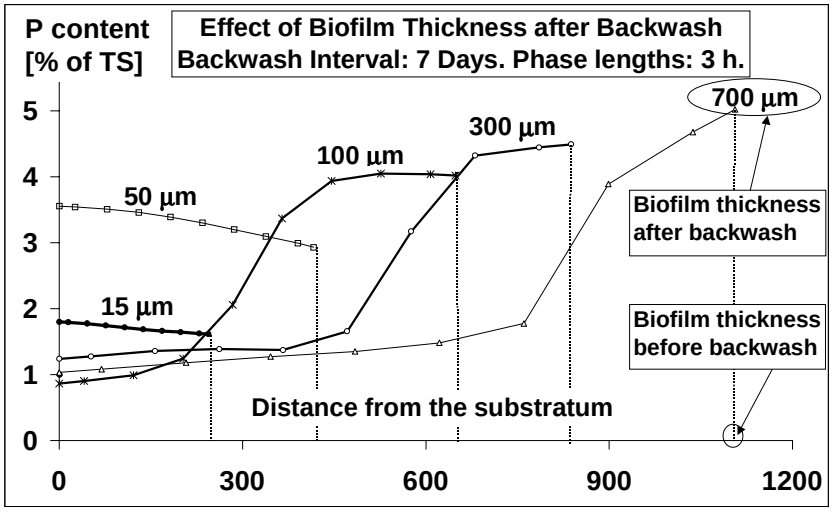

Figure 9.12. Modelled phosphorus contents in different layers of the biofilm before backwash. Backwash interval: 7 days, and phase lengths: 3 hours. Different biofilm thicknesses after backwash were modelled, this thickness is indicated by each curve. E.g. for the 700 µm thickness after backwash, the biofilm just before backwash is 1100 µm (x-axis). The points on the curves are not measure-points, but used to distinguish between the different modelled curves.

The highest ratio of the slow-growing PAOs is in all cases found closest to the substratum, equivalent to the 'oldest' parts of the biofilm, Fig. 9.13a. For very thin films, the competitive advantage of the PAOs is hampered in the favour of the faster growing non-PAO heterotrophs - a certain mean cell residence time in the biofilm is required for the slow-growing PAOs to dominate the biofilm over the faster growing non-PAO heterotrophs. Competition for space in a biofilm consisting of bacteria with different growth rates is also known from e.g. simultaneous nitrification and COD removal, where nitrifiers have been shown to reside in deeper layers of the biofilm overgrown by faster growing heterotrophs. For a biofilm thickness of 15 µm after backwash, non-PAOs constitute more than 95 % of the bacteria cell mass in the film. A biofilm thickness of ~60 µm after backwash sets the dividing line between when non-PAOs and PAOs dominate the biofilm, Fig. 9.13b.

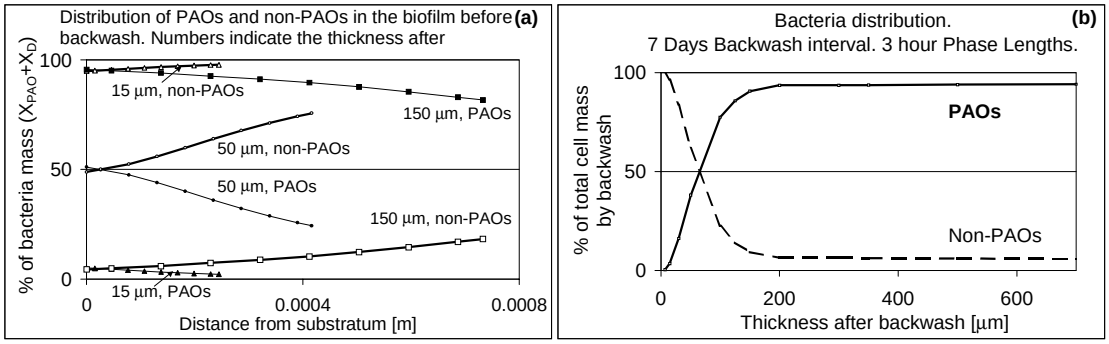

Figure 9.13. Modelled competition between PAOs and non-PAOs in the continuous system for a backwash interval of 7 days and phase lengths of 3 hours. (a) shows distributions inside the biofilm (b) shows the integrated amount [%] over the total biofilm depth. For thin biofilms, <60 µm after backwash, the faster-growing non-PAOs dominate the film.

A major parameter for the outcome of the competition between the PAOs and non-PAO heterotrophic denitrifiers was identified to be the respective decay rate. Figure 9.14 shows the effect of PAO decay rates in the interval 0 - 0.4 d^{-1} on the percentage of PAOs versus non-PAOs in the biofilm at the time of backwash. The decay rate of the denitrifying heterotrophs was kept constant at 0.24 d^{-1}, the backwash interval was 7 days and 3 hours phase lengths were used. The biofilm thickness after backwash was 200 µm. As seen from the figure, a PAO decay rate of 0.175 d^{-1} sets the dividing line between when PAOs, respectively non-PAOs, dominate the biofilm.

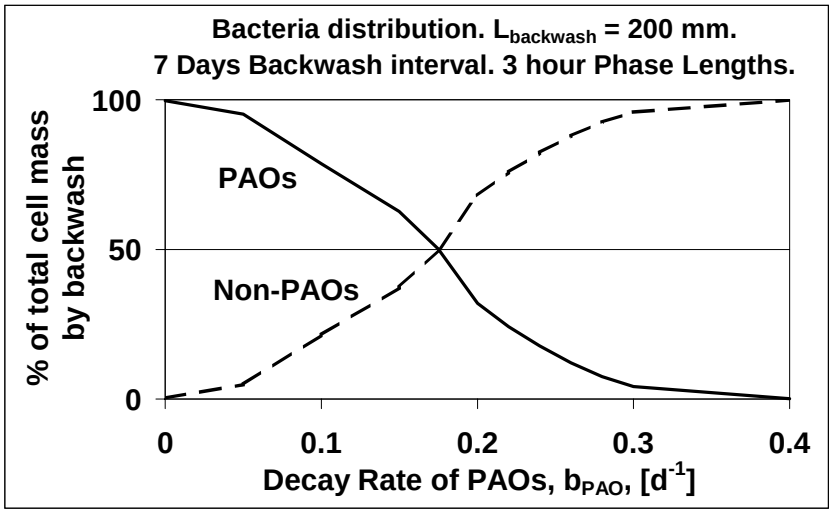

Figure 9.14. Modelled competition between PAOs and non-PAOs in the continuous system for different values of the PAO decay rate. The integrated amount [% of total cell mass] over the total biofilm depth before backwash is shown as a function of the PAO decay rate. The decay rate of non-PAOs was kept constant at 0.24 d^{-1}. Backwash interval: 7 days, phase lengths: 3 hours, and biofilm thickness after backwash: 200 µm. Based on literature information, the decay rate of PAOs was for all other simulations 0.05 d^{-1}.

Wentzel *et al.*, 1989, reported decay rates of PAOs of 0.04 d^{-1} as oppose to 0.24 d^{-1} for heterotrophs. Smolders *et al.*, 1994b found a PAO decay rate of 0.06 d^{-1}. These findings were the basis of the modelling made here, where the decay rate was set to 0.05 d^{-1} for PAOs and 0.24 d^{-1} for denitrifying heterotrops. Little research has been made regarding the decay rate of PAOs. The ASM2d uses a decay rate of PAOs that is half of the one for heterotrophs (0.2 d^{-1} and 0.4 d^{-1}, respectively). If this is used, the heterotrophic fraction in the biofilm at steady state is significantly higher than for the simulations reported here.
Another important aspect of decay is the accumulation of inert particles inside the film, which increases for increasing decay. Due to the significant importance of the low decay rate of PAOs for the competitive advantage over non-PAO heterotrophs this could deserve further research attention.

9.1.1.2 Influence of Backwash Interval

Figure 9.15 illustrates the effect of different backwash intervals for different biofilm thicknesses after backwash. The phase lengths are as above 3 hours. The backwash intervals: 1, 3 and 7 days are shown, and also one point for a backwash interval of 21 days and a very thin, 15 μm, biofilm thickness after backwash. A total curve for a 21 day interval could not be made, since the biofilm thickness for the thin thickness before backwash already was ~1100 μm and a thicker thickness would be problematic for the calculation, since not enough room is available in the reactor volume (in practice = clogging).

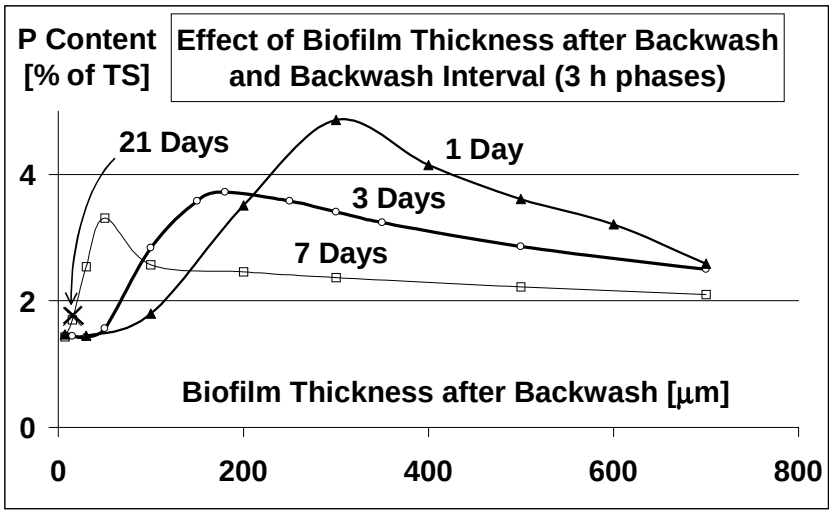

Figure 9.15. Effect of backwash interval and biofilm thickness after backwash on the average P content of the total biofilm biomass (average over the total biofilm depth at the time of backwash).

The figure illustrates the average phosphorus content for the *total* biofilm depth. It is seen that the maximum phosphate concentration of the biomass is obtained for increasing biofilm thicknesses after backwash for decreasing backwash

interval. The explanation is the same as discussed above – the balance between diffusion and growth/death of the two considered types of organisms. For the tested backwash intervals, the highest average P content of the total biomass, 4.9 %, was found for the combination of a 1 day backwash interval with a biofilm thickness of 300 μm after backwash.
The point for a 21 day backwash interval has been included to indicate which average P content could be expected, if sloughing of the biofilm where e.g. one third of the thickest parts of the biomass detach during backwash, as discussed in section 9.3.3. During the experimental investigations it was found that approximately one third of the total amount of biomass detached during the weekly backwash. According to the model, an average P content of 1.8 % is to be expected for a biofilm growing from 15 μm to ~1100 μm during 21 days. The longer backwash interval makes an advantage for the slow-growing PAOs, so that even for the very thin biofilm thickness after backwash they compete well with the non-PAOs. Before backwash, PAOs make up 77 % of the total bacteria mass in the biofilm, Fig. 9.16.

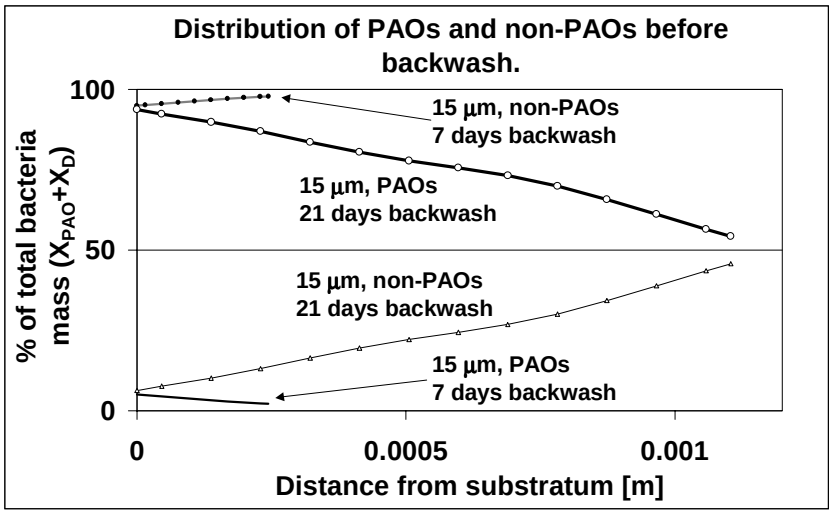

Figure 9.16. Effect of backwash interval on the competition between PAOs and non-PAOs for a very thin biofilm thickness after backwash (15 μm). For a 7 days interval, non-PAOs dominate the film (>95 %), but for 21 days interval, PAOs compete well and makes up 77 % of the bacteria cell mass at the time of backwash (integration over the total biofilm depth).

For the backwash intervals 1, 3 and 7 days, also the average P content of the biomass removed by backwash (in the model), i.e. the biomass above the biofilm thickness after backwash, has been calculated. Figure 9.17 shows the results of these calculations. The data from Fig. 9.15 of the average P content taken over the complete biofilm depth are included for comparison.

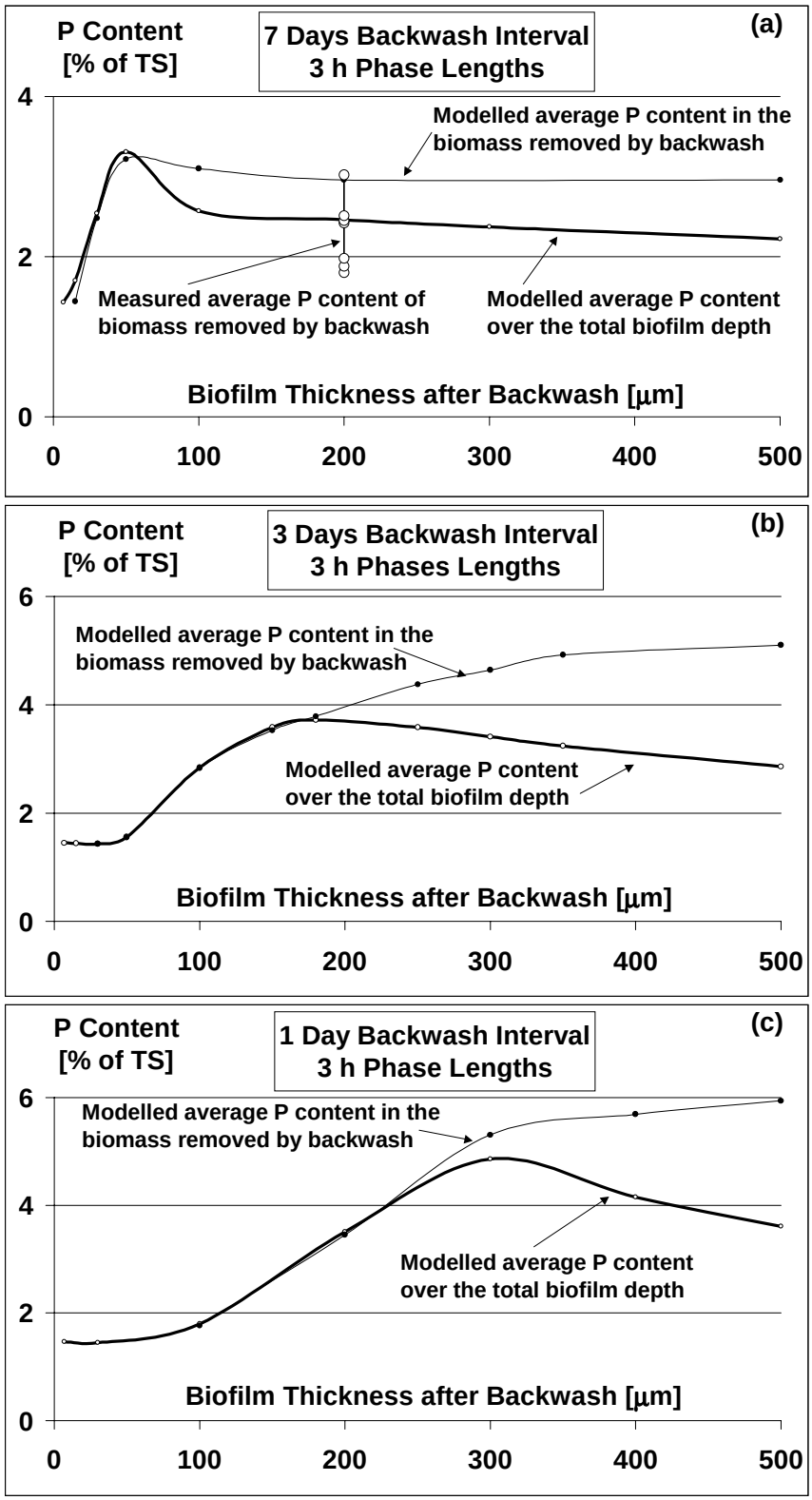

Figure 9.17. Average P contents of the total biomass at the time of backwash, and of the biomass detached by backwash (i.e. the biomass above the specified biofilm thickness after backwash). 3 hour phase lengths. (a) 7 days backwash interval. (b) 3 days backwash interval. (c) 1 day backwash interval.

The curves for the average P content of the biomass removed by backwash and of the complete biomass follow each other until diffusion limitation becomes of significance. For biofilm thicknesses above this point, the average P content of the biomass removed by backwash (the top layers) are higher than the average of the total biomass. The highest average P contents of the detached biomass are found for the shortest backwash interval. This is because the biofilm thickness before backwash is smallest, the shorter the backwash interval and hence, the relative mass of bacteria with PP storage (not diffusion limited part of the film) is higher. Experimental findings are included in Fig. 9.17(a). Experimentally, 7 days backwash interval was used. The biofilm thickness after backwash varied in the interval 0-469 μm, but was predominantly above 100 μm (Fig. 8.11). The measured P contents of the detached biomass are plotted against a thickness of 200 μm. As seen, it cannot from these data be concluded whether backwash in practise removed mainly the top or cohesive parts of the biofilm (sloughing), a tendency of the latter is found. For a conclusion based on the measured P content of detached biomass, a different combination of biofilm thickness and backwash interval, would have been preferential. Considering measuring uncertainty etc. a greater difference of the average P content of the total biomass and the top biomass would be needed to conclude from measured data, e.g. a 1 day backwash interval with a biofilm thickness of ~500 μm after backwash.

9.1.1.3 Influence of Phase Length

From the above, it is clear that the highest P contents of the biomass is found in the phosphate penetrated layers of the biofilm. For very thin films, diffusion limitation does not limit the process, but PAOs loose the competition for space in the biofilm with faster growing non-PAO organisms. The growth of the competing organisms is based on the transition period between two phases in the continuous system, where organic matter and electron donor are present simultaneously. A way to suppress this growth would therefore be to run the system with longer phase lengths, whereby the relative time periods for growth of non-storing organisms would be reduced. Figure 9.18 shows the results of simulations where different phase lengths: 3, 5 and 8 hours were modelled for a biofilm thickness of 300 μm after backwash. Different backwash intervals were tested. The longer the phase lengths, the higher the average P content. For 8 hours phase lengths, phosphorus contents as high as 16 % was found in the biomass removed by backwash by a 3 days backwash interval and 300 μm biofilm thickness after backwash.

The longer phase lengths result in a reduced ratio of non-PAOs in the film, Fig. 9.19. The biofilm by the time of backwash is thinner than for shorter phase lengths, because no non-PAOs take up space, and because the longer anoxic phases lead to less accumulation of PHB in the film. The longer anoxic phase length additionally leads to higher phosphorus contents of the bacteria cells in the phosphate-penetrated region of the film. It is characteristic that the thickness of the top phosphate rich layer of the biofilm (~300 μm) not increase

significantly by the use of longer phase lengths, only the stored phosphate *concentration*. This indicates that the bacteria still have excess storage capacity available, no depletion of PHB occur even for the 8 hour phase lengths. One could have expected that longer phase lengths would cause depletion of the stored PHB or completion of the poly-phosphate storage capacity in the top layer of the biofilm, whereby uptake would cease allowing for deeper penetration of phosphate as a function of time during one anoxic phase. Apparently, none of these criteria were reached. As previously discussed, the PHB levels in practise could deserve investigation.

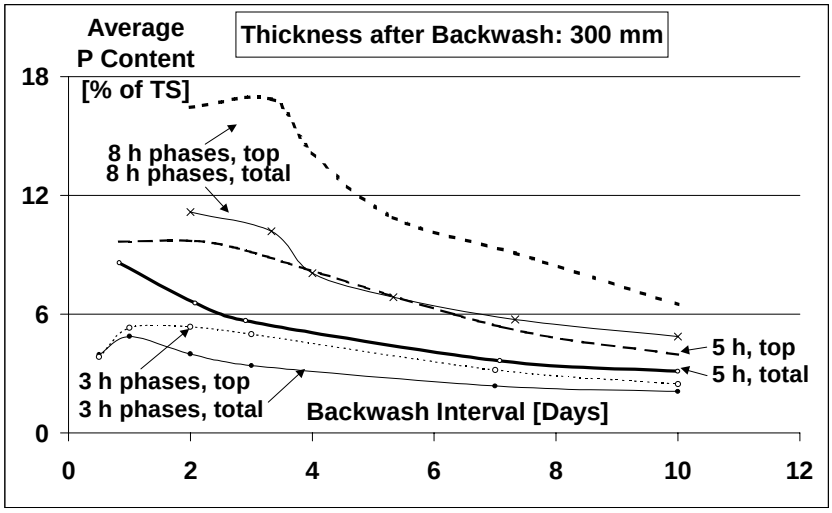

Figure 9.18. Effect of different phase lengths in regard to the average phosphorus content of the biomass by the time of backwash. 'top' refers to the biomass above the biofilm thickness after backwash (300 μm), i.e. the biomass detaching during backwash, whereas 'total' is the total biomass.

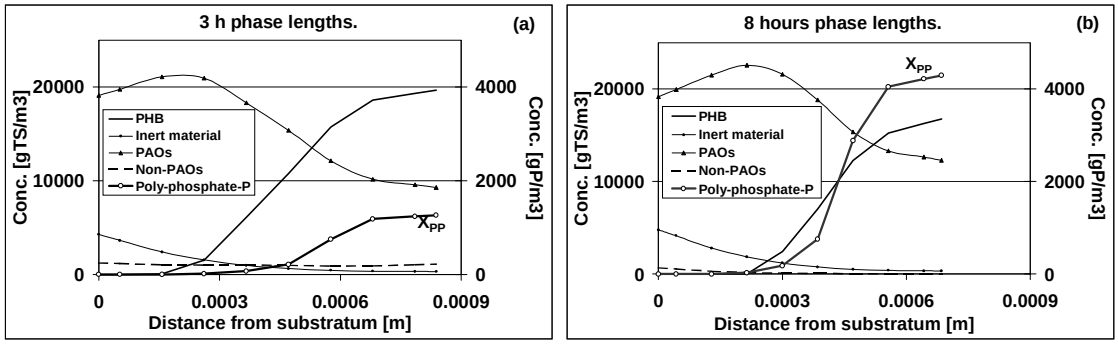

Figure 9.19. Modelled distribution of particulate compounds inside the biofilm before backwash for a biofilm thickness of 300 μm after backwash, 7 days backwash interval and (a) 3 hours phase lengths or (b) 8 hours phase lengths.

9.1.1.4 Phosphate Removal Capacity - Active Biomass Concentration

In the above discussion, focus was on the achievable phosphorus content of the biomass. Elevated phosphorus contents of the biomass is one criteria for EBPR, however not the only one. Another question is the phosphate removal capacity in terms of how much phosphate can be removed from the water phase, which is determined by the amount of active PAO biomass. Figure 9.20 shows the modelled outlet concentration of phosphate in the continuous system after backwash for a biofilm thickness of 50 and 350 μm after backwash, respectively. 3 hours phase lengths and a 7 days backwash interval was used. The thin film after backwash avoids phosphate diffusion limitation in the biofilm, but the low biomass concentration has a significant negative effect on the mass of phosphate that is involved in the EBPR process. For the 350 μm thick biofilm, only the very first cycle after backwash is influenced. No steady level is reached for the thin biofilm, and the mass of phosphate involved in the bio-P metabolism (amplitude of the curve) is much smaller than for the thick film. The difference between the two cases of limitation: 1) Limitation due to a low mass of PAOs (thin film) or 2) Limitation due to phosphate diffusion limitation (thick film) is reflected in the shape of the outlet concentration curves. These agree with the hypothesis outlined in chapter 6.3 of increasing amplitude of the curve for an increasing mass of PAOs in a fully penetrated thin biofilm, whereas a stable level is reached for the thicker film where diffusion limitation controls the process. The curve trend of the thin biofilm (increasing amplitude) was observed during the upstart of the experimental runs in PART B, indicating full penetration of the biofilm during this period, whereas more stable concentration levels were observed later in the experimental period.

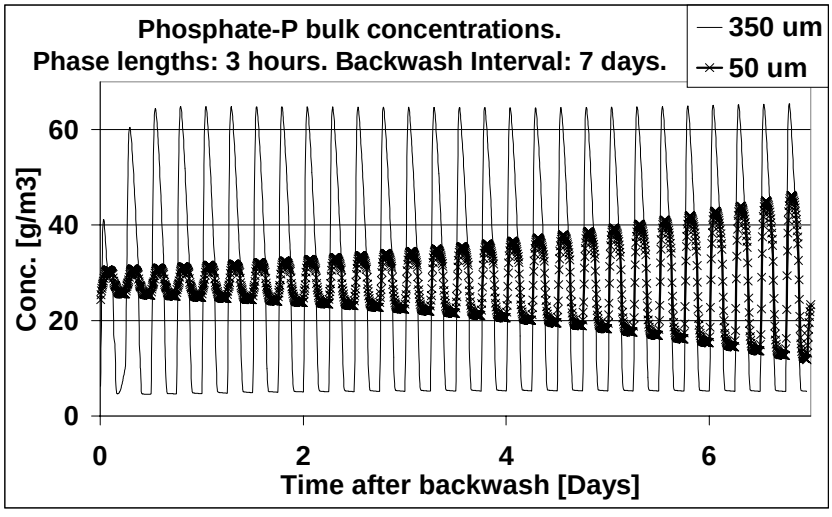

Figure 9.20. Effect of different biofilm thicknesses after backwash, 50 and 350 μm, on the bulk concentrations of phosphate. The amplitude of the curve can be taken as an indication of the EBPR activity – the bigger the amplitude, the higher amounts of phosphate is involved in the polyphosphate-storage process.

When relatively thin biofilms are required in order to avoid diffusion limitation and hence significant inactive parts of the biofilm, one can ask, if this then still lead to higher volumetric biomass concentrations in biofilters compared to activated sludge systems. Usually, higher biomass contents are stated as one of the advantages of biofilters over AS. The experimentally investigated reactor had a very high biomass content, ~20 gTS/l, but as illustrated, only a fraction of this was actively contributing to the phosphorus removal process. To answer the question whether biofilters generally contain higher amounts of *active* biomass than activated sludge systems, investigations are needed. In order to give an idea, a small, approximate calculation shall be given here, however this should be seen only as a speculative and inaccurate theoretical evaluation. Imagine the use of a spherical carrier material with a radius of 3 mm (comparable to Biolith used experimentally). The porosity of Biolith is ~0.45. If a uniform biofilm thickness of *250 μm* is attached to this carrier (the penetration depth of phosphate in most simulations), the number of carriers in a 1 L reactor volume would be:

$$\begin{aligned} &\textit{Volume of Sphere}: \frac{4}{3}\cdot\pi\cdot r^3 \quad (\mathrm{r} = \text{radius}) \\ &\text{Spheres pr. 1 L reactor volume}: \quad \frac{(1-0.45)\cdot 1\cdot 10^{-3} m^3}{\frac{4}{3}\cdot\pi\cdot(0.003m+0.00025m)^3} = 3825\ spheres/L \end{aligned} \tag{9.1}$$

Hence, the wet biomass volume in 1 L would be:

$$\text{Wet Biomass Volume pr. 1 L reactor volume}:$$

$$3825\ spheres/L \cdot \left(\frac{4}{3}\cdot\pi\cdot(0.00325m)^3 - (0.003m)^3\right) = 1.17\cdot 10^{-4}\ \mathrm{m}^3/L \tag{9.2}$$

With a solid fraction of 0.36 in the biofilm matrix and a biomass dry density of 70.000 gTS /m^3 this corresponds to a solid biomass density of *3.0 g TS/L*. Activated sludge plants are typically operated with suspended solids concentrations of ~4 g TS/L.

9.5 Key Results of PART C of The Study

1) The simplified 1-D biofilm model incorporated in AQUASIM was in good qualitative agreement with the experimental observations and hypothesis outlined in chapter 6.3.

2) The model revealed that the experimentally found low average phosphorus contents of the biomass that detached during backwash (2.4 %) could be explained by phosphate diffusion limitation. For backwash once a week and 3 hour phase lengths (as used experimentally), the modelled average P contents over the total depth of the film was ~ 2.5 % and of the top layers removed during the modelled backwash ~ 3.0 %.

3) When operating the system with a thin biofilm (<60 μm after a weekly backwash) denitrifying heterotrophs almost completely out-competed the PAOs and not much bio-P activity remained. However, PAOs stayed in the system, and their activity improved with increasing thickness of the growing biofilm.

4) A way to improve the phosphorus content of the biomass in the studied system was to keep the biofilm thin (either by short backwash intervals or an adequate backwash procedure) combined with the use of longer phase lengths. The thin biofilm avoids diffusion limitation, and the long phase lengths suppress the growth of denitrifying heterotrophs. The longer phase lengths additionally allow the bacteria to take up higher amounts of phosphate. In this way, phosphorus contents as high as 16 % was found (8 hours phases, 3 day backwash interval and 300 μm biofilm thickness after backwash). The payoff when using thin biofilms was low biomass concentrations in the reactor and hence low absolute amounts of phosphate removed from the bulk water.

The model revealed a delicate balance between phase lengths, backwash frequency and biofilm thickness in regard to obtainable phosphorus contents of the biomass and the relative ratio of PAOs and non-PAO heterotrophs. This relationship has never been addressed in reported studies of EBPR with biofilms, which makes it appear as if good EBPR in many cases might have been achieved on the basis of an accidental fortunate combination of the different parameters.
In order to control EBPR in a biofilter system, a well-controlled backwash strategy is required. Backwash intervals as well as optimal biofilm thickness and phase lengths have to be evaluated in relation to wastewater composition and removal objectives. Modelling appears to be a valuable tool in such an evaluation due to the complexity of the process. A way to control a biofilm thickness within a defined interval in a practical biofilter is still to be revealed.
To avoid competition between the two groups of organisms, a complete separation of COD and nitrate may be a solution. This may be difficult in a continuous flow system exposed to varying wastewater compositions, but is perhaps better done in e.g. sequencing batch biofilm reactors with 100 % water exchange ratio.
For a practical system operated with wastewater, the additional complexity of adsorption and on-going hydrolysis of particulate COD complicates the process regarding competition between PAOs and non-PAOs.

10. Summarising Discussion of The Study

HYPOTHESIS: It was hypothesised that a thick biofilm could be problematic in regard to phosphate removal due to consequences of diffusion limitation and zonation in the film. A relatively dense biofilm structure was expected based on the operating conditions with: High nutrient availability, high shear, a multispecies bacterial community and a low growth rate of PAOs. For a dense biofilm structure, molecular diffusion into the biofilm would be the major transport mechanism, leading to zonation in the biofilm. If phosphate was the limiting substrate, no excess phosphate removal was expected, since all phosphate taken up would be released in the following anaerobic phase by COD penetrating the film deeper than the poly-phosphate rich layers. Low average phosphate contents of the biomass from a thick biofilm for EBPR was expected due to diffusion limitation of phosphate.

PART A of the study verified that a 1-dimensional approach of the biofilm with molecular diffusion serving as the main transport mechanism was a reasonable approach. ½ and 0 order rates in the bulk water was observed according to the theory of the biofilm diffusion model, where transition from ½ to 0 order rate will take place once the bulk concentrations get high enough to fully penetrate the film. In order to compare different batch experiments, the initial release or uptake rates during batch tests were used.
It appeared that the bacteria in the deeper layers were able to perform immediately when met with substrate – as indicated by batch tests, where high substrate concentrations were tested. This was a bit surprising, since the bacteria in these layers most likely would have emptied their internal storage pools and some time for regeneration would have been expected.
The biological P activity as indicated by maximum phosphate concentrations in the outlet during anaerobic phases and minimum phosphate concentrations during anoxic phases varied over the 1½ year period of operation despite the use of well-defined, non-changed operation and synthetic wastewater. These variations were attributed to hypothesised shifts of the microbial population in the biofilm.
Mass balances of the continuous operation indicated that no excess P removal took place, since the same mass of phosphate was released during anaerobic phases as taken up during anoxic phases. The mass stayed constant during steady state operation, which indicated only partly penetration of the film. For a fully phosphate penetrated biofilm, increasing mass of phosphate taken up and released would be expected between subsequent cycles, due to an increasing amount of biomass (as indicated by an increasing amplitude of the phosphate outlet concentration curve). However, the mass balances of the continuous operation were difficult due to changing inlet concentrations between the two

phases and a very high sensitivity of the calculation to the exact value of the inlet concentration.
Stoichiometric coefficients of the phosphate removal process were low compared to values stated in the literature. The stoichiometry of phosphate released pr. COD taken up was: 0.25 g P/g COD in Nov'97 and decreased during the study to a final value of 0.14 g P/g COD in Dec'98. However, this might be due to lower pH (regulated to 7) in the latest part of the study. The literature cites a value of 0.46 g P/g COD for activated sludge cultures at pH = 7 (Smolders *et al.*, 1994a). The coefficient of phosphate taken up per nitrate removed during anoxic batch tests was observed: 0.65 g P/g N = 0.058 mol P/ mol e^- (Nov'97-Jan'98). Kuba *et al.*, 1993, cites a value of 2.1 g P/g N for an enhanced denitrifying PAO activated sludge culture.
The low coefficients during both anaerobic and anoxic phases indicate the presence of other bacteria with the capacity of storing COD under anaerobic conditions and degrading it via nitrate during anoxic periods, or a different phosphate metabolism of PAO biofilm bacteria compared to previously studied activated sludge cultures. Since Kerrn-Jespersen *et al.*, 1994, found stoichiometric coefficients of an EBPR biofilm system in agreement with Kuba *et al.*, 1993, the presence of other bacteria appear as the most likely reason.
The yield coefficient in the system was estimated from measured bulk outlet concentrations of COD and masses of total solids removed from the system. The coefficient was 0.23-0.27 g TS/g COD. This is low compared to aerobic systems, but in agreement with the finding of Kuba *et al.*, 1993, who found a yield coefficient of 0.25-0.30 for an anaerobic/anoxic AS EBPR system. A low yield is identical to a low sludge production.

PART B of the study showed that denitrifying PAO activity could be induced in two different biofilms originating from a semi-full scale and, respectively, pilot-scale EBBR SBBRs operated with oxygen as the electron acceptor. Two separate experimental runs were performed. During the first run, a decrease in the denitrifying bio-P activity was observed after 1 month following a change in the anaerobic phase length. This was speculated to be a shift in the microbial population caused by the changed operation. In the second run, biomass samples were collected regularly (the mass removed by backwash) and analysed with fluorescent in situ hybridisation (FISH) and confocal laser scanning microscopy (CLSM). A similar decrease in the activity was seen after 1 month, despite no change of the phase lengths. Hence, the decrease after one month should be seen as a start-up phenomenon. FISH could detect a noticeable shift in the microbial population mainly within the first 2 weeks of upstart. Almost all bacteria belonging to the alpha subclass of *Proteobacteria* disappeared and characteristic clusters of the beta and gamma subclasses were lost. Over the 4 months period, small clusters of Gram-positive bacteria with a high DNA G+C content (GPBHGC) were gradually completely replaced by filamentous GPBHGC. No significant change could be detected around the time of the peak performance.

The characteristic morphology reported for glycogen accumulating organisms (tetrads) was not detected in neither the aerobic nor denitrifying EBPR biofilm sludge. For the denitrifying sludge additionally no bacteria belonging to the alpha subclass of *Proteobacteria* remained, the typical GAO organism has been identified as a member of this group (Blackall *et al*., 1997). This indicate, that GAOs did not accumulate in the biofilm, at least not the typical type known from activated sludge systems. Hence, the low stoichiometric coefficients of the system could not be attributed to the typical GAO organism.
Most cells were detectable with the general *Bacteria* probe. This indicated that all bacteria (i.e. also those residing in deeper layers) were relative active at the time of backwash, since otherwise not enough rRNA to bind the probe would have been produced. This was in agreement with the observations during batch test of PART A.
The diversity of the microbial population of the denitrifying biofilm was low with a characteristic short, oval rod from the beta group of *Proteobacteria* making up the major fraction.
The biofilm thickness was measured by staining with Flourescein 5-isothiocyanate (FITC) prior to microscopic investigation. FITC binds to amino groups and therefore proteins and amino sugar. Hence both cells and extracellular polymer substances (EPS) of the biofilm were stained. The biofilm thickness of the denitrifying bio-P biofilm was very heterogeneous and therefore it was not possible to determine an average thickness. For one spot sample before backwash, the thickness varied in the range of 67 to 1096 μm, mainly above 400 μm, and after backwash 0 to 469 μm, mainly above 100 μm. The aerobic biofilm from the bench-scale reactor was more homogeneous and thinner. Before backwash, the typical thickness was 100-200 μm, and after 0-50 μm. The aerobic biofilm community was inhabited by many protozoan as evident especially after backwash. Most of these apparently stayed attached during backwash, while the bacteria cells between them detached.
The phosphate contents of both types of biofilm biomass (denitrifying and aerobic) was consistently low, 24 ± 4 mg P/g TS, compared to the reports in the literature of phosphate removing sludge (up to 16 %). This was for the denitrifying biofilm speculated to be due to phosphate limitation during the anoxic phases. The situation for the aerobic biofilm was different, since it was operated in a SBR mode with low P contents after the aerobic phase, in this case, a limitation in the available mass of phosphate occurred. The phosphate contents of this biofilm was immediately elevated to 35 ± 2 mg P/g TS by feeding the reactor additional phosphate.

PART C of the study illustrated by modelling that only relatively low phosphate contents of the biomass could be obtained in the investigated continuous system with 3 hour phase lengths. For a biofilm thickness after the weekly backwash of 200 μm, the average phosphate content of the detached biomass during backwash was ~3 %, which agrees well with the findings of

PART B. It also showed, that low P contents was not a result of accumulation of other organisms in the biofilm, since PAOs dominated the biofilm (GAOs were not included in the model). A way to improve the phosphate content of the biomass in the studied system was to keep the biofilm thin (either by short backwash intervals or an adequate backwash procedure) combined with the use of longer phase lengths. The thin biofilm avoids diffusion limitation, and the long phase lengths suppress the growth of denitrifying heterotrophs. The longer phase lengths additionally allow the bacteria to take up higher amounts of phosphate. In this way, phosphate contents as high as 16 % was found (8 hours phases, 3 day backwash interval and 300 μm biofilm thickness after backwash). The payoff when using thin biofilms was low biomass concentrations in the reactor and hence low absolute amounts of phosphate removed from the bulk water. The use of a thin biofilm and longer phase lengths were not tested experimentally. However, the good qualitative agreement of the model with the available experimental data supports the reliability of the model as an appropriate indicator of real phenomena.
A significantly lower decay rate of the PAOs compared to denitrifying heterotrophs was identified as one of the key factors for their competitive advantage in the considered system.
The high sensitivity of e.g. biofilm thickness (and possibly other non-identified parameters) to the competition between the two organisms included in the model, indicate well, why the process displayed significant variability during the 1½ year period of PART A. In reality an interplay between several species is to be expected, e.g. also sulphate reducing bacteria in the bottom of a thick biofilm.
The model was not calibrated and used default values from the Activated Sludge Model 2d (except for the decay rate), hence the exact numerical values should be taken with some reservation. The model was in qualitative agreement with the experimental observations and hypotheses, which illustrated its strength as an explanatory tool for enhancement of understanding of the considered biofilm process, despite the very simplified model structure.

EBPR in biofilms - literature: Generally no reports of biofilm thickness are given for studies of EBPR in biofilms. According to the findings of this study, this is a crucial parameter for understanding observed phosphate contents of different biofilm sludges. The highest reported average phosphate content, up to 8-10 %, for a biofilm system with EBPR was supplied by Kerrn-Jespersen *et al*., 1994. They also used a continuous system with nitrate as the electron acceptor. However, between each phase, tap water was used to flush the reactor in order to avoid simultaneous presence of nitrate and acetate. This would avoid competition with denitrifying heterotrophs, which can explain the obtained high phosphate content. Goncalves *et al*., 1994a, used a continuous system similar to the one tested in this study. They reported phosphate contents of maximum 4.1 %. Almost all other studies applied SBR modes, where competition with

heterotrophs are better controlled due to avoidance of simultaneous presence of COD and electron acceptor.

Outlook – Up-scaling? For further studies of the investigated system, or other systems with EBPR in biofilms, it would be interesting to use microbial characterisation methods, possibly including PP, glycogen and PHB measurements, on a micro-sliced biofilm. This could be used to test e.g. the presence of sulphate reducing bacteria, and for a definitive verification of the modelling results of this study, i.e. the zonated biofilm structure with different storage concentrations in different distances from the biofilm surface. Also an experimental verification of the modelled relationships between phase lengths, biofilm thickness and backwash intervals could be desirable.
Regarding up-scaling of the process, a computer model for the total larger-scale system, where several reactors are needed (alternating tanks and a nitrification reactor) is recommended as the first step. In this study, the possible consequences and significance of diffusion was illustrated. For a real continuous flow system, this might be even more important, since these shall be operated with lower substrate concentrations in the tanks (e.g. totally mixed) whereby lower penetration of the film is expected. The question, whether the principle of the investigated system could function in practice – given optimal operating conditions such as relatively long phase lengths combined with thin biofilms – still has to be answered. In this regard, the active amount of biomass in a biofilter compared to activated sludge systems should be investigated.
The current study applied excess COD and nitrate, the possible combinations of limiting substrate for different wastewater compositions are numerous and should be tested. Similarly, different ratios of the anoxic and anaerobic phase lengths could be investigated – here the ratio was kept constant at 1 for all model simulations (equal length of the two phases).

11. Conclusion

A lab-scale biofilm for combined removal of nitrate and phosphorus was build up via a continuous flow system alternating between anaerobic and anoxic conditions. Batch experiments with different start concentrations of acetate, nitrate or phosphate verified ½ and 0 order removal rate in the bulk water outside the film depending on the concentration. This was taken as an indication of a zonation of the biofilm with molecular diffusion acting as the major transport mechanism for soluble compounds.

Relatively low stoichiometric coefficients of the process, 0.25 g P/g COD for anaerobic phosphate release and 0.65 g P/g N for anoxic uptake, were determined via batch tests with no simultaneous presence of COD and nitrate. The findings indicate the presence of other bacteria in the biofilm capable of storage or that the PAOs are capable of changing their metabolism according to the availability of phosphate.

A simplified one-dimensional computer model was developed based on the simulation program AQUASIM. The modelling results were in good qualitative agreement with the experimental observations. This agreement rendered model extrapolations reasonable as indicators of the likely practical behaviour of the system under changed operating conditions.
According to the computer model, a very thin biofilm thickness (< ~60 μm) was disadvantageous for the competitive advantage of PAOs over denitrifying heterotrophs for the considered 3 hours phase lengths. However, by combining a thin film with longer phase lengths, high average P contents (16 %) could be achieved due to no diffusion limitation and suppression of the growth of non-PAO denitrifying heterotrophs. The payoff was a reduced phosphate removal capacity due to the consequently low amounts of biomass. The need of relatively thin biofilms to avoid diffusion limitation reduce the concentration of the active biomass and might thus reduce the volumetric removal rate to a level similar to (or lower than) activated sludge systems?

Answers to the open questions of chapter 3 (p. 65) are as follows:

1. Continuous alternation with nitrate as the only electron acceptor is possible with a biofilm. The bio-P activity remained throughout a 1½-year test period, but the activity varied significantly despite the use of well-defined operation and synthetic feed. The reason was speculated to be shifts in the microbial population. Modelling results verified that e.g. the biofilm thickness has a serious influence on the competition between organisms with different growth and decay rates in a multi-species biofilm.

2. The build up of a denitrifying EBPR biofilm took approximately 1 month when inoculum from an activated sludge plant based on aerobic EBPR was used.

3. Induction of denitrifying EBPR in a biofilm acclimatised with oxygen was possible and took 2 weeks for biofilms originating from different reactor-scales.

4. Zonation in a biofilm could be verified by an EBPR biofilm. ½ and 0 order bulk rates were observed depending on the bulk concentration and hence penetration depth.

5. A thick biofilm lead to release of acetate by decaying bacteria in the bottom of the film during anoxic phases, and this likely cause the release of phosphate in this part (provided that remaining polyphosphate storage is available). However, the significance of such a release was low and could not be detected in the continuous operation (via the model) – likely, any released phosphate was immediately taken up again by the use of nitrate.

6. It appeared from both batch tests and microbiological characterisation that all cells in the biomass were active by the time of backwash once a week, despite diffusion limitation during most of the time between backwashes. This was surprising and in contrast to the computer model where reduced reaction rates of the first cycle after backwash were revealed, resulting from empty storage pools of the 'buried' bacteria.

7. The denitrifying PAOs of the biofilm in this study was apparently different from the aerobic PAO organism that recently was identified as important for aerobic laboratory bio-P processes (*Rhodocyclus* like clone). However, a specific characterisation of the denitrifying PAO of this study was not achieved nor attempted. More general knowledge of PAOs with the development of rRNA targeting probes is needed before a sufficiently precise characterisation and hence distinction may be made.

8. Whether biofilm PAOs are different from activated sludge PAOs cannot be answered for the same reasons as given above.

9. Low P contents of thick biofilms for EBPR were found (2.4 ± 0.4 %). The computer model indicated this to be due to depletion of internal phosphate storage pools of bacteria residing in the deep layers. The bacteria in the deep layers did not contribute to EBPR.

10. The typical reported type of GAO organism was not observed in the investigated biofilm. The observed low P contents could be explained solely

by diffusion limitation. However, reduced stoichiometric coefficients indicated the presence of either non-PAO organisms capable of storage or that the PAOs could adjust their metabolism according to the time periods where phosphate was available or not.

The following recommendations are given regarding future research on EBPR in biofilters:

I. On-line measurements of in particular phosphate in order to record the history of the biomass.

II. Awareness of the delicate balance between substrate concentrations, biofilm thickness, backwash interval, phase lengths etc. that exists in a biofilm system for EBPR.

III. Use of a system that allows for biofilm thickness control.

IV. Investigation of the biofilm detachment mode during e.g. backwash.

V. Use of a micro-slicing technique to investigate zonation. Poly-phosphate and PHB measurements or staining methods could be elegant tools for a direct experimental verification of zonation in an EBPR biofilm.

VI. Continued characterisation and development of new gene probes for the organisms involved in EBPR and as important, the competing organisms.

VII. Investigations of the system behaviour when particulate organic matter is included, e.g. by the use of real wastewater.

VIII. Computer modelling of the total system (i.e. several alternating tanks and a nitrification reactor) before up-scaling. The modelling should include tests of different wastewater compositions and different operating conditions in order to elucidate optimal process configuration. A complete model is necessary to evaluate whether a biofilm process in a given situation can be recommended compared to an activated sludge system.

12. Acknowledgements

The host of the Ph.D.-study was the Department of Environmental Science and Engineering (IMT) at the Technical University of Denmark (DTU), Lyngby, with Professor Poul Harremoës as the main supervisor. I would like to greatly thank him for getting the idea of the project and for assisting with highly qualified scientific supervision and discussions as well as advice and friendly support throughout the project period. Associate Professor Hans Mosbæk was my second supervisor, and he assisted with invaluable help concerning especially the technical development and operation of the computer controlled experimental setup. I thank him for always being very quick to offer help whenever a problem occurred with the computer program, electrical connections or on-line measurement systems. Also for always being optimistic during the occasional breakdowns of the equipment that otherwise would have made me very anxious. My third supervisor, Associate Professor Mogens Henze, was always capable of answering questions regarding the metabolism of phosphorus removal, and he also deserves the credit for regular discussion forums between the university researchers involved in bio-P related topics.

1 year of the study was spent at the Department of Water Quality Control and Waste Management at the Technical University of Munich (TUM) in Germany. This stay was financed by the EU-project BioToBio (Biological Nitrogen Removal: From Biofilms To Bioreactors) and partly by the Research Center for Fundamental Studies of Aerobic Biological Wastewater Treatment (SFB 411, Deutsche Forschungsgemeinschaft). I address my great thanks to Professor Peter Wilderer who let me come and take part in his research team. He had inspiring ideas, was always very accommodating and introduced me among others to the microbiology group at his institute. Dr. Stefan Wuertz leads this group, and he welcomed me to take part in his workgroup, whereby I got the opportunity to learn microbial characterisation methods. In this context, I like to send my most grateful thanks to Dipl.-Biol. Lisa Müller, who very committed and interested supervised me during the learning process and microbial investigation period. Also my thanks to Dr. Martina Hausner for always helpfully and qualified answering questions regarding microbiology and microscopy. My colleague Patrik Arnz deserves my special thank. He operated the aerobic EBPR SBBR reactor that was used for supply of biofilm samples, and he offered biofilm and EBPR discussions of high value to me. The TUM-administer of the BioToBio project: Dr. Brigitte Helmreich deserves a special thank for smilingly helping with all the administrative work regarding my contract and stay in Germany. The laboratory personnel helped with analysis of water and biomass samples for which I thank them. I also like to thank the TUM-workshop for assistance in setting up the experimental setup that I brought along from Denmark.

Dr. Eberhard Morgenroth discussed scientifically the bio-P-process in biofilms and was helpful in assisting with good advice and suggestions, whenever I had questions, especially regarding the computer program: AQUASIM. I thank him for letting me implement the by him developed backwash procedure in my AQUASIM model. I thank Dr. Natuschka Lee from the Microbiology Department at TUM for discussions and advice regarding the use of microbial methods in biological phosphate removal sludge. Especially for providing me with samples of the recently developed probe for the *Rhodocyclus* like groups of bacteria and for showing me traditional staining methods of sludge samples. The IMT-librarians Grete Hansen and Helle Offenberg were always very helpful in procuring all kinds of literature, and I gladly acknowledge this as a very valuable help. The IMT-secretariat was always very kind and helpful and deserves a special thank for forwarding all my mail to Germany, during my stay there. Of my Danish colleagues, I like to address my special thanks to: Marianne Lange, Klaus Dircks, Rasmus Boe-Hansen and Eric Warnaars, whom all supported me and added fun to the study period, I appreciate their help and understanding greatly. Shabbir H. Ghewala, whom I met when he visited IMT and worked next to me in the laboratory, I thank for his friendly and colloquial support throughout the study, also after our ways separated. I could continue this list, since all my colleges at both of the technical universities have been very kind and supporting, and I thank all of them warmly.

For an especially pleasant stay in Germany, also outside of the university building, I thank my very special friend and colleague, Christian Ekkerlein. I appreciate greatly his support, patience and understanding throughout the often very time-consuming study-period.

I would also like to thank the many private Danish funds that were willing to support me financially and hereby making it possible for me to attend conferences etc. in foreign countries and supporting my stay in Germany. I thank, in alphabetical order, the following funds: Augustinus Fonden; Christian og Ottilia Brorsons Rejselegat for yngre videnskabsmænd og –kvinder; COWIfonden; Familien Hede Nielsens Fond; Frimodt-Heineke Fonden; Fabriksejer, Ingeniør Valdemar Selmer Trane og hustru Elisa Tranes Fond; Ingeniør Alexandre Haynman og hustru Nina Haynmans Fond; Knud Højgaards Fond, Løvens Kemiske Fabriks Forskningsfond and Marie Henckels Mindelegat.

For support “behind the scenes”, I also like to thank my brother, Claes Falkentoft. He deserves my happy thank for travelling with me to Munich and staying there for one half year. This made the stay lots of fun also outside of the institute and easier to laugh at the sometimes rather frustrating situations, one occasionally encounters when starting life in a foreign country. All of my family and friends, my very good friend, Mette Boysen, my uncle, Torben Skov, my sisters, Christel and Charlotte, and my parents, Lykke and Karsten Falkentoft, deserve a tremendous thank for always cheering me up, for supportive shoulder claps, for showing their belief in me and for their interest in my study.

13. References

Abu-ghararah, Z. H. and Randall, C. W. (1991) The effect of organic compounds on biological phosphorus removal. *Wat. Sci. Tech.* **23**, 585-594.

Amann, R. (1995) In-situ identification of micro-organisms by whole cell hybridization with rRNA-targeted nucleic acid probes. In Molecular Microbial Ecology Manual. Akkerman, A. D. L., van Elsas, J. D. and de Bruijn, F. J. (eds). Kluwer Academic Publishers. 1-15.

Amann, R. I., Krumholz, L. and Stahl, D. A. (1990a) Fluorescent-oligonucleotide probing of whole cells for determinative phylogenetic, and environmental studies in microbiology. *J. Bacteriol.* **172**, 762-770.

Amann, R. I., Binder, B.J. , Olson, R.J., Chisholm, S.W., Devereux, R., Stahl, D. A. (1990b) Combination of 16S rRNA-targeted oligonucleotide probes with flow cytometry for analyzing mixed microbial populations. *Appl. Environ. Microbiol*. **56**, 1919-1925.

Amann, R. I., Stromley, J., Devereux, R., Key, R. and Stahl, D. A. (1992) Molecular and microscopic identification of sulfate-reducing bacteria in multispecies biofilms. *Appl. Environ. Microbiol.* **58**(2), 614-623,

Amann, R. I., Ludwig, W. and Schleifer, K. (1995) Phylogenetic Identification and In Situ Detection of Individual Microbial Cells without Cultivation. *Microbiol. Rev.* **59**, 143-169.

Andreadakis, A. D. (1993) Physical and chemical properties of activated sludge flocs. *Wat. Res*. **27**, 1707-1714.

Appeldorn, K. J., Kortsee, G. J. J. and Zehnder, A. J. B. (1992) Biological phosphate removal by activated sludge under defined conditions. *Wat. Res.* **26**(4), 453-460.

Arcangeli, J. and Arvin, E. (1995) A membrane de-oxygenator for the study of anoxic processes. *Wat. Res.* **29**(9), 2220-2222.

Arnz, P., Esterl, S., Nerger, C., Delgado, A. and Wilderer, P. A. (2000a). Simultaneous loading and draining as a means to enhance efficacy of Sequencing Biofilm Batch Reactors. *Wat. Res.* **34**(5), 1763-1766).

Arnz, P, Arnold, E. and Wilderer, P. (2000b) Enhanced biological phosphorus removal in a semi full-scale SBBR. To be presented at the IWA Paris2000 Post-congress symposium on sequencing batch reactors (SBR), Narbonne, France, July 2000. *Wat. Sci. Tech.* (2001, in press).

Arun, V., Mino, T. and Matsuo, T. (1989) Metabolism of carboxylic acids located in and around the glycolytic pathway and the TCA cycle in the biological phosphorus removal process. *Wat. Sci. Tech.* **21**, 363-374.

Arvin, E. (1983) Observations supporting phosphate removal by biologically mediated chemical precipitation – A review. *Wat. Sci. Tech.* **15**, Capetown, 43-63.

Arvin, E. (1985) Biological removal of phosphorus from wastewater. *CRC Critical Reviews in Environmental Control.* **15**(1), 25-63.

Arvin. E. and Harremoës, P. (1990) Concepts and models for biofilm reactor performance. *Wat. Sci. Tech.* **22**(1/2), 171-192.

Arvin, E. and Kristensen, G. H. (1983). Phosphate precipitation in biofilms and flocs. *Wat. Sci. Tech.* 15, Capetown, 65-85.

Arvin, E. and Kristensen, G. H. (1985). Exchange of organics, phosphate and cations between sludge and water in biological phosphorus and nitrogen removal processes. *Wat. Sci. Tech.* **17**(11/12), 147-162.

ASM (2000) American Society for Microbiology. http://www.asmusa.org/

Atkinson, B. and Davies, I. J. (1974) The overall rate of substrate uptake (reaction) by microbial films. Part I – A biological rate equation. *Trans. Instn. Chem. Engrs.* **52**, 248-259.

Auling, G., Pilz, F., Busse, H.-J., Karrasch, S., Streichan, M. and Schon, G. (1991) Analysis of the polyphosphate-accumulating microflora in phosphorus eliminating anaerobic-aerobic activated sludge systems by using diaminopropane as a biomarker for rapid estimation of *Acinetobacter* spp. *Appl. Environ. Microbial.* **57**, 3685-3692.

Baetens, D. and Hosten, L. (1996) Biological phosphorus removal using SBR technology: Phenomenological aspects during start up period. *IAWQ Conference on SBR Technology*, Germany.

Baetens, D., Vanrolleghem, P. A., van Loosdrecht, M. C. M. and Hosten, L. H. (1999) Temperature effects in bio-P removal. *Wat. Sci. Tech.* **39**(1), 215-226.

Bakke, R., Characklis, W. G., Turakhia, M. H. and Yeh, A.-I. (1990) Modeling a monopopulation biofilm system: *Pseudomonas aeruginosa*. In: Characklis, W: G. and Marschall, K. C. (eds.) Biofilms. Wiley. New York. 487-522.

Banister, S. S., Pitman, A. R. and Pretorius, W. A. (1998) The solubilisation of N and P during primary sludge acid fermentation and precipitation of the resultant P. *Water SA*. **24**(4), 337-342.

Barak, Y. and van Rijn, J. (2000) Atypical Polyphosphate Accumulation by the Denitrifying Bacterium Paracoccus denitrificans. *Appl. Environ. Microbiol.* **66**(3), 1209-1212.

Barker, P. S. and Dold, P. L. (1996). Denitrification behaviour in biological excess phosphorus removal activated sludge systems. *Wat. Res.* **30**(4), 769-780.

Barnard, J. L. (1974) Cut P and N without chemicals. *Water and Wastes Engineering* **11**, 33-36.

Barnard, J. L. (1976) A review of biological phosphorus removal in the activated sludge process. *Water S.A.* **2**(3), 136-144.

Barnard, J. L., Stevens, G. M. and Leslie, P. J. (1985) Design strategies for nutrient removal plant. *Wat. Sci. Tech.* **17**(11/12), 233-242.

Bayly, R. C., Duncan, A., May, J. W., Schembri, M., Semertjis, A., Vasiliadis, G. and Raper, W. G. C. (1991) Microbiological and genetic aspects of the synthesis of polyphosphate by species of Acinetobacter. *Wat. Sci. Tech.* **23**, Kyoto, 747-754.

Beacham, A. M., Seviour, R. J., Lindrea, K. C. and Livingston, I. (1990) Genospecies diversity of *Acinetobacter* isolates obtained from a biological nutrient removal pilot plant of a modified U.C.T. configuration. *Wat. Res.* **24**, 23-29.

Beimfohr, C., Krause, A., Amann, R., Ludwig, W., Schleifer, K.-H. (1993) In situ identification of Lactococci, Enterococci and Streptococci. *System. Appl. Microbiol*. **16**, 450-456.

Belia, E. and Smith, P. G. (1997) The bioaugmentation of sequencing batch reactor sludges for biological phosphorus removal. *Wat. Sci. Tech.* **35**(1), 19-26.

Biesterfeld, S., Figueroa, L., Hernandez, M. and Russel, P. (1998) Use of fluorescent oligonucleotide probes to characterize vertical population distributions of nitrifying bacteria in a full-scale nitrifying trickling filter. *Proceedings of the IAWQ Conference on Microbial Ecology of Biofilms: Concepts, Tools and Applications.* 8-10 Oct., Lake Bluff, Illinois, USA.

Bishop, P. L. (1997) Biofilm structure and kinetics. *Wat. Sci. Tech.* **36**(1), 287-294.

Bishop, P. and Rittman, B. (1995) Modelling heterogeneity in biofilms. Report from the IAWQ Conference and Workshop on Biofilm Structure, Growth and Dynamics, Noordwijkerhout, The Netherlands. *Wat. Sci. Tech.* **32**(8), 263-265.

Blackall, L. L., Rossetti, S., Christensson, C., Cunningham, M., Hartman, P., Hugenholtz, P. and Tandoi, V. (1997) The characterization and description of representatives of 'G' bacteria from activated sludge plants. *Lett. Appl. Microbiol.* **25**, 63-69.

Boller, M., Gujer, W. and Tschui, M. (1994) Parameters affecting nitrifying biofilm reactors. *Wat. Sci. Tech.* **29**(10-11), 1-11.

Boller, M., Kobler, D. and Koch, G. (1997) Particle separation, solids budgets and headloss development in different biofilters. *Wat. Sci. Tech.* **36**(4), 239-247.

Bond, P. L., Hugenholtz, P., Keller, J., Blackall, L. (1995) Bacterial Community Structures of Phosphate-Removing and Non-Phosphate-Removing Activated Sludges from Sequencing Batch Reactors. *Appl. Environ. Microbiol.* **61**(5), 1910-1916.

Bond, P. L., Keller, J. and Blackall, L. L. (1999) Bio-P and non-bio-P bacteria identification by a novel microbial approach. *Wat. Sci. Tech.* **39**(6), 13-20.

Bonting, C. F. C., Kortsee, G. J. J., Boekestein, A. and Zehnder, A. J. B. (1993) The elemental composition dynamics of large polyphosphate granules in Acinetobacter strain 210A. *Arch. Microbiol.* **159**, 428-434.

Bordacs, K. and Chiesa S. C. (1989) Carbon flow patterns in enhanced biological phosphorus accumulating activated sludge cultures. *Wat. Sci. Tech.* **21**, 387-396.

Borregaard, V. R. (1997) Experience with nutrient removal in a fixed-film system at full-scale wastewater treatment plants. *Wat. Sci. Tech.* **36**(1), 129-137.

Bortone, G., Malaspina, F., Stante, L. and Tilche, A. (1994) Biological nitrogen and phosphorus removal in an anaerobic/anoxic sequencing batch reactor with separated biofilm nitrification. *Wat. Sci. Tech.* **30**(6), 303-313.

Bortone, G., Saltarelli, Alonso, V., Sorm, R., Wanner, J. and Tilche, A. (1996) Biological anoxic phosphorus removal – the Dephanox process. *Wat. Sci. Tech.* **34**(1-2), 119-128.

Bougthon, W. H., Gottfried, R. J., Sinclair, N. A. and Yall, I. (1971) Metabolic factors affecting enhanced phosphorus uptake by activated sludge. *Appl. Microbiol.* **22**(4), 571-577.

Bouwer, E. J. (1987) Theoretical investigation of particle deposition in biofilm systems. *Wat. Res.* **21**(12), 1489-1498.

Brdjanovic, D., Hooijmans, C. M., van Loosdrecht, M. C. M., Alaerts, G. J. and Heijnen, J. J. (1996) The dynamic effects of potassium limitation on biological phosphorus removal. *Wat. Res.* **30**(10), 2323-2328.

Brdjanovic, D., van Loosdrecht, M. C. M., Hooijmans, C. M., Alaerts, G. J. and Heijnen, J. J. (1997) Temperature effects on physiology of biological phosphorus removal. *J. Env. Eng.* **Feb**., 144-153.

Brdjanovic, D., van Loosdrecht, M. C. M., Hooijmans, C. M., Mino, T., Alaerts, G. J. and Heijnen, J. J. (1998a) Effect of polyphosphate limitation on the anaerobic metabolism of phosphorus-accumulating microorganisms. *Appl. Microbiol. Biotechnol.* **50**, 273-276.

Brdjanovic, D., Slamet, A., van Loosdrecht, M. C. M., Hooijmans, Alaerts, G. J. and Heijnen, J. J. (1998b) Impact of excessive aeration on biological phosphorus removal from wastewater. *Wat. Res.* **32**(1), 200-208.

Brdjanovic, D., van Loosdrecht, M. C. M., Hooijmans, C. M., Mino, T., Alaerts, G. J. and Heijnen, J. J. (1999) Innovative methods for sludge characterization in biological phosphorus removal systems. *Wat. Sci. Tech.* **39**(6), 37-43.

Brodish, K. E. U. (1985) Interaction of different groups of micro-organisms in biological phosphate removal. *Wat. Sci. Tech.*, **17**(11/12), 89-97.

Brown, J. W. (1999) Microbial Diversity. Course: MB 409, NCSU, USA. Lecture notes on the internet adress: http://www.mbio.ncsu.edu/micro/MB409/infor/syllabus.html. Based on the book: Brock Biology of Microorganisms, and Perry and Staley: Microbiology: Dynamics & Diversity.

Bryers, J. D. (1993) Bacterial Biofilms. *Curr. Opin. Biotechnol.*, **4**, 197-204.

Bryers, J. D. (1994) Biofilms and the technological implications of microbial cell adhesion. *Colloids and Surfaces B: Biointerfaces*. **2**, 9-23.

Bryers, J. D. (1984) Biofilm formation and chemostat dynamics: Pure and mixed culture considerations. *Biotechnol. and Bioeng.* **26**, 948-958.

Buchan, L. (1983) Possible biological mechanism of phosphorus removal. *Wat. Sci. Tech.* **25**, 83-92.

Bungartz, H. J., Kuehn, M., Hausner, M. and Wuertz, S. (2000) Fluid flow and transport in defined biofilms: Experiments and numerical simulations on a microscale. *Proceedings of the IAWQ Conference on Biofilm Systems*. Oct. 1999, New York. *Wat. Sci. Tech*. (in press).

Buckman Labs (2000) Biofilm Information Release. http://www.buckman.com/eng/biofilm2.htm

Bønlykke, H. and Kristensen, L. C. (1995) Biologisk P-fjernelse i biofilmreaktorer. (In Danish. English title: Biological P removal in biofilm reactors). Master of Science project at the Dep. of Env. Science and Engineering. Technical University of Denmark.

Carucci, A., Lindrea, K., Majone, M. and Ramadori, R. (1995) Dynamics of the anaerobic utilization of organic substrates in an anaerobic/aerobic sequencing batch reactor. *Wat. Sci. Tech.* **31**(2), 35-43.

Carucci, A., Majone, M., Ramadori, R. and Rossetti, S. (1997) Biological phosphorus removal with different organic substrates in an anaerobic/aerobic sequencing batch reactor. *Wat. Sci. Tech.* **35**(1), 161-168.

Carucci, A., Lindrea, K., Majone, M. and Ramadori, R. (1999) Different mechanisms for the anaerobic storage of organic substrates and their effect on enhanced biological phosphate removal (EBPR). *Wat. Sci. Tech.* **39**(6), 21-28.

Castillo, P. A., González-Martínez, S. and Tejero, I. (1999a) Biological phosphorus removal using a biofilm membrane reactor: Operation at high organic loading rates. *Wat. Sci. Tech.* **40**(4-5), 321-329.

Castillo, P. A., González-Martínez, S. and Tejero, I. (1999b) Observations during start-up of biological phosphorus removal in biofilm reactors. *Proceedings of the IAWQ Conference on Biofilm Systems. New York, USA, 17-20 Oct. 1999.*

CBE (2000) The Center for Biofilm Engineering, an NSF Engineering Research Center at Montana State University – Bozeman. USA. http://www.erc.montana.edu/

CEC (1991) Council of European Communities. Directive concerning urban wastewater treatment (91/271/EEC). *Official Journal L135/40.*

Cech, J. S. and Hartman, P. (1990). Glucose induced break down of enhanced biological phosphate removal. *Envir. Technol.* **11**, 651-656.

Cech, J. S. and Hartman, P. (1993). Competition between polyphosphate and polysaccharide accumulating bacteria in enhanced biological phosphate removal systems. *Wat. Res.* **27**(7), 1219-1225.

Cech, J. S., Hartman, P. and Macek, M. (1994) Bacteria and protozoa population dynamics in biological phosphate removal systems. *Wat. Sci. Tech.* **29**(7), 109-117.

Christiansen, P. and Hollesen, L. (1994) Biologisk fjernelse af p i biofilm reaktor. (In Danish. English title: Biological removal of P in a biofilm reactor). Master of Science project at the Dep. of Env. Science and Engineering. Technical University of Denmark.

Christiansen, P., Hollesen, L. and Harremoës, P. (1995) Liquid film diffusion on reaction rate in submerged biofilters. *Wat. Res.* **29**(3), 947-952.

Christensson, M., Blackall, L. L. and Welander, T. (1998) Metabolic transformations and characterisation of the sludge community in an enhanced biological phosphorus removal system. *Appl. Microbiol. Biotechnol*. **49**, 226-234.

Cloete, T. E., Steyn, P. L. and Buchan, L. (1985) An aut-ecological study of *Acinetobacter* in activated sludge. *Wat. Sci. Tech.* 17(11/12), 139-146.

Comeau, Y., Rabinowitz, B., Hall, K. J., and Oldham, W. K. (1985) Phosphorus release and uptake in enhanced biological phosphorus removal. *Proceedings of the 8th Symposium on Wastewater Treatment, Montréal*, 301-323.

Comeau, Y., Hall, K. J., Hancock, R. E. W. and Oldham, W. K. (1986) Biochemical model for enhanced biological phosphorus removal. *Wat. Res.* **20**(12), 1511-1521.

Confer, D. R. and Logan, B. E. (1997) Molecular weight distribution of hydrolysis products during biodegradation of model macromolecules in suspended and biofilm cultures I. Bovine serum albumin. *Wat. Res.* **31**(9), 2127-2136.

Confer, D. R. and Logan, B. E. (1998) Location of protein and polysaccharide hydrolytic activity in suspended and biofilm wastewater cultures. *Wat. Res.* **32**(1), 31-38.

Converti, A., Rovatti, M. and Del Borghi, M. (1995) Biological removal of phosphorus from wastewaters by alternating aerobic and anaerobic conditions. *Wat. Res.* **29**(1), 263-269.

Costerton, J. W., Lewandowski, Z., de Beer, D., Caldwell, D., Korber, D. and James, G. (1994) Biofilms, the Customized Microniche. *J. Bacteriol.* **176**(8), 2137-2142.

Costerton, J. W. (1995) Overview of microbial biofilms. *J. Industrial Microbiol*. **15**, 137-140.

Costerton, J. W. (1999a) Introduction to biofilm. *Int. J. Antimicrobial Agents*. **11**, 217-221.

Costerton, J. W. (1999b) The Role of Bacterial Exopolysaccharides in Nature and Disease. Chapter 15. *J. Ind. Microbiol. & Biotechn.* **22**, 551-563.

Crocetti, G. R., Hugenholtz, P., Bond, P. L., Schuler, A., Keller, J., Jenkins, D. and Blackall, L. L. (2000) Identification of Polyphosphate-Accumulating Organisms and Design of 16S rRNA-Directed Probes for Their Detection and Quantitation. *Appl. Environ. Microbiol.* **66**(3), 1175-1182.

Danesh, S. and Oleszkiewicz, J. A. (1997) Use of a new anaerobic-aerobic sequencing batch reactor system to enhance biological phosphorus removal. *Wat. Sci. Tech.* **35**(1), 137-144.

Davies, D. G., Parsek, M. R., Pearson, J. P., Iglewski, B. H., Costerton, J. W. and Greenberg, E. P. (1998) The Involvement of Cell-to-Cell Signals in the Development of a Bacterial Biofilm. *Science*. **280**, 295-298.

de Beer, D., Stoodley, P., Roe, F. and Lewandowski, Z. (1994) Effects of Biofilm Structures on Oxygen Distribution and Mass Transport. *Biotechnol. and Bioeng.* **43**(11), 1131-1138.

de Beer, D. and Stoodley, P. (1995) Relation between the structure of an anaerobic biofilm and transport phenomena. *Wat. Sci. Tech.* **32**(8), 11-18.

de Beer, D. and Schramm, A. (1999) Micro-environments and mass transfer phenomena in biofilms studied with microelectrodes. *Wat. Sci. Tech.* **39**(7), 173-178.

Deinema, M. H., Habets, L. H. A., Scholten, J., Turkstra, E. and Webers, H. A. A. M. (1980) The accumulation of polyphosphate in *Acinetobacter* spp. *FEMS Microbiol. Lett*. **9**, 275-279.

Deinema, M. H., van Loosdrecht, M. and Scholten, A. (1985) Some physiological characteristics of *Acinetobacter* spp. accumulating large amounts of phosphate. *Wat. Sci. Tech.* **17**(11/12), 119-125.

DeLong, E. F., Wickham, G. S. and pace, N. R. (1989) Phylogenetic stains: ribosomal RNA-based probes for the identification of single microbial cells. *Science*. **243**, 1360-1363.

Doll, W., Hollender, J., Kornberger, L. and van der Krol, D. (1999) Enzymatische und regulatorische Untersuchungen zur Phosphat- und Kohlenstoffspericherung von Bakterien des belebten Schlammes. Institut für Hygiene und Umweltmedizin. Aachen, Germany. Arbeitsbericht zum Forshungsvorhaben DO 237/11-2. Deutsche Forchungsgemeingschaft. (In German).

Edward, O. W. and Huffmann, E. O. (1959) Diffusion of aqueous solutions of phosphoric acid at 25 ^{o}C. *Journal of Physical Chemisty* **63**, 1830-1833.

Einfeldt, J. (1992) The implementation of biological phosphorus and nitrogen removal with the Bio-Denipho process on a 265,000 PE treatment plant. *Wat. Sci. Tech.* **25**, 161-168.

Erhart, R. (1997) *In situ* Analyse Mikrobieller Biozönosen in Abwasserreinigungsanlagen. *Ph.D. thesis* (in German) Fakultät für Chemie, Biologie und Geowissenshaften, Technische Universität München.

Ferris, M. J., Nold, S. C., Revsbech, N. P. and Ward, D. M. (1997) Population structure and physiological changes within a hot spring microbial mat community following disturbances. *Appl. Environ. Microbiol.* **63**(4), 1367-1374.

Filipe, C. D. M. and Daigger, G. T. (1998) Development of a revised metabolic model for the growth of phosphorus-accumulating organisms. *Water Environ. Res.* **70**(1), 67-79.

Filipe, C. D. M. and Daigger, G. T. (1999) Evaluation of the Capacity of Phosphorus-Accumulating Organisms To Use Nitrate and Oxygen as Final Electron Acceptors: A Theoretical Study on Population Dynamics. *Water Environ. Res.* **71**(6), 1140-1150.

Fleit, E. (1995) Intracellular pH regulation in biological excess phosphorus removal systems. *Wat. Res.* **29**(7), 1787-1792.

Flemming, H.-C. (1995) Sorption sites in biofilms. *Wat. Sci. Tech.* **32**(8), 27-33.

Flemming, H.-C. and Melo, L. (1995) Unwanted biofilms: Report from the discussion session. Report from the IAWQ Conference and Workshop on Biofilm Structure, Growth and Dynamics, Noordwijkerhout, The Netherlands. *Wat. Sci. Tech.* **32**(8), 267-268.

Fuhs, G. W. and Chen, M. (1975) Microbiological Basis of Phosphate removal in the Activated Sludge Process for the Treatment of Wastewater. *Microb. Ecol.* **2**, 119-138.

Fukase, T., Shibata, M. and Mijayi, X. (1982) Studies on the mechanism of biological phosphorus removal. (Abstract and figures in English, but the rest in Japanese). *Jap. J. Wat. Pollut. Res.* **5**, 309-317.

Fukase, T., Shibata, M. and Miyaji, Y. (1985) Factors affecting biological removal of phosphorus. *Wat. Sci. Tech.* **17**(11/12), 187-198.

Garzón-Zúñiga, M. A. and González-Martínez, S. (1996) Biological phosphate and nitrogen removal in a biofilm sequencing, batch reactor. *Wat. Sci. Tech.* **34**(1-2), 293-301.

Gerber, A., Mostert, E. S., Winther, C. S. and Devilliers, R. H. (1986) The effect of acetate and other short-chain carbon compounds on the kinetics of biological nutrient removal. *Water SA.* **12**, 7-12.

Gersberg, R. M. and Allen, D. W. (1985) Phosphorus uptake by *Klebsiella pneumoniae* and *Acinetobacter calcoaceticus*. *Wat. Sci. Tech.* **17**(11/12), 113-118.

Gieseke, A., Arnz, P., Schramm, A., Amann, R. and Wilderer, P. (1999) Nutrient removal with a sequencing batch biofilm reactor: Process parameters and microscale investigations. *Proceedings of the IAWQ Conference on Biofilm Systems. New York, USA, 17-20 Oct. 1999.*

Giovannoni, S. J., DeLong, E. F., Olsen, G. J. and Pace, N. R. (1988) Phylogenetic group-specific oligodeoxynucleotide probes for identification of single microbial cells. *J. Bacteriol.* **170**, 720-726.

Gjaltema, A., van der Marel, N., van Loosdrecht, M. C. M. and Heijnen, J. J. (1997a) Adhesion and Biofilm Development on Suspended Carriers in Airlift Reactors:

Hydrodynamic Conditions versus Surface Characteristics. *Biotechnol. and Bioeng.* **55**(6), 880-889.

Gjaltema, A., Vinke, J. L., van Loosdrecht, M. C. M. and Heijnen, J. J. (1997b) Abrasion of Suspended Biofilm Pellets in Airlift Reactors: Importance of Shape, Structure, and Particle Concentrations. *Biotechnol. and Bioeng.* **53**(1), 88-99.

Goncalves, R. F. and Rogalla, F. (1992a) Continuous Biological Phosphorus Removal in a Biofilm Reactor. *Wat. Sci. Tech.* **26**(9-11), 2027-2030.

Goncalves, R. F. and Rogalla, F. (1992b) Biological phosphorus removal in fixed films reactors. *Wat. Sci. Tech.* **25(**12), 165-174.

Goncalves, R. F., Nogueira, F. N., Le Grand, L. and Rogalla, F. (1994a) Nitrogen and phosphorus removal in submerged biofilters. *Wat. Sci. Tech.* **30**(11), 1-12.

Goncalves, R. F., Charlier, A. C. and Sammut, F. (1994b) Primary fermentation of soluble and particulate organic matter for wastewater treatment. *Wat. Sci. Tech.* **30**(6), 53-62.

González-Martinez, S. and Wilderer, P. A. (1991) Phosphate removal in a biofilm reactor. *Wat. Sci. Tech.* **23**, 1405-1415.

Greenburg, A. E., Klein, G. and Kaufman, W. J. (1955) Effects of phosphorus on the activated sludge process. *Sew. Ind. Wastes.* **27**(3), 277-282.

Hagedorn-Olsen, C., Møller, I. H., Tøttrup, H. and Harremoës, P. (1994) Oxygen reduces denitrification in biofilm reactors. *Wat. Sci. Tech.* **29**(10-11), 83-91.

Harremoës, P. (1978) Biofilm kinetics. In Mitchell, R. (ed.). Water pollution microbiology, 71-110. John Wiley, New York, 1978.

Harremoës, P. (1994?) Newsletter in the IAWQ Biofilm Group – including M. Nielsen's findings, in the years 1993-1995. More detailed information on this reference could not be provided.

Harremoës, P., Henze, M., Arvin, E. and Dahi, E. (1989) Teoretisk Vandhygiejne. (In Danish. English title: Theoretical Water Hygiene"). 3rd edition. Polyteknisk Forlag. Denmark.

Harremoës, P. (1997) Transient experimentation for process understanding and control. *International Conference on Environmental Biotechnology*, Belgium, April 1997.

Hascoet, M. C., Florentz, M. and Granger, P. (1985) Biochemical aspects of enhanced biological phosphorus removal from wastewater. *Wat. Sci. Tech.* **17**(11/12), 23-41.

Helness, H. and Ødegaard, H. (1999) Biological phosphorus removal in a sequencing batch moving bed biofilm reactor. *Wat. Sci. Tech.* **40**(4-5) 161-168.

Helmer, C. and Kunst, S. (1997) Low temperature effects on phosphorus release and uptake by microorganisms in EBPR plants. *Wat. Sci. Tech.* **37**(4-5), 531-539.

Henze, M. (1996a) Biological phosphorus removal from wastewater: processes and technology. *WQI*, July/August, 32-36.

Henze, M. (1996b) Biological phosphorus removal from wastewater. Processes and technology. *Special Seminar on 'International Trends in Water Environment Management'*, Tokyo, 23. April 1996.

Henze, M. (1999) Personal communication.

Henze, M., Kristensen, G. H. and Strube, R. (1994) Rate-capacity characterization of wastewater nutrient removal processes. *Wat. Sci. Tech.* **29**(7), 101-107.

Henze, M., Gujer, W., Mino, T., Matsuo, T., Wentzel, M. C. and Marais, G. v. R. (1995) Activated Sludge Model No. 2. IAWQ Scientific and Technical Reports, No.3. IAWQ. London.

Henze, M., Harremoës, P., la Cour Jansen, J., Arvin, E. (1997) Wastewater Treatment. Biological and Chemical Processes. 2nd edn. Springer-Verlag Berlin Heidelberg.

Henze, M., Gujer, W., Mino, T., Matsuo, T., Wentzel, M. C., Marais, G. v. R. and Van Loosdrecht, M. C. M. (1999) Activated Sludge Model No. 2D. IAWQ Task Group. *Wat. Sci. Tech.* **39**(1), 165-182.

Hermanowicz, S. W. (1998) A model of two-dimensional biofilm morphology. *Wat. Sci. Tech.* **37**(4-5), 219-222.

Hermanowicz, S. W. (1999) Two-dimensional simulations of biofilm development: Effects of external environmental conditions. *Wat. Sci. Tech.* **39**(7), 107-114.

Hesselmann, R. P. X., Werlen, C., Hahn, D., van der Meer, J. R. and Zehnder, A. J. B. (1999) Enrichment, Phylogenetic Analysis and Detection of a Bacterium That Performs Enhanced Biological Phosphate Removal in Activated Sludge. *System. Appl. Microbiol.* **22**, 454-465.

Heymann, J. B., Eagle, L. M., Greben, H. A. and Potgieter, D. J. J. (1989) The isolation and characterization of volutin granules as subcellular components involved in biological phosphorus removal. *Wat. Sci. Tech.* **21**, 397-408.

Hiraishi, A., Ueda, Y. and Ishihara, J. (1998) Quinone Profiling of Bacterial Communities in Natural and Synthetic Sewage Activated Sludge for Enhanced Phosphate Removal. *Appl. Environ. Microbiol.* **64**(3), 992-998.

Isaacs, S. (1997) Automatic adjustment of cycle length and aeration time for improved nitrogen removal in an alternating activated sludge process. *Wat. Sci. Tech.* **35**(1), 225-232.

Jahn, A. and Nielsen, P. H. (1995) Extraction of extracellular polymeric substances from biofilms using a cation exchange resin. *Wat. Sci. Tech.* **32**(8), 157-164.

James, G. A., Beaudette, L. and Costerton, J. W. (1995) Interspecies bacterial interactions in biofilms. *J. Ind. Microbiol.* **15**, 257-262.

Janning, K. F. (1995) TOC analyse af spildevandsprøver indeholdende partikulært organisk stof og methanol. (In Danish, English title: TOC analysis of wastewater treatment samples containing particulates and methanol). Student project at the Dep. of Env. Science and Engineering. Technical University of Denmark.

Janning, K. F. (1998) Hydrolysis and oxidation of particulate organic matter in biofilters. *Ph.d.-Thesis.* Department of Environmental Science and Engineering, Technical University of Denmark.

Janning, K. F., Nielsen, M. and Harremoës, P. (1995) Evaluating and modelling the kinetics in a full-scale submerged denitrification filter. *Wat. Sci. Tech.* **32**(8), 115-123.

Janning, K. F., Mesterton, K. and Harremoës, P. (1997) Hydrolysis and degradation of filtrated organic particulates in a biofilm reactor under anoxic and aerobic conditions. *Wat. Sci. Tech.* **36**(1), 279-286.

Jansen, J. la Cour and Harremoës, P. (1984) Removal of soluble substrates in fixed films. *Wat. Sci. Tech.* **17**, 1-4.

Jardin, N. and Pöpel, H. J. (1994) Phosphate release of sludges from enhanced biological P-removal during digestion. *Wat. Sci. Tech.* **30**(6), 281-292.

Jenkins, D. and Tandoi, V. (1991) The applied microbiology of enhanced biological phosphate removal – accomplishments and needs. *Wat. Res.* **25**(12), 1471-1478.

Jenkins, D. Richard, M. G. and Daigger, G. T. (1993) Manual on the Causes and Control of Activated Sludge Bulking and Foaming. New York. Lewis Publishers.

Jones, M. and Stephenson, T. (1996) The effect of temperature on enhanced biological phosphate removal. *Env. Techn.* **17**, 965-976.

Kämpfer, P., Erhart, R., Beimfohr, C., Böhringer, J., Wagner, M. and Amann, R. (1996) Characterization of Bacterial Communities from Activated Sludge: Culture-Dependent Numerical Identification Versus In Situ Identification using Group- and Genus-Specific rRNA-Targeted Oligonucleotide Probes. *Microbial Ecol.* **32**, 101-121.

Kawaharasaki, M., Kanagawa, T., Tanaka, H. and Nakamura, K. (1998) Development and application of 16S rRNA-targeted oligonucleotide probe for detection of the phosphate-accumulating bacterium *Microlunatus phosphovorus* in an enhanced biological phosphorus removal process. *Wat. Sci. Tech.* **37**(4-5), 481-484.

Kawaharasaki, M., Tanaka, H., Kanagawa, T. and Nakamura, K. (1999) *In situ* identification of polyphosphate-accumulating bacteria in activated sludge by dual staining with rRNA-targeted oligonucleotide probes and 4',6-diamidino-2-phenylindol (DAPI) at a polyphosphate-probing concentration. *Wat. Res.* **1**, 257-265.

Kerrn-Jespersen, J. P. and Henze, M. (1993) Biological phosphorus uptake under anoxic and aerobic conditions. *Wat. Res.* **27**(4), 617-624.

Kerrn-Jespersen, J. P., Henze, M. and Strube, R. (1994) Biological phosphorus release and uptake under alternating anaerobic and anoxic conditions in a fixed-film reactor. *Wat. Res.* **28**(5), 1253-1255.

Kim, H.-S. and Chung, T. H. (1996) Changes in composition of the intracellular phosphorus in a SBR process. *Proceedings of the 1st IAWQ international conference on Sequencing Batch Reactor Technology*. Munich, Germany, March 1996.

Kortsee, G. J. J., Appeldoorn, K. J., Bonting, C. F. C., van Niel, E. W. J. and van Veen, H. W. (1994). Biology of polyphosphate-accumulating bacteria involved in enhanced biological phosphorus removal. *FEMS Microbiol. Rev.* **15**, 137-153.

Kreikenbohm, R. and Stephen, W. (1985) Application of a two-compartment model to the wall growth of Pelobacter acidigallici under continuous culture conditions. *Biotechnol. and Bioeng.* **27**, 296-301.

Kristensen, G. H. and Christensen, F. R. (1982) Application of cryo-cut method for measurements of biofilm thickness. *Wat. Res.* **16**, 1619-1621.

Kuba, T., Smolders, G., van Loosdrecht, M. C. M. and Heijnen, J. J. (1993) Biological phosphorus removal from wastewater by anaerobic-anoxic sequencing batch reactor. *Wat. Sci. Tech.* **27**(5-6), 241-252.

Kuba, T., Wachtmeister, A., van Loosdrecht, M. C. M. and Heijnen, J.J. (1994) Effect of nitrate on phosphorus release in biological phosphorus removal systems. *Wat. Sci. Tech.* **30**(6), 263-269.

Kuba, T., van Loosdrecht, M. C. M. and Heijnen, J. J. (1996a) Phosphorus and nitrogen removal with minimal COD requirements by integration of denitrifying dephosphatation and nitrification in a two-sludge system. *Wat. Res.* **30**(7), 1702-1710.

Kuba, T., van Loosdrecht, M. C. M. and Heijnen, J. J. (1996b) Effect of cyclic oxygen exposure on the activity of denitrifying phosphorus removing bacteria. *Wat. Sci. Tech.* **34**(1/2), 33-40.

Kuba, T., van Loosdrecht, M. C. M., Brandse, F. A. and Heijnen, J. J. (1997a) Occurrence of denitrifying phosphorus removing bacteria in modified UCT-type wastewater treatment plants. *Wat. Res.* **31**(4), 777-786.

Kuba, T., van Loosdrecht, M. C. M., Brandse, F. A. and Heijnen, J. J. (1997b) Biological dephosphatation by activated sludge under denitrifying conditions: pH influence and occurrence of denitrifying dephosphatation in a full-scale waste water treatment plant. *Wat. Sci. Tech.* **36**(12), 75-82.

Kühl, M. and Jorgensen, B. B. (1992) Microsensor measurements of sulfate reduction and sulfide oxidation in compact microbial communities of aerobic biofilms. *Appl. Environ. Microbiol*. **58**, 1164-1174.

Kumar, P., Mehrotra, I. and Viraraghavan, T. (1996) Biological Phosphorus Removal: Effect of Low Temperature. *J. Cold Regions Eng.* **10**(2), 63-76.

Kwok, W. K., Picioreanu, C., Ong, S. L., van Loosdrecht, M. C. M., Ng, W. J. and Heijnen, J. J. (1998) Influence of Biomass Production and Detachment Forces on Biofilm Structures in a Biofilm Airlift Suspension Reactor. *Biotechnol. and Bioeng.* **58**(4), 400-407.

Lacamp, B., Hansen, F., Penillard, P. and Rogalla, F. (1993) Wastewater nutrient removal with advanced biofilm reactors. *Wat. Sci. Tech.* **27**(5-6), 263-276.

Larose, A., Perrier, M. and Comeau, Y. (1997) Respirometric control of the anaerobic period duration of an SBR Bio-P process. *Wat. Sci. Tech.* **36**(5), 293-300.

Larsen, T. A. and Harremoës, P. (1994) Degradation mechanisms of colloidal organic matter in biofilm reactors. *Wat. Res.* **28**(6), 1443-1452.

Lawrence, J. R., Korber, D. R., Hoyle, B. D., Costerton, J. W. and Caldwell, D. E. (1991) Optical Sectioning of Microbial Biofilms. *J. Bacteriol.* **173**(20), 6558-6567.

Lazarova, V. and Manem, J. (1995) Biofilm characterization and activity analysis in water and wastewater treatment. *Wat. Res.* **29**(19), 2227-2245.

Lazarova, V., Bellahcen, D., Rybacki, D., Rittman, B. and Manem, J. (1998) Population dynamics and biofilm composition in a new three-phase circulating bed reactor. *Wat. Sci. Tech.* **37**(4-5), 149-158.

Lee, N., Nielsen, P. H., Andreasen, K. H., Juretschko, S., Nielsen, J. L., Schleifer, K.-H. and Wagner, M. (1999) Combination of Fluorescent In Situ Hybridization and Microautoradiography – a New Tool for Structure-Function Analyses in Microbial Ecology. *Appl. Environ. Microbiol.* **65**(3), 1289-1297.

Lee, S. E., Kim, K. S., Ahn, J. H. and Kim, C. W. (1997) Comparison of phosphorus removal characteristics between various biological nutrient removal processes. *Wat. Sci. Tech.* **36**(12), 61-68.

Levin, G. V. and Shapiro, J. (1965) Metabolic uptake of phosphorus by waste-water organisms. *J. Wat. Poll. Contr. Fed.* **37**(6), 800-821.

Levin, G. V., Topol, G. J. and Samworth, R. B. (1972) Pilot plant tests of a phosphate removal process. *J. Wat. Poll. Contr. Fed.* **44**(10), 1940-1954.

Levine, A. D., Tchobanoglous, G. and Asano, T. (1985) Characterization of the size distribution of contaminants in wastewater: treatment and reuse implications. *J. Wat. Poll. Contr. Fed*. **57**(7), 805-816

Lewandowski, Z., Webb, D., Hamilton, M. and Harkin, G. (1999) Quantifying biofilm structure. *Wat. Sci. Tech.* **39**(7), 71-76.

Li, D. and Ganczarczyk, J. (1991) Size distribution of activated sludge flocs. *J. Wat. Poll. Contr. Fed*. **63**, 806-814.

Lide, D. R. (Editor in Chief) (1992) Handbook of Chemistry and Physics. 73rd edition.

Lie, E., Christensson, M., Jönsson, K., Østgaard, K., Johansson, P. and Welander, T. (1997) Carbon and phosphorus transformations in a full-scale enhanced biological phosphorus removal process. *Wat. Res.* **31**(11), 2693-2698.

Lindrea, K. C., Pigdon, S. P., Boyd, B. and Lockwood, G. A. (1994) Biomass characterization in a nitrification-denitrification biological enhanced phosphorus removal (NDBERP) plant during start-up and subsequent periods of good and poor phosphorus removal. *Wat. Sci. Tech.* **29**(7), 91-100.

Liu, W.-T., Mino. T., Nakamura, K. and Matsuo, T. (1994) Role of Glycogen in Acetate Uptake and Polyhydroxyalkanoate Synthesis in Anaerobic-Aerobic Activated Sludge with a Minimized Polyphosphate Content. *J. Ferment. Bioeng.* **77**(5), 535-540.

Liu, W.-T., Mino, T., Matsuo, T. and Nakamura, K. (1996a) Biological phosphorus removal processes – effect of pH on anaerobic substrate metabolism. *Wat. Sci. Tech.* **34**(1-2), 25-32.

Liu, W.-T., Mino, T., Nakamura, K. and Matsuo, T. (1996b) Glycogen accumulating population and its anaerobic substrate uptake in anaerobic-aerobic activated sludge without biological phosphorus removal. *Wat. Res.* **30**(1), 75-82.

Liu, W.-T., Nakamura, K., Matsuo, T. and Mino, T. (1997) Internal energy-based competition between polyphosphate- and glycogen-accumulating bacteria in biological phosphorus removal reactors – effect of P/C feeding ratio. *Wat. Res.* **31**(6), 1430-1438.

Lötter, L. H. (1985) The role of bacterial phosphate metabolism in enhanced phosphorus removal from the activated sludge process. *Wat. Sci. Tech.* **17**(11/12), 127-138.

Lötter, L. H. and Pitman, A. R. (1992) Improved biological phosphorus removal from the enrichment of reactor feed with fermentation products. *Wat. Sci. Tech.* **26**(5-6), 943-953.

Lötter, L. H., Wentzel, M. C., Loewenthal, R. E., Ekama, G. A. and Marais, G. v. R. (1986) A study of selected characteristics of *Acinetobacter* spp. isolated from activated sludge in anaerobic/anoxic/aerobic and aerobic systems. *Wat. S. A.* **12**, 203-208.

Malmvig, H. (1996) Introduction to Radiometer Selectrode® S. Measuring with Ion Selective Electrodes. 3rd edition. This manual was supplied with the buy of the nitrate electrode by Radiometer Copenhagen, Lyon, France, in 1996. However, no publication year is written on the manual itself.

Malnou, D., Meganck, M., Faup, G. M. and du Rostu, M. (1984) Biological phosphorus removal: Study of the main parameters. *Wat. Sci. Tech.* **16**, 173-185.

Mamais, D. and Jenkins, D. (1992) The effects of MCRT and temperature on enhanced biological phosphorus removal. *Wat. Sci. Tech.* **26**(5-6), 955-965.

Manz, W., Amann, R., Ludwig, W., Wagner, M., Schleifer, K.H. (1992) Phylogenetic oligodeoxynucleotide probes for the major subclasses of proteobacteria: problems and solutions. *System. Appl. Microbiol*. **15**, 593-600.

Manz, W., Szewzyk, U., Eriksson, P., Amann, R., Schleifer, K. H. and Stenström ,T.-A. (1993) In situ identification of bacteria in drinking water and adjoining biofilms by hybridization with 16S and 23S rRNA-directed fluorescent oligonucleotide probes. *Appl. Environ. Microbiol.* **59**, 2293-2298.

Marais, G. v. R. and Ekama, G. A. (1976) The Activated Sludge Process. PART I: Steady State Behaviour. *Water SA.* **2**(4), 163-200.

Marais, G. v. R., Loewenthal, R. E. and Siebritz, I. P. (1983) Review: observations supporting phosphate removal by biological excess uptake. *Wat. Sci. Tech.* **15**, 15-41.

Masuda, S., Watanabe, Y. and Ishiguro, M. (1991) Biofilm properties and simultaneous nitrification and denitrification in aerobic rotating biological contactors. *Wat. Sci. Tech.* **23**(7-9), 1355-1363.

Matsuo, Y. (1994) Effect of the anaerobic solids retention time on enhanced biological phosphorus removal. *Wat. Sci. Tech.* **30**(6), 193-202.

Maurer, M., Gujer, W., Hany, R. and Bachmann, S. (1997) Intracellular carbon flow in phosphorus accumulating organisms from activated sludge systems. *Wat. Res.* **31**(4), 907-917.

Maurer, M. and Boller, M. (1999) Modelling of phosphate precipitation in wastewater treatment plants with enhanced biological phosphorus removal. *Wat. Sci. Tech.* **39**(1), 147-163.

McClintock, S. A., Randall, C. W. and Patterkine, V. M. (1993) Effect on temperature and mean cell residence time on biological nutrient removal processes. *Wat. Environ. Res.* **65**(5), 110-118.

Meinhold, J., Pedersen, H., Arnold, E., Isaacs, S. and Henze, M. (1998) Effect of continuous addition of an organic substrate to the anoxic phase on biological phosphorus removal. *Wat. Sci. Tech.* **38**(1), 97-105.

Meinhold, J. Filipe, C. D. M., Daigger, G. T. and Isaacs, S. (1999) Characterization of the denitrifying fraction of phosphate accumulating organisms in biological phosphate removal. *Wat. Sci. Tech.* **39**(1), 31-42.

Melasniemi, H., Hernesmaa, A., Pauli, AS-L, Rantanen, P. and Salkinoja-Salonen, M. (1998) Comparative analysis of biological phosphate removal (BPR) and non-BPR activated sludge bacterial communities with particular reference to *Acinetobacter*. *Journ. of Industrial Microbiol. & Biotechn.* **21**, 300-306.

Mino, T., Arun, V., Tsuzuki, Y. and Matsuo, T. (1987) Effect of phosphorus accumulation on acetate metabolism in the biological phosphorus removal process. Advances in *Water Pollution Control.* Biological phosphate removal from wastewaters. Ramadori, R. (ed.). Pergamon Press, Oxford.

Mino, T., Satoh, H. and Matsuo, T. (1994) Metabolisms of different bacterial populations in enhanced biological phosphate removal processes. *Wat. Sci. Tech.* **29**(7), 67-70.

Mino, T., Liu, W.-T., Kurisu, F. and Matsuo, T. (1995) Modelling glycogen storage and denitrification capability of microorganisms in enhanced biological phosphate removal processes. *Wat. Sci. Tech.* **31**(2), 25-34.

Mino, T., Van Loosdrecht, M. C. M. and Heijnen, J. J. (1998) Microbiology and biochemistry of the enhanced biological phosphate removal process. *Wat. Res.* **32**(11), 3193-3207.

Miyamoto-Mills, J., Larson, J., Jenkins, D. and Owen, W. (1983) Design and operation of a pilot-scale biological phosphate removal plant at the Central Contra Costa Sanitary District. *Wat. Sci. Tech.* **15**(3/4), 153-179.

Montgomery, D. C. (1991) Design and Analysis of Experiments. Arizona State University. 3rd ed. John Wiley and Sons. Singapore.

Morgenroth, E. (1998) Enhanced Biological Phosphorus Removal in Biofilm Reactors. *Ph.D.-Thesis*. Technical University of Munich, Germany.

Morgenroth, E. and Wilderer, P. (1998) Modelling of enhanced biological phosphorus removal in a sequencing batch biofilm reactor. *Wat. Sci. Tech.* **37**(4-5), 583-587.

Morgenroth, E. and Wilderer, P. (1999) Controlled biomass removal – the key parameter to achieve enhanced biological phosphorus removal in biofilm systems. *Wat. Sci. Tech.* **39**(7), 33-40.

Morgenroth, E., Eberl, H. and van Loosdrecht, M. C. M. (2000) Evaluating 3-D and 1-D mathematical models for mass transport in heterogenous biofilms. *Proceedings of the IAWQ Conference on Biofilm Systems. New York, USA, 17-20 Oct. 1999. Wat. Sci. Tech*. (in press).

Muñoz-Colunga, A. and González-Martínez, S. (1996) Effects of population displacements on biological phosphorus removal in a biofilm SBR. *Wat. Sci. Tech.* **34**(1-2), 303-313.

Murnleitner, E., Kuba, T., Van Loosdrecht, M. C. M. and Heijnen, J. J. (1997) An integrated metabolic model for the aerobic and denitrifying biological phosphorus removal. *Biotechnol. and Bioeng.* **54**(5), 434-450.

Muyzer, G. and Ramsing, N. B. (1995) Molecular methods to study the organization of microbial communities. *Wat. Sci. Tech.* **32**(8), 1-9.

Møller, H. (1994) Delrapport, EF 487, Udkast. Unpublished student report at the Technical University of Denmark.

Nakumara, K., Masuda, K. and Mikami, E. (1991) Isolation of a new type of polyphosphate accumulating bacterium and its phosphate removal characteristics. *J. Ferment. Bioeng.* **69**, 368-371.

Nakamura, K., Hiraishi, A., Yoshimi, Y., Kawaharasaki, M., Masuda, K. and Kamagata, Y. (1995) Microlunatus phosphovorus gen. nov., sp. nov., a new Gram-positive polyphosphate-accumulating bacterium isolated from activated sludge. *Int. J. Syst. Bacetriol.*, **45**, 17-22.

Nicholls, H. A. and Osborn, D. W. (1979) Bacterial stress: Prerequisite for biological removal of phosphorus. *J. Wat. Poll. Contr. Fed.* **51**(3), 557-569.

Nielsen, M. (1993) Diffusionsbegrænsning i en Bio-P biofilm. (In Danish, English title: Diffusion limitation in a Bio-P biofilm). Student project at the Dep. of Env. Science and Engineering. Technical University of Denmark.

Nielsen, P. H, and Harremoës, P. (1995) Solids: Report of the discussion session. Report from the IAWQ Conference and Workshop on Biofilm Structure, Growth and Dynamics, Noordwijkerhout, The Netherlands. *Wat. Sci. Tech.* **32**(8), 273-275.

Nielsen, P. H., Jahn, A. and Palmgren, R. (1997) Conceptual model for production and composition of exopolymers in biofilms. *Wat. Sci. Tech.* **36**(1), 11-19.

Nielsen, P. H. and Keiding, K. (1998) Disintegration of activated sludge flocs in presence of sulfide. *Wat. Res.* **32**, 313-320.

Nielsen, A. T., Liu, W.-T., Filipe, C., Grady, L. Jr., Molin, S, and Stahl, D. A. (1999a) Identification of a Novel Group of Bacteria in Sludge from a Deteriorated Biological Phosphorus Removal Reactor. *Appl. Environ. Microbiol.* **65**(3), 1251-1258.

Nielsen, P. H., Andreasen, K., Lee, N. and Wagner, M. (1999b) Use of microautoradiography and fluorescent in situ hybridization for characterization of microbial activity in activated sludge. *Wat. Sci. Tech.*, **39**(1), 1-9.

Norsker, N. H., Nielsen, P. H. and Hvitved-Jacobsen, T. (1995) Influence of oxygen on biofilm growth and potential sulfate reduction in gravity sewer biofilm. *Wat. Sci. Tech.* **31**(7), 159-167.

Noguera, D. R., Pizarro, G., Stahl, D. A. and Rittmann, B. E. (1999a) Simulation of multispecies biofilm development in three dimensions. *Wat. Sci. Tech.* **39**(7), 123-130.

Noguera, D. R., Okabe, S. and Picioreanu, C. (1999b) Biofilm modelling: Present status and future directions. *Wat. Sci. Tech.* **39**(7), 273-278.

Oerther, D. B., Danalewich, J., Dulekgurgen, E., Leveque, E., Freedman, D. L. and Raskin, L. (1998) Bioaugmentation of sequencing batch reactors for biological phosphorus removal: Comparative rRNA sequence analysis and hybridization with oligonucleotide probes. *Wat. Sci. Tech.*, **37**(4-5), 469-473.

Ohtake, H., Takahashi, K., Tsuzuki, Y. and Toda, K. (1985) Uptake and release of phosphate by a pure culture of *Acinetobacter Calcoaceticus*. *Wat. Res.* **12**, 1587-1594.

Okabe, S., Matsuda, T., Satoh, H., Itoh, T. and Watanabe, Y. (1998) Sulfate reduction and sulfide oxidation in aerobic mixed population biofilms. *Wat. Sci. Tech.* **37**(4-5), 131-138.

Oldham, W. K. (1985) Full scale optimization of biological phosphorus removal at Kelowna, Canada. *Wat. Sci. Tech.* **17**(11/12), 243-257.

Olsen, G. J., Lane, D. J., Giovannoni, S. J., Pace, N. R. and Stahl, D. A. (1986) Microbial ecology and evolution: a ribosomal RNA approach. *Ann. Rev. Microbiol.* **40**, 337-365.

Osborn, D. W. and Nicholls, H. A. (1978) Optimisation of the activated sludge process for the biological removal of phosphorus. *Prog. Wat. Tech.* **10**(1/2), 261-277.

Paffoni, C., Gousailles, M., Rogalla, F. and Gilles, P. (1990) Aerated biofilters for nitrification and effluent polishing. *Wat. Sci. Tech.* **22**(7/8), 181-189.

Pastorelli, G., Canziani, R., Pedrazzi, L. and Rozzi, A. (1999) Phosphorus and nitrogen removal in moving-bed sequencing batch biofilm reactors. *Wat. Sci. Tech.* **40**(4-5), 169-176.

Pereira, H., Lemos, P., Reis, M. A. M., Crespo, J. P. S. G., Carrondo, M. J. T. and Santos, H. (1996) Model for carbon metabolism in biological phosphorus removal processes based on in vivo ^{13}C-NMR labelling experiments. *Wat. Res.* **30**(9), 2128-2138.

Peyton, B. M. (1996) Effects of shear stress and substrate loading rate on *Pseudomonas Aeruginosa* biofilm thickness and density. *Wat. Res.* **30**(1), 29-36.

Petersen, B., Temmink, H., Henze, M. and Isaacs, S. (1998) Phosphate uptake kinetics in relation to PHB under aerobic conditions. *Wat. Res.* **32**(1), 91-100.

Picioreanu, C., van Loosdrecht, M. C. M. and Heijnen, J. J. (1998a) A New Combined Differential-Discrete Cellular Automaton Approach for Biofilm Modeling: Application for Growth in Gel Beads. *Biotechnol. and Bioeng.* **57**(6), 718-731.

Picioreanu, C., van Loosdrecht, M. C. M. and Heijnen, J. J. (1998b) Mathematical Modeling of Biofilm Structure with a Hybrid Differential-Discrete Cellular Automaton Approach. *Biotechnol. and Bioeng.* **58**(1), 101-116.

Picioreanu, C., van Loosdrecht, M. C. M. and Heijnen, J. J. (1999) Discrete-differential modelling of biofilm structure. *Wat. Sci. Tech.* **39**(7), 115-122.

Pitman, A. R. (1991) Design considerations for nutrient removal activated sludge plants. *Wat. Sci. Tech.* **23**, Kyoto, 781-790.

Pitman, A. R. (1999) Management of biological nutrient removal plant sludges – change the paradigms? *Wat. Res.* **33**(5), 1141-1146.

Pochana, K., Keller, J. and Lant, P. (1999) Model development for simultaneous nitrification and denitrification. *Wat. Sci. Tech.* **39**(1), 235-243.

Pramanik, J., Trelstad, P. L., Schuler, A. J., Jenkins, D. and Keasling, J. D. (1999) Development and validation of a flux-based stoichiometric model for enhanced biological phosphorus removal metabolism. *Wat. Res.* **33**(2), 462-476.

Ramsing, N., Kuhl, M. and Jorgensen, B. (1993) Distribution of sulfate-reducing bacteria, O_2, and H_2S in photosynthetic biofilms determined by oligonucleotide probes and microelectrodes. *Appl. Environ. Microbiol.* **59**(11), 3840-3849.

Randall, A. A., Benefield, L. D. and Hill, W. E. (1994) The effect of fermentation products on enhanced biological phosphorus removal, polyphosphate storage, and microbial population dynamics. *Wat. Sci. Tech.* **30**(6), 213-219.

Randall, A. A., Benefield, L. D. and Hill, W. E. (1997) Induction of phosphorus removal in an enhanced biological phosphorus removal bacterial population. *Wat. Res.* **31**(11), 2869-2877.

Rasmussen, K. and Lewandowski, Z. (1998) The accuracy of oxygen flux measurements using microelectrodes. *Wat. Res.* **32**(12), 3747-3755.

Reichert, P. (1994) AQUASIM: A tool for simulation and data analysis of aquatic systems. *Wat. Sci. Tech.* **30**(2), 21-30.

Reichert, P. and Wanner, O. (1997) Movement of solids in biofilms: Significance of liquid phase transport. *Wat. Sci. Tech.* **36**(1), 321-328.

Riemer, M. and Harremoës, P. (1978) Multi-component diffusion in denitrifying biofilms. *Prog. Wat. Tech.* **10**(5/6), 149-165.

Rittmann, B. E. (1982) The Effect of Shear Stress on Biofilm Loss Rate. *Biotechnol. and Bioeng.* **24**, 501-506.

Rittmann, B. E., Pettis, M., Reeves, H. W. and Stahl, D. A. (1999) How biofilm clusters affect substrate flux and ecological selection. *Wat. Sci. Tech.* **39**(7), 99-105.

Rodrigo, M. A., Seco, A., Penya-roja, J. M. and Ferrer, J. (1996) Influence of sludge age on enhanced phosphorus removal in biological phosphorus removal in biological systems. *Wat. Sci. Tech.* **34**(1-2), 41-48.

Roller, C., Wagner, M., Amann, R., Ludwig, W. and Schleifer, K. (1994) *In situ* probing of Gram-positive bacteria with high DNA G+C content using 23S rRNA-targeted oligonucleotides. *Microbiol.* **140**, 2849-2858.

Romanski, J., Heider, M. and Wiesmann, U. (1997) Kinetics of anaerobic orthophosphate release and substrate uptake in enhanced biological phosphorus removal from synthetic wastewater. *Wat. Res.* **31**(12), 3137-3145.

Rovatti, M. C., Nicolella, C., Converti, A., Ghihliazza, R. and Difelice, R. (1995) Phosphorus removal in Fluidized-Bed Biological Reactor (FBBR). *Wat. Res.* **29**(12), 2627-2634.

Santegoeds, C. M., Muyzer, G. and de Beer, D. (1998) Biofilm dynamics studied with microsensors and molecular techniques. *Wat. Sci. Tech.* **37**(4-5), 125-129.

Satoh, H., Mino, T. and Matsuo, T. (1992) Uptake of organic substrates and accumulation of polyhydroxyalkanoates linked with glycolysis of intracellular carbohydrates under anaerobic conditions in the biological excess phosphate removal process. *Wat. Sci. Tech.* **26**(5-6), 933-942.

Satoh, H., Mino, T. and Matsuo, T. (1994) Deterioration of enhanced biological phosphorus removal by the domination of microorganisms without polyphosphate accumulation. *Wat. Sci. Tech.* **30**(6), 203-211.

Satoh, H., Remey, W. D., Koch, F. A., Oldham, W. K., Mino, T. and Matsuo, T. (1996) Anaerobic substrate uptake by the enhanced biological phosphorus removal activated sludge treating real sewage. *Wat. Sci. Tech.* **34**(1-2), 9-16.

Scheer, H. (ed.) (1995) Vermehrte biologische Phosphorelimination in der Abwasserreinigung. Abschlussbericht eines Erfahrungsaustausches deutschsprachiger Hoschschulen. Mitteilungen der Oswald-Schulze-Stiftung. Heft 19.

Scheer, H. and Seyfried, C. F. (1996) Enhanced biological phosphate removal: Modelling and design in theory and practice. *Wat. Sci. Tech.* **34**(1-2), 57-66.

Schmid, M., Thill, A. Purkhold, U., Walcher, M., Bottero, J. Y., Ginestet, P., Urbain, V., Nielsen, P. H., Wuertz, S. and Wagner, M. (2000) Monitoring of activated sludge floc settling based on confocal laser scanning microscopy and image analysis (Submitted to *Wat. Res.*).

Schuppler, M., Wagner, M., Schön, G. and Göbel, U. B. (1998) *In situ* identification of nocardiaform actinomycetes in activated sludge using fluorescent rRNA-targeted oligonucleotide probes. *Microbiol.* **144**, 249-259.

Schramm, A., Larsen, L. H., Revsbech, N. P., Ramsing, N. B., Amann, R. and Schleifer, K.-H. (1996) Structure and function of a nitrifying biofilm as determined by in situ hybridization and the use of microelectrodes. *Appl. Environ. Microbiol.* **62**(12), 4641-4647.

Schramm, A., Santegoeds, C. M., Nielsen, H. K., Ploug, H., Wagner, M., Pribyl, M., Wanner, J., Amann, R. and de Beer, D. (1999) On the Occurrence of Anoxic

Microniches, Denitrification, and Sulfate Reduction in Aerated Activated Sludge. *Appl. Environ. Microbiol*. **65**(9), 4189-4196.

Seviour, R. J. and Blackall, L. L. (editors) (1998) The Microbiology of Activated Sludge. Chapman & Hall. London.

Shapiro, J., Levin, G. V. and Humberto, Z. G. (1965) Metabolic uptake of phosphorus by wastewater organisms. *J. Wat. Poll. Contr. Fed.* **37**(6), 800-824.

Shin, H.-S. and Park, H.-S. (1991) Enhanced nutrient removal in porous biomass carrier sequencing batch reactor (PBCSBR). *Wat. Sci. Tech.* **23**, Kyoto, 719-728.

Sicko-Goad, L. M., Crang, R. E. and Jensen, T. E. (1975) Phosphate metabolism in blue-green algae. IV. In situ analysis of polyphosphate bodies by X-ray energy dispersive analysis. *Cytobiol.* **11**, 430-437.

Sieker, C. (1999) Kombination der Denitrifikation und der vermehrten biologischen Phosphorelimination in einer alternierend betriebenen Biofiltrationsanlage (in German). *Ph.D.-thesis.* June 1999. Technical University of Berlin.

Simpkins, M. J. and McLaren, A. R. (1978) Consistent Biological Phosphate and Nitrate Removal in an Activated Sludge Plant. *Prog. Wat. Tech.* **10**(5/6), 433-442.

Smolders, G. J. F. (1995) A metabolic model of the biological phosphorus removal. Stoichiometry, kinetics and dynamic behaviour. Ph. D.-Thesis. Technical University of Delft, The Netherlands.

Smolders, G. J. F., van der Meij, J., Van Loosdrecht, M. C. M. and Heijnen, J.J. (1994a) Model of the anaerobic metabolism of the biological phosphorus removal process: Stoichiometry and pH influence. *Biotechnol. and Bioeng*. **43**, 461-470.

Smolders, G. J. F., van der Meij, J., Van Loosdrecht, M. C. M. and Heijnen, J.J. (1994b) Stoichiometric model of the aerobic metabolism of the biological phosphorus removal process. *Biotechnol. and Bioeng*. **44**, 837-848.

Smolders, G. J. F., van Loosdrecht, M. C. M. and Heijnen, J. J. (1994c) pH: Key factor in the biological phosphorus removal process. *Wat. Sci. Tech.* **29**(7), 71-74.

Smolders, G. J. F., van Loosdrecht, M. C. M. and Heijnen, J. J. (1996) Steady-state analysis to evaluate the phosphate removal capacity and acetate requirement of biological phosphorus removing mainstream and sidestream process configurations. *Wat. Res.* **30**(11), 2748-2760.

Snaidr. J., Amann, R., Huber, I., Ludwig, W. and Schleifer, K.-H. (1997) Phylogenetic Analysis and In Situ Identification of Bacteria in Activated Sludge. *Appl. Environ. Microbiol*. **63**(7), 2884-2896.

Speitel, G. E. and DiGiano, F. A. (1987) Biofilm shearing under dynamic conditions. *J. Environ. Eng. ASCE*. **113**, 464-475.

Spring, S., Amann, R., Ludwig, W., Schleifer, K.-H. and Pedersen, N. (1992) Phylogenetic diversity and identification of nonculturable magnetotactic bacteria. *System Appl. Microbiol*. **15**, 116-122.

Srinath, E. G., Sastry, C. A. and Pillay, S. C. (1959) Rapid removal of phosphorus from sewage by activated sludge. *Water and Waste Treatment.* **11**, 410.

Stahl, D. A., Flesher, B., Mansfield, H. R. and Montgomery, L. (1988) The use of phylogenetically based hybridization probes for studies of ruminal microbial ecology. *Appl. Environ. Microbiol*. **54**, 1079-84.

Standard Methods for examination of Water and WasteWater (1995) 19. Edition.

Stante, L., Cellamare, C. M., Malaspina, F., Bortone, G. and Tilche, A. (1997) Biological phosphorus removal by pure culture of *Lampropedia* spp. *Wat. Res.* **31**(6), 1317-1324.

Stewart, P. S. (1993) A Model of Biofilm Detachment. *Biotechnol. and Bioeng.* **41**(1), 112-117.

Stewart, P. S., Murga, R., Srinivasan, R. and de Beer, D. (1995) Biofilm structural heterogeneity visualised by three microscopic methods. *Wat. Res.* **29**(8), 2006-2009.

Stoodley, P., de Beer, D. and Lewandowski, Z. (1994) Liquid flow in biofilm systems. *Appl. Env. Microbiol.* **60**, 2711-2716.

Sudiana, I. M., Mino, T., Satoh, H. and Matsuo, T. (1998). Morphology, In-situ characterization with rRNA targeted probes and respiratory quinone profiles of enhanced biological phosphorus removal sludge. *Wat. Sci. Tech.* **38**(8-9), 69-76.

Sudiana, I. M., Mino, T., Satoh, H., Nakamura, K. and Matsuo, T. (1999) Metabolism of enhanced biological phosphorus removal and non-enhanced biological phosphorus removal sludge with acetate and glucose as carbon sources. *Wat. Sci. Tech.* **39**(6), 29-35.

Surampalli, R. Y., Tyagi, R. D., Scheible, O. K. and Heidman, J. A. (1997) Nitrification, denitrification and phosphorus removal in sequential batch reactors**.** *Bioresource Techn.* **61**, 151-157.

Suresh, N., Wartburg, R., Timmerman, M., Wells, J., Coccia, M., Roberts, M. F. and Halvorson, H. O. (1985) New strategies for the isolation of microorganisms responsible for phosphate accumulation. *Wat. Sci. Tech.* **17**(11/12), 99-111.

Surman, S. B., Walker, J. T., Goddard, D. T., Morton, L. H. G., Keevil, C. W., Weaver, W., Skinner, A., Hanson, K., Caldwell, D. and Kurtz, J. (1996) Comparison of microscope techniques for the examination of biofilms. *J. Microbiol. Methods.* **25**, 57-70.

Tasli, R., Artan, N. and Orhon, D. (1997) The influence of different substrates on enhanced biological phosphorus removal in a sequencing batch reactor. *Wat. Sci. Tech.* **35**(1), 75-80.

Temmink, H., Petersen, B., Isaacs, S. and Henze, M. (1996) Recovery of biological phosphorus removal after periods of low organic loading. *Wat. Sci. Tech.* **34**(1-2), 1-8.

Tijhuis, L., Hijman, B., van Loosdrecht, M. C. M. and Heijnen, J. J. (1996) Influence of detachment, substrate loading and reactor scale on the formation of biofilms in airlift reactors. *Appl. Microbial. Biotechnol.* **45**, 7-17.

Toettrup, H., Rogalla, F., Vidal, A. and Harremoës, P. (1994) The treatment trilogy of floating filters: From pilot to prototype to plant. *Wat. Sci. Tech.* **29**(10-11), 23-32.

Truelar, M. G. and Characklis, W. G. (1982) Dynamics of Biofilm Processes. *J. Wat. Poll. Contr. Fed.* **54**(9), 1288-1301.

Ubukata, Y. and Takii, S. (1994) Induction method of excess phosphate accumulation for_phosphate removing bacteria isolated from anaerobic/aerobic activated sludge. *Wat. Sci. Tech.* **30**(6), 221-227.

van Loosdrecth, M. C. M., Eikelboom, D., Gjaltema, A., Mulder, A., Tijhuis, L. and Heijnen, J. J. (1995) Biofilm Structures. *Wat. Sci. Tech.* **32**(8), 35-43.

van Loosdrecht, M. C. M. and Heijnen, J. J. (1997) Importance of bacterial storage polymers in bioprocesses. *Wat. Sci. Tech.* **35**(1), 41-47.

van Loosdrecht, M. C. M., Hooijmans, C. M., Brdjanovic, D. and Heijnen, J. J. (1997a) Biological phosphate removal processes. *Appl. Microbiol. Biotechnol.* **48**, 289-296.

van Loosdrecht, M. C. M., Picioreanu, C. and Heijnen, J. J. (1997b) A more unifying hypothesis for biofilm structures. *FEMS Microbiol. Ecol.* **24**, 181-183.

Vinconneau, J. C., Schaack, F., Boschet, A. F., Chevalier, D., Villesot, D., Jaubert, M., Laval, Ch. and Lambert, S. (1985) The problem of phosphorus in France – its presence in natural waters and biological phosphorus removal. *Wat. Sci. Tech.* **17**(11/12), 1-9.

Vlekke, G. J. F. M., Comeau, Y. and Oldham, W. K. (1988) Biological phosphate removal from wastewater with oxygen or nitrate in sequencing batch reactors. *Environ. Technol. Lett.* **9**, 791-796.

Wachtmeister, A., Kuba, T., van Loosdrecht, M. C. M. and Heijnen, J. J. (1997) A sludge characterization assay for aerobic and denitrifying phosphorus removing sludge. *Wat. Res.* **31**(3), 471-478.

Wagner, M., Amann, R., Lemmer, H. and Schleifer, K.-H. (1993) Probing Activated Sludge with Oligonucleotides Specific for *Proteobacteria*: Inadequacy of Culture-Dependent Methods for Describing Microbial Community Structure. *Appl. Environ. Microbiol*. **59**(5), 1520-1525.

Wagner, M., Erhardt, R., Manz, W., Amann, R., Lemmer, H., Wedi, D. and Schleifer, K. (1994a). Development of an r-RNA-Targeted Oligonucleotide Probe Specific for the Genus *Acinetobacter* and its Application for In Situ Monitoring in Activated Sludge. *Appl. Environ. Microbiol.*, 792-800.

Wagner, M., Amann, R., Kämpfer, P., Assmus, B., Hartmann, A., Hutzler, P., Springer, N. and Schleifer, K. (1994b) Identification and *in situ* Detection of Gram-negative Filamentous Bacteria in Activated Sludge. *System. Appl. Microbiol.* 17, 405-417.

Wanner, J., Cech, J. S. and Kos, M. (1992) New process design for biological nutrient removal. *Wat. Sci. Tech.* 25, 445-448.

Wanner, O. (1995) New experimental findings and biofilm modelling concepts. *Wat. Sci. Tech.* 32(8), 133-140.

Wanner, O. (1998) The Best Biofilm Model. *Proceedings of The First International Workshop on Biofilms in Aerobic Wastewater Treatment: An Interdisciplinary Approach.* Munich, Germany, 16-18.

Wanner, O. and Gujer, W. (1984) Competition in biofilms. *Wat. Sci. Tech*. 17(2/3), 27-44.

Wanner, O. and Gujer, W. (1986) A multispecies biofilm model. *Biotechnol. and Bioeng.* **28**, 314-328.

Wanner, O. and Reichert, P. (1996) Mathematical Modeling of Mixed-Culture Biofilms. *Biotechnol. and Bioeng.* **49**(2), 172-184.

Wentzel, M. C., Lötter, L. H., Loewenthal, R. E. and Marais, G. v. R. (1986) Metabolic Behaviour of *Acinetobacter* spp. in Enhanced Biological Phosphorus Removal – a Biochemical Model. *Water SA* **12**(4), 209-224.

Wentzel, M. C., Dold., P. L., Loewenthal, R. E., Ekama, G. A. and Marais, G. v. R. (1987) Experiments towards establishing the kinetics of biological excess phosphorus removal. Advances in *Water Pollution Control.* Biological

phosphate removal from wastewaters. Ramadori, R. (ed.). Pergamon Press, Oxford.

Wentzel, M. C., Ekama, G. A., Loewenthal, R. E., Dold, P. L., and Marais, G. A. (1989) Enhanced polyphosphate organism cultures in activated sludge systems. Part II: Experimental behaviour. *Water SA.* **15**(2), 71-88.

Wentzel, M. C., Lötter, L. H., Ekama, G. A., Loewenthal, R. E. and Marais, G. A. (1991). Evaluation of biochemical models for biological excess phosphorus removal. *Wat. Sci. Tech*. **23**, 567-576.

Wentzel, M. C. and Ekama, G. A. (1997) Principles in the design of single-sludge activated-sludge systems for biological removal of carbon, nitrogen and phosphorus. *Wat. Environ. Res.* **69**(7), 1222-1231.

Wiechers, H. N. S. (1985) Preface of "Enhanced biological phosphorus removal from wastewaters". *Wat. Sci. Tech.* **17**(11/12), ix-x.

Wild, D., Kisliakova, A. and Siegrist, H. (1996) P-fixation by Mg, Ca and Zeolite A during stabilization of excess sludge from enhanced biological P-removal. *Wat. Sci. Tech.* **34**(1-2), 391-398.

Wimpenny, J. W. T. and Colasanti, R. (1997) A unifying hypothesis for the structure of microbial biofilms based on cellular automaton models. *FEMS Microbiol. Ecol.* **22**, 1-16.

Xavier, J. B., Malhó, R., Reis, A. M. and Almeida, J. S. (2000) Description of biofilm formation by determination of developmental axis. *Proceedings of the IAWQ Conference on Biofilm Systems*. Oct. 1999, New York. *Wat. Sci. Tech*. (in press).

Yu, T. and Bishop, P. L. (1998) Stratification of microbial metabolic processes and redox potential change in an aerobic biofilm studied using microelectrodes. *Wat. Sci. Tech*. **37**(4-5), 195-198.

Zhang, X., Bishop, P. L. and Kupferle, M. J. (1998) Measurement of polysaccharides and proteins in biofilm extracellular polymers. *Wat. Sci. Tech.* **37**(4-5), 345-348.

Ødegaard, H., Rusten, B. and Westrum, T. (1994) A new moving bed biofilm reactor – applications and results. *Wat. Sci. Tech.* **29**(10-11), 157-165.

14. List of Symbols and Abbreviations

For a list with explanations of the constant parameters used in the computer model, please refer to Table 9.2, p. 146. For a list of abbreviations of the applied gene probes, please refer to Table 8.2, p. 131.

Symbol	**Explanation**
α	Slope
a_x	The activity of the ion species X
A	Absorbance
A^*	Biofilm surface ares
A_2	Anaerobic-Anoxic
AC	Acetic acid (or Alternating Current)
AO	Anaerobic-Oxic
AS	Activated Sludge
ASM	Activated Sludge Model
β	Relative penetration depth of a compound into a biofilm
BAS	Biofilm Airlift Reactor
BF	Biofilm
BOD_5	5-day Biological Oxygen Demand [$gO_2\ m^{-3}$]
C	Concentration of a compound [$g\ m^3$]
C^*	Concentration of a compound by the biofilm surface [$g\ m^3$]
$C_{PO4,ana,in}$	Inlet conc. of phosphate during anaerobic phase
$C_{PO4,ano,in}$	Inlet conc. of phosphate during anoxic phase
CA	Cellular Automaton
CLSM	Confocal Laser Scanning Microscope
COD	Chemical Oxygen Demand [$gO_2\ m^{-3}$]
D	Diffusion coefficient
DC	Direct Current
DPB	Denitrifying phosphorus removing bacteria
E	Electrode potential of a half-cell
E_0	Standard electrode potential for a half-cell
EBPR	Enhanced biological phosphorus removal
ED	Entner-Doudoroff pathway
EMP	Embden-Meyerhof-Parnas Pathway
EPS	Extrapolymeric Substances
F	Faraday's constant [96487 Coulomb equiv.$^{-1}$]

FITC	Fluorescein 5-isothiocyanate
FISH	Fluorescent in situ hybridisation
GAO	Glycogen Accumulating Organism
GPB	Gram positive bacteria
HAc	Acetic Acid
HGC	High DNA G+C content
I	Light intensity or ionstrength
k_{0A}	Zero order area specific rate constant [g m^2 d^{-1}]
$k_{½a}$	Half order rate constant [$g^{½}$ $m^{-½}$ d^{-1}]
k_{1A}	First order area specific rate constant [d^{-1} m^{-2}]
k_d and k_d'	Detachment coefficients
k_{0f}	Zero order rate constant inside biofilm
L	Biofilm thickness
$L_{base\ thickness}$	Biofilm thickness after backwash
μ	Growth rate [d^{-1}]
M^+	Positively charged cation
M_P	Mass of phosphate
$M_{P,removed}$	Net mass of phosphate removed during one cycle
MAR	Microautoradiography
MBBR	Moving Bed Biofilm Reactor
MCRT	Mean cell residence time
N	Flux of a substance into a biofilm or a number indicator
ND	Nitrification-Denitrification
PAO	Phosphate Accumulating Organism
PBC	Porous Biomass Carrier
PBS	Phosphate buffer
PCR	Polymerase Chain Reaction
PE	Person Equivalent
PFA	Paraformaldehyde
PHA	Polyhydroxyalkanoates
PHB	Polyhydroxybuturate
PHV	Polyhydroxyvaleric acid
$P_{cycle,area}$	The area of the phosphate outlet curve during a cycle
Q	Water flow [m^3 d^{-1}]
ρ_f	Biofilm volumetric density
r	Radius
r_a	Area specific removal rate [g m^2 d^{-1}]

$r_{a,max}$	Maximum area specific removal rate [g m^2 d^{-1}]
r_f	Reaction rate inside biofilm [g m^3 d^{-1}]
R	The gas constant [8.3143 Joule $^oK^{-1}$ $Mole^{-1}$] or Regression coefficient
S	Concentration of a soluble compound [g m^3]
S_{in}	Concentration of a soluble compound in the inlet [g m^3]
S_{out}	Concentration of a soluble compound in the outlet [g m^3]
$S_{transition}$	Conc. that lead to transition from ½ to 0 order bulk reaction rate
SBR	Sequencing Batch Reactor
SBBR	Sequencing Batch Biofilm Reactor
SBMBBR	Sequencing Batch Moving Bed Biofilm Reactor
SCFA	Short Chain Fatty Acid
SRB	Sulphate Reducing Bacteria
SRT	Sludge Retention Time
SS	Suspended Solids (dry mass) [g m^3]
SVI	Sludge Volume Index
τ	surface shear stress
t	time [d]
T	Absolute temperature [^oK]
T_{ana}	Anaerobic phase length
T_{ano}	Anoxic phase length
TCA	Tricarboxylic Acid cycle
TOC	Total Organic Carbon
TS	Total Solids [g m^3]
UCT	University of Capetown
V	Volume
VSS	Volatile Suspended Solids [g m^3]
WWTP	Wastewater Treatment Plant
x	Position co-ordinate, e.g. distance from the substratum in a biofilm [m]
X_D	Concentration of denitrifying bacteria inside a biofilm [g m^3]
X_f	Biomass concentration inside a biofilm [g m^3]
X_I	Concentration of inert particulates inside a biofilm [g m^3]
X_{PAO}	Concentration of phosphate accumulating bacteria inside a biofilm [g m^3]
X_{PP}	Concentration of poly-phosphate inside a biofilm [gP m^3]
Y_{obs}	Observed Yield coefficient
γ_1 and γ_2	Activity coefficients or mono-, respectively, divalent ions
z	Position co-ordinate or the charge number of an ionic species

Appendix 4.1

Phosphate reagent

A dilution of 1:2 was used for the phosphate reagent compared to the reagent from ASTM D 515-68 non referee method B. This turned out to be a sufficient strong concentration for the investigated concentration range, and was desirable due to the high price of the chemical $(NH_4)_6Mo_7O_{24}*4H_2O$.

Preparation of 5 liter phosphate reagent:

a: 200 g ammoniummolybdate, is dissolved in 2000 ml destilled water (if necessary with heating and then cooled to room temperature).

b: 5 g ammonium vanadate, NH_4VO_3, is dissolved in a mixture of 1500 ml destilled water and 1000 ml nitric acid, HNO_3, density 1.42 g/cm^3.

Solution a is poured into solution b.
The solution is diluted to a total volume of 10 L (add 5.5 L).